Die Expeditionen ANTARKTIS XIII/1-2 des Forschungsschiffes „POLARSTERN" 1995/96

The Expeditions ANTARKTIS XIII/1-2 of the Research Vessel "POLARSTERN" in 1995/96

Herausgegeben von / Edited by
Ulrich Bathmann, Mike Lucas, Victor Smetacek
unter Mitarbeit der Fahrtteilnehmer /
with contributions of the participants

Ber. Polarforsch. 221 (1997)
ISSN 0176 - 5027

ANTARKTIS XIII/1 - 2

09 NOVEMBER 1995 - 24 JANUARY 1996

KOORDINATOR/COORDINATOR

Ernst Augstein

ANT XIII/1: Bremerhaven - Cape Town

FAHRTLEITER

Kapt. H. Jonas

ANT XIII/2: Cape Town - Cape Town

FAHRTLEITER/CHIEF SCIENTIST

Victor Smetacek

ANT XIII/1 FAHRTVERLAUF

Aus dem Bericht des Kapitäns und Fahrtleiters Kapt. Jonas mit Beiträgen der Wissenschaftler.

Der Fahrtabschnitt ANT XIII/1 begann am 9. November 1995 in Bremerhaven mit 8 Wissenschaftlern und 5 zusätzlichen Personen an Bord. Mit Erreichen der spanischen Hoheitsgewässer begannen am Morgen des 12.11.95 die kontinuierlichen Forschungsarbeiten.

Der Tag der Abfahrt Bremerhaven war gekennzeichnet durch verhältnismäßig geringe Luftdruckgegensätze und dementsprechend geringe Windgeschwindigkeit von 3 bis 4 Bft um Südwest. Am 10.11.95 entwickelte sich im Raum der Biskaya ein kräftiges Tief, das langsam nordwärts zog. An seiner Vorderseite verstärkte sich im Ärmelkanal der Wind auf Süd bis Südost 6 bis 7. Nach vorübergehender Abnahme verstärkte sich westlich der Biskaya auf der Rückseite des Tiefs der Wind auf 8 bis 9 und drehte dabei auf West. Die Wellenhöhe erreichte 4 Meter (12.11.95). Am Südrand des umfangreichen Tiefs über dem Nordatlantik hielt danach ein Südwestwind der Stärke 5 bis 6 bis zum 15.11. an. Erst ab 16.11. nahm im Raum der Kanarischen Inseln der Wind auf 2 bis 3 ab.

Am 16.11.95 wurde die Verankerung CI-5 nördlich von Gran Canaria aufgenommen und CI-6 an gleicher Stelle ausgelegt. Die Verankerungen enthalten Sedimentfallen und Strömungsmesser. Mit den Sedimentfallen werden über ein Jahr die sedimentierenden Partikel quantitativ und qualitativ gesammelt, sodaß der Jahresgang der Sedimentation bestimmt werden kann. An den Proben wurde zunächst visuell die Zusammensetzung der Sinkstoffe untersucht, anschließend wurden verschiedene chemische Untersuchungen durchgeführt: Bestimmung des Gehaltes an organischer Substanz, an Karbonat und Silikat und Messung der stabilen Sauerstoff- und Kohlenstoffisotope an Karbonat, sowie der Kohlenstoffisotope an der organischen Substanz. Nach Abschluß der Verankerungsarbeiten wurden anschließend noch einige Tests an ANP und GPS gefahren, um dann am Abend nach Las Palmas abzulaufen. Am 17.11. wurden die 5 zusätzlichen Personen ausgeschifft.

Westlich von Mauretanien wurde am 19.11. die Verankerung CB-6 aufgenommen und CB-7 auf Pos. 21°15,4`N, 020°41,8`W ausgelegt. Mittags waren diese Arbeiten abgeschlossen und die Fahrt Nonstop außerhalb der 200sm Wirtschaftszonen nach Kapstadt fortgesetzt. Abends setzte der NO-Passat mit Bft 5 ein bis zur Intertropischen Konvergenzzone. Diese wurde in der Nacht zum 22.11. bei ca. 5°N durchquert. Zum Leidwesen unserer "Regenfänger" traten nur wenige Regenschauer und Gewitter auf. Von den Mallungen war kaum etwas zu spüren, denn schon am 22.11. setzte der SO-Passat mit Stärke 5 Bft ein. Die Luft-Temperaturen stiegen auf über 30°C an, die höchste Wassertemperatur wurde mit 30,5°C gemessen. Die Sonnenanbeter hielten sich in Grenzen (nur Esel und Weiße gehen in die pralle Sonne), dagegen wurde der Seewasserpool auf dem Achterschiff ausgiebig frequentiert. Am 23.11. um 1832 UTC wurde der Äquator bei 12°16`W überlaufen.

Im Verlauf dieser Reise wurden vom CO_2-Projekt des Kieler Instituts für Meereskunde kontinuierlich 4 verschiedene Analysesysteme betrieben. Hauptziel der Reise war die Aufnahme eines lückenlosen Oberflächenschnittes des CO_2-Partialdruckes in Oberflächenwasser und Atmosphäre entlang der gesamten Fahrtroute. Dieses Ziel konnte in vollem Umfang erreicht werden. Der umfangreiche, zeitlich (und somit auch räumlich) hochaufgelöste Datensatz zeigte eine mäßige Untersättigung (ca. 10-30 µatm) des Oberflächenwassers bezüglich CO_2 im Bereich der subtropischen Wirbelsysteme des Nord- und Südatlantiks. Äquatoriale Breiten sind demgegenüber durch eine Übersättigung von bis zu 50 µatm gekennzeichnet. Dieses Phänomen ist auf das Vorhandensein von äquatorialem Auftrieb zurückzuführen, durch den nährstoff- und damit auch CO_2-reiches Wasser aus Tiefen von wenigen Hundert Metern an die Oberfläche gelangt. Der atmosphärische CO_2-Gehalt lag während der gesamten Reise sehr stabil zwischen 359 und 361 ppmv. Ein Sprung von etwa +1.5 ppmv wurde beim Durchqueren der Intertropischen Konvergenzzone (ITCZ) beobachtet. Um die Interpretierbarkeit und Aussagekraft der CO_2-Partialdruckmessungen zu ergänzen, wurden Begleitmessungen von Gesamtkarbonatgehalt, Alkalinität und Nährsalzkonzentrationen (NO_2, NO_3, PO_4, SiO_4) mit hochgenauen

Analysesystemen durchgeführt. Die Rohdaten zeigen eine sehr gute Übereinstimmung mit den Ergebnissen der kontinuierlichen CO_2-Partialdruckmessungen. Insbesondere konnten die Auswirkungen des äquatorialen Auftriebs in den deutlich erhöhten Nährsalzkonzentrationen klar identifiziert werden.

Wetterbestimmend ab Äquator war ein umfangreiches Hochdruckgebiet mit seinem Zentrum im Raume der Gough Insel mit einem Kerndruck von meist 1030 hPa oder etwas darüber. Ein breiter Keil erstreckte sich bis zur Ascension Insel. Am Nordostrand dieses Keiles wehte zunächst ein ziemlich gleichmäßiger Südostpassat mit einer Stärke von 4 bis 5 Bft. Am 28.11. setzte über dem gesamten südafrikanischen Raum stärkerer Druckfall ein, so daß sich der Luftdruckgradient merklich verschärfte. Schon in der Nacht zum 29.11. erreichte der Wind Bft. 6 bis 7 und wehte dann am 29. und 30. fast durchweg mit Stärke 7, erreichte sogar kurzzeitig Bft 8. Erst am 1.12. flaute der Wind auf 6 bis 5 Bft ab und drehte auf Süd.

Die Reise endete planmäßig am 2. Dezember 1995 in Kapstadt. (Abb. 1)

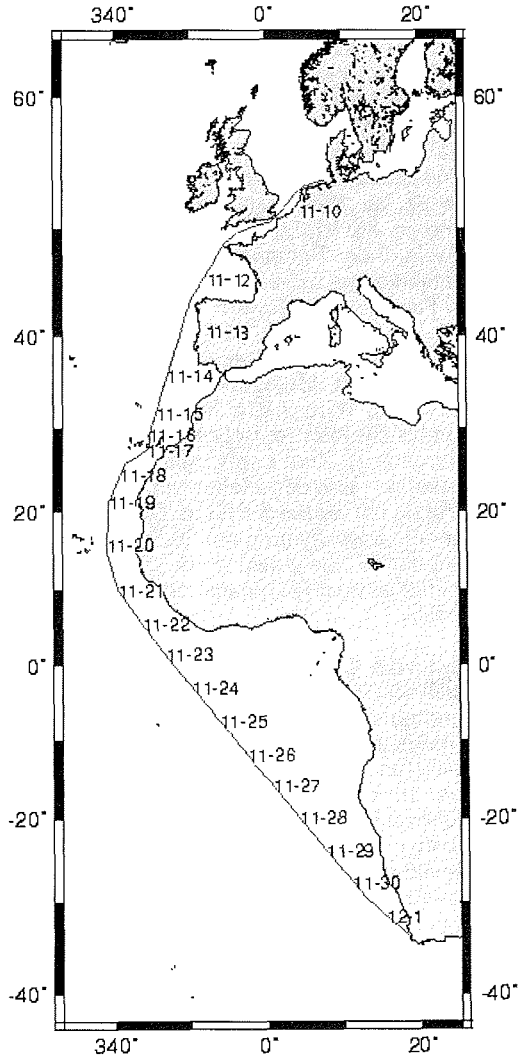

ANT XIII/2 EINLEITUNG UND FAHRTVERLAUF

V. Smetacek, U. Bathmann

Die Expedition ANT XIII/2 (Frontendynamik und Biologie) wurde als Teil der internationalen Joint Global Ocean Flux Study (JGOFS) durchgeführt. Dieses Programm hat das Ziel, den Kohlenstoffkreislauf zu bestimmen, in diesem Fall die Prozesse, die zum Eintrag atmosphärischen CO_2 in den Ozean führen, wie der Einbau von CO_2 in biogenes Material (Primärproduktion), dessen Umwandlung im pelagischen Nahrungsgeflecht und das Absinken in tiefe Ozeanschichten. Am Anfang dieser Prozesse, auch Biologische Pumpe genannt, steht das Phytoplankton, dessen wichtigste Vertreter Flagellaten und Diatomeen sind. Die Flagellaten dominieren verschiedene Algenklassen des Pico- und Nanoplanktons, während bei Diatomeen kettenbildende Arten oder solche mit langen Fortsätzen häufig sind. Während die Flagellatenbiomasse selten 0.3 mg Chlorophyll *a* m^{-2} übersteigt, ist die der Diatomeen weitaus höher; sie tritt aber räumlich und zeitlich begrenzt auf. Es gilt, die Faktoren solch einer Blütenbildung zu verstehen, um die biochemischen Kreisläufe im Meer zu begreifen und zu quantifizieren, da diese Stoffkreisläufe den vertikalen Partikelfluß und die CO_2 -Aufnahme des Ozeans bestimmen.

Während der ersten JGOFS Expedition des FS "*Polarstern*" (ANT X/6), die im Oktober/November 1992 entlang des 6°W Meridians zwischen 58° S und 47° S stattfand, wurde die Entwicklung einer Diatomeenblüte an der Polarfrontzone beobachtet, die zur Untersättigung des Ozeans mit CO_2 führte. Da die hohen Eisenkonzentrationen im Meerwasser während dieser Blüte stark abnahm, wird vermutet, daß Eisenverfügbarkeit die Produktion im Südpolarmeer limitiert. Die Ozeanschichtung in dieser Region war sehr flach, dennoch wurde hohe Diatomeenbiomasse in tiefen, lichtlimitierten Zonen gefunden. Eine dynamische Hydrographie muß demnach zu einer Überschichtung von Oberflächenwasser mit tieferem bewirkt haben. Eine wichtige Erkenntnis der Expedition ANT X/6 war, daß das Verständnis der mesoskaligen Dynamiken an Ozeanfronten essentiell für das Verständnis chemischer und biologischer Prozesse ist, die ihrerseits den vertikalen Partikeltransport dieser Meeresgebiete bestimmen.

Um die eben beschriebenen Prozesse zu verstehen, muß die Datenerfassung auf adäquaten, d.h. viel feineren Skalen erfolgen als bisher. Das Schleppsystem "Sea Soar", das ständig zwischen Meeresoberfläche und ca. 400 m Wassertiefe geschleppt wird, nimmt Daten des Unterwasser-Lichtfeldes, der Temperatur- und Salzgehaltsschichtung und der Phytoplanktonfluoreszenz auf, aus denen die Höhe der Phytoplanktonbiomasse und der Primärproduktion abgeleitet werden. Mit den zusätzlichen Daten aus kontinuierlichen Oberflächenproben wurde ein Bild der Hydrographie und Verteilung der Biologie in je einem groben (ca. 75 km Transektabstand) und einem feinen (13 km Transektabstand) dreidimensionalen Grid gewonnen. Zusätzlich wurden diskrete Wassersäulen beprobt mit den Geräten: CTD-Rosette, Go-Fo-Flaschen am Kevlarseil, Multi-, Bongo, Midwater-Netz, *in situ*-Pumpen.

Akkumulation von Diatomeenbiomasse im Plankton kann durch verstärktes Zellwachstum erzeugt werden oder bei verminderten Verlustraten (Zellsterben, Parasitenbefall, Absinken, Wegfressen) auftreten. Wachstumsfaktoren (Lichtklima, Nährsalz- und Eisengehalt) wurden in Beziehung zur Hydrographie untersucht, und die Wachstumsraten des Phytoplanktons direkt und indirekt gemessen. Mikroskopische Untersuchungen halfen, die verschieden Arten von Phytoplanktonverlust (Parasiten, Absinken, Wegfraß) semi-quantitativ abzuschätzen. Der Bestand des Mesozooplanktons wurde durch konventionelle Netzfänge, durch akkustische (ADCP) und optische *in situ* Verfahren (optischer Planktonzähler) erfaßt. Absinken partikulärer Substanz wurde über die Uran/Thorium-Differenz und über verankerte Sinkstoffallen ermittelt.

Fahrtverlauf

FS "*Polarstern*" verließ Kapstadt planmäßig am Montag den 4.12. mit 71 Eingeschifften und 44 Besatzungsmitgliedern. Außerhalb der Hoheitsgewässer begannen die wissenschaftlichen Arbeiten mit der Dauerregistrierung von physikalischen und biologischen Daten aus der Ozeandeckschicht durch SeaSoar und mit verschiedenen anderen On-Line Registrierungen. Die geplante Auswechslung von 3 Verankerungen auf dieser Route zwischen 50° und 57° war leider nicht erfolgreich, so daß unmittelbar Kurs auf Neumayer genommen wurde (Abb. Cruise track). Dort angekommen herrschte Schneetreiben, und eine mehrere 100m breite Barriere aus aufgetürmten Eisschollen war der Küste vorgelagert. An der schmalsten Stelle der sehr harten Barriere begannen die Rammaktivitäten, die erst am nächsten Morgen erfolglos abgebrochen wurden. Montag Nacht bestätigte sich, daß die Eisbarriere noch einige Zeit unüberwindbar bleiben würde, und daher verließen wir die Bucht und begannen die Untersuchungen an der Polarfront. Zuvor war ein Teil des Sommerteams auf Neumayer per Hubschrauber abgesetzt worden.

Das Forschungsvorhaben mußte gekürzt werden, um die verbleibende Zeit optimal zu nutzen. Die Wiederholung des SeaSoar Transekts begann zwischen 54° und 50°S. Eine Phytoplanktonblüte hatte sich entlang der Polarfront zwischen 52° und 50°S mit niedrigerer Biomasse im Süden entwickelt. Nach Beendigung des ersten Transekts am 23. 12. begannen zwischen 52° und 50°S die Registrierungen mit SeaSoar in einem Raster, bestehend aus 7 meridionalen Transekten, die 75 km auseinander lagen und 270 km lang waren. Zudem wurden im Oberflächenwasser kontinuierlich verschiedene andere Parameter gemessen. Stationen dienten zur Kalibrierung des Sea Soar und versorgten verschiedene Gruppen mit Probenmaterial; eine Kurzzeitverankerung bestückt mit akustischen und mechanischen Strömungsmessern und Sinkstoffallen wurde am nordöstlichen Rand des Untersuchungsgebietes ausgebracht. Sturmbedingt wurden weitere Stationsarbeiten zugunsten der Aufnahme einer feinskaligen Matratze durch SeaSoar (elf 123 km lange, 13 km voneinander entfernte Transekte) aufgegeben. Nach weiteren 12 CTD Stationen wurden die Arbeiten am 7.1. abgebrochen und der zweite Anlauf zur Entladung gestartet, die dann am 14.1., nach erfolglosem Versuch einer Meereisentladung, innerhalb von 2 Tagen über die Schelfeiskante abgeschlossen wurde.

Die verbliebenen 40 Stunden Forschungszeit wurden an der Polarfront zum Bergen der Kurzzeitverankerung und für weitere wichtige Kalibrations- und Stationsarbeiten verwendet. Die Fahrt endete am 24. Januar 1996 planmäßig in Kapstadt.

Zwei weitere wichtige Ereignisse wurden während der Fahrt begangen. Zum Neujahr wechselte die Bereederung von "*Polarstern*". Kapitän Jonas sowie elf Besatzungsmitglieder gingen mit Ende dieser Reise in den Ruhestand.

ANT XIII/2 INTRODUCTION AND CRUISE ITINERARY

U.V. Bathmann, M. Lucas,.V. Smetacek

Rationale

The cruise ANT XIII/2 (Frontal dynamics and biology) was carried out as part of the international Joint Global Ocean Flux Study (JGOFS) dedicated to measurement of the carbon cycle with particular focus on processes leading to CO_2 drawdown from the atmosphere and transfer of biogenic matter via vertical flux to the ocean interior and the sediments. This biological carbon pump is driven by the marine phytoplankton which can be grouped into two categories: pico and nanoplanktonic flagellates belonging to various algal classes and the diatoms which tend to be chain-forming or possess large cells. Whereas the biomass of flagellates rarely exceeds about 0.3 mg chlorophyll m^{-2}, diatoms give rise to blooms of much higher biomass that are, however, spatially and temporally restricted in their occurrence. Understanding the factors leading to build-up of diatom blooms is essential to understanding and quantifying marine biogeochemical cycles as it is this group which has the greatest impact on vertical flux and CO_2 drawdown.

During the first JGOFS cruise of RV "*Polarstern*" (ANT X/6), conducted in October/November 1992 along the 6°W meridian between 58° S and 47° S, build-up of diatom blooms was observed in the Polar Frontal Zone concomitant with strong undersaturation of CO_2 . As higher iron concentrations were found here that were depleted with progress of the blooms, a strong case could be made for iron limitation of Southern Ocean productivity. However, the region was also characterised by shallower mixed layers although substantial diatom biomass often extended to depths where growth rates must have been light-limited. It was assumed that the phytoplankton distribution pattern was caused by the dynamics of the frontal zone which led to subduction of surface layers. Hence the blooms must have arisen under favorable light conditions prevailing in a shallow mixed layer. A major outcome of ANT X/6 was the need to assess mesoscale dynamics of water masses along fronts in order to understand chemical and biological processes mediating vertical particle flux occurring there.

A prerequisite to understanding these processes and the various causative mechanisms is data collection at adequate scales normally not achieved by conventional station spacing.This is because of the complex dynamics of frontal systems. The towed undulating sensor package Sea Soar, the main instrument employed on ANT XIII/2, enables rapid, detailed mapping of the surface ocean down to about 400 m depth and the major aim of this cruise was to measure physical, chemical and biological parameters using this instrument along the Polar Frontal Zone. A suite of additional properties was assessed simultaneously both continuously and in water samples taken from the sea surface. An impression of the overall hydrography and biology of the frontal system was obtained on the basis of a coarse-scale SeaSoar survey and a small-scale (13 km grid spacing) three-dimensional survey (ca. 100 x 100 km). A number of water column stations was carried out through the survey area. Gear deployed at these stations included a CTD rosette, Go-Flo bottles mounted on Kevlar wire for iron measurements, multinet, Bongonet, Rectangular Midwater trawl and in situ pumps.

Diatom biomass accumulation can be achieved in two ways: a) by increasing growth rates and/or b) by decreasing mortality due to cell death, sinking, parasites and grazing. Factors influencing growth rates (underwater light climate, macronutrient and iron availabilty) in relation to hydrography were studied in detail. Growth rates of phytoplankton were assessed using various direct and indirect measurements. Mortality rates are more difficult to assess directly. Microscopic assessment of fresh samples enabled estimation of losses due to cell death by unfavourable environmental factors and by grazing by parasitoids and protozoa. Biomass and composition of metazooplankton was also assessed both by conventional netting, ADCP data and by means of optical plankton counters mounted on the SeaSoar and the Multinet. Sinking out of particulate matter was followed by Uranium/Thorium budgets and moored sediment traps.

Cruise itinerary

RV "*Polarstern*" left Cape Town as planned on the morning of 4th Dec. with 71 passengers and 44 crew members on board. The intention was to first steam to the Neumayer station, disembark personnel and supplies and then return to the study area along the Polar Front. SeaSeaSoar was deployed and various measurements in surface waters commenced within a few days after departure. The planned recovery and deployment of three moorings on the way South had to be cancelled due to bad weather. On arrival at Neumayer station we found that a formidable barrier of heavily ridged, fast ice several 100 meters broad adjoined the shelf ice. Visibility was very poor and ramming proved to be of no avail. Personnel were transported to the station during a short period of relatively good visibility by helicopters. Strong winds further compressed the loose pack-ice and it became clear that the barrier was impregnable all along the Bay in the foreseeable future. It was decided to return to the Polar Front and unload the cargo later: 10 extra days which had to be deducted from research time.

The research strategy had to be changed to make optimal use of the limited time at our disposal. It was decided to commence the study by repeating the SeaSoar transect between 54° and 50°S covered on the way south. After completing this first transect on the evening of the 23rd Dec., Sea Soar mapping of a coarse-scale grid started along the bloom, comprising a series of 7 longitudinal transects, each 270 km long and 75 km apart between 52° and 50°S. After completing the SeaSoar grid on Friday 29th, a chain of current meters and two sediment traps for collecting sinking material was moored to the east of the box and several stations carried out. Another storm forced us to interrupt station work and SeaSoar was deployed again, this time to cover a small-scale grid comprising 11 north/south transects 123 km long and spaced at intervals of 13 km. After completing the grid, a total of 12 stations were carried out: 3 along the western margin of the grid and 9 through its centre. Research was stopped on 7th Jan. as we had to return to Neumayer. The fast-ice barrier was still there and resisted all attempts at ramming. After an unsuccessful attempt to unload supplies on the fast ice to the west of the Station, "*Polarstern*" managed to dock alongside one of the shelf-ice protrusions to the north of the station. After two busy days all equipment and fuel was successfully unloaded.

"*Polarstern*" next returned to the Polar Front and in the remaining 40 hrs research time, the mooring was recovered and several stations carried out to improve calibration and validation of SeaSoar data. The cruise ended as planned on 24th Jan. in Cape Town.

Two other, non-scientific events were celebrated during the cruise. On New Years day the management of "*Polarstern*" was transferred from the Hapag-Lloyd Transport and Service GmbH to the new contractor - Martini GmbH. Captain Jonas together with 11 crew members retired at the end of the cruise; most of them have been on "*Polarstern*" for the last 10 years, so this was the end of an era.

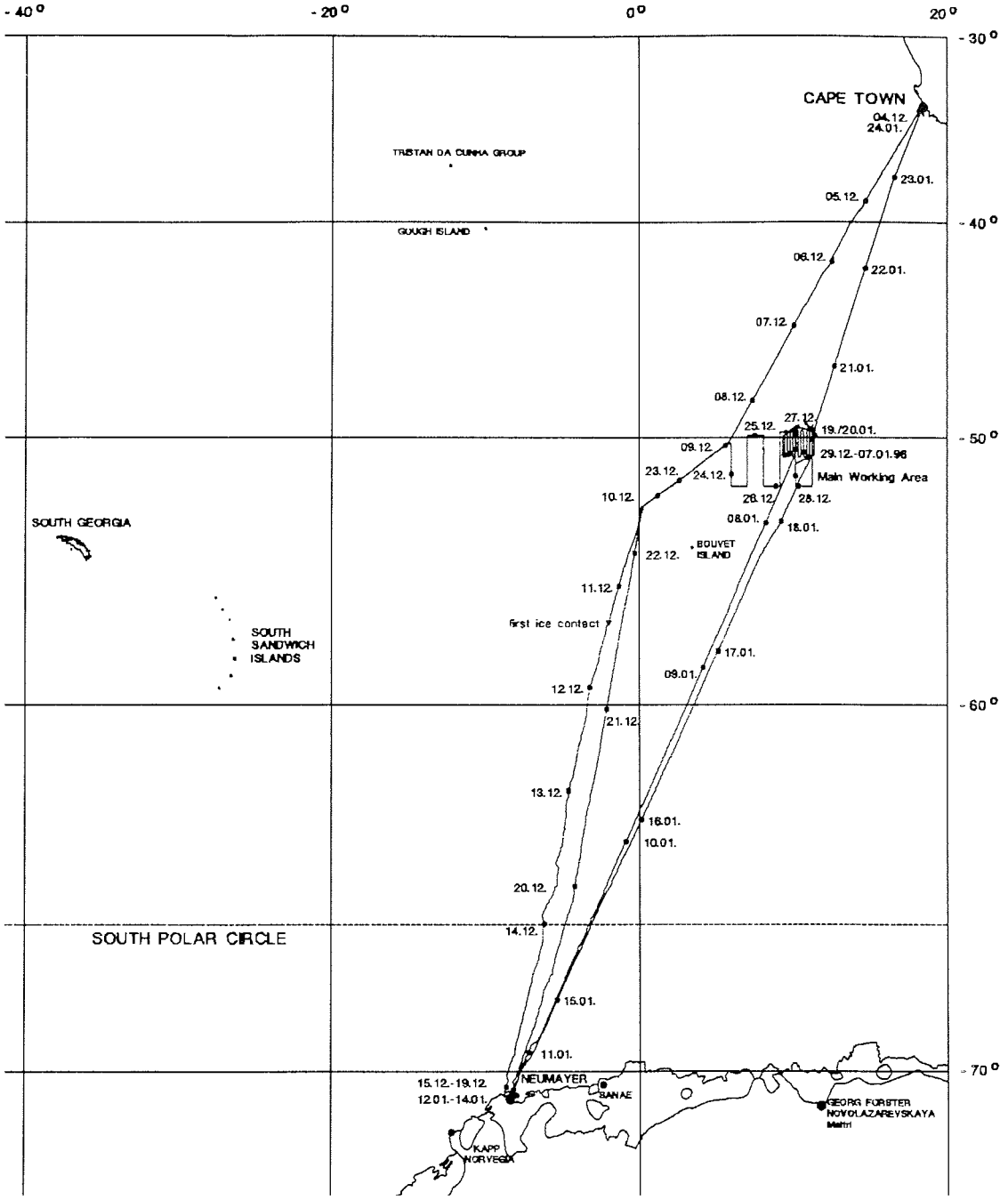

Fig. Cruise Track of RV "*Polarstern*"-Cruise ANT XIII/2 from 4 December 1995 to 24 January 1996

1. WETTER / WEATHER

J. England

Am 04.12. pünktlich 10 Uhr UTC verließ das Schiff Kapstadt bei strahlendem Sonnenschein. Zwischen einem Tief über der Kapprovinz und einem kräftigen und umfangreichen Hochdruckgebiet bei 30 Grad Süd und 0 Grad, von dem aus sich ein Hochkeil bis in das Seegebiet südlich Afrikas erstreckte, wehte zunächst nur ein schwacher Westwind der Stärke 2 bis 3, der später auf Süd bis Südost drehte und auf Stärke 4 zunahm. Etwa in Höhe des Kaps der Guten Hoffnung sank die Wassertemperatur in einem Gebiet mit kaltem Auftriebswasser rapide auf etwa 14 Grad ab, so daß das Schiff in ein dichtes Nebelgebiet geriet. Der Taupunkt lag einige Grade über der Wassertemperatur. Abends stieg die Wassertemperatur wieder auf 20 Grad an und das Nebelgebiet wurde verlassen. Auch in den Folgetagen bestimmte das erwähnte Hochdruckgebiet das Wetter. Die Stärke der südlichen Winde betrug dabei zwischen Bft 4 und 6. Die Sichtverhältnisse waren gut, so daß am 05.12. der erste Hubschrauberflug rund um das Schiff durchgeführt werden konnte.

Inzwischen hatte sich bei South Georgia ein kräftiges Tiefdruckgebiet gebildet, das rasch südostwärts zog und am 07.12. mit einem Kerndruck von etwa 955 hPa 350 sm südöstlich der Insel Corbeta lag. Dieses Tief drängte den für die Fahrt bisher günstigen langgestreckten Hochkeil nach Osten ab. Damit gelangte das Schiff in zunehmendem Maße an die Vorderseite des umfangreichen Sturmtiefs, so daß der Wind über Nord nach West drehte und auf 6 bis 7 Bft zunahm. Die Kaltfront überquerte das Schiff am 08.12. in den frühen Morgenstunden. Dabei trat zeitweise Windstärke 8 auf.

Das bisher wetterbestimmende umfangreiche Tief nördlich von Sanae füllte sich am 09.12. allmählich auf. Der Wind wehte anfangs noch mit 7 Bft um West, nahm aber unter Zwischenhocheinfluß bis zum Abend auf 4 Bft ab. Inzwischen hatte sich nordöstlich von South Georgia ein weiteres kräftiges Tief entwickelt, das mit seinen Fronten in der Folgezeit rasch ostwärts zog. Am 10.12 wehte der Wind mit Stärke 8 bis 9 aus Nordwest. Im Bereich eines breiten Warmsektors herrschte in der relativ milden und feuchten Luft ganztags Nebel. Das langgestreckte Starkwindfeld südlich des Tiefs löste sich am 11.12. merklich auf, da das Tief sehr rasch nach Osten abgezogen war. Die Windgeschwindigkeit ging auf 5 bis 4 Bft zurück. Die auch nachts noch schlechte Sicht besserte sich tagsüber nur langsam.

In der Nacht zum 12.12. bildete sich westlich der "*Polarstern*" ein verhältnismäßig kleines, aber kräftiges Tief, das rasch ostwärts zog. Dabei frischte der Wind bereits in der zweiten Nachthälfte auf nicht erwartete 8 Bft auf und drehte auf Nordwest. Schneefall und Nebel beeinträchtigten dabei in starkem Maße die Sichtverhältnisse. In den Morgenstunden überquerte die Kaltfront das Schiff. Danach trat eine deutliche Sichtbesserung auf über 30 km ein. Der Wind drehte auf West zurück, blieb aber zunächst noch bei 7 bis 6 Bft. Erst nachmittags flaute der Wind ab und erreichte abends nur noch Stärke 4.

Am 13.12. bestimmte ein breiter Zwischenhochkeil das Wetter. Es wehte dabei ein mäßiger Südwestwind der Stärke 5 bis 6.

Am 15.12. bestimmte ein langsam ziehendes Tief westlich des Schiffes das Wettergeschehen mit auffrischendem Wind aus Nordost bis Ost, der die Stärke 7, zeitweise auch 8 erreichte. Ab Mittag trat leichter bis mäßiger Schneefall auf. Im Zusammenhang mit dem Schneefall und der Zufuhr feuchter Luft vom Meer her trat eine permanente Sichtverschlechterung ein. Dadurch konnte der Hubschrauber nicht zur Eiserkundung vor Neumayer starten.

Am 16.12. brachte ein Zwischenhochkeil eine allmähliche Wetterbesserung. Es trat kaum noch Schneefall auf und die Sicht besserte sich bis zum Abend auf über 20 km. Der Wind kam aus Ost und nahm von Stärke 6 auf Stärke 4 ab. Bis mittags herrschte allerdings Whiteout, so daß erst nachmittags geflogen werden konnte.

Am 17.12. zog von Nordwesten her ein Tief heran, so daß ab Nachmittag anhaltender Schneefall mit entsprechend schlechter Sicht aufkam und der Wind auf Stärke 6 auffrischte. Der Schneefall hielt die ganze Nacht und den Vormittag des Folgetages an und der Wind verstärkte sich auf 8 bis 9 Bft. Gegen Mittag hörte der Schneefall auf, die Sicht besserte sich, der Wind drehte auf Nordwest und nahm rasch bis zum Abend auf Stärke 4 bis 3 ab, so daß Hubschrauberflüge möglich wurden.

Am 19.12. streifte ein ostwärts vom Liegeplatz nach Südosten ziehendes Tiefdruckgebiet das Schiff mit seinem Schneefallgebiet. Vormittags gab es einen Nebeleinbruch ohne Aussicht auf baldige Besserung. Der Wind wehte dabei schwach um Nordost mit 2 bis 4 Bft.

Da das Eis vor Neumayer Base noch zu stark war um es erfolgreich durchdringen zu können, wurde beschlossen, zunächst wieder nach Norden zu fahren, um wenigstens die meereskundlichen Forschungen weiter betreiben zu können. Gegen 11 Uhr UTC verließ die "*Polarstern*" deshalb die Atkabucht. Nachmittags besserte sich bei West 4 Bft das Wetter. In der Nacht zum 20.12. näherte sich von Nordnordwesten ein Sturmtief, so daß der Wind auf Nord drehte und 8 bis 9 Bft erreichte. Am 20.12. nahm vormittags und mittags der Wind verhältnismäßig rasch wieder ab, so daß nachmittags nur noch 3 bis 4 Bft gemessen wurden. Nördlich des Tiefs hatte sich ein breiter Keil des Südatlantikhochs aufgebaut, der im Laufe des 21.12. in zunehmendem Maße wetterbestimmend wurde. Nachmittags bildete sich in der relativ warmen Nordströmung anhaltend dichter Nebel, der auch die ganze Nacht und bis zum Folgetag mittag noch anhielt.

Am 22.12.zog ein kräftiges Sturmtief westlich des Schiffes südsüdostwärts, dessen Starkwindfeld zu einer Zunahme des Nordwindes auf 7, nachmittags zeitweise auch 8 Bft führte. Das Tief zog weiter nach Süden genau auf Neumayer Base zu. In einer langgestreckten Nordströmung herrschte am 23 .12. Windstärke 6 bis 7. In der "warmen" und feuchten Luftmasse hielt ganztags und auch noch in der Nacht der Nebel an. Am 24.12. ging frühmorgens die Kaltfront des Sturmtiefs durch, so daß eine deutliche Sichtbesserung eintrat, der Wind auf Südwest bis West drehte und auf 4 bis 3 Bft abflaute.

Am 25.12. führte ein Zwischenhochkeil anfangs nochmals zu sonnigem und windschwachem Weihnachtswetter. Nachmittags setzte von Norden her ein "klassischer" Bewölkungsaufzug vor einem von Nordwesten heranziehenden kräftigen Sturmtief ein. Der Wind verstärkte sich aber zunächst noch nicht wesentlich. Erst in der zweiten Nachthälfte nahm der Nordostwind auf Stärke 6 bis 7 zu. Obwohl das Tief nur etwa 200 bis 250 sm westlich der "*Polarstern*" nach Südsüdosten zog und wir im Bereich der stärksten Winde lagen, brachte der an sich sehr kräftige Wirbel am 26.12. nur 7 bis 8 Bft. Der Wind drehte dabei auf Nord. Ab Mittag bildete sich im Warmsektor wieder anhaltender Nebel aus. Nachts verstärkte sich dann der Wind auf Stärke 8 und drehte auf Nordwest. Am Vormittag des 27.12. nahm auf der Rückseite des Sturmtiefs der Wind weiter zu und Am Nachmittag nahm unter Zwischenhocheinfluß der Wind rasch ab, so daß abends nur noch 5 Bft aus Südwest gemessen wurden. Am 28.12. brachte der breite Zwischenhochkeil ruhiges Wetter mit einem Nordostwind der Stärke 4. Auch am 29.12. blieb der schwache Nordwind von 4 Bft tagsüber größtenteils noch erhalten. Erst nachmittags und abends nahm der Wind auf 6 Bft zu, da ein von Westnordwesten heranziehendes Tief zunehmend an Einfluß gewann. Den ganzen Tag herrschte zum Teil dichter Nebel.

Ein Tiefdruckwirbel zog am 30.12. relativ langsam nur etwa 150 sm westlich des Schiffes nach Südosten. Der Wind drehte dabei von Nordwest auf West und schwankte tagsüber um Stärke 7. Im Bereich eines nachfolgenden Troges frischte abends und nachts der Wind zeitweise auf 9 Bft auf. Auch am 31.12. hielt tagsüber der starke Wind mit 9 Bft noch an und kam dabei aus West bis Südwest. Erst gegen Abend flaute der Wind rasch ab.

In der Sylvesternacht zog ein weiterer Sturmwirbel südlich der "*Polarstern*" rasch ostwärts, so daß der Wind zeitweise Stärke 8 bis 9 erreichte.

Vom 02. bis 05.01. herrschte am Nordrand eines umfangreichen Zentraltiefs störungsfreies und ruhiges Wetter. Der Wind wehte aus westlichewn Richtungen mit Windstärken zwischen 2 und

5 Bft. Eine über einen Zeitraum von mehreren Tagen fast glatte See mit einer nur geringer Dünung dürfte in diesen Breiten nicht allzu oft auftreten.

In der Nacht zum 06.01. zog von Westen her ein Tief heran, so daß der Wind auf Stärke 6, vormittags auf Stärke 7 auffrischte und aus Richtung Nordost kam. Mittags und nachmittags zog das Tief fast genau über unsere Position hinweg, so daß der Wind auf 4 bis 5 Bft abnahm und auf West drehte. Auf der Rückseite nahm der Wind abends wieder auf Stärke 6, nachts auf Stärke 7 zu. Am Morgen des 07.01. flaute dann der Wind rasch auf 5 bis 4 Bft ab. Tagsüber brachte ein Zwischenhochkeil einige Stunden Sonne und ruhige See bei 1 bis 3 Bft. Nachmittags kündigte ein rascher Bewölkungsaufzug ein westlich von Bouvet Island ostwärts ziehendes kräftiges Sturmtief an, so daß für die Nacht und den Folgetag Windstärken bis 10 Bft aus Nord angenommen wurden. Deshalb drehte das Schiff vorzeitig nach Süden Richtung Neumayer Base ab. Diese Maßnahme erwies sich als richtig, da auf diese Weise das Tiefzentrum, das nur wenig südlich der Ausgangsposition ostwärts vorbeizog, durchquert wurde und der Wind schon nachts auf Stärke 5 zurückging. Tagsüber flaute südlich des Tiefzentrums der Wind sogar auf 3 Bft ab, während in unserem bisherigen Wirkungsbereich bei 50 Süd und 10 Ost dem Gradienten nach ganztägig mindestens Windstärke 10 aus West geherrscht haben muß. Eine mächtige Dünung zeugte davon, daß ringsum Sturm aufgetreten ist.

Am 09.01. wehte in einem gradientschwachen Gebiet nur ein schwacher Ost- bis Nordostwind der Stärke 3 bis 4. Die See hatte sich wieder beruhigt. Auch vom 10. bis 12. 01. hielt das windschwache Wetter an. Vor Neumayer Base traten zeitweise driftende Nebelfelder und Whiteout-Erscheinungen auf. Am 12.01. schneite es tagsüber leicht. Durch die schlechten Sichtbedingungen wurde der Einsatz des Hubschraubers stark beeinträchtigt bzw. überhaupt verhindert.

Am späten Vormittag des 13.01. begannen die Entladearbeiten an der Eisbarriere. Es herrschte schwacher Wind aus vorwiegend westlichen Richtungen der Stärke 2. Vormittags schneite es zeitweise, nachmittags traten noch einzelne Schneeschauer auf. Die Sichtbedingungen für den Hubschrauber waren dadurch zu schlecht, so daß er nicht fliegen konnte. Am 14.01. war es bis zum zeitigen Nachmittag sonnig und es herrschte sehr gute Sicht. Nachmittags zogen Wolken auf und es schneite zeitweise leicht. Der Wind kam vorwiegend aus Nordwest bis Nord und nahm gegen Tagesende von Stärke 2 auf Stärke 4 zu. Am Spätabend verließ die "*Polarstern*" die Eisbarriere vor Neumayer.

Am 15. und 16.01. herrschte im Bereich geringer Luftdruckgegensätze verhältnismäßig ruhiges Wetter. Der Wind kam vorwiegend aus westlichen Richtungen meist mit 3 bis 4 Bft. Am 17.01. nahm unter dem Einfluß eines weit nach Süden reichenden kräftigen Keils des Südatlantikhochs der Wind auf 5 bis 6 Bft zu und kam dabei aus Südwest bis West. Am 18.01. zog von Westen her ein kräftiges Sturmtief heran, so daß der Wind auf Stärke 8 bis 9, in der Nacht vorübergehend auf 10 zunahm. Der Wind drehte dabei von Nord nach West. Am 19.01. hielt der starke Wind zunächst noch an, nahm aber im Laufe des Nachmittags bis zum Abend auf 6 Bft ab. Nachts flaute der Wind weiter ab auf Stärke 5 bis 4.

Am 20.01. war der letzte Tag wissenschaftlicher Aktivitäten. Der Wind hatte erwartungsgemäß abgenommen auf 3 Bft, so daß morgens eine Tiefseeboje gefunden und geborgen werden konnte. Außerdem wurden noch einige Stationen durchgeführt. Dann ging es endgültig auf Kapstadtkurs.

Am 21.01. brachte ein umfangreiches und kräftiges Sturmtief zum Abschluß noch einmal eine Windstärke von 9 bis 10 Bft aus West. Danach nahm der Wind bis zum Einlaufen in Kapstadt allmählich ab.

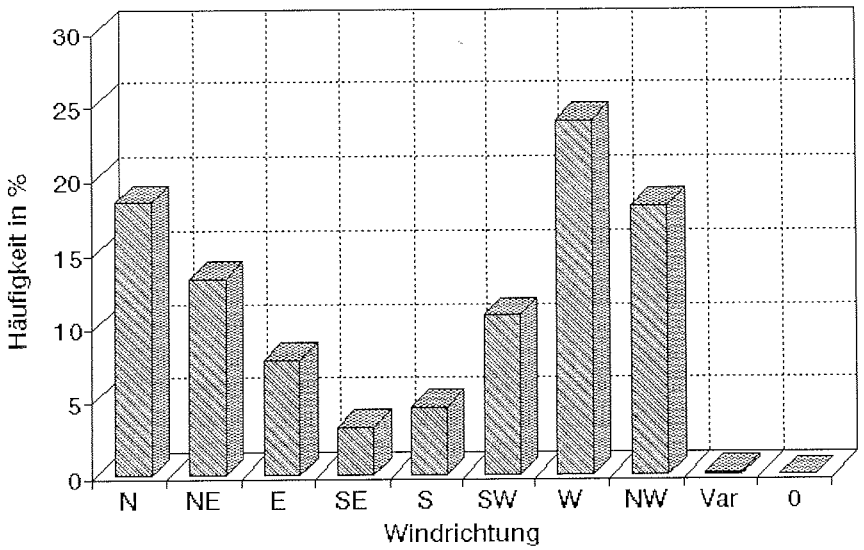

Fig. 1.1 Wind direction expressed in percentages during ANT XIII/2

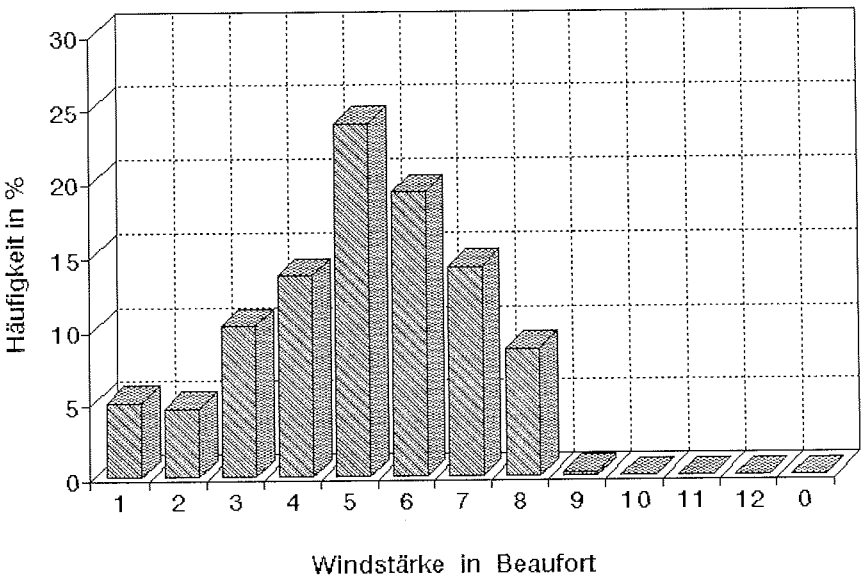

Fig. 1.2 Wind velocity expressed in percentages during ANT XIII/2

2. SEA ICE OBSERVATIONS AND ICEBERGS

N.W. van den Brink, J.A. van Franeker

Introduction

Sea ice is a striking phenomena of the Southern Ocean. In winter it extends to well over 20 million square kilometres in extent, which in summer is reduced to about 4 million square kilometres. Sea ice cover plays an important role in the Antarctic ecosystem. It influences the light regime in the water column, the stability and salinity of the underlying water and it acts as a substrate for ice-algae communities (Schalk et al. 1990). Hence sea ice has a strong impact on the primary production of the ecosystem in this area. The distribution of top-predators can also be related to sea ice distribution as it provides an important habitat and platform from which to extend foraging and breeding ranges (van Franeker 1991, 1992, van Franeker et al., in press). Furthermore, since sea ice reflects 80% of the incoming solar radiation, its extent and albedo characteristics play an important role in controlling the earth's heat balance. It is therefore of importance to assess sea ice distribution in order to unravel questions of structure and processes in the Antarctic ecosystem. Icebergs too are important. While melting, they provide a source of freshwater and (micro)-nutrients, and attract some species of penguins that use it as a resting place and as a further extension of their foraging ranges.

Methods

Sea ice observations followed the methods of Ackley et al. (1992) (SO-JGOFS protocol) and were similar to the methods used to make sea ice observations during an earlier cruise (ANT X/6) in 1992. At regular intervals observations were made on the percentage cover of ice, on the different types of ice and on some characteristics of the ice such as thickness, floe size, snow cover, the occurrence of ice-algae and the degree of ridging. Nomenclature of ice types follows the WMO standards (World Meteorological Organisation 1985). Weather and visibility permitting, observations were made and the situation was integrated over a range around the ship extending to several km. Data collected according to the SO-JGOFS protocol are summarised in a data-base (ANT XIII/2.ICE (ASCII format)) compiled at the Computer Department of AWI. Ice cover has been categorised into three types: snow-covered ice (first year or older), new ice (grease, nilas, grey ice etc.) or brash ice (fragments of rotting ice). Such ice types play different roles as a habitat for top predators or algae and also influence light conditions in the water column in different ways. In addition to this the size (average, minimum and maximum) of the floes, water temperature and salinity are given. This information and the ice type is of relevance to its melting or freezing status.
Additional to sea ice observations based on the SO-JGOFS protocol, records of sea ice were also made in association with ten minute observations of marine top predators (van Franeker and van den Brink, 1996). At the end of each ten minute observation period, average ice cover, average maximum and minimum floe size and maximum and minimum ice cover were recorded. These 10 minute based ice observations will be included in the ANT XIII/2 surface-database, and therefore are available for cruise participants.

Results

The results presented here are preliminary and based on the JGOFS protocol observations. Figures 2.1 to 2.3 show the ice cover and the mean floe size of the sea ice during transects 4,5 and 10 respectively. Figures 2.4 to 2.6 show the number of icebergs detected within 12 Nautical Miles of the ship and surface salinity along the three transects. No further details are given on transect 11, because except at the very beginning of this transect at approximately 70° South, no further sea ice was encountered on this transect. With regards to the small-scale grid, no ice or icebergs were recorded during this part of the cruise.

SEA ICE

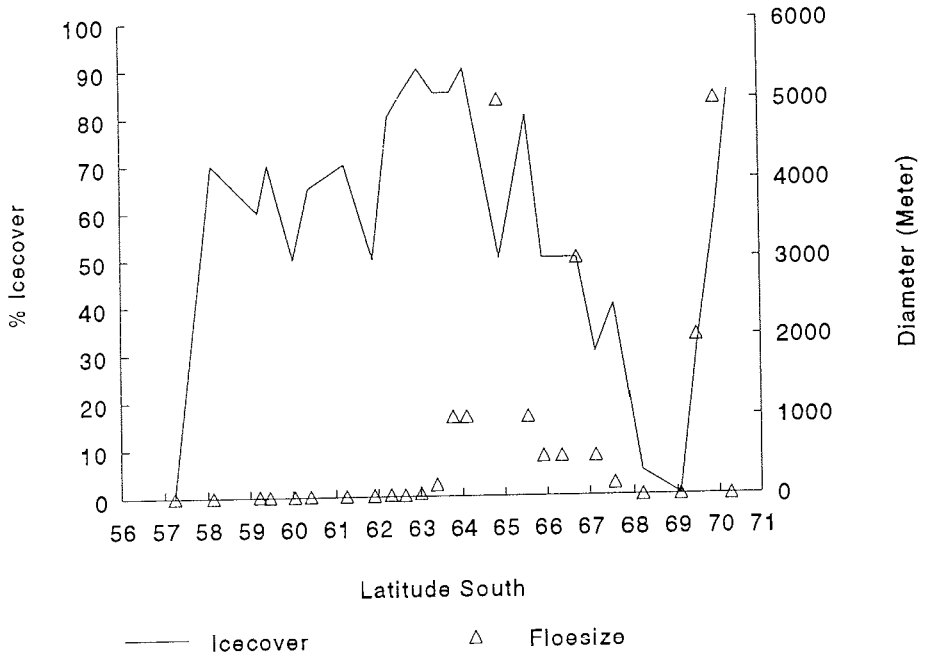

Fig. 2.1 Ice cover (%) and floe diameter (m), transect 4, voyage south ANT-XIII/2 (SO-JGOFS '95)

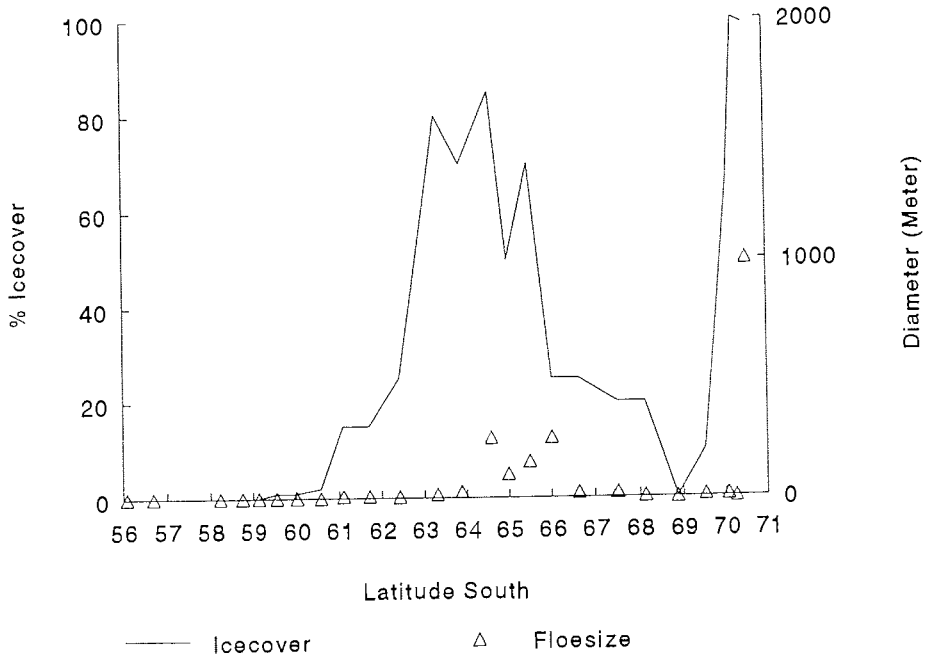

Fig. 2.2 Ice cover (%) and floe diameter (m), transect 5, voyage north ANT-XIII/2 (SO-JGOFS '95)

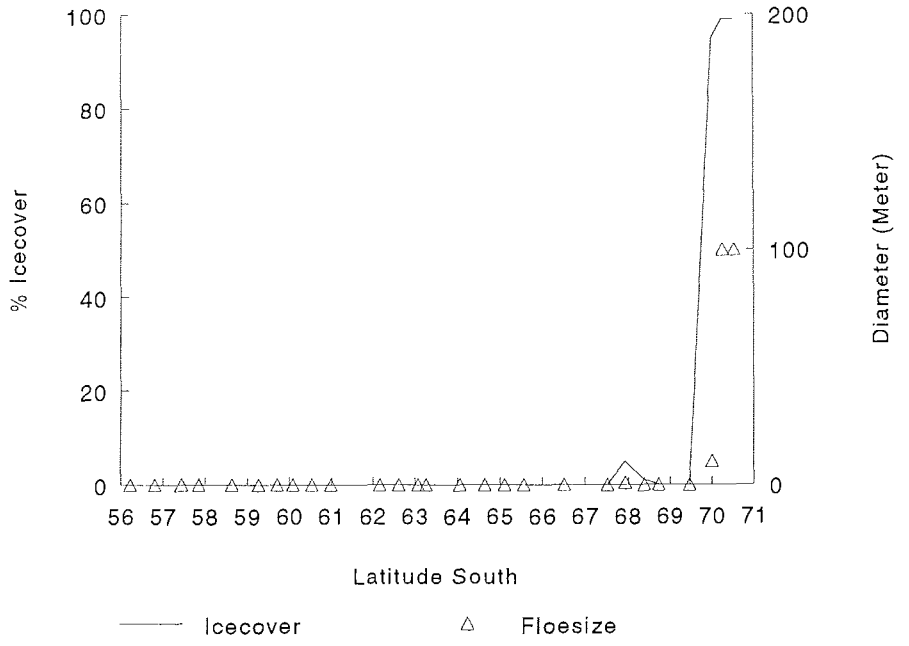

Fig. 2.3 Ice cover (%) and floe diameter (m), transect 10, voyage south ANT-XIII/2 (SO-JGOFS '95)

At 12 December 1995 the ice edge was located at approximately -58.12° South (Fig 2.1). North of this point no ice was recorded. From 58°S to 62°S the sea ice cover ranges from 50 to 70 %. Floes were small and in general the sea ice was rotting. However this did not result in a decrease in salinity (Fig. 2.4). Further south the ice cover increased, which coincided with an increase in floe size. It is likely that some melting of the sea ice occurred in this areas revealed by a salinity decrease in this area. South of 66° S the average ice cover decreased, and between 68°S and 69°S (almost) open water was encountered. Further south the ice cover increased to 90% close to the continent. Returning from South to North on Transect 5 with a 4 day delay, the situation had changed dramatically (Fig. 2.2). The polynya at 69° S still existed. Slightly North of this polynya the ice cover decreased in a time span of 6 days from 50 % to 25 % on average. Floes were also smaller on transect 5. This melting process coincided with a small decrease in salinity. However slightly more north of 66° S the salinity decreased rapidly, indicating melt. In this area the ice cover had not changed yet in percentage, but the large floes occurring at transect 4 were fragmented into much smaller ones (note the scale difference between floe size in figures 2.1 and 2.2). In this area the ice was melting rapidly. Between 63° S and 62°S the ice cover decreased 80 % to 20 %, reducing to less then 10 % further north. In the area between 62° S and 57° S the ice (coverage of 60 % on average) had disappeared in a period of 8 to 9 days. However this did not result in any decrease in salinity.

On transect 10, about two weeks later, we only detected some sea ice at 68° S and more heavy densities while approaching the continent. This transect was just east of transect 4 and 5. This area consisted of a funnel shaped region which showed low ice cover on satellite maps throughout the period of the entire cruise. Hence the differences between ice cover of transect 4 and 5 or of transect 10 are partly seasonal changes but probably reflect also regional differences. It seems that in this funnel shaped region, water from lower latitudes is being transported South between the eastern boundary of the Weddell Sea Gyre and the Antarctic Coastal Current. The temperatures at 64° S on transect 4 and 5 were respectively -1.7 and -1.4 °C, whereas the temperature at this latitude on transect 10 was 0.1°C. Additional to the ice cover, the colour imparted to the sea ice by ice algae was noted as brown ice. Brown ice occurred at all latitudes at which we found ice. The intensity seemed higher at the northern edge of the ice fields, which is in agreement with the situation in 1992. Highest densities of ice algae were mostly at the

interface between the ice and snow layer, or at the base of the ice floes. This is also in agreement with the situation found during the previous cruise in 1992.

ICEBERGS

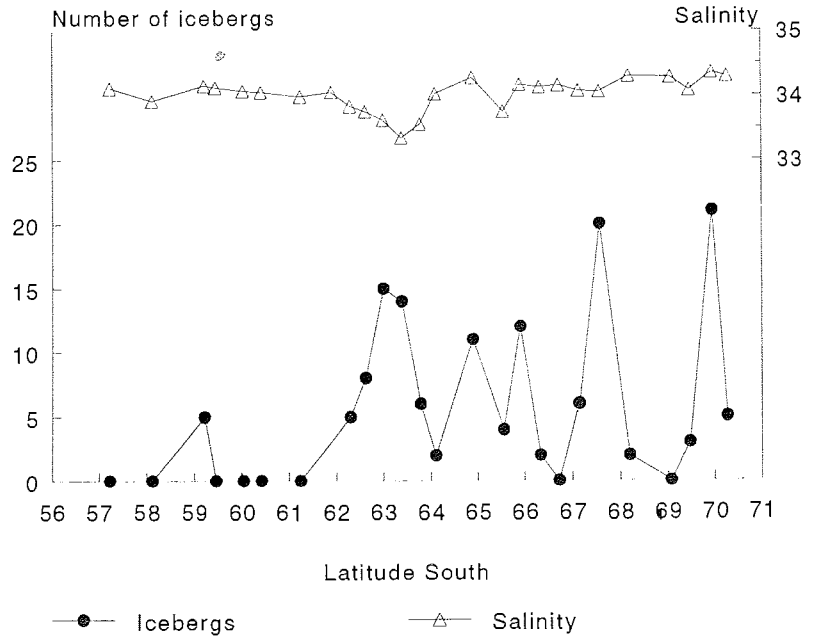

Fig. 2.4 Icebergs within 12 Nautical miles range and salinity, transect 4, voyage south ANT-XIII/2 (SO-JGOFS '95)

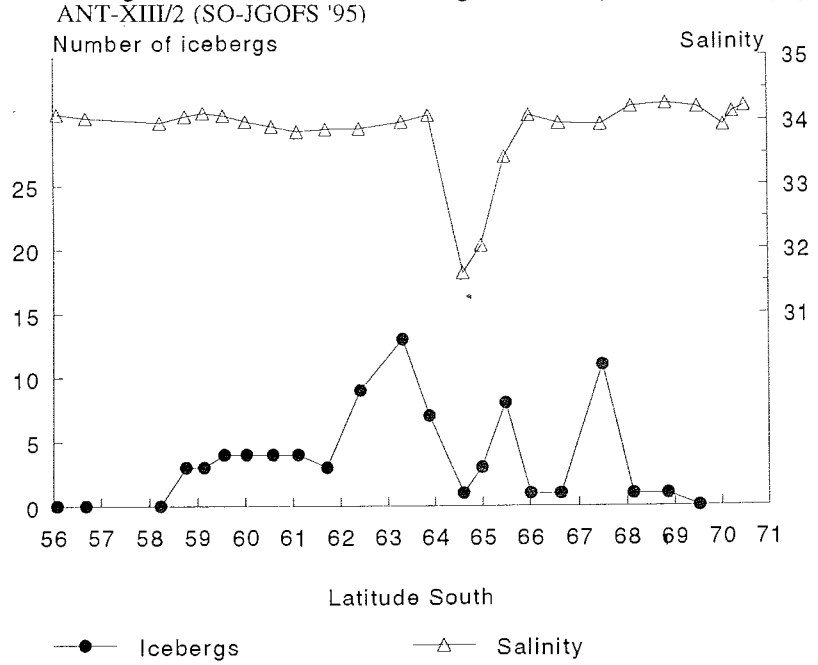

Fig. 2.5 Icebergs within 12 Nautical miles range and salinity, transect 5, voyage north ANT-XIII/2 (SO-JGOFS '95)

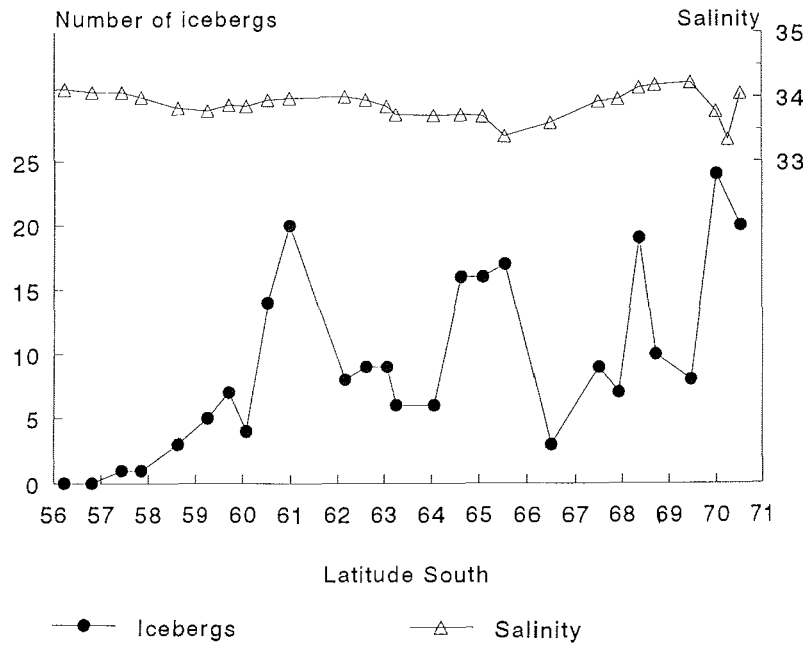

Fig. 2.6 Icebergs within 12 Nautical miles range and salinity, transect 10, voyage south ANT-XIII/2 (SO-JGOFS '95)

Figures 2.4 to 2.6 present the numbers of icebergs seen within a range of 12 Nautical Miles (Nm) from the ship along the different transects. On transect 4, most icebergs were located south of 62° S. On average we encountered 3 to 10 icebergs within the 12Nm range. Maximum numbers were up to 20 bergs within 12Nm. Compared to a previous cruise in October/ November 1992 (ANT-X/6), the numbers of icebergs reported here are much fewer. In 1992 up to 60 were counted within 12 Nm from the ship. In 1992 the icebergs accumulated at around 56° S and moved southward. In the present study a small peak in density was found at 63° S, but this was only 15 bergs within range. A possible explanation may be interannual variation in iceberg calving from continental glaciers and also that the 1992 study was 6° further west. Differences in current patterns can also result in differences in iceberg densities. On transect 5 the densities were slightly lower then on transect 4. However the small peak at 63° S was still there, although slightly lower (10 icebergs within range). On transect 10 the densities of icebergs were higher then on transects 4 or 5 with up to 25 icebergs within range. There was no peak at 63° S on transect 5. The relatively higher number of icebergs in this region contrasts with the proposed explanation for the low sea ice cover in this area, i.e.. that water was transported in from the north resulting in higher water temperatures and low sea ice cover. The exact mechanism is unclear but perhaps icebergs in this region originate from the Weddell Sea Gyre.

References

Ackley, S.F., Eicken H., van Franeker J.A. and Wadhams P. 1992 Protocol for ship and airborne observations on the structure, physical properties and coverage of sea ice in the framework of Southern Ocean (SO) JGOFS activities. AWI Bremerhaven.

Schalk, P.H., Brey, T., Bathamnn, U., Arntz, W., Gerdes, D., Dieckman, G., Ekau, W., Gradinger, R., Nöthig, E., Schnack-Schiel, S.B., Siegel, V., Smetacek, V and van Franeker, J.A. 1990. Towards a conceptual model for the Antarctic marine ecosystem. ICES C.M. 1990/L:30.

van Franeker, J.A. Sea Ice Cover and Icebergs. Cruise Report *Polarstern* ANT-X/6. Ber. zur Polarforschung.
van Franeker, J.A. 1991. Top predators as indicators for ecosystem events in the confluence zone and marginal ice zone of the Weddell and Scotia Seas. EPOS Symposium, 22 to 27 May 1991, Bremerhaven. Abstracts: 26.
van Franeker, J.A. 1992. Top predators as indicators for ecosystem events in the confluence zone and marginal ice zone of the Weddel and Scotia Seas, Antarctica, November 1988 to January 1989 (EPOS Leg 2). Polar Biol. 12:93-102.
van Franeker, J.A., Bathmann, U.V. and Mahlot, S. (in press). Carbon fluxes to Antarctic Top predators. Deep Sea Research.
World Meteorological Organisation. 1985. WMO sea ice nomenclature, terminology, codes and illustrated glossary. WMO/DMM/BMO No. 259-TP145. Secretariat of the WMO, Genf.

3. PHYSICAL CONTROL OF PRIMARY PRODUCTION AT FRONTS IN THE CIRCUMPOLAR CURRENT CLOSE TO THE GREENWICH MERIDIAN

V. Strass, R. Pollard, H. Leach

Introduction

Physical processes relevant to marine primary production play a central role in the climate system as a feedback mechanism between possible climate changes which may result from alterations of the CO_2 concentration in the atmosphere and the drawdown of carbon into the deep ocean and sediments by way of the biological pump. The primary goal of the measurements conducted during ANT-XIII/2 was to reveal those physical processes which could explain the existence of the 'Antarctic Paradox', the low mean level of primary production within a nutrient rich environment.

The relevant physical processes are best revealed by comparison of physical measurements made in the productive and the less productive regions within the circumpolar current. Previously existing data suggest that fronts are regions of enhanced production; one example is the Polar Front and its associated benthic opal belt, indicating sedimentation of silica rich biogenic material which is increased in the climatological mean. The view of the Polar Front as a region of enhanced primary production is supported by our new measurements.

The physics of fronts can influence primary production by horizontal advection, or by frontal dynamics which forces vertical motion and the associated variation of stratification during frontal formation and decay. Vertical motion can resupply the euphotic zone with nutrients (macro and micro nutrients, e.g. iron) in one place and transport phytoplankton down into the euphotic layer and force sedimentation in another place while the variation in stratification influences the depth of the mixed layer within which the densest blooms favourably occur. The relevant horizontal scales, however, may be quite small (a few tens of kilometres) and the time scales quite short (some days), posing considerable demands on the measuring system being used.

The fundamental physical measurements during this cruise resolved these scales with the use of an instrument package (SeaSoar + VM_ADCP) which allowed the density and velocity structures of a front to be measured simultaneously with other physical and biological variables down to 400 m depth at high horizontal resolution in quasi-synoptic manner. The SeaSoar undulates vertically through the water column while being towed behind the ship moving at almost cruising speed. (Tab. 1) The vessel mounted ADCP (Acoustic Doppler Current Profiler) measures the horizontal current profile in the depth range of the top few hundred meters. In addition to its main purpose, the VM_ADCP can be used to detect zooplankton abundance by evaluating the backscatter amplitude. The SeaSoar + VM_ADCP measurements were complemented by a number of deep CTD (Conductivity Temperature Depth) stations to reveal the deeper hydrographic structure and to allow the collection of water samples from depth by use of the attached rosette sampler. Information on the temporal variability of the velocity profile and sedimentation at one position in the survey area was obtained from moored instruments.

The initial measurement strategy was to perform two long SeaSoar transects extending between the South African shelf break and the ice edge off Antarctica (one transect at the beginning of the cruise and the second repeated along the same line at the end) to reveal the temporal changes of the upper ocean physical conditions and the associated changes in primary production on a large scale. The second purpose of the first long section was to reveal the productive frontal structure on which to centre the 3-dimensional SeaSoar mapping grids. The temporal development of the mesoscale front and eddy structure was planned to be studied by repeating the frontal mapping in exactly the same region with a delay of one to two weeks. Within the time interval, a coarse resolution SeaSoar survey of the upstream area was planned to asses the influence of advection into the main survey area. However, the repetition of the fine-scale survey as well as the second long SeaSoar transect had to be cancelled due to time constraints resulting from the adverse ice conditions off Neumayer which forced us to visit the station a second time for re-supply purposes.

4. UNDERWAY MEASUREMENTS OF HYDROGRAPHIC AND BIOLOGICAL VARIABLES USING THE TOWED UNDULATOR "SEASOAR"

R.T. Pollard, J.F. Read, J.T. Allen, M.J. Griffiths, A.C. Naveira, P. Gwilliam

Introduction

The SeaSoar system comprises a NBIS CTD, a Chelsea Instruments fluorometer and a Focal Technologies optical plankton counter (OPC) within a CI SeaSoar vehicle. This winged vehicle is towed behind the ship at 8 - 9 knots on 750m of faired cable, and profiles between the surface and 300-500m every few km. With this combination, SeaSoar was able to serve as the primary survey tool, not only for the physics of the upper ocean (CTD, PAR), but also for phytoplankton (fluorometer) and zooplankton (OPC) in the size range 250μm to 3 mm. In the 7 week cruise, SeaSoar was towed for a total of 15.2 days, covering 6155 km. SeaSoar provides detailed temperature, salinity and density information. The one major physical variable that it does not measure is velocity. This was provided by the ship's Acoustic Doppler Current Profiler (ADCP), data from which were logged together with navigation and meteorological data from the ship's POLDAT system.

The SeaSoar tows were split into 3 main surveys (Tab. 4.1):
- a long section from 41.8°S to 57.3°S (Runs 2 and 3) to locate the positions of the major fronts and measure their biological productivity;
- a Course Scale Survey (CSS, Run 6) in the vicinity of the Polar Front to locate large scale (50-100 km) meanders and eddies;
- and a Fine Scale Survey (FSS, Run 8) to resolve the scales of physical and biological patchiness, primarily in tongues a mere 15 km across and 60 - 100 km long.

A very considerable amount of data was collected during these surveys, over 1.3 million data cycles of CTD and fluorometer data after averaging to one per second and over 30 million particles counted by the OPC. The data were processed on 3 Sun workstations and displayed mainly in the form of colour contour sections and maps. The most difficult and time-consuming task during data collection was to obtain well-calibrated salinities. The CTD is specially fitted with dual conductivity cells, which are both subject to biological fouling because of the high productivity of the survey area. Every 4 hours, plots were produced and the salinities derived from the two cells intercompared. Most often, the two cells do not foul simultaneously, so that it is possible, though laborious, to correct each offset. Absolute calibration was achieved by comparing near-surface salinities with those from a thermosalinograph in the ship's bow-propeller shaft, itself calibrated by water samples drawn from the bow-prop intake every half-hour and analysed on a salinometer. Final absolute accuracies are 0.01 in salinity, and less than 2mK in temperature. To summarise the data, five separate data reports have been produced for the various instruments. Here, only a few representative plots can be shown for each survey.

Table of SeaSoar deployments on AntXIII/2

Run		time (Z)	day/date	latitude	longitude	distance run (km)
001	start	1347	339/5xii95	39°05.9'S	14°43.9'E	679
	end	1834	339/5xii95	39°38.8'S	14°15.0'E	753
	duration	4h47m	mean speed 8.3 kt			74 km
Reason for recovery						End of trial
002	start	0931	340/6xii95	41°46.7'S	12°46.4'E	1036
	end	0300	343/9xii95	50°13.5'S	5°46.0'E	2127
	duration	2d17h29m	mean speed 8.9 kt			1091 km
Reason for recovery						End of run - mooring position reached
003	start	1427	343/9xii95	50°21.3'S	5°31.3'E	2195
	end	2117	345/11xii95	57°19.5'S	2°06.3'W	3185
	duration	2d6h50m	mean speed 9.7 kt			990 km
Reason for recovery						End of run - ice reached
6.1-3	start	1845	356/22xii95	54°00.6'S	0°05.8'W	6954
	end	1848	359/25xii95	50°28.2'S	8°05.3'E	8235
	duration	3d0h3m	mean speed 9.7 kt			1281 km
Reason for recovery						End of run - station position
6.4-5	start	2240	359/25xii95	50°29.1'S	8°07.8'E	8248
	end	0930	361/27xii95	49°54.9'S	10°15.3'E	8844
	duration	1d10h50m	mean speed 9.2 kt			596 km
Reason for recovery						Cable problem - need to reterminate
6.6-7	start	1715	361/27xii95	49°28.2'S	10°31.4'E	8903
	end	0845	363/29xii95	49°27.8'S	11°24.6'E	9555
	duration	1d15h34m	mean speed 8.8 kt			652 km
Reason for recovery						End of survey
8.1	start	0900	001/1i96	49°41.5'S	11°19.8'E	10292
	end	1430	001/1i96	50°25.0'S	11°23.1'E	10376
	duration	5h30m	mean speed 8.2 kt			84 km
Reason for recovery						Vehicle not flying - kelp holdfast around wing
8.1-11	start	1500	001/1i96	50°27.8'S	11°23.3'E	10381
	end	0627	005/5i96	50°48.6'S	9°30.0'E	11768
	duration	3d15h27m	mean speed 8.5 kt			1387 km
Reason for recovery						End of survey
Totals						
	duration	15d4h30m	mean speed 9.0 kt			6155 km

Table 4.1 SeaSoar deployments on ANT XIII/2

Preliminary Results

Long SeaSoar transects

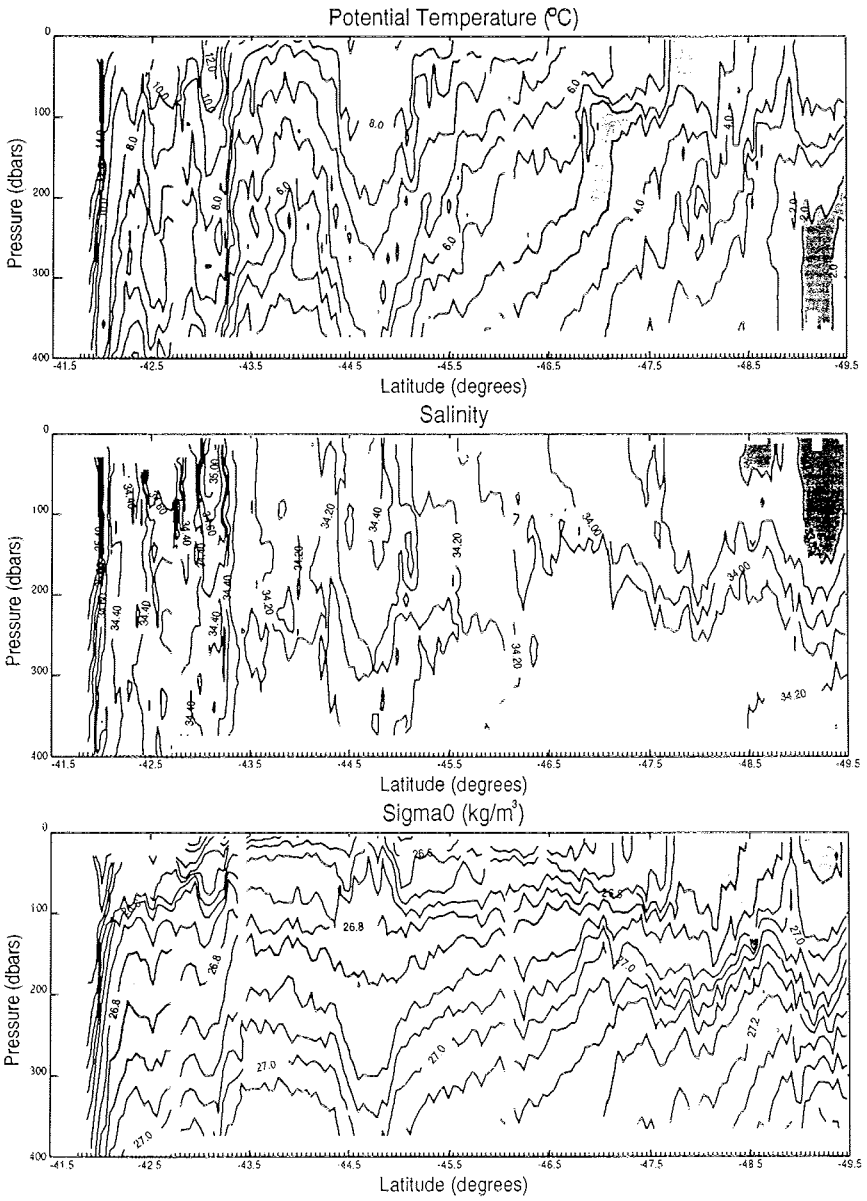

Fig. 4.1 Section 41.5-49.5°S
The Subtropical Front was crossed at 42°S shortly after SeaSoar was deployed. There is a striking anticyclonic eddy at 44.5-45°S. The outcrop to the surface of the 4°C isotherm at 48.5°S marks the Subantarctic Front, south of which there is a surface salinity minimum (shaded) of less that 33.85 ppu. The northern limit of the Polar Front can just be seen at 49.5°S in the downward plunge of the 2°C subsurface temperature minimum.

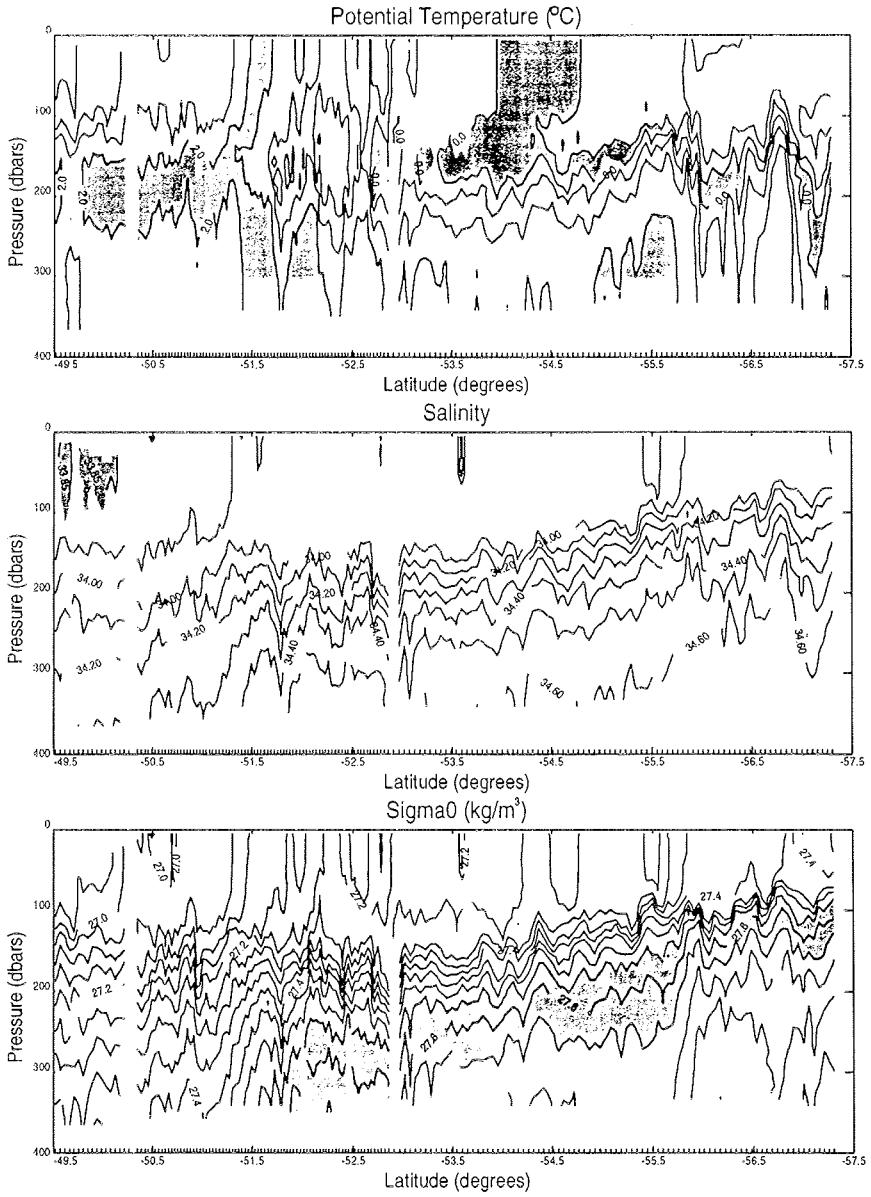

Fig. 4.2 Section 49.5-57.5°S
The Polar Front is unusually broad, as seen by the extended 2°C temperature minimum between 49.5°S and 51.5°S. The upslope to the south of isopycnals at 51-51.5°S indicates the main frontal jet. Note the mixed layer depths of up to 100m, caused by strong winds during the section which was itself early in austral spring.

Course Scale Survey (CSS)

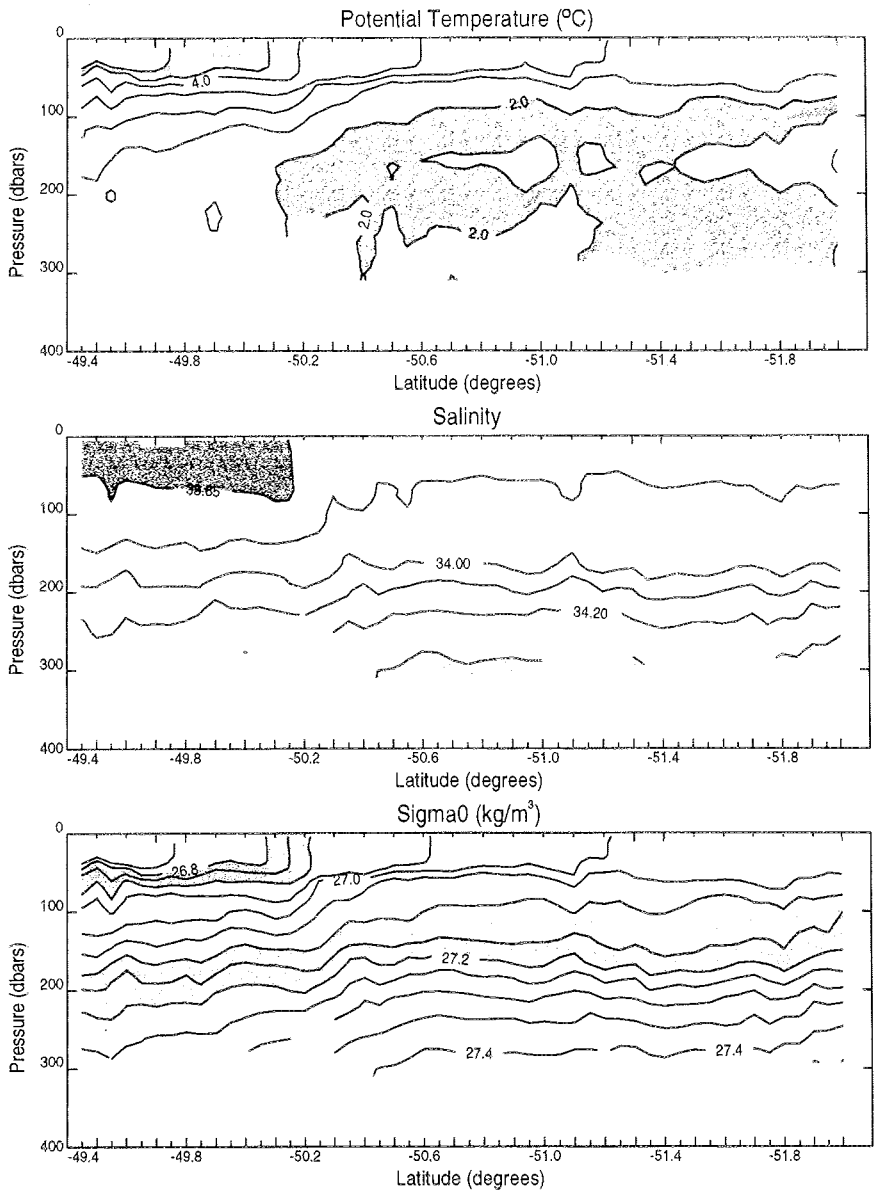

Fig. 4.3 Section of T, S, s_0, Run 6.6
Run 6.6 was the penultimate leg of the Course Scale Survey, and was chosen as the central transect for the Fine Scale Survey and CTD line. There are several indicators of the Polar Front at 50.2-50.5°S: the northern limit of the 2°C subsurface temperature minimum; the southern limit of the surface salinity minimum; sloping isopycnals; and the change in separation of the 27.1 and 27.2 kg m^{-3} isopycnals (shaded)

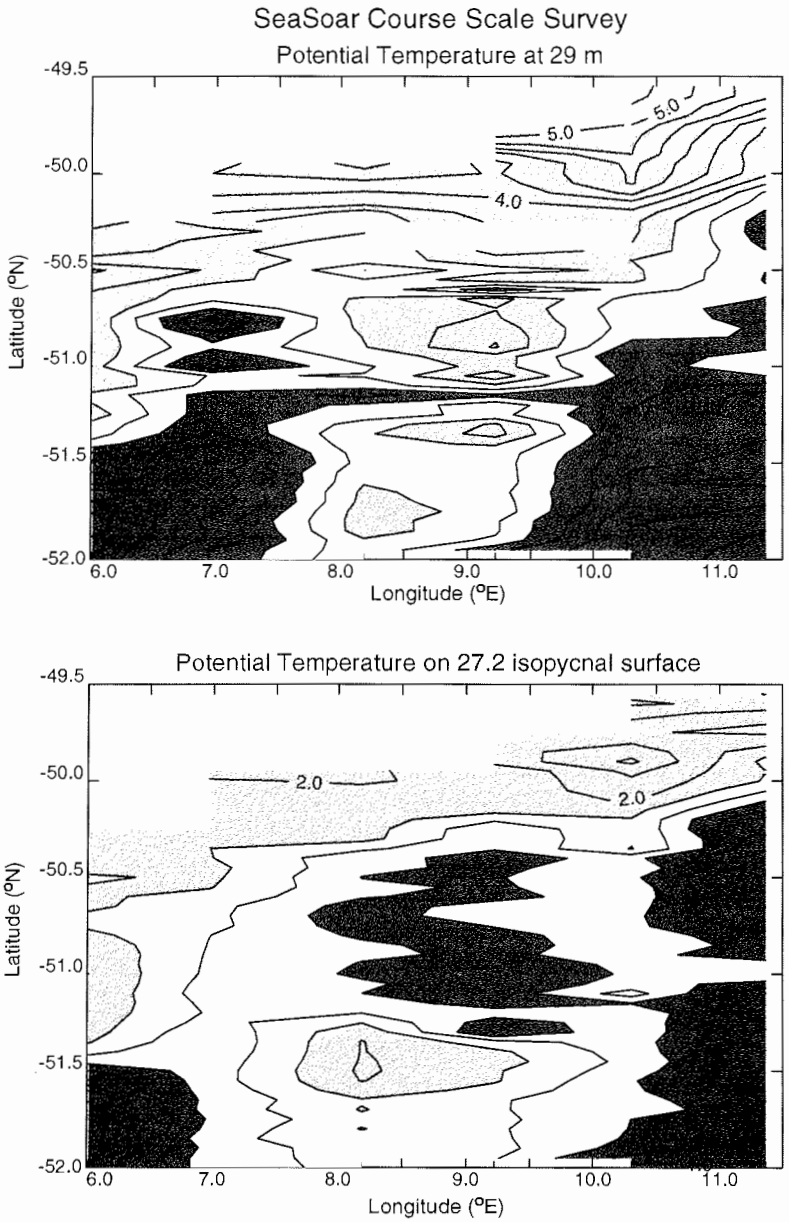

Fig. 4.4 Maps of temperature at 29m and 27.2 kg m^3

A depth of 29 m lies within the surface mixed layer, and the density surface 27.2 kg m^{-3} is well beneath the mixed layer lying between 150 m and 230 m (compare Fig. 4.3). The 1.8°C isotherm on 27.2 (boundary between white and light shading) is a simple indicator of the Polar Front. At 6°E, the western edge of the CSS, currents are strongest at 51.5°S (Fig. 4.4) where there is a strong north-south temperature gradient; likewise at 50°S, 11.5°E, the eastern edge. The southern current jet turns south out of the survey area at 7°E, bounding the dark shaded temperature areas, and re-enters the area at 10°E. There are several barely resolved eddies in the centre of the survey area. Note for example the cold core eddy on the 27.2 isopycnal around 51°S, 9°E, also shown by clockwise currents (Fig. 4.4). The pattern at 29 m is notably different, with warm water in that area, apparently drawn south in a meander, which is much better resolved by the FSS.

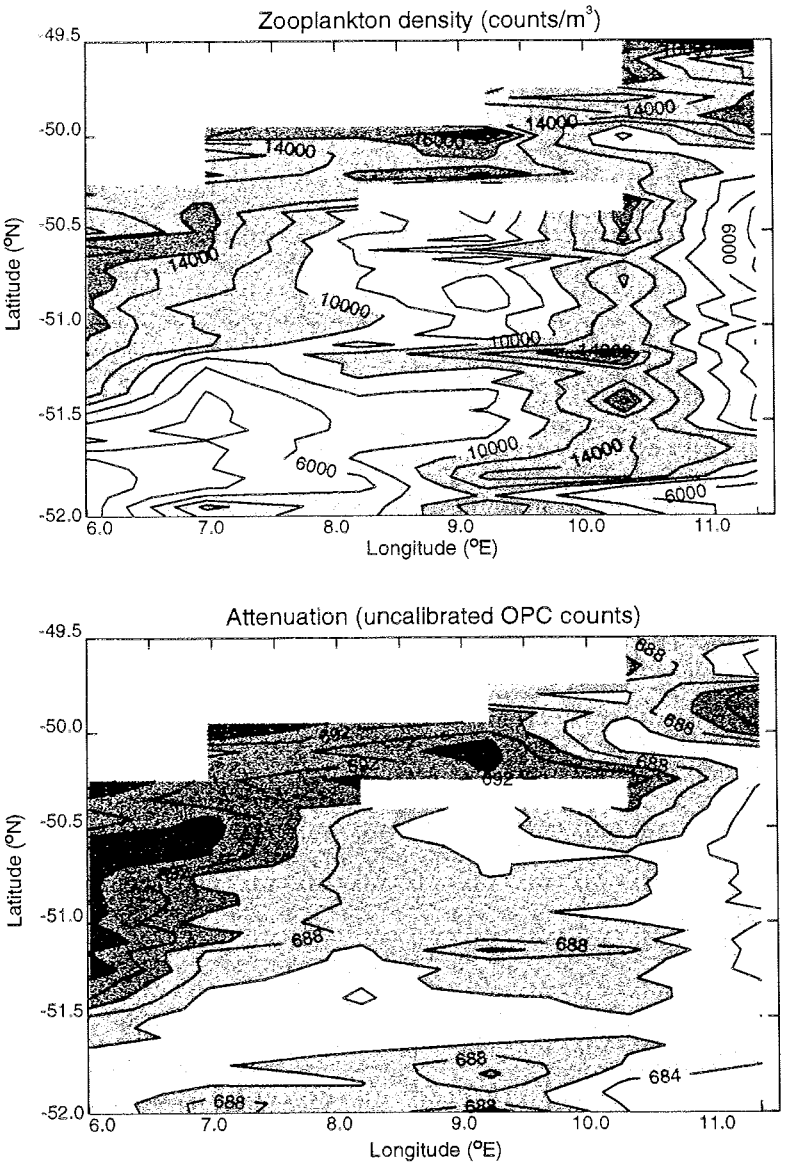

Fig. 4.5 Maps of OPC counts and attenuance
Zooplankton density at 29 m and light attenuance (a useful qualitative measure of phytoplankton) both show features broadly correlating with the physical structures (Fig. 4.5). Note in particular the higher values north of the Polar Front and the southward extending tongue along 10.5°E

Fine Scale Survey (FSS)

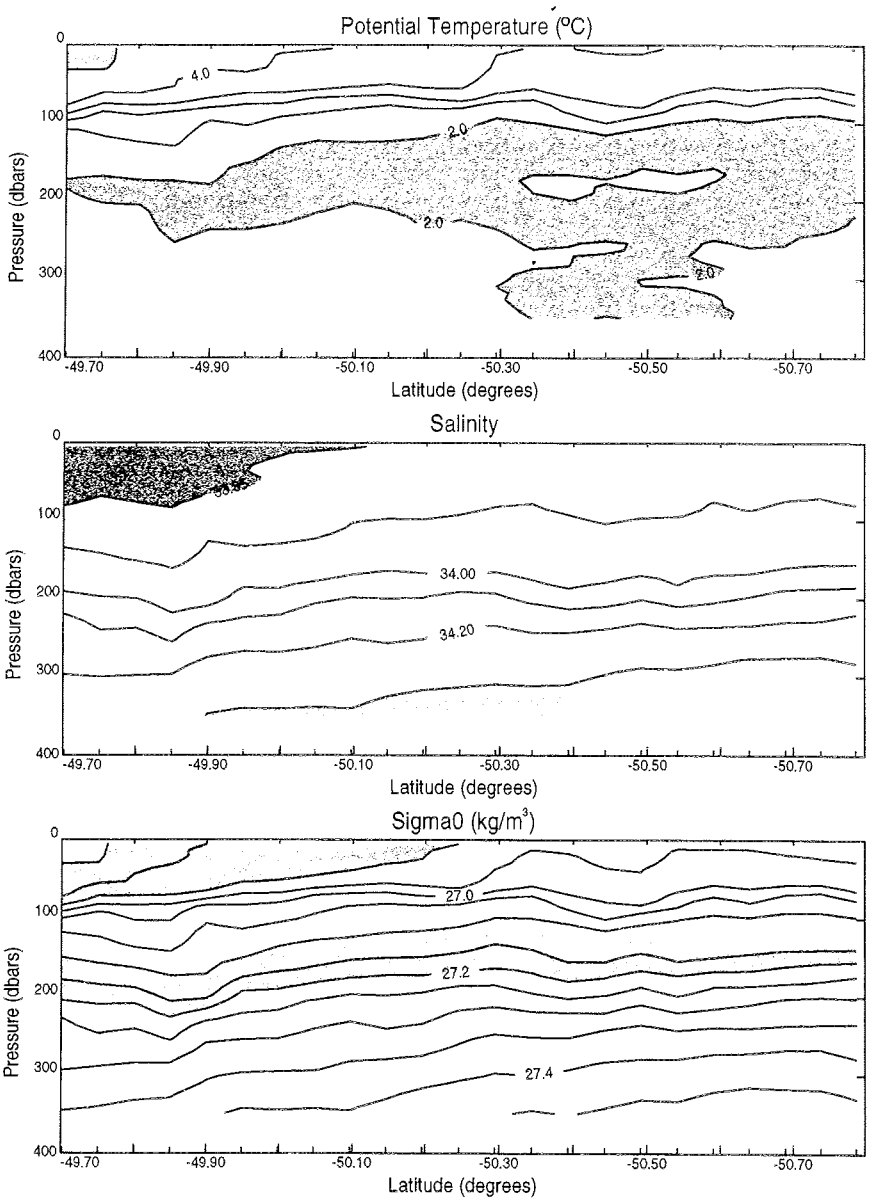

Fig. 4.6 Section of T, S, s_0, Run 8.7
Section 8.7 is the FSS repeat of leg 6.6 (Fig. 4.3). The two surveys were a week apart. Comparison shows that the surface outcrop of the front is more diffuse, with the 4°C isotherm, 33.85 isohaline and 26.9 kg m^{-3} isopycnal sloping over several tens of km from 100 m to the surface.

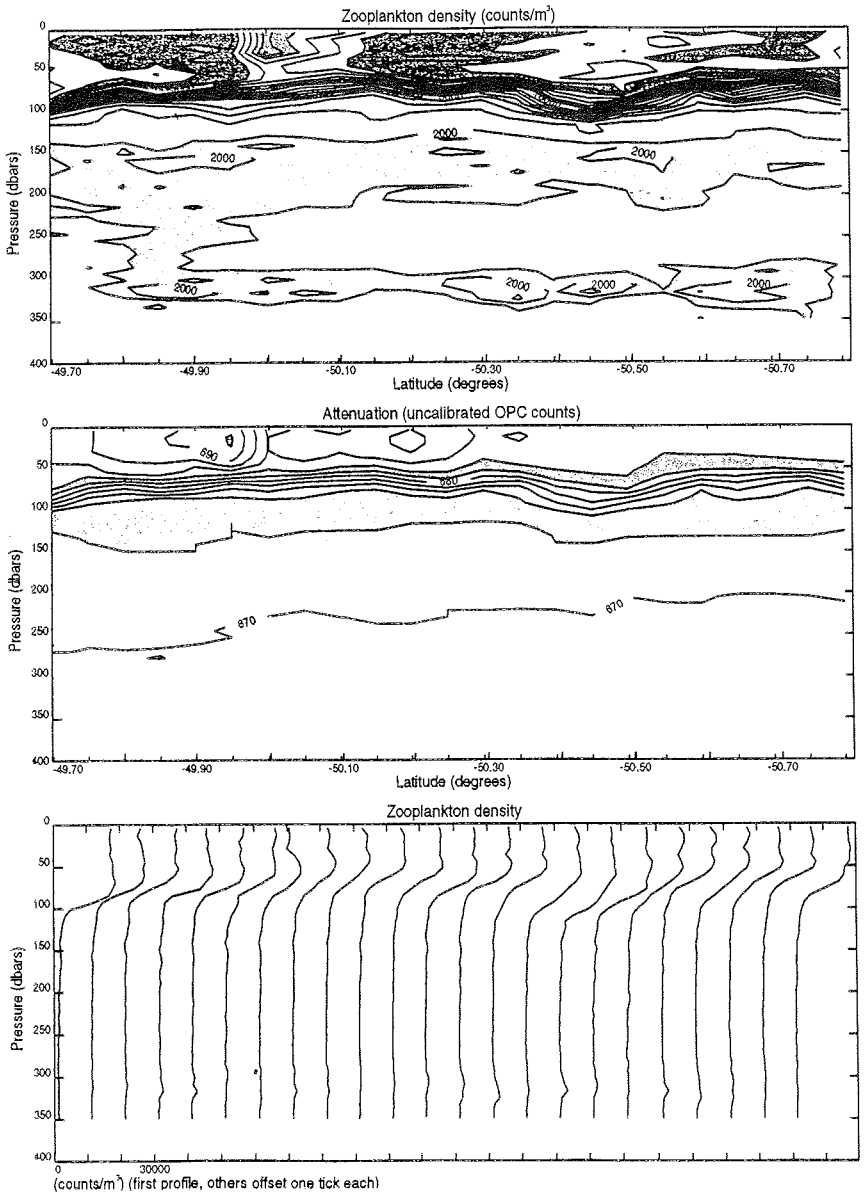

Fig. 4.7 Section of OPC counts and attenuance, Run 8.7
In contrast to Fig. 4.6, OPC sections for Run 8.7 show strong changes at 50.0°S, with low values across 15 km between 49.95°S and 50.1°S. This will be shown (Fig. 4.9) to be the northeastern tip of a tongue of lower values, probably drawn out from the cold core eddy mentioned in Fig. 4.5. The profiles of zooplankton density (10000 counts m^{-3} per tick, each profile offset by one tick) are fairly independent of depth from the surface to 50 m, but this was not generally the case. On this leg, for example, the size classes from 500-1000m had a subsurface maximum density of 7000, increasing from less than 5000 at the surface.

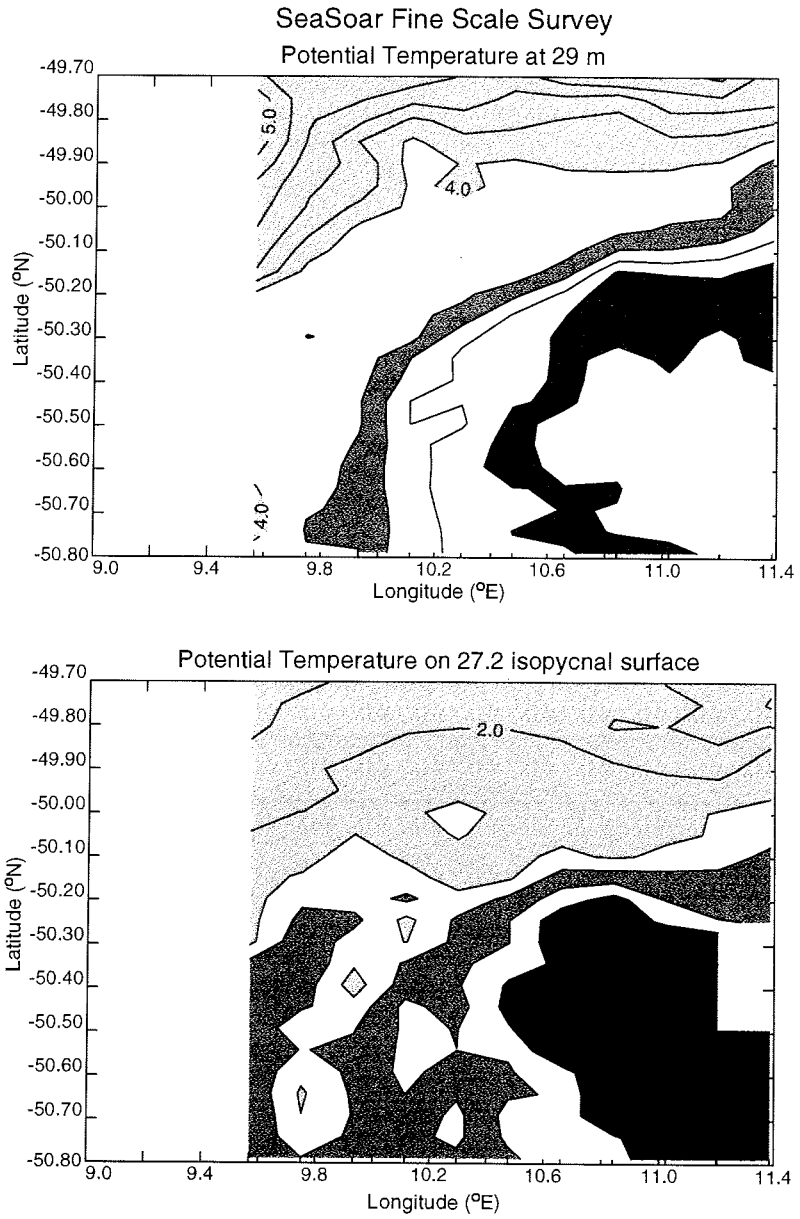

Fig. 4.8 Maps of temperature at 29m and 27.2 kg m^3
The 27.2 isopycnal map of temperature is particularly revealing, showing a dark-shaded tongue of cold water extending northeastwards into the survey area from the southwestern corner. This tongue reaches as far northeast as 50°S, 10.3°E on leg 8.7 (Fig. 4.6), seen in this map by the small white area of temperature colder than 1.8°C. East of the cold tongue is a warm tongue extending southward along 9.8°E. Neither of these tongues is revealed by the 29 m temperatures, but their importance to biological patchiness will be shown in Fig. 4.9.

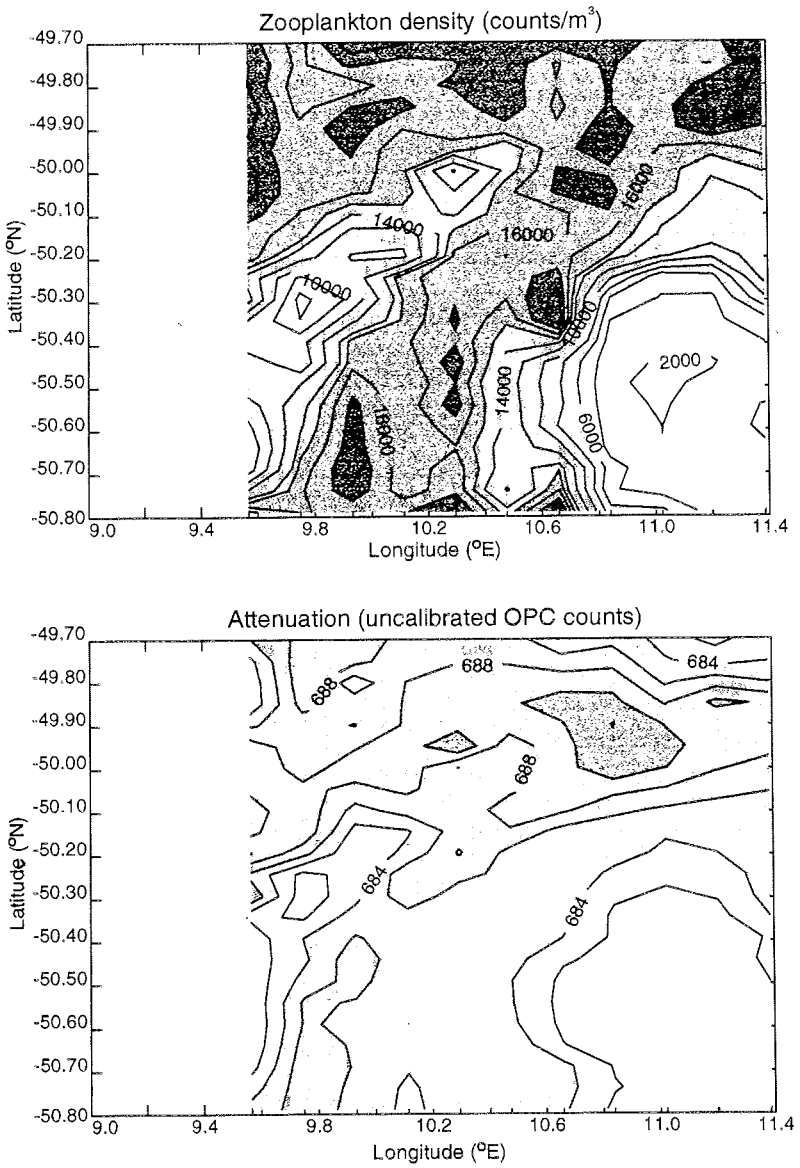

Fig. 4.9 Maps of OPC counts and attenuance
Streaks of high attenuance along 50°S and 9.8°E indicate where phytoplankton biomass was highest at 29 m. The southward extending high streak corresponds exactly to the warm tongue of Fig. 4.8. Particularly low values of both phytoplankton and zooplankton abundance are found in the cold water of southern origin in the southeast corner of the FSS. Values are also low in the cold tongue of Fig. 4.8. Note however that the southward extending band of high zooplankton density is broader and somewhat to the east of the streak of high attenuance.

5. UNDERWAY MEASUREMENTS OF CURRENTS AND ACOUSTIC BACKSCATTER BY USE OF THE VM_ADCP

V.H. Strass, H. Fischer, J.T. Allen

Vertical profiles of ocean currents and acoustic backscatter down to roughly 300 m depth were continuously measured (Figs. 5.1, 5.2 & 5.3) with a Vessel Mounted Acoustic Doppler Current Profiler (VM_ADCP; manufactured by RDI, 150 kHz nominal frequency), installed in the ship's hull behind an acoustically transparent plastic window for ice protection. The instrument settings were chosen to give a vertical resolution of 4 m, and a temporal resolution of 2 min after ensemble averaging. The VM_ADCP data collected cover almost the entire cruise, except for the last transect back to Cape Town when we unfortunately encountered irreparable electronic problems with the ADCP deck unit.

Calibration data for the ADCP velocity measurements were obtained prior to the cruise during the ship's passage through the shallow waters of the North Sea and English Channel on leg ANT-XIII/1 with the ADCP operating in bottom track mode. The pre-cruise collection of calibration data was made possible with the help of the ship's electronic engineers, which is thankfully acknowledged.

Calibration data for the backscatter signal were taken during the cruise. This calibration, however, only accounts for physical influences such as electronic noise levels of the individual transducer heads and losses of sound energy with distance from the transducer due to beam spreading, absorption, and scattering. To relate the backscatter signal to zooplankton abundance, it has to be calibrated with net catches, as were obtained regularly with the Multinet and occasionally with the Rectangular Midwater Trawl (see contribution of U. Bathmann and C. Dubischar). Given the 150 kHz acoustic frequency, the most effective scatterers are expected to be found in the 1 cm size class. Species dependent differences in backscatter strength (due to the relative contribution by soft tissue, hard shells and gaseous inclusions) will, however, account for large variations of the obtained signal.

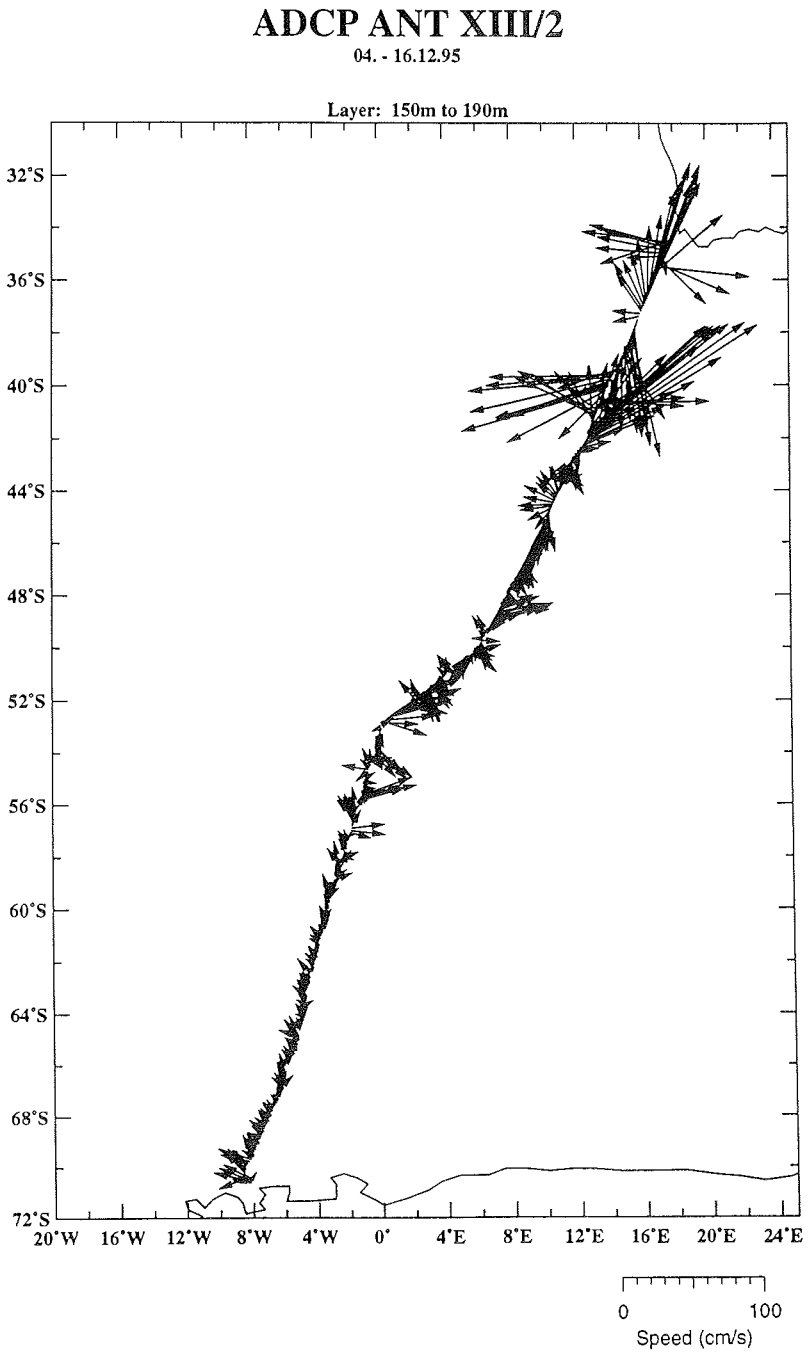

Fig. 5.1 Horizontal currents in the depth range 190 to 230 m
These were obtained with the Vessel Mounted Acoustic Doppler Current Profiler (VM_ADCP; RDI 150 kHz) during the first transect from Cape Town to Neumayer Station, Antarctica. The large currents north of 42°S are related to the Agulhas Retroflection. The various bands of enhanced eastward velocities between 48 and 58°S reveal the Circumpolar Current as being composed of a series of distinct fronts: the Subantarctic Front at 48.5°S, the Polar Front between 50 and 52°S, and the Weddell Front around 55°S.

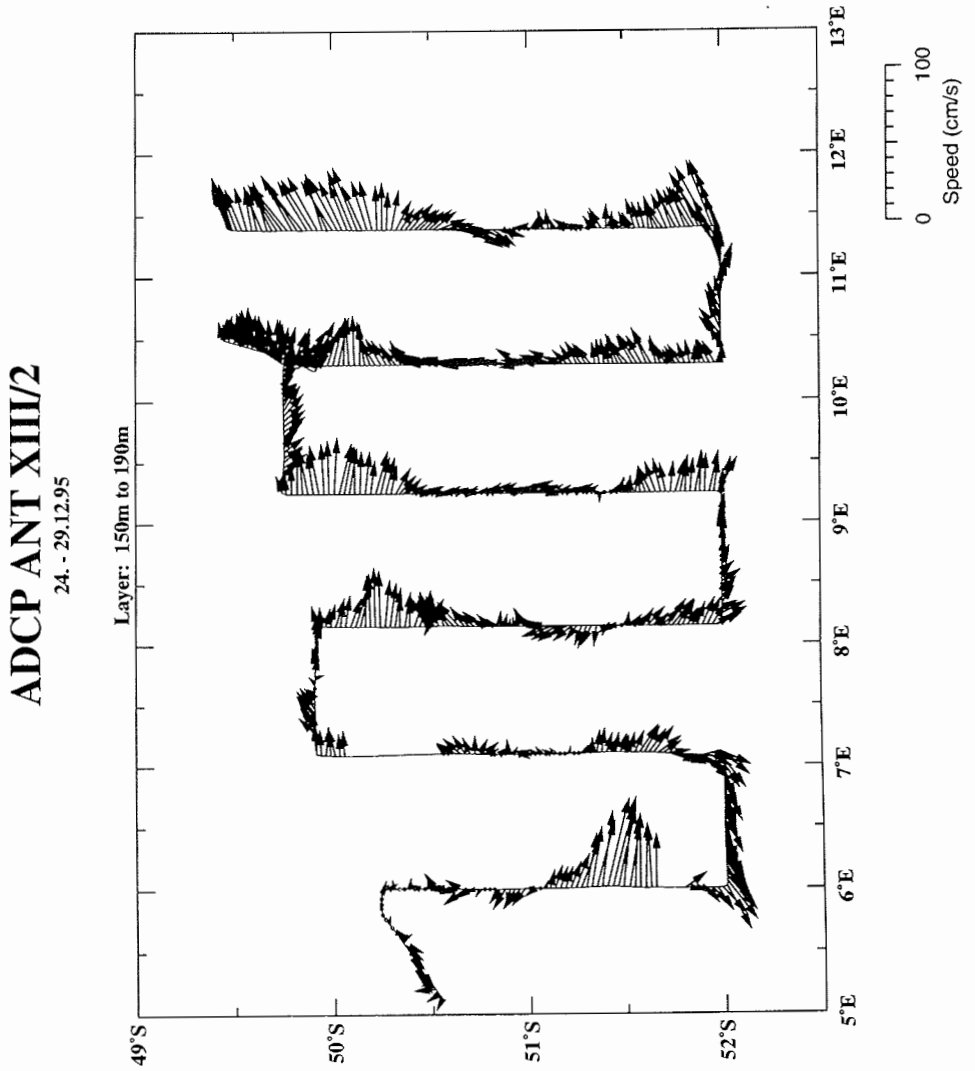

Fig. 5.2 Current vectors in the depth range 150-190m
ADCP current vectors across the CSS show the two branches of the Polar Front, the southern between 51.5°S and 52°S, the northern north of 50.5°S. In between, the alternating northward and southward currents indicate barely resolved eddies as well as temporal changes.

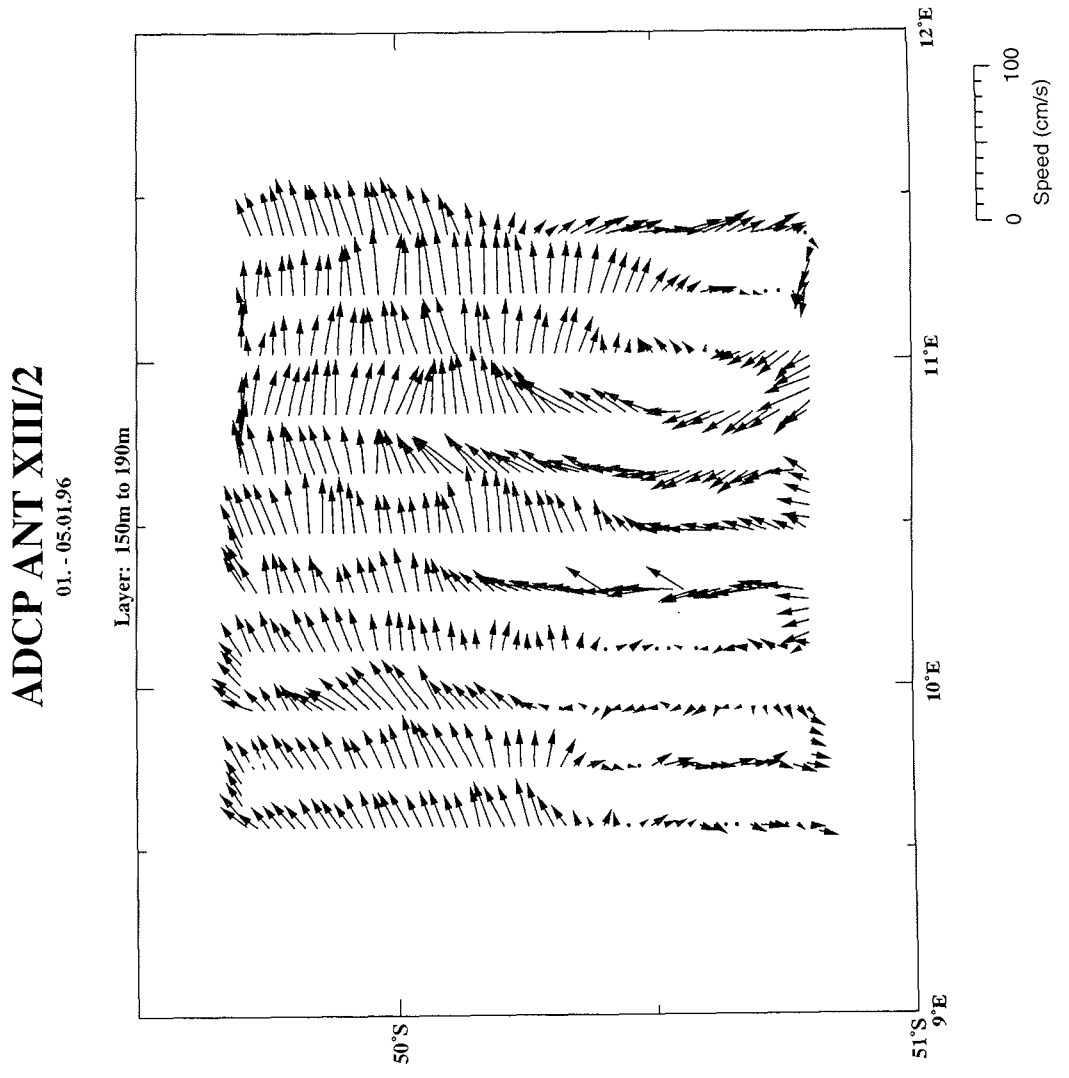

Fig. 5.3 Current vectors in the depth range 150-190m
The flow across the FSS is mostly eastwards, but northward flow converges into the front in the southern half of the survey between 10.5°E and 11.0°E. Flow around a cyclonic eddy in the southwest corner of the FSS is also just resolved.

6. CTD STATIONS AND WATER BOTTLE SAMPLING

V.H. Strass, R. Timmermann, H. Fischer, M. Hofmann, P. Gwilliam, A. Wischmeyer

Complementary to the fine resolution SeaSoar survey of the near-surface layers, the deep physical structure of the Polar Front was investigated with an array of hydrographic stations where a CTD (Conductivity-Temperature-Depth sonde) was deployed to the sea floor (Fig. 6.1). Other CTD casts to intermediate depths were conducted at the endpoints of the various SeaSoar runs for calibration checks of the SeaSoar sensors and to collect water samples for biological and chemical analysis with the attached Rosette sampler. Altogether, 58 CTD casts were performed at 30 stations.

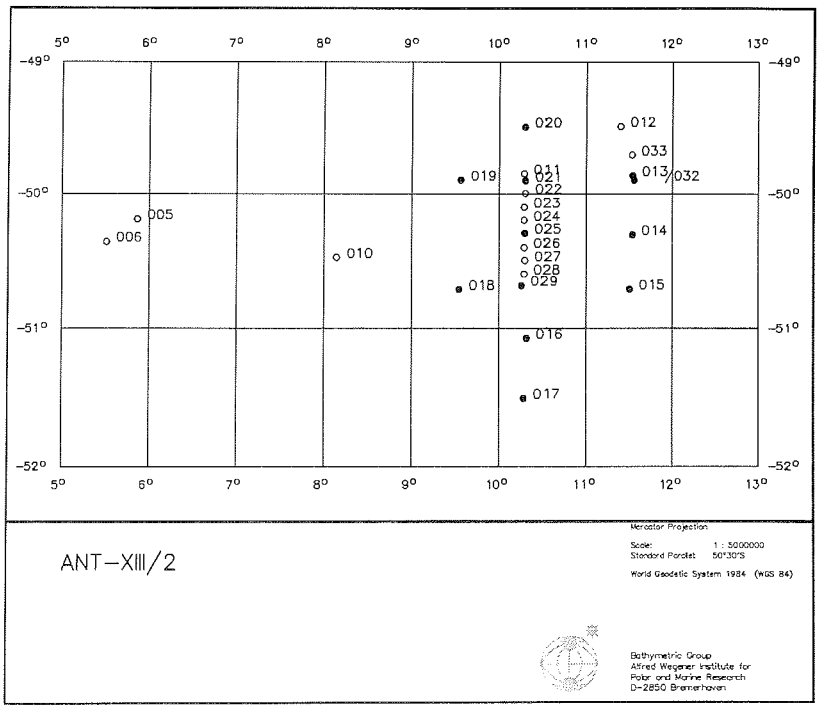

Fig. 6.1 Map showing the positions of CTD stations performed in the Polar Front area. Solid dots denote stations at which the CTD was lowered down to the sea floor, open circles those stations with only shallow CTD casts to a maximum depth of 500 m. Stations 013 and 032 were performed at the location of the mooring AWI-235, the first on the day of deployment (29. Dec. 1995) and the latter on the day of recovery (20. Jan. 1996). Six further CTD stations were deployed outside the area shown here.

The CTD employed was a NBIS Mark III, connected to a General Oceanics rosette water sampler with 24 x 12-liter bottles. The CTD temperature and pressure sensors were calibrated just prior to the cruise at the Scripps Institution of Oceanography, La Jolla, California. The performance of the instrument during the cruise was controlled by use of SIS reversing thermometers and pressure gauges attached to the water bottles. The readings of the CTD conductivity cell (from which, in combination with the temperature and pressure measurements,

salinity is calculated according to the UNESCO Practical Salinity Scale, PSS78) were corrected against salinity samples taken from the bottles. The bottle salinity samples were determined with a Guildline Autosal 8400 B salinometer with reference to I.A.P.S.O Standard Seawater. As neither a significant pressure dependency of the conductivity cell nor a temporal drift over the period of the cruise was observed, a uniform conductivity correction was applied to all stations. The achieved accuracy is estimated to be 3mK in temperature, 3 dbar in pressure, and 0.004 PSU (Practical Salinity Units) in salinity.

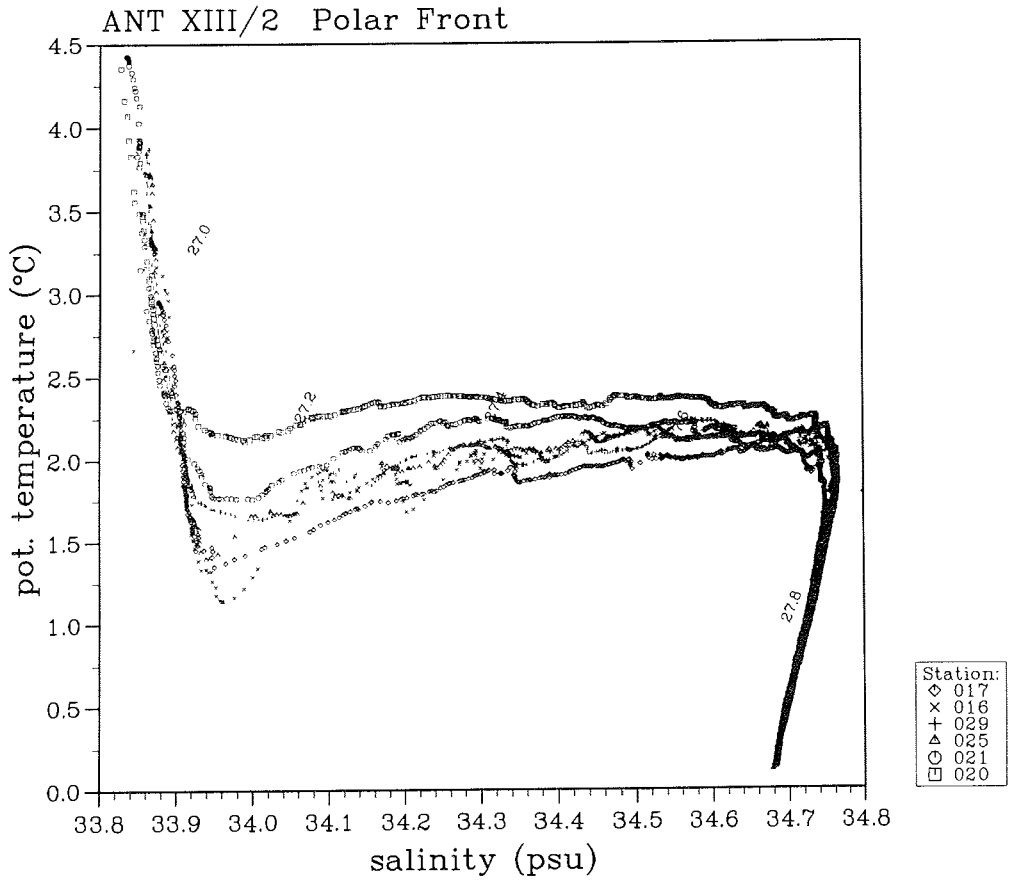

Fig. 6.2 θ/S (potential temperature / salinity) diagram showing the thermohaline water mass changes across the front, as derived from the meridional section of deep CTD stations (see Fig. 6.1). The shapes of profiles from the individual stations indicate the presence of four major water masses: Warm and fresh (θ of about 4 °C and S around 33.85) Antarctic Surface Water (AASW) on top; below, just above the 27.2 isopycnal, the relatively cold (1.5 to 2.0 °C) and fresh (33.95 PSU) Winter Water (WW); further down the warmer (about 2.0 °C) and saline (exceeding 34.7 PSU) Circumpolar Deep Water (CDW); approaching the bottom the profiles tend to merge into the thermohaline properties of the very cold Antarctic Bottom Water (AABW). The WW is found in the depth range between 100 and 300 m, the CDW is centred at about 500 m, but tends to rise slightly between the northern and southern stations. The strongest meridional gradient of the thermohaline properties (i.e. largest difference between stations) occurs in the range of the Winter Water.

The deep CTD stations reveal the thermohaline water mass changes across the Polar Front (above, Fig. 6.2). Associated with the thermohaline changes are differences in the vertical density structure between stations. These horizontal gradients of the vertical density structure imply geostrophic transports of water mass (below, Fig. 6.3) if balance between the pressure gradient and the Coriolis force is assumed.

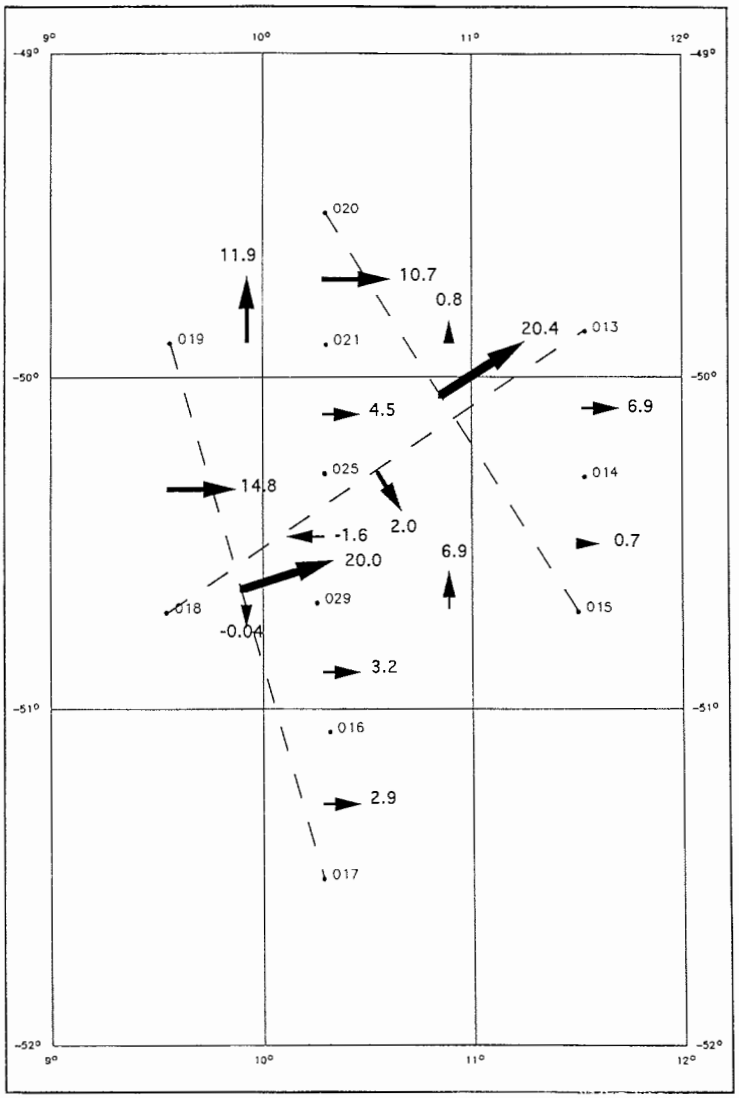

Fig. 6.3 Geostrophic transports of water volume relative to the bottom, calculated from the density field obtained from the deep CTD stations. The number at each arrow gives the transport in Sverdrups (10^6 m^3 s^{-1}) between the sea surface and bottom, perpendicular to the cross section between each pair of stations. The major transport in the area, accounting for about 20 Sv, occurs in an east-northeasterly direction.

A quasi-continuous vertical profile of chlorophyll concentration can be derived from the optical measurements made with a SEATECH transmissiometer connected to the CTD. Though the transmissiometer is not specifically designed for the measurement of phytoplankton chlorophyll, it nevertheless measures the transmission of light at 660 nm, i.e. close to the red absorption peak of chlorophyll. A possible calibration is suggested by the linear regression line drawn to the scatter plot of chlorophyll concentration versus light transmission (Fig. 6.4). Despite the scatter, the correlation is considered reasonable compared to the much larger scatter normally encountered with *in situ* fluorescence measurements of chlorophyll where daylight usually has a strong influence and requires a very laborious treatment for its removal. It must, however, be pointed out that a correlation between transmission and chlorophyll as obtained can only be expected from the euphotic zone in open ocean regions. The decrease of transmission in the bottom nepheloid layer revealed by the deep CTD profiles, for instance, is certainly due to the presence of light attenuating particles other than chlorophyll. The meridional distribution of light transmission across the Polar Front in the top 250 m is shown in Fig. 6.5, together with the distributions of temperature, salinity, and density.

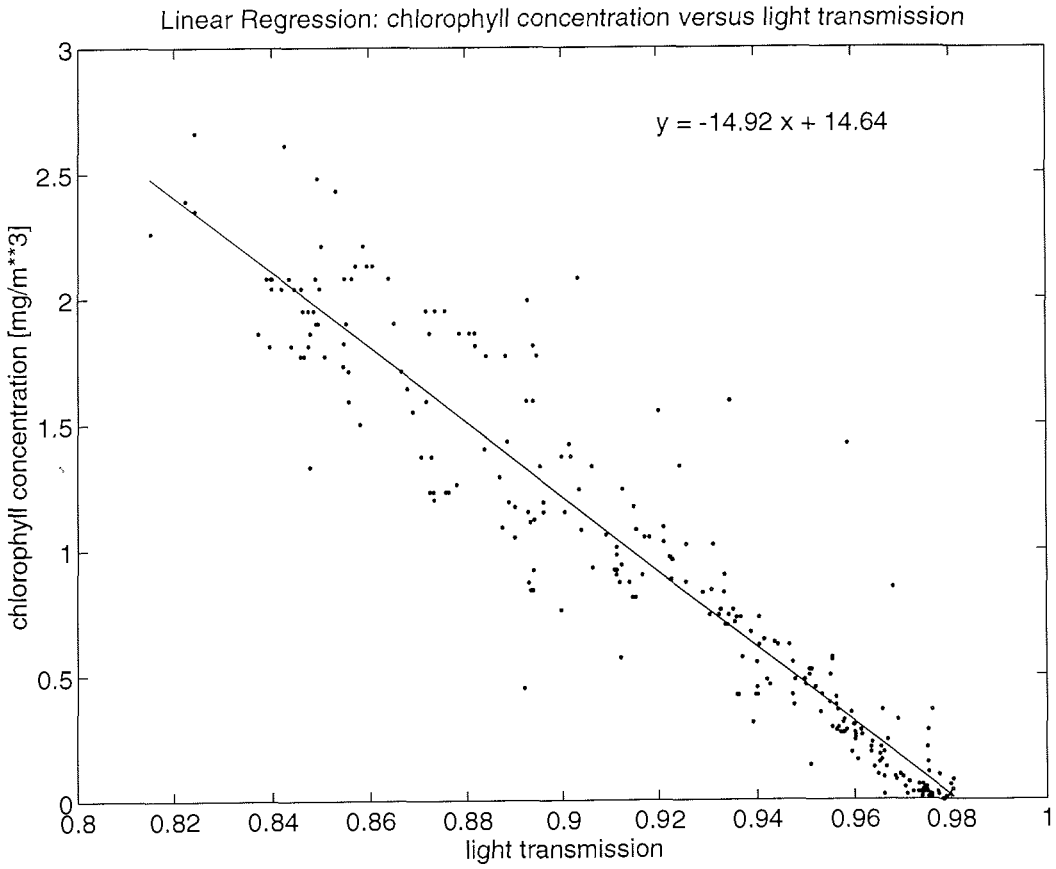

Fig. 6.4 Correlation between the concentration of chlorophyll *a* and the transmission of light at λ = 660 nm. According to the linear regression, the chlorophyll concentration could be calculated from the measurements of transmission as Chl = 14.64 - 14.92*transmission. The data are collected from the top two hundred meters of all stations. The chlorophyll concentrations were determined from extracts drawn from the rosette bottle samples (see contribution by U. Bathmann)

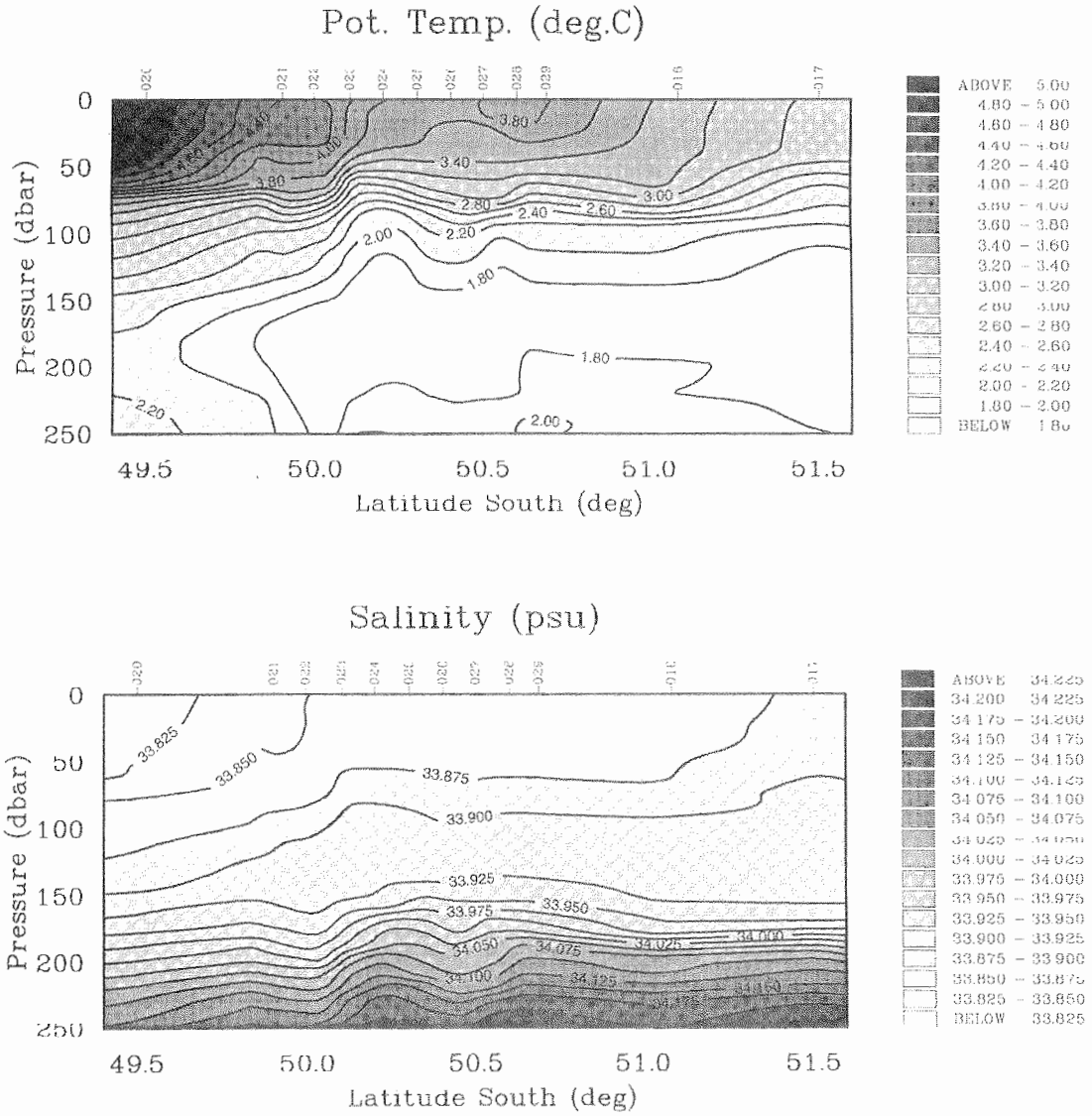

Fig. 6.5 a-d Meridional section across the Polar Front of potential temperature, salinity, density sigma-t, and light transmission as obtained from the CTD stations; only the upper 250 m are reproduced. Station numbers are indicated on the upper x-axis; the station positions are shown in Fig. 6.1. An interpretation of the plotted light transmission data in terms of chlorophyll concentrations is suggested by the negative correlation shown in Fig. 6.4. Accordingly, the lowest transmission of below 0.85 compares to a chlorophyll concentration of about 2 mg m^{-3}, while the highest transmission values indicate a chlorophyll concentration of less than 0.2 mg m^{-3}. The low transmission values or high chlorophyll concentrations, respectively, are generally confined to the upper mixed layer which extends from the surface to the top of the seasonal pycnocline between 50 and 75 m depth.

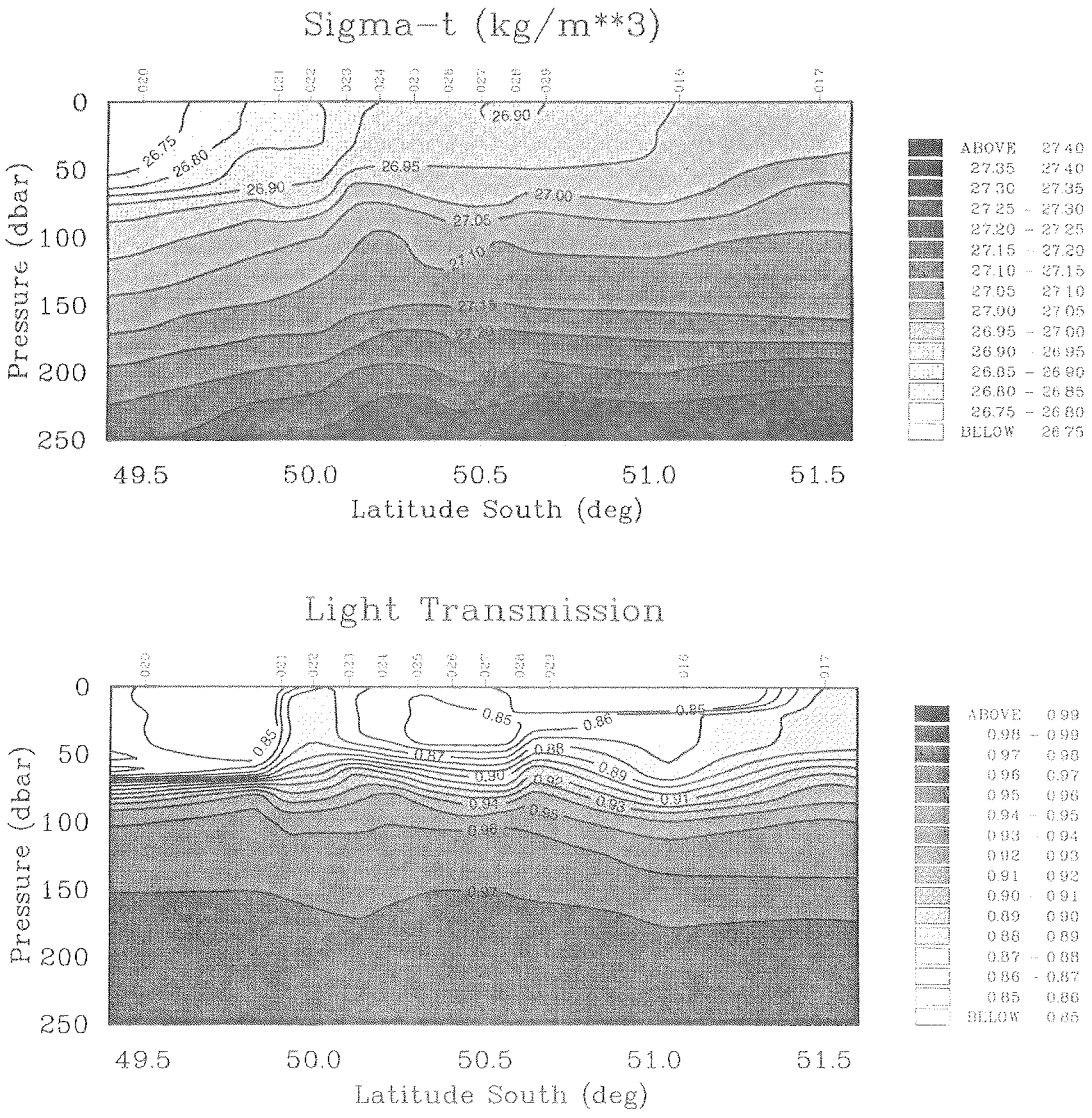

Fig. 6.5 a-d (cont`d.) The shallow pycnocline appears to be maintained by a cross-frontal circulation through which warmer and lighter surface water from the north overlays the colder and denser water below. Evidence of a subsurface chlorophyll maximum is found around stations 026 and 027. Note also the meridional interruption of the high upper mixed layer chlorophyll concentrations between stations 021 and 024, which seems to be associated with an upward displacement of the isotherms, isohalines, and isopycnals at this location, which is close to the position of the Polar Front as defined by the northernmost extension of the 2°C isotherm in the Winter Water layer.

7. MEASUREMENTS BY MOORED INSTRUMENTS

V.H. Strass, H. Fischer, M. Hofmann, A. Wischmeyer, R. Timmermann

To monitor the temporal variations of currents, hydrographic properties, and sedimentation, a mooring was deployed for the duration of the frontal survey. It was deployed at the eastern, downstream, margin of the survey grid, within a band of high current velocities as identified by the shipborne VM_ADCP velocity measurements. This location of the mooring (almost identical with the position of stations 013 and 032, see previous section, Fig. 6.1) was chosen to relate the sedimentation of particles caught in the traps with production in the intensely surveyed upstream area. The mooring was well equipped (see Fig. 7.1) with 6 rotor current meters, 1 acoustic current meter, 1 Acoustic Doppler Current Profiler, and 2 sediment traps. The current meters also carried thermometers, while one carried a conductivity cell and another a complete CTD. All instruments worked properly. An example of the current meter time series obtained is given in Fig. 7.2. A conceptual integration of the VM_ADCP and moored current meters leads to the idealised view of the streamlines shown in Fig. 7.3.

Fig. 7.1(over-leaf) Schematic drawing of mooring AWI-235, deployed for the duration of the frontal survey and located close to station positions 013 and 032 (ref. section 6, Fig. 6.1). The mooring carried 2 sediment traps (HDW-SF) manufactured by Howaldt Deutsche Werft, 1 self-contained Acoustic Doppler Current Profiler (ADCP; RDI) operating at a sound frequency of 150 kHz, 1 FSI acoustic current meter + CTD (3D-ACM), and 6 Aanderaa rotor current meters (RCM8). The uppermost Aanderaa current meter (type VTCP) also carried sensors for temperature and conductivity; the other deeper ones carried sensors for temperature only. The ADCP was configured to measure the velocity profile up to the surface with a vertical resolution of 8 m. All current meters were set to a sampling interval of 30 min. Connection between mooring line and anchor weight was through a pair of acoustic releases (EG&G). The echo amplitude measurements retrieved from the ADCP after recovery indicate a from-surface distance of 152 m, i.e. an instrument depth which is about 40 m shallower than the planned depth distribution indicated in the drawing.

Mooring ID : AWI235 Position : 49 53.09 S 11 32.42 E
Project : ANT XIII/2 Deployed : 29.12.95
Waterdepth : 4159 m Released : 20.01.96
Volker Strass

-Depth-Dist.	Segments	Instruments		Time-in	Time-out
		XT6000	Code H	14:50	06:25
	8 Floats				
	40 m				
	20 m				
- 132-4028		HDW-SF		14:57	06:20
	4 Floats				
	40 m				
	20 m				
- 192-3968		ADCP		15:04	06:07
	200 m				
	4 Floats				
- 397-3763		RQM8 VTCP	SN 9200	15:14	06:33
- 398-3762		3D-ACM	SN 1388	15:14	06:33
	40 m				
	20 m				
	6 Floats				
	40 m				
	20 m				
- 523-3637		HDW-SF		15:26	06:45
	20 m				
	40 m				
	4 Floats				
- 588-3572		RQM8 VTP	SN 9783	15:29	06:48
	2*40 m				
	2*200 m				
	20 m				
	4 Floats				
-1093-3067		RQM8 VTP	SN 9182	15:44	07:00
	500 m				
	500 m				
	4 Floats				
-2099-2061		RQM8 VT	SN 9190	16:00	07:16
	500 m				
	500 m				
	4 Floats				
-3105-1055		RQM8 VT	SN 9186	16:17	07:32
	1000 m				
	6 Floats				
-4106- 54		RQM8 VT	SN 9391	16:37	07:47
		2*EG&G	14104/14105		
	50 m				
	3 m Kette				
	Anker 1000kg	16:43			

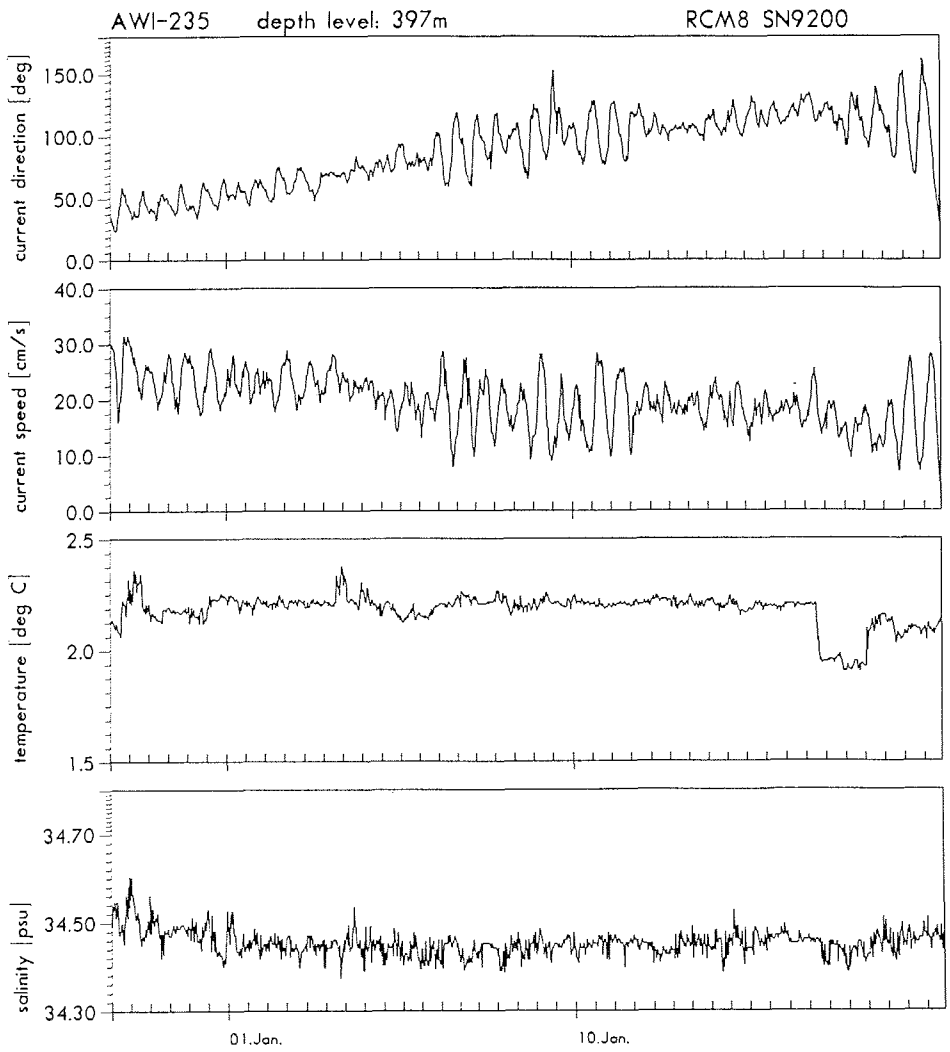

Fig. 7.2 Time series of current direction, current speed, temperature, and salinity obtained from the Aanderaa current meter at 397 m nominal depth (preliminary invalidated data, e.g. salinity probably about 0.1 PSU too high). The velocity fluctuations appear to be dominated by semi-diurnal tidal motions. This seems to hold true also for the deeper layers; not represented here. Closer to the surface (as suggested by the ADCP measurements), inertial oscillations predominate. A longer-term shift affects the mean (tidal and inertial variations removed) current direction at all depth levels in a fashion similar to what is seen in the figure. At the beginning of the time series, the mean current sets in a northwesterly direction (45 °). During the following 2 to 3 weeks it gradually changes to a west-southwesterly direction (120°), and later tends to swing back during the last days of the deployment period. This longer-term shift of the flow is probably associated with a displacement of the frontal meander structure. It is interesting to note also the sudden occurrence of a temperature minimum during January 16 and 17 (3rd panel). As the occurrence of that anomaly is associated with a mean flow from the west-northwest, and not from the south, where low temperatures at that depth are more likely to be found, it indicates that this anomaly must have been advected in along a curved path.

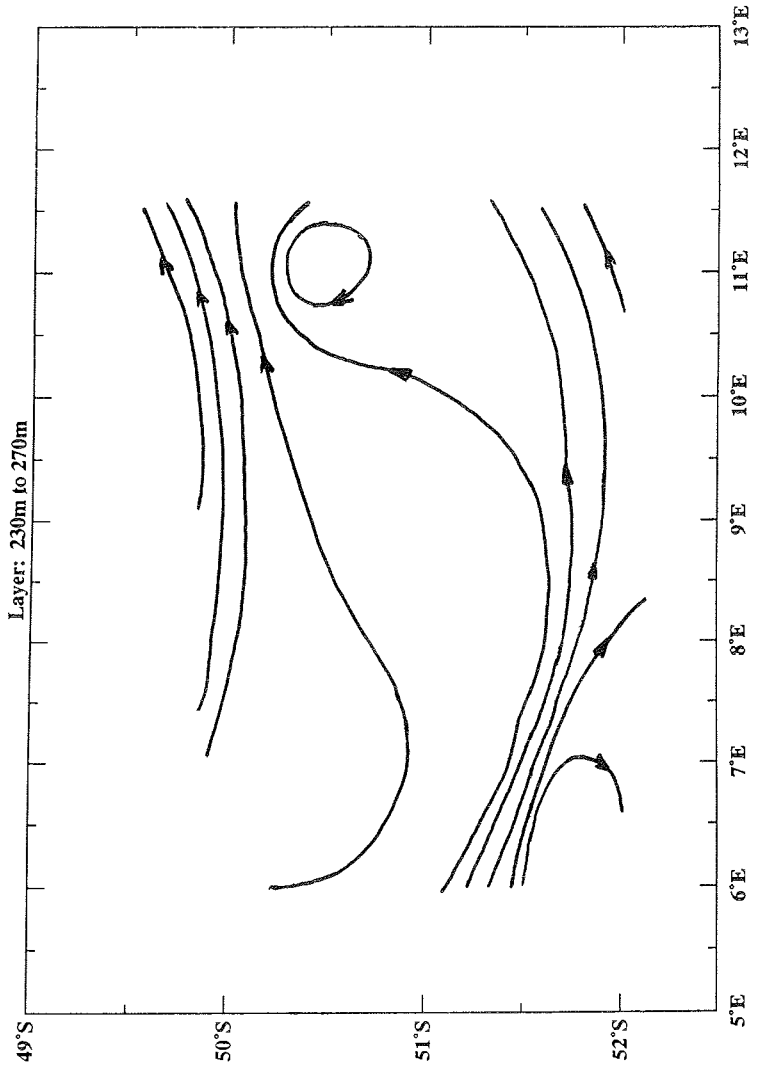

Fig. 7.3 Idealised streamlines indicating the likely mean pattern of flow during the frontal survey. This pattern is suggested by combining the horizontal current structure as obtained from the ship-borne ADCP measurements with the current meter time series of mooring AWI-235 (described in Figs. 7.1 & 7.2) and another mooring, PF-8, positioned at the northwestern corner of the coarse scale survey area. This was deployed in Dec. 1994 and recovered in April 1996 during *Polarstern* cruise ANT-XIII/4

8. NUTRIENTS, DISSOLVED AND PARTICULATE MATTER

C. Hartmann, B. Hollmann, G. Kattner, K.-U. Richter, A. Terbrüggen

Sampling and Methods

Nutrients were determined from underway samples, from CTD Niskin bottles and from Goflo bottles. The determinations of nitrate, nitrite, ammonium, silicate and phosphate generally followed the routinely used methods for sea water analyses and were performed with a Technicon Autoanalyser II system. Underway samples were taken from about 8 m depth by means of the membrane pump installed on board *Polarstern*. During the four long sections towards Neumayer station and back to the main investigation area, samples were taken each half hour. During the large and small scale surveys in the Polar Front area, samples were collected every 15 minutes. Samples from the CTD casts were generally taken from the six productivity light depths (100, 50, 25, 10, 1 & 0.1%) and further down to 500 m. Nutrients were also analysed from a few casts to the bottom.

In addition to the nutrient determinations, dissolved organic nitrogen was analysed by the peroxodisulfate oxidation method with the Autoanalyser. Samples for dissolved organic carbon (DOC) measurements were collected, stored deep frozen in glass ampoules and will be analysed later in the home laboratory. Samples for DOC and DON determinations from 8 CTD casts.

Particulate organic matter (POM) was collected at 10 stations within the large scale survey area and at 7 stations in the small scale one as well as from one CTD cast at St. 29. From the ship's membrane pump sea water was filtered through a cascade of filters with different pore sizes. First, 40 L was filtered through a gauze of 100 µm mesh size, retaining the larger organisms and particles. The water was then passed through different polycarbonate filters resulting in particle size classes of 20-8, 8-3 and 3^{-1} µm. Finally the filtrate was passed through a quartz fibre filter of 0.3 µm pore size. The filtration systems containing the 8, 3 and 1 µm filters were equipped with stirrers so that the particles did not settle on the filters. All particulate fractions were collected on quartz fibber filters and deep frozen prior to later analyses. From all POM size groups, carbon and nitrogen will be determined as well as their stable isotopes, ^{13}C and ^{15}N.

After the filtration procedure, the particle-free filtrate was passed through XAD resins to extract the dissolved organic material (DOM). Exactly 20 L of filtrate were extracted on three different resins in the sequence of XAD 7, XAD 4 and XAD 2. This sequence of XAD resins allows the most complete extraction of DOM. The DOM together with the resins was deep frozen and will be later eluted. From the eluates, carbon and nitrogen as well as their stable isotopes will be determined and compared with those of the particulate fractions.

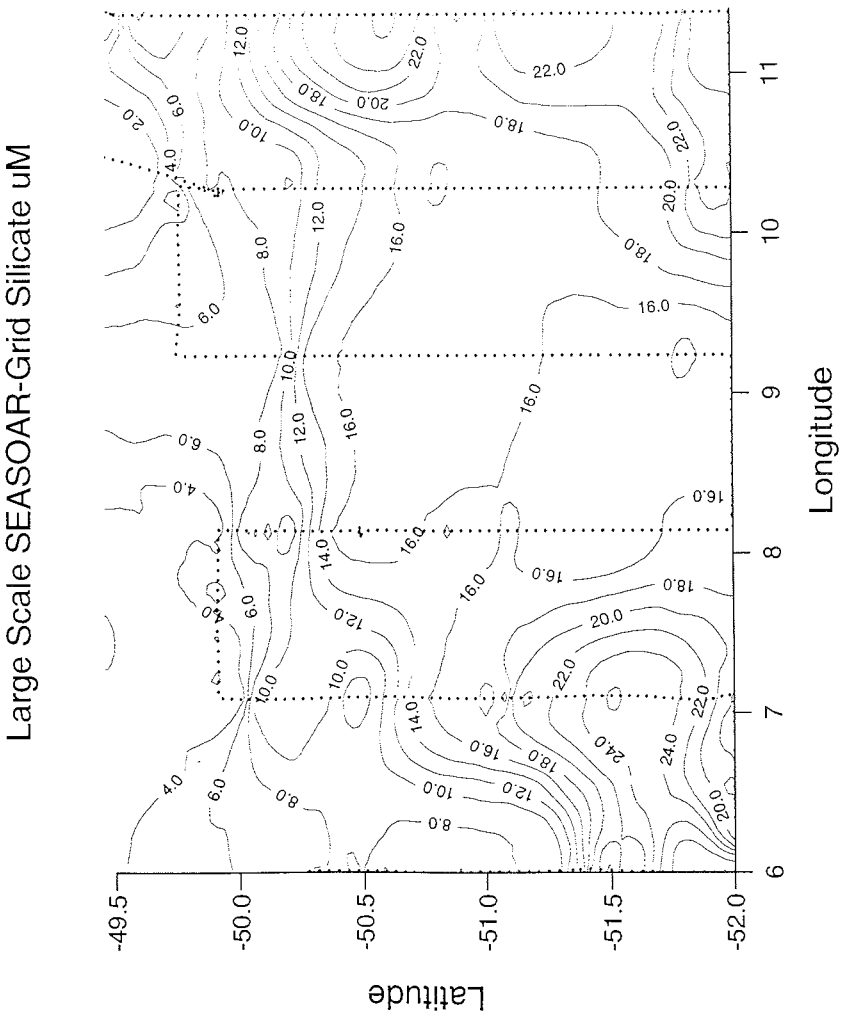

Fig. 8.1a and b The large scale survey area is clearly marked by large gradients in silicate concentrations in the surface water. Silicate values ranged from > 28 to < 2 µM. In the south western corner of this area, highest concentrations were found, whereas at the northern boundary, silicate concentrations were low, with lowest values in the north eastern most region of the survey area. In the south east, high silicate values of upto 25 µM were measured which extended further to the north than at the western boundary of the study area. In the north, a sharp south to north gradient from high values to nearly silicate depleted areas occurred.

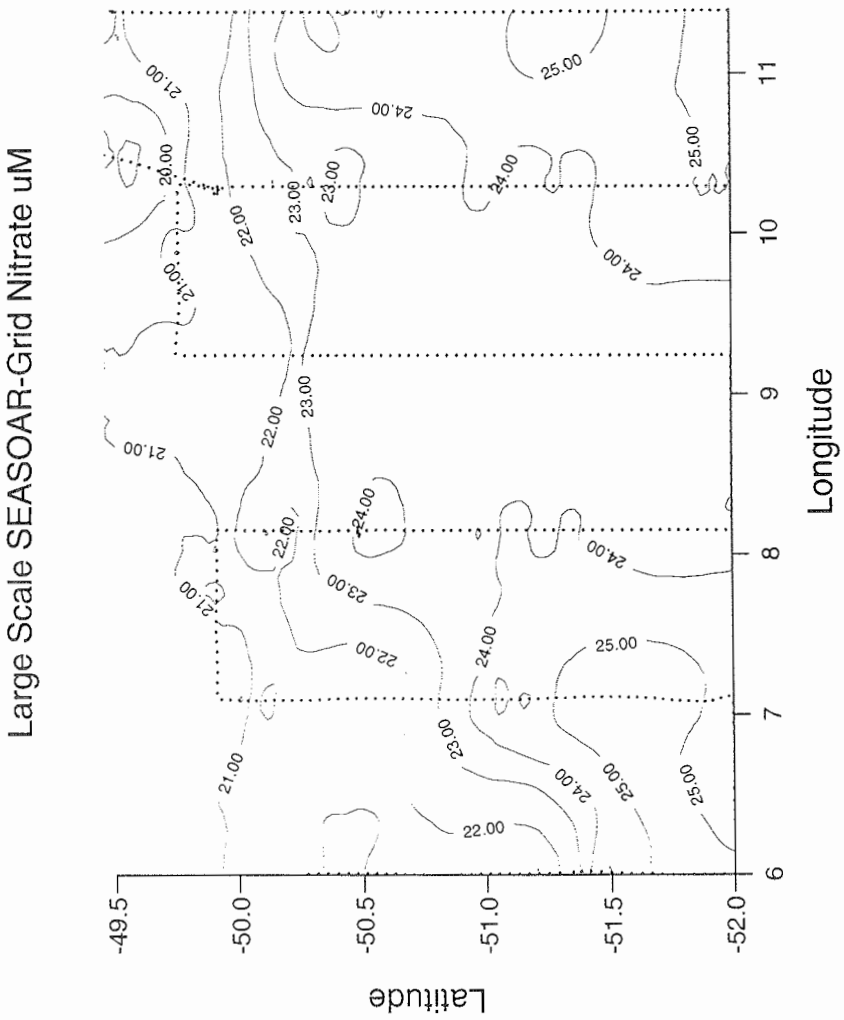

Fig. 8.1a and b (cont`d.) In the central part of the survey area, silicate concentrations were about 16 µM, declining northwards. The two spots of very high silicate concentrations in the east and west probably originated from the same polar ACC water, known for its high silicate concentrations. In the northern part, the depletion of silicate matched the regions of elevated chlorophyll distribution. Nitrate distribution in the large scale survey region follows essentially that of silicate. Highest concentrations of more than 25 µM were found in the south western and south eastern part, whereas lowest values of about 20 µM were measured in the north. Nitrate depletion was less marked than that of silicate. The phosphate distribution (not shown) was similar to both other nutrients, with a maximum of 1.7 µM and minimum of 1.3 µM.

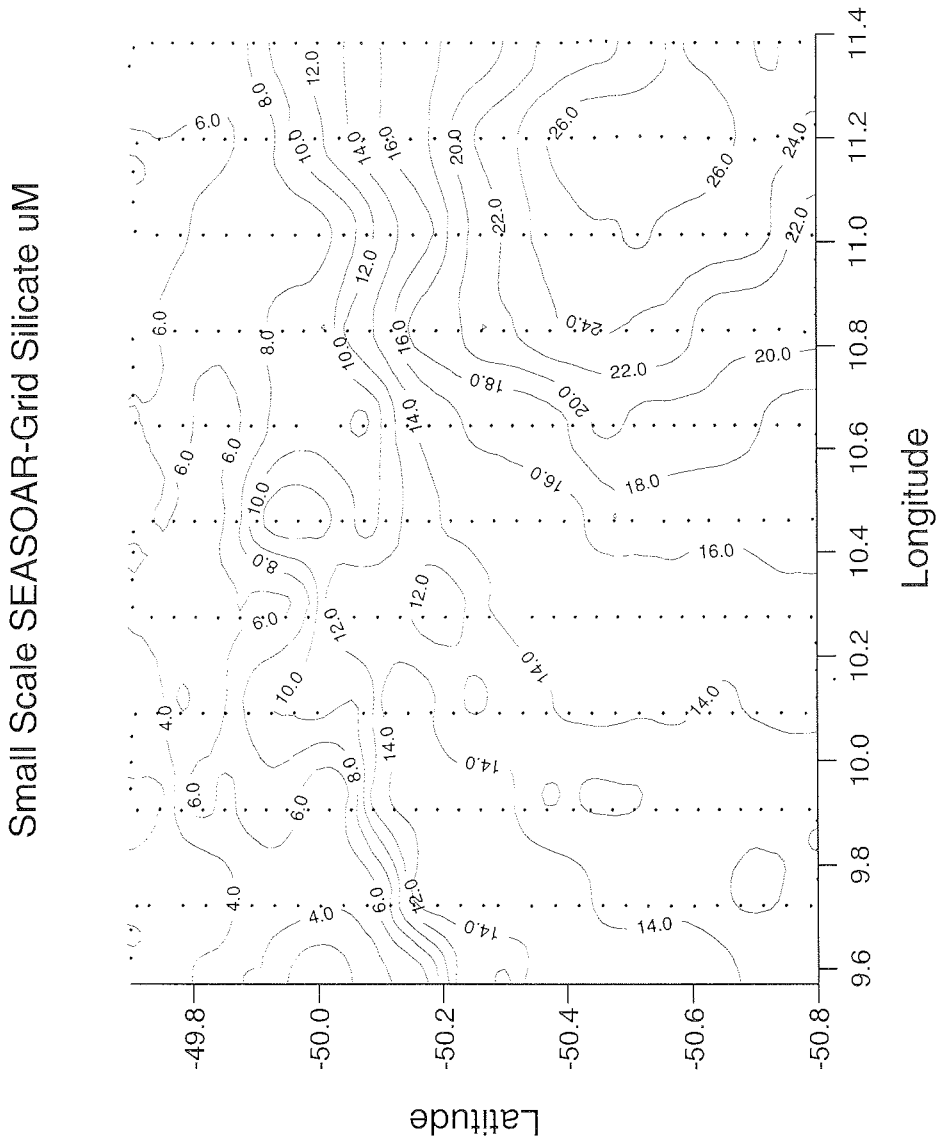

Fig. 8.2 a and b In the small scale survey area, where the north eastern part of the large scale survey was repeated with a much higher resolution, the nutrient distribution in the surface was generally similar to that monitored during the large scale survey. The silicate rich (26 µM) south eastern region accorded well with that of the large scale survey, extending only somewhat further to the west. The higher sampling resolution nevertheless revealed some small scale structure in nutrient distribution. For example, a band of slightly lower silicate values extended

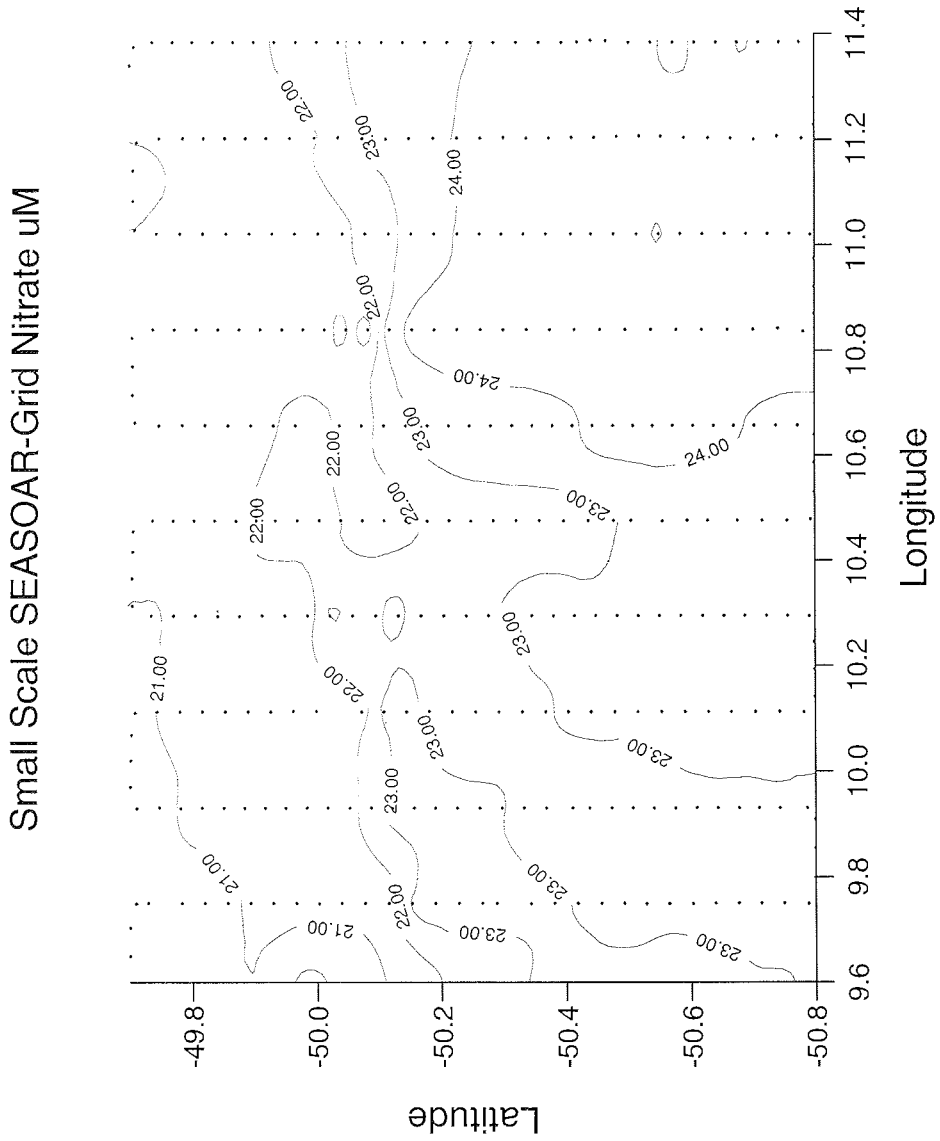

Fig. 8.2 a and b (cont`d.) from the south western part up to the north east, declining to the lower northern values of between 6 and 2 µM. Again nitrate and phosphate (not shown) were similarly distributed. Nitrate values of > 24 µM were present in the south east and lower values of about 21 µM in the north. Phosphate ranged between 1.7 and 1.3 µM.

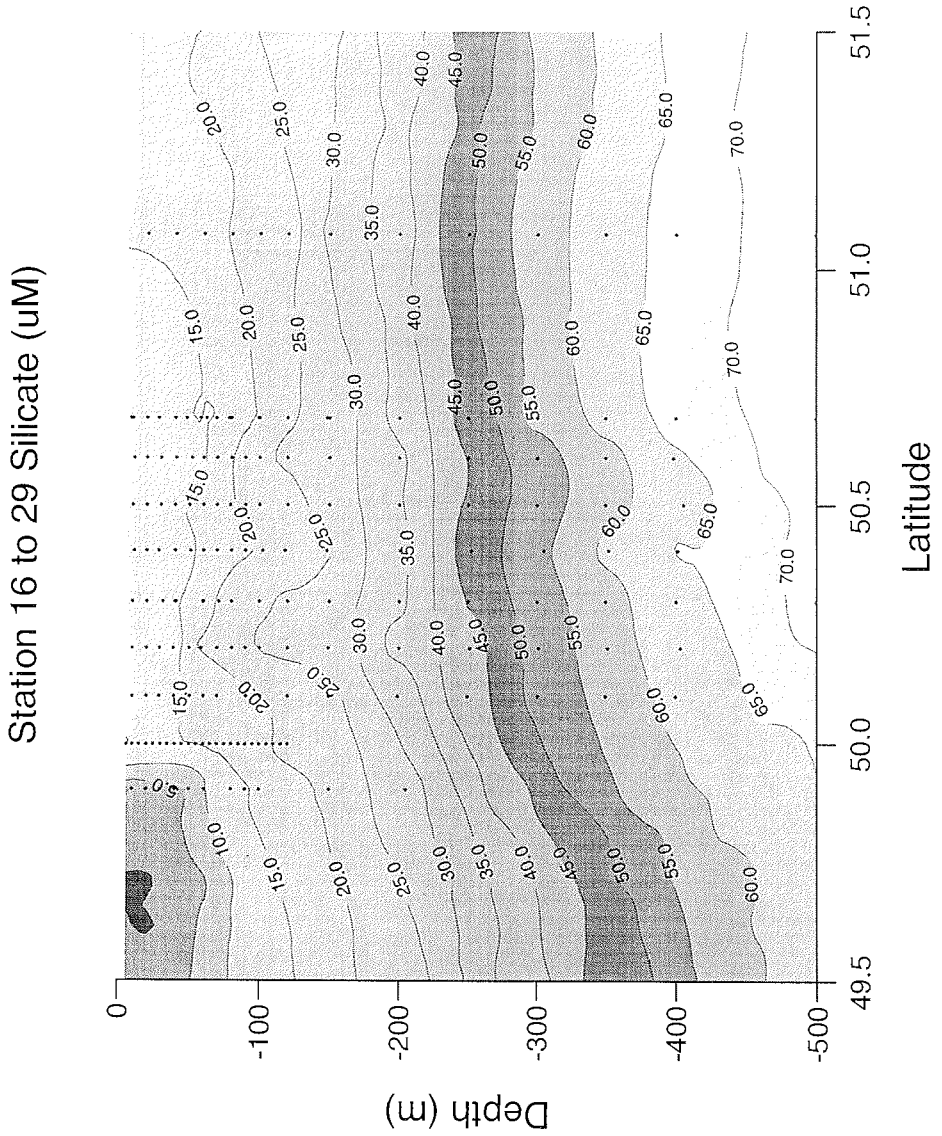

Fig. 8.3 a and b Fig. 3 shows the nutrient distribution from the north to south section through the large and small scale survey areas. Stations 20 (north) to 29 were successively occupied whereas stations 16 and 17 (south) were occupied some days earlier. Silicate values increased from the surface (about 20-30 µM) to more than 70 µM at 500 m depth. In accordance with the surface mapping,

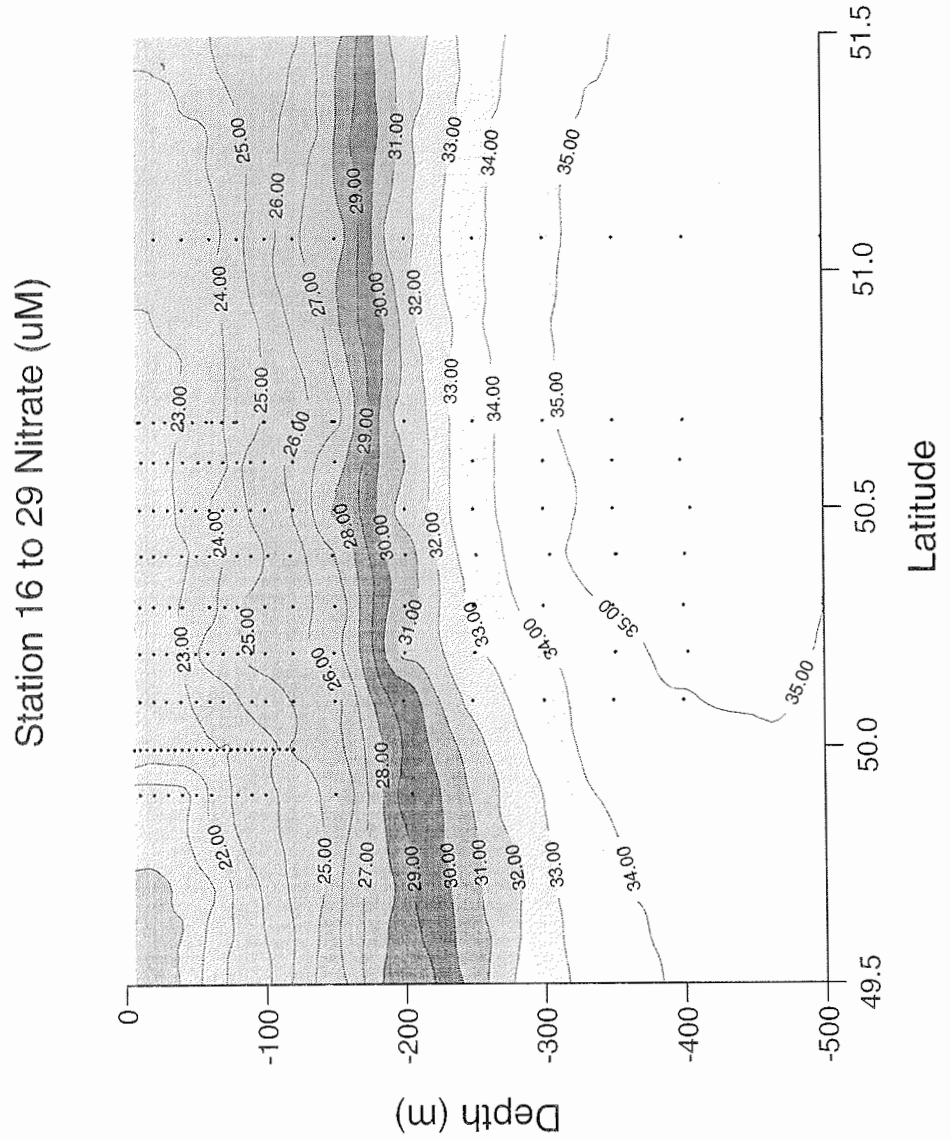

Fig. 8.3 a and b (cont`d.) lowest silicate values were found in the northern part of the section, increasing to about 20 µM in the south. Below the mixed layer, nutrients were rather homogeneously distributed with only slight variability. Nitrate values increased from (about 20 µM) in the surface layer to about 35 µM at 400 to 500 m depth. The low values of about 20 µM in the surface layer were found in the north and increased to 24 µM toward the south.

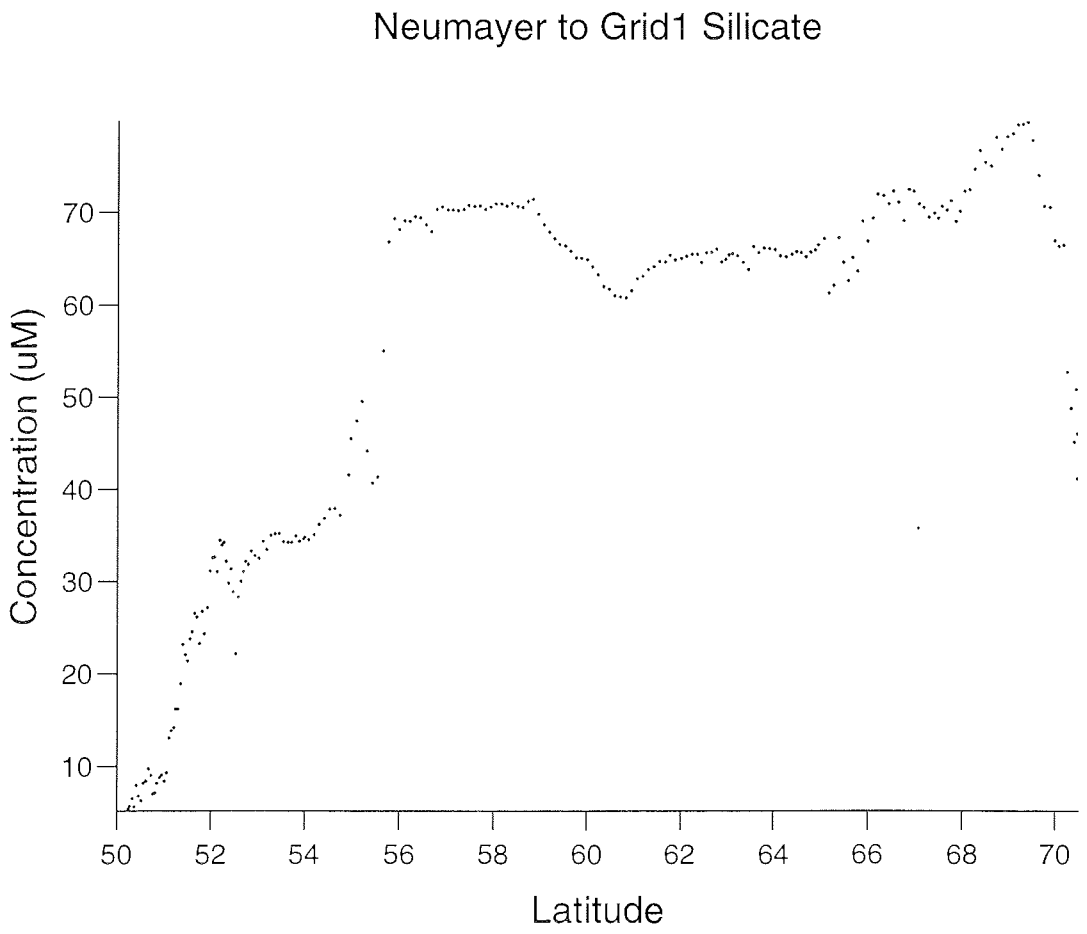

Fig. 8.4 a and b During the four transects from the main investigation area in the Polar Front to Neumayer station, surface nutrient concentrations were measured every 30 minutes. As an example, the nutrient distribution of the transect from Neumayer to 50°N is shown in Fig. 8.4. In the Polar Front area, silicate

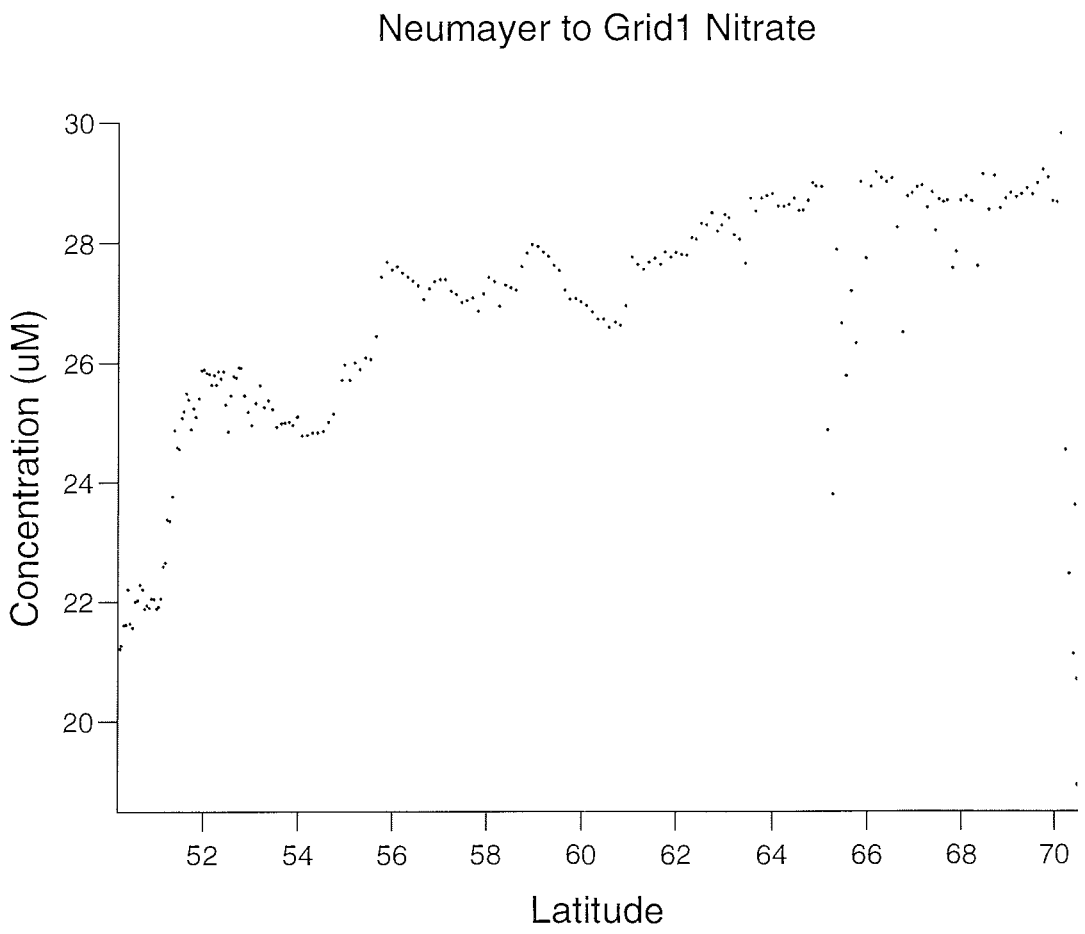

Fig. 8.4 a and b(cont`d.) concentrations increased from < 10 μM to ca. 37 μM and increased further between 54°S and 55°S to values of about 60μM to 70 μM. Where silicate concentrations increased sharply, so too did nitrate. Values of 20 μM of nitrate in our northern investigation area rose to 26 μM in the Polar Front area, increasing further (in parallel with silicate) to 28 μM with slight but variable increases further south.

9. FIELD DISTRIBUTION OF IRON IN A SECTION OF THE ANTARCTIC POLAR FRONTAL ZONE.

J.T.M. de Jong, J. den Das, K.R. Timmermans, H.J.W. de Baar

Introduction

The contradicting situation of low primary production in several remote ocean provinces in spite of replete nutrients (nitrate, phosphate and silicate), was first observed in the Antarctic ocean in 1928 - 1929 (Ruud, 1930) and became known as the 'Antarctic Paradox'. Ever since, the idea of iron deficiency in such a High Nutrient Low Chlorophyll (HNLC) area has been offered as an explanation to account for this (Gran, 1931) Many investigators have tried to study the biogeochemical behaviour of iron and to elucidate the role that iron plays as an essential micronutrient in the ecology and physiology of oceanic phytoplankton. Initially they were quite unsuccessful due to the lack of sensitive analytical methods, and more notably, due to problems of contamination during sampling and sample processing (de Baar, 1994). Iron is obviously one of the most abundant elements on board a steel research vessel but it exists at trace levels in oceanic waters. To illustrate this, concentrations in open ocean waters generally range between (sub) surface values of < 0.05 nM and several nM in deeper waters. (Bruland et al., 1994; Landing & Bruland, 1987; Martin & Gordon, 1990; Nolting et al., 1991; Westerlund & Öhman, 1991). Values can be higher in neritic coastal waters (Martin et al., 1990; Nolting et al., 1991), upwelling areas and frontal systems (de Baar et al., 1995; Powell et al, 1995), and areas affected by aeolian input (Donaghay et al., 1991; Duce & Tindale, 1991)

For several years a vigorous debate has been going on, focusing on the emphasis given by some investigators (Martin et al., 1994) that iron is the most important limitation to primary production in HNLC regions, while others (Banse, 1990; Buma et al., 1991; de Baar et al., 1990; de Baar, 1994; Dugdale & Wilkerson, 1990; Lancelot et al., 1993; Price et al., 1991) have argued that other limiting factors are at work, such as light intensity, temperature, zooplankton grazing, particle sinking as well as limitation by other trace elements (e.g. Mn, Co, Zn).

To assess the exact role of iron in phytoplankton bloom development, it is vital that accurate chemical analyses of iron is performed in combination with *in situ* measurements of several other sensitive physical, chemical and biological parameters. Such a multidisciplinary approach to study the Antarctic Paradox has already been carried out successfully during the European *Polarstern* Study (EPOS) in the Weddell and Scotia Seas (1988/89), ANT X/6, in the Polar Frontal Zone at 6° W (1992) and ANT XII/4 (1995) in the Antarctic sector of the South-East Pacific.

Methods

During cruise ANT XIII/2 the structure of a sector of the Polar Frontal Zone was studied. The work was characterized by high density sampling and profiling of a small area of the frontal system, mainly focused on the Fine Scale Survey (FSS).

Spatial distribution of iron:
A total of 15 vertical profiles were measured, notably at stations 5, 8, 9, 10, 13, 15, 16, 18, 19, 20, 21, 25, 29, 30 and 32. The majority of them where situated in the FSS area. A number of stations were also occupied between the primary research area and the German base 'Georg von Neumayer' to gather data on iron concentrations in the Antarctic Circumpolar Current (ACC) and the Weddell Sea.

To prevent sample contamination, trace metal clean techniques were applied. Samples were taken at depths of 20, 40, 60, 80, 100, 150, 200, 300, 400 and 500 meters using trace metal clean, Teflon-coated General Oceanics GoFlo samplers with a volume of 12 l. These bottles were attached to a Kevlar hydrowire and tripped using Teflon messengers. On retrieval, the bottles were mounted in closable, wooden cabinets outside a Class-100 clean air container. Via

Teflon tubing through the wall of the lab, the bottles were subsampled as follows: first macronutrient sampling, followed by unfiltered sampling for shipboard iron analysis and other trace metals. The GoFlo's were then pressurized to 1.0 bar and connected to Teflon filter holders (with typically 0.4 µm pore size polycarbonate membrane filters) for size-fractionation using clean, in-line filtered nitrogen. Again subsamples were collected for iron analysis and other trace metals. All samples were acidified to pH = 2 with ultraclean quartz distilled concentrated nitric acid.

In between the station work and during the SeaSoar transects, surface water was sampled. Parts of the Course Scale Survey (CSS) (transects 6.1, 6.2, 6.4 and 6.7) were covered at half hour intervals, and most of the FSS (transects 8.3 until 8.11) at one hour intervals. Samples were taken using a peristaltic pump connected to a polyurethane coated towing torpedo (1m length and 50 kg) by acid cleaned polyethylene tubing. The torpedo was towed alongside the ship at a distance of several meters from the hull at a maximum speed of 15 knots. A water sample was delivered to and filtered (0.4 µm) in the clean air container every hour. On transects 11.2 and 11.3 from Neumayer station to the north, surface water was sampled at roughly four hour intervals when large volumes (20 - 40 l) of sea water were also filtered through several pre-weighed polycarbonate filters to determine trace metals in suspended particulate matter (SPM) back in the home laboratory. This involves a three step sequential leaching technique with dilute acetic acid rinsing, dilute aqua regia rinsing and total digestion of the residue. Focusing on Fe, Mn and Al, we hope to distinguish between the biogenic or terrigenous nature of the SPM.

Total dissolvable (unfiltered) and total dissolved iron (< 0.4 µm) were measured on-board using a recently developed flow injection technique with in-line pre-concentration on a chelating resin followed by chemiluminescence detection (FIA-CL) (Obata et al., 1993, Landing et al., 1986). Iron from an acidified sample is buffered and pre-concentrated onto a column of immobilized 8-hydroxyquinoline. After a loading time of four minutes, the column is washed with deionized water and the iron is eluted with dilute hydrochloric acid. The iron mixes with luminol, hydrogen peroxide and ammonium hydroxide to produce chemiluminescence in the flow cell of a photomultiplier tube connected to a photon counter. The chemiluminescence occurs as a result of the iron catalyzed oxidation of luminol (3-aminophtalhydrazide) by hydrogen peroxide, producing blue light. The accuracy of the method was checked and confirmed using NASS-4 reference sea water. Throughout the cruise, the blank and detection limit (3x standard deviation of blank) remained constant at 0.025 and 0.015 nM respectively. Reproducibility was typically 2% at the 0.3 nM concentration and better than 5% at the 0.1 nM concentration.

The other trace metals (Mn, Cd, Ni, Cu, Zn, Pb and Co) will be analyzed in the home laboratory using a FIA-CL method for Mn and for the other metals the conventional method of dithiocarbamate complexation, extraction into chloroform and digestion of the extract in nitric acid, followed by measurement with Graphite Furnace Atomic Absorption Spectrophotometry (Nolting & De Jong, 1995).

Iron stress in phytoplankton

By measuring the ratio between the proteins flavodoxine and ferrodoxine, it is possible to examine the extent to which phytoplankton are iron depleted. Both proteins have the same function, but only ferrodoxine contains iron. In conditions of iron depletion, the cells adapt their metabolism to this situation and switch over to flavodoxine. These proteins can be determined using western blotting and immunofluorescence techniques. Sampling was done daily using large volume filtrations (typically 30 L over cellulose nitrate membrane filters, 0.4 µm pore size) of sea water from the ship's pump. Each of the 60 collected filters was thoroughly rinsed with some deionized water and the residue was collected in a centrifuge tube. After centrifuging the residue was transferred into small polyethylene vials and stored at -25° C for later analysis.

Preliminary results and discussion

During cruise ANT X/6 (de Baar et al., 1995) high dissolved iron concentrations of up to 4 nM were found in the upper 150 meters of the Polar Frontal Zone at 6° W, coinciding with the occurrence of a diatom bloom and CO_2 drawdown from the atmosphere. It was hypothesized that the iron was derived from a continental source, be it via atmospheric input or via resuspension of iron from continental shelf sediments of South America and/or the Antarctic Peninsula. The continental signature of the iron was demonstrated by a good correlation with dissolved and particulate Al and particulate Fe:Al ratio's fitting the crustal abundance ratio (Löscher et al., in press). The input of iron from sea-ice and icebergs was deemed to be negligible as the analysis of the iron concentrations in sea ice, glacial ice and surface water in the wake of an iceberg showed that there can only be a significant enhancement of iron in situations of stratification of the water column. The latter is however not expected to happen often in the stormy environment of the Polar Front, where the wind mixed layer sometimes exceeds 100 meters in depth.

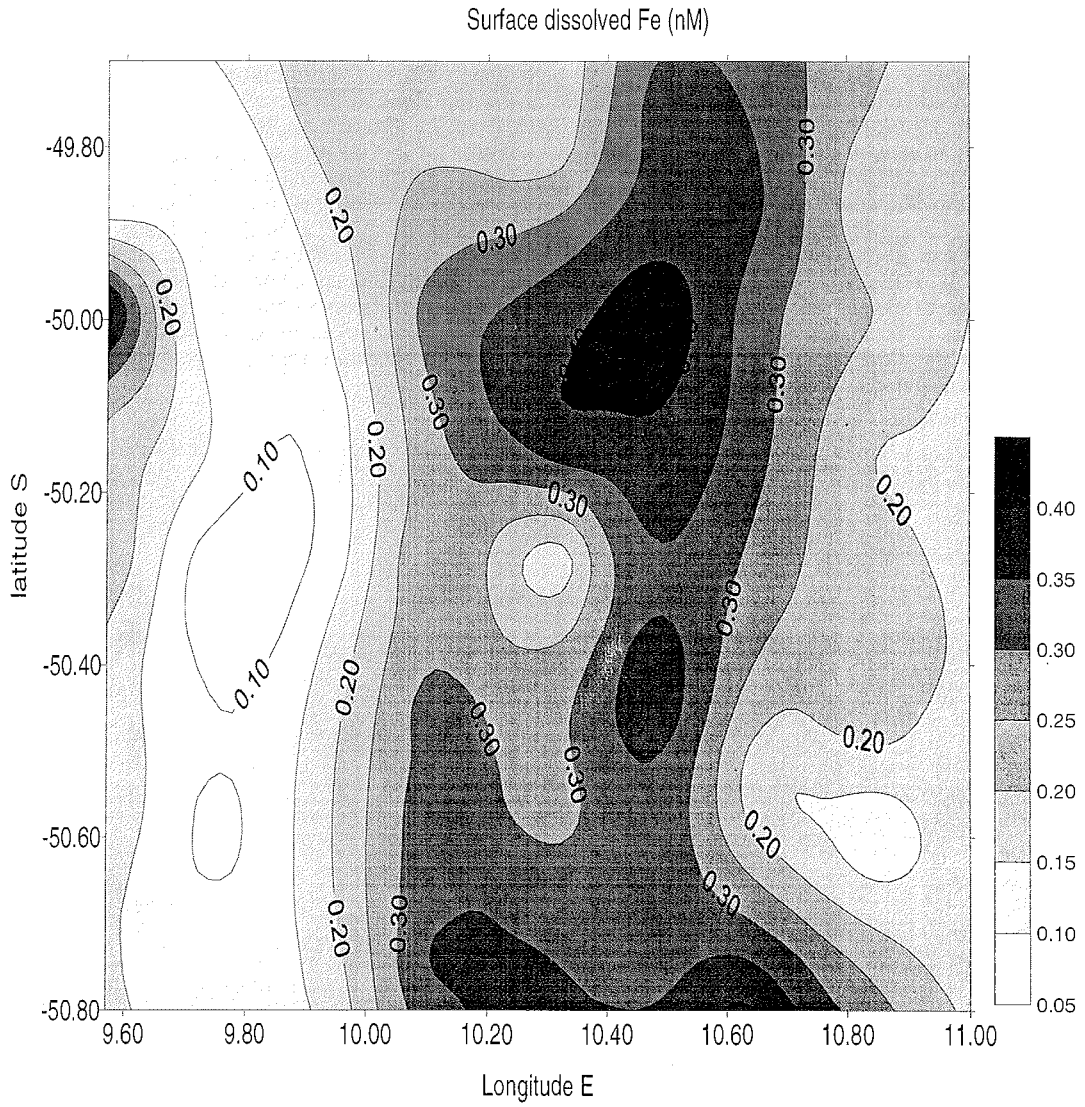

Fig. 9.1 Surface dissolved iron during the Fine Scale Survey.
Dissolved iron concentrations observed in Polar Front surface layer at 11° E were generally an order of magnitude lower than three years before at 6° W, ranging between 0.05 and 0.4 nM in the FSS. However, in the CSS west of the FSS, higher values between 0.4 and 0.8 nM were measured (not shown). These data seem to indicate a belt of high values between 50°30' S and 52° S at 6° E, which might bend off to the north while narrowing to one degree width just north of the FSS at 11° E. From this belt it appears that a tongue of slightly higher iron concentrations extends south in the middle of the FSS. This zone of higher iron values (0.3 - 0.4 nM) appears to be correlated with an area of higher chlorophyll, although higher chlorophyll is also present in places with depleted iron. Two phases of plankton succession might be present: one that was growing on sufficient iron supply and another that was decaying due to iron deficiency.

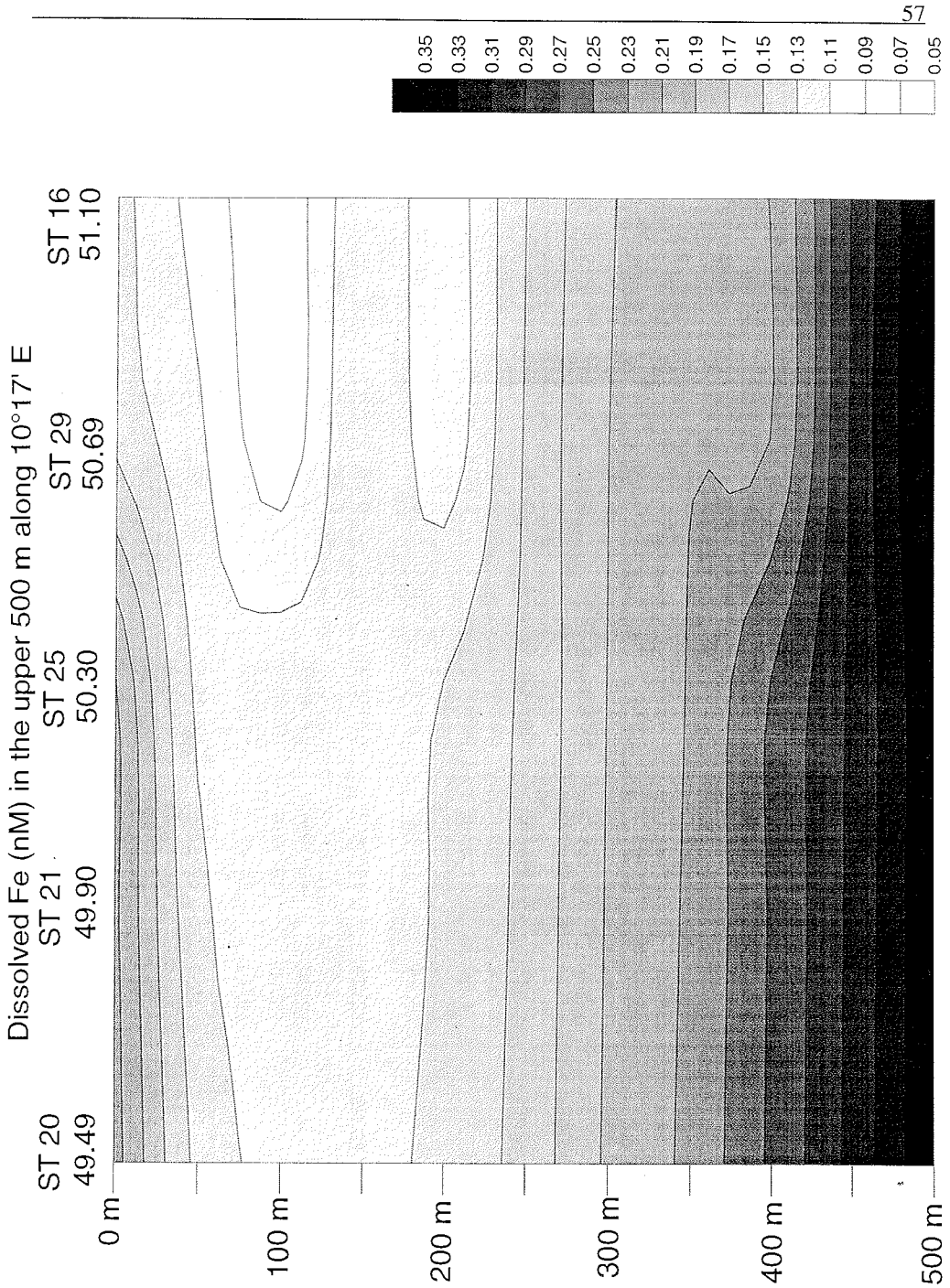

Fig. 9.2 Dissolved iron in the upper 500 m along a transect at 10°17' E.
The vertical profiles from transect 9.2, running from north to south through the middle of the FSS, show some very clear trends. Iron profiles below 100 m show a nutrient-type distribution, with values starting at 0.06 - 0.11 nM rising to uniform values of 0.33 ± 0.02 nM at 500 m (n = 5 stations). The upper 100 m are characterized by remarkable iron enrichment of up to 0.3 nM in the northern part of the transect, consistent with the observed surface tongue of the same concentrations.

surface Fe

date	time	lat S	long E	diss Fe (<0.4µ) (nM)		
23.12.95	23:00			0.75	av.	0.69
	23:10	50°38.3'	04°57.1'	0.63	st.dev.	0.08
	23:20			0.39	mean	0.33
	23:35			0.4	st.dev.	0.06
	23:45			0.32		
	24:00			0.38		
	00:15	50°31.7	05°10.2'	0.23		
	00:30			0.31		
	00:45	50°27'.8	05°18'.5	0.29		
24.12.95	13:30	51°45.6'	06°002'	0.79	av.	0.71
	14:00	51°50.4'	06°00.3'	0.56	st.dev.	0.16
	14:30	51°55.8'	06°00.2'	0.83		
	15:30	52°00.5'	06°07.3'	0.85		
	15:45	52°00'	06°11'	0.52	0.54 (25.12)	
25.12.95	12:00	49°54.3'	07°35.7'	0.38		
				0.24	av.	0.37
	12:30	49°54.4'	07°42.9'	0.44	st.dev.	0.09
	13:10	49°54.6'	07°53.4'	0.46		
	13:30	49°54.6'	07°58.5'	0.32		
	14:00	49°54.5'	08°07.5'	0.53	av.	0.60
	14:35	49°58.1'	08°09.4'	0.55	st.dev.	0.08
	15:10	50°03.5'	08°09.3'	0.74		
	16:15	50°13.9'	08°09.1'	0.55		
	16:50	50°19.2'	08°09.0'	0.63		
	17:15	50°22.9'	08°09.1'	0.58		

Tab. 9.1 Surface dissolved iron along transect 11.2 and 11.3.
Running north after our visit to Neumayer, surface measurements began to show the following pattern. Initial concentrations close to the continent were almost 0.5 nM, decreasing to around 0.2 nM when the distance from the melting sea ice and the continent increased. The crossing of a *Phaeocystis* bloom between 65° S and 63° S concurred with higher iron values of upto almost 0.5 nM. These higher concentrations are likely to originate from melting sea ice. As remarkable was the decrease at 63°30' where the bloom maximum was located, implying active biological uptake or passive adsorption on to the *Phaeocystis* colonies.

One can speculate why iron in this part of the Polar Frontal Zone at this time of year (or even this very year) is lower than the situation encountered three years ago:-

a) - the studied area is more to the east and a dilution of the earlier proposed iron input from the land masses far in the west has resulted in the observed concentrations. Evidence that the Polar Frontal waters have been in contact with continental waters was given by the regular sighting and even catching of healthy *Macrocystis*, a seaweed that grows in sea water a few tens of meters deep.

b) - the study took place about two months later in the season than during the 1992 cruise. It was then early spring (October - November), whereas now it was full summer. This implies that two months longer of primary productivity may have lowered the early season iron concentrations. Whether these are limiting concentrations or that in the end the concentrations will become limiting, remains to be seen.

c) - 1992 happened to be a remarkably rich year for icebergs, and indeed many were spotted in the Polar Front. This year hardly any icebergs were sighted in the Polar Front. This gives new life to the hypothesis that melting of icebergs can play a significant role in enriching the Polar Front with iron. Another possible source of Fe is thought to be its release from the continental shelf. As ^{228}Ra (5.8 years half-life) is released from the seafloor and accumulates to high activities in shallow waters, it is a suitable tracer of shelf waters. We (see Section 17) have collected 19 samples for ^{228}Ra analysis, distributed over the latitude range from 45°S to the Antarctic continent, with emphasis on the region around the Polar Front. Radium was co-precipitated with $BaSO_4$ from 60-Liter samples, and will be analysed by gamma and alpha spectroscopy.

In conclusion, iron concentrations in the Polar Frontal Zone were enhanced, but much less so than previously observed elsewhere in the PFZ. Also, areas of higher iron concentration coincided with higher chlorophyll concentrations. Additional measurements and data analysis are needed to further clarify the observed distribution and behaviour of iron in the Polar Front at this time.

References

Banse, K. (1990). Does iron really limit phytoplankton production in the offshore subarctic Pacific? Limnology and Oceanography, 35, 772 - 775.

Bruland, K. W., Orians, K. J., & Cowen, J. P. (1994). Reactive trace metals in the stratified central North Pacific. Geochimica et Cosmochimica Acta, 58(15), 3171 - 3182.

Buma, A. G. J., de Baar, H. J. W., Nolting, R. F., & van Bennekom, A. J. (1991). Metal enrichment experiments in the Weddell - Scotia Seas: Effects of iron and manganese on various plankton communities. Limnology and Oceanography, 36(8), 1865 - 1878.

de Baar, H. J. W. (1994). von Liebig's law of the minimum and plankton ecology. Progress in Oceanography, 33, 347 - 386.

de Baar, H. J. W., Buma, A. G. J., Nolting, R. F., Cadée, G. C., Jacques, G., & Tréguer, P. J. (1990). On iron limitation in the Southern Ocean: experimental observations in the Weddell and Scotia Seas. Marine Ecology Progress Series, 65, 105 - 122.

de Baar, H. J. W., de Jong, J. T. M., Bakker, D. C. E., Löscher, B. M., Veth, C., Bathmann, U., & Smetacek, V. (1995). Importance of iron for plankton blooms and carbon dioxide drawdown in the Southern Ocean. Nature, 373, 412 - 415.

Donaghay, P. L., Liss, P. S., Duce, R. A., Kester, D. R., Hanson, A. K., Villareal, T., Tindale, N. W., & Gifford, D. J. (1991). The role of episodic atmospheric nutrient inputs in the chemical and biological dynamics of oceanic ecosystems. Oceanography, 4(2), 62-70.

Duce, R. A., & Tindale, N. W. (1991). Atmospheric transport of iron and its deposition in the ocean. Limnology and Oceanography, 36(8), 1715-1726.

Dugdale, R. C., & Wilkerson, F. P. (1990). Iron addition experiments in the Antarctic: a reanalysis. Global Biogeochemical Cycles, 4(1), 13 - 19.

Gran, H. H. (1931). On the conditions for the production of plankton in the sea. Rapports et Proces verbaux des Réunions, Conseil International pour l'Exploration de la Mer, 75, 37 - 46.

Lancelot, C., Mathot, S., Veth, C., & de Baar, H. J. W. (1993). Factors controlling phytoplankton ice-edge blooms in the marginal ice-zone of the northwestern Weddell Sea during sea ice retreat in 1988: field observations and mathematical modelling. Polar Biology, 13, 377 - 387.

Landing, W. M., & Bruland, K. W. (1987). The contrasting biogeochemistry of iron and manganese in the Pacific Ocean. Geochimica et Cosmochimica Acta, 51, 29 - 43.

Landing, W. M., Haraldsson, C., & Paxéus, N. (1986). Vinyl polymer agglomerate based transition metal cation chelating ion-exchange resin containing the 8-hydroxyquinoline functional group. Analytical Chemistry, 58, 3031 - 3035.

Löscher, B. M., de Jong, J. T. M., de Baar, H. J. W., Veth, C., & Dehairs, F. (1996). The distribution of iron in the Antarctic Circumpolar Current. Deep-Sea Research, (in press)

Martin, J. H., Coale, K. H., Johnson, K. S., Fitzwater, S. E., Gordon, R. M., Tanner, S. J., Hunter, C. N., Elrod, V. A., Nowicki, J. L., Coley, T. L., Barber, R. T., Lindley, S., Watson, A. J., van Scoy, K., Law, C. S., Liddicoat, M. I., Ling, R., Stanton, T., Stockel, J., Collins, C., Anderson, A., Bidigare, R., Ondrusek, M., Latasa, M., Millero, F. J., Lee, K., Yao, W., Zhang, J. Z., Friederich, G., Sakamoto, C., Chavez, F., Buck, K., Kolber, Z., Greene, R., Falkowski, P., Chisholm, S. W., Hoge, F., Swift, R., Yungel, J., Turner, S., Nightingale, P., Hatton, A., Liss, P., & Tindale, N. W. (1994). Testing the iron hypothesis in ecosystems of the equatorial Pacific Ocean. Nature, 371, 123 - 129.

Martin, J. H., Gordon, R. M., & Fitzwater, S. E. (1990). Iron in Antarctic waters. Nature, 345, 156 - 158.

Nolting, R. F., de Baar, H. J. W., van Bennekom, A. J., & Masson, A. (1991). Cadmium, copper and iron in the Scotia Sea, Weddell Sea and Weddell/Scotia Confluence (Antarctica). Marine Chemistry, 35, 219 - 243.

Nolting, R. F., & de Jong, J. T. M. (1994). Sampling and analytical methods for the determination of trace metals in surface seawater. International Journal of Environmental Analytical Chemistry, 57, 189 - 196.

Obata, H., Karatani, H., & Nakayama, E. (1993). Automated determination of iron in seawater by chelating resin concentration and chemiluminescence detection. Analytical Chemistry, 65, 1524 - 1528.

Powell, R. T., Whitney King, D., & Landing, W. M. (1995). Iron distributions in surface waters of the South Atlantic. Marine Chemistry, 50, 13 - 20.

Price, N. M., Andersen, L. F., & Morel, F. M. M. (1991). Iron and nitrogen nutrition of equatorial Pacific plankton. Deep-Sea Research, 38(11), 1361 - 1378.

Ruud, J. T. (1930). Nitrates and phosphates in the Southern Seas. Rapports et proces verbaux des réunions, Conseil International pour l'Exploration de la Mer, 5, 347 - 360.

Westerlund, S., & Öhman, P. (1991). Iron in the water column of the Weddell Sea. Marine Chemistry, 35, 199 - 217.

10. BIOGENIC PRODUCTION OF NEUTRAL AND IONIC METHYL HEAVY METAL SPECIES IN POLAR WATER REGIONS

O. Schedlbauer

Introduction

In polar regions, the determination of heavy metal concentrations have been carried out, but little is known about their speciation. Different species of have different properties, especially with regard to geochemical transport, toxicity or bioavailability. Therefore it is necessary to identify and determine heavy metal species to acquier more precise and detailed information on, for example, geochemical cycles and their global sources and sinks. Biomethylation is one such important biogeochemical process.

In anthropogenically influenced regions, it is difficult to relate organo-metal compounds in the environment to definite primary sources. It is however, in principle, possible to prove the biogenic production of such compounds in the "clean room" environment of the Antarctic. As such, it is also possible to determine the contribution of these compounds to the global biogeochemical cycle of heavy metals.

For the determination of neutral and ionic methylated heavy metal compounds, the elements mercury, lead, cadmium and thallium need to be considered. High enrichment factors, especially for cadmium and lead in Antarctic snow and aerosol samples (Radlein & Heumann, 1992) suggest an emission of volatile organic heavy metal compounds from polar seas. Since the south polar sea is an important source for the biomethylation of bromine, iodine, sulphur and selenium (Reifenhauser & Heumann 1992, Tanzer & Heumann 1990,1992), it can be assumed also, that biomethylation of heavy metals is also taking place in polar seas. Their high volatility causes high exchange rates of methylated heavy metal compounds between the ocean and the atmosphere and because of this, biomethylation is an important process for the biogeochemical cycle of heavy metals.

Methods

The determination of cadmium and lead species was carried out by DPASV (Differential Pulse Anodic Stripping Voltammetry) on board RV "*Polarstern*" during the cruise. With the help of a purge and trap system and GC-CVAFS (Gas Chromatography-Cold Vapour Atomic Fluorescence Spectrometry), mercury species will be examined in the home laboratory. Similarly, the corresponding thallium species will be assessed later with IDMS (Isotope Dilution Mass Spectrometry).

Sampling

A number of different sea water samples were analysed. Surface samples were taken from the ship's membrane pump (depth 8m) and from a surface torpedo (NIOZ, depth 1m). To obtain water from various depths, the CTD-rosette (AWI) and the kevlar dip system (NIOZ) were used. Aerosol samples were also collected onto glass fibre filters on the bridge-deck for later examination in the home laboratory. Snow samples from the Antarctic will also be analysed after June 1996.

Results

During the cruise, samples from 39°S to 70°S were analysed on board. In 15 - 20 % of these samples, methylated compounds of Cadmium and Lead were detectable as the ionic compounds $MeCd^+$ and Me_3Pb^+. The north-south-profiles are shown in figures 10.1 and 10.2.

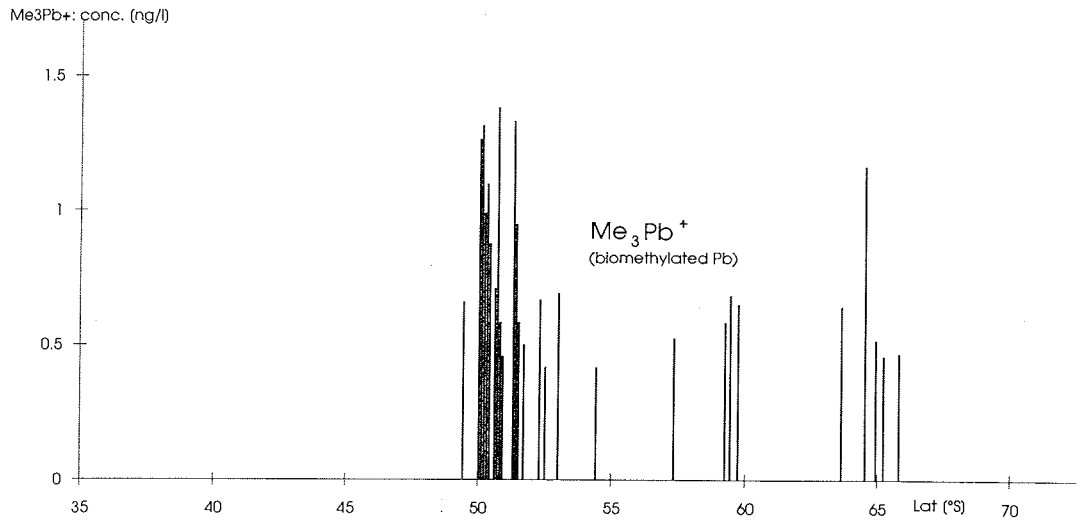

Fig. 10.1 North/South profile of methylated lead during ANT XIII/2

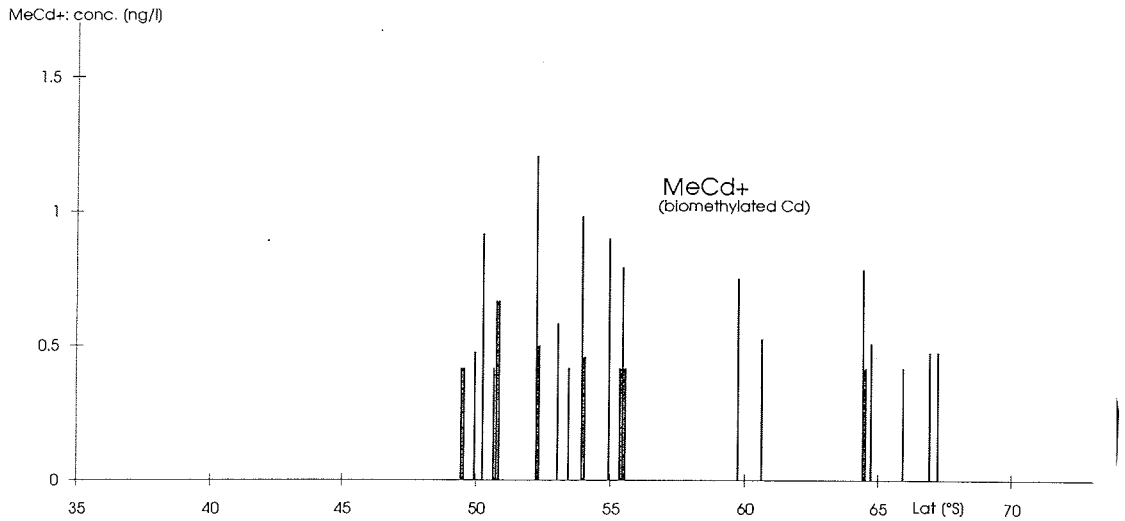

Fig. 10.2 North/South profile of methylated Cd during ANT XIII/2

As shown, methylated lead was frequently detected in the Polar Front region which correlates well with the high biological activity of this area. Methylated cadmium was also frequently detected in this area, but also a few degrees further south in the Antarctic Circumpolar Current. This may imply different biological sources for these two species. Less frequently, methylated cadmium and lead were detected in the area of 60°S and 64°S where the peaks at 64°S correlate with high chlorophyll biomass in this area as well.

Depth profiles from 10m to 500m also show the correlation between methylated compounds and biological activity (figures 10.3 and 10.4). In the upper water column, where chlorophyll and bacterial concentrations are high, it is possible to detect methylated compounds, but not at greater depths where there is less biological activity.

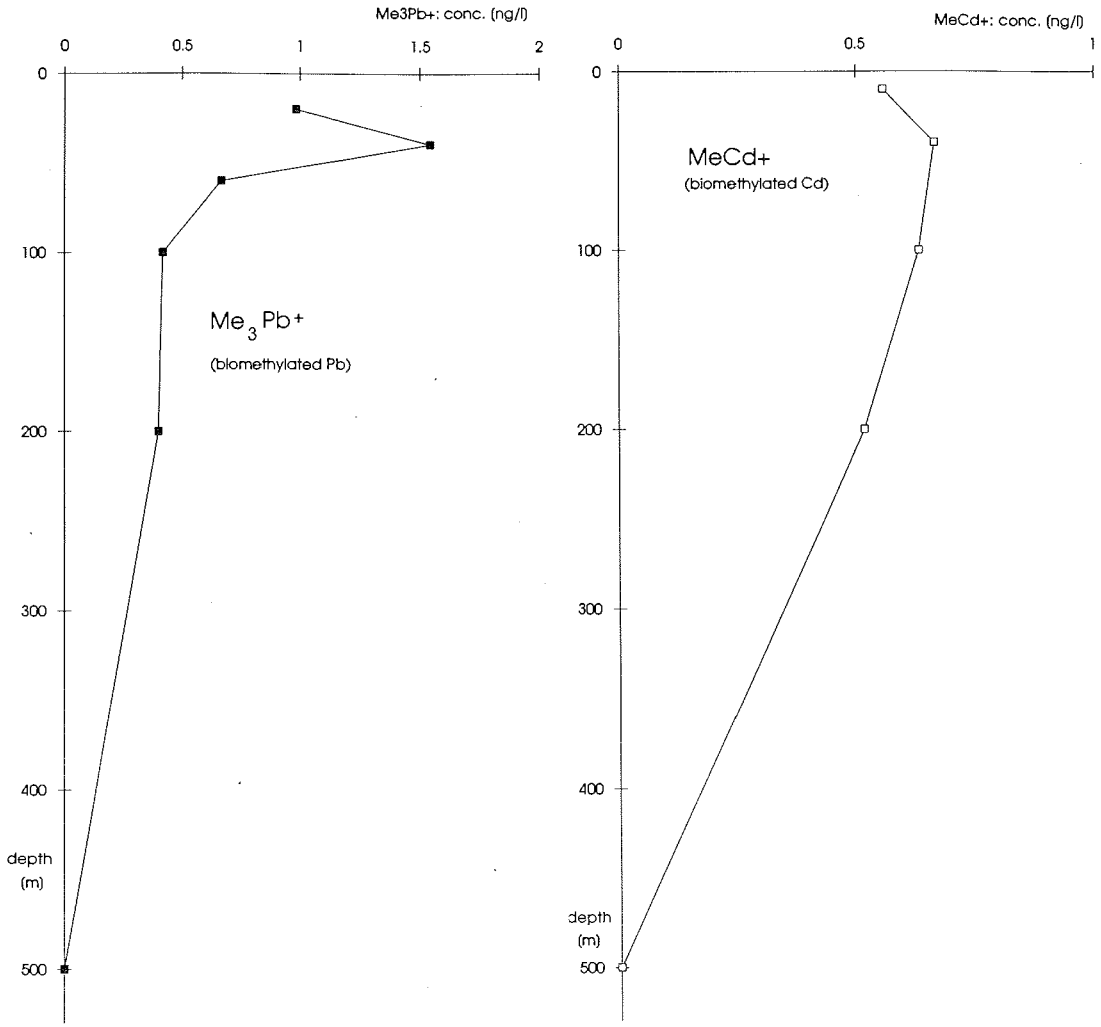

Fig. 10.3 and 10.4 Depth profiles, Sta. 9 and 32 during ANT XIII/2

In summary, it is very probable that the biomethylation of heavy metals is taking place in marine systems, including the Polar Front region of the Southern Ocean, although the biological species that produce these compounds are still unknown

11. THE CARBON DIOXIDE SYSTEM IN ANTARCTIC WATERS

M. Stoll, I. Zondervan, E. de Jong

Introduction

Modifications to the global carbon cycle through fossil fuel combustion and changes in land use have led to an increase in the concentration of atmospheric carbon dioxide which has the potential to increase the greenhouse effect of the atmosphere.
Most of the oceans are able to take up this excess CO_2, but at a rate vastly slower than the one associated with anthropogenic perturbations, due to the renewal times of deep and bottom waters of the oceans which are typically of the order of a 1000 years. Thus, studies in areas where interactions between deep and surface oceans occur, such as the Weddell Sea, are vital for the study of CO_2 uptake and re-distribution.
An objective of this project was to gain knowledge of the CO_2 distribution in the Weddell Sea, where the initial properties of a major part of the abyssal world oceans are generated. Another objective was to determine the potential of Antarctic waters to take up atmospheric CO_2. This is especially important for the frontal regions of the Antarctic Circumpolar Current (ACC) and for regions of seasonal ice cover. Data from this cruise will be combined with data from previous cruises. The ensuing CO_2 database from the Weddell Sea and the ACC may also be used in a modelling effort in which carbon transport and air-sea gas exchanges are calculated.

Sampling and Methods

Work at sea
The cruise started from Cape Town and several sections were studied in detail. Mostly underway measurements were performed for the parameters TCO_2 and pCO_2. At some parts also alkalinity was determined underway. At selected stations TCO_2 determinations for the watercolumn were done. A coarse grid section and a fine-scale grid were sampled in detail.

TCO_2
TCO_2 (total inorganic carbon content) was determined by a high-precision coulometric method and automated sample stripping system. Briefly, the method is as follows. A sample of seawater is acidified with phosphoric acid and stripped with high purity N_2 gas. The carrier gas plus extracted CO_2 is led through a solution containing ethanolamine and an indicator. This solution is electrochemically back-titrated to its original colour and the amount of Coulombs used is equivalent to the amount of CO_2 in the sample. Data obtained were processed onboard and calibrated against an internationally recognized TCO_2 standard (Dickson). Final data will be made available after postprocessing the data in the shore laboratory.

pCO_2
Continuous measurements of the partial pressure of CO_2 (pCO_2) in water and marine air were done using an infra-red analyzer (Li-Cor). A continuous water supply is led through an equilibrator where approximately every 4 to 5 minutes the headspace gas is analyzed for its CO_2 content thus giving pCO_2 in the surface water. Marine air was pumped continuously from the crows nest into the laboratory and subsampled after every fourth equilibrator reading. The equipment was calibrated with reference gases, traceable against NOAA standard gases. Obtained data were processed onboard. Final data will be available pending recalibration of the reference gases ashore.

Preliminary results

Total CO_2 and pCO_2.
Some preliminary data are plotted versus latitude where a comparison is made between 4 sections (-70°S to -50°S), running from the Coarse Scale Survey (CSS) region towards Neumayer. The first pair of sections (figures 11.1 & 11.2) fell in the time period 09/12 to 14/12 and 19/12 to 23/12.

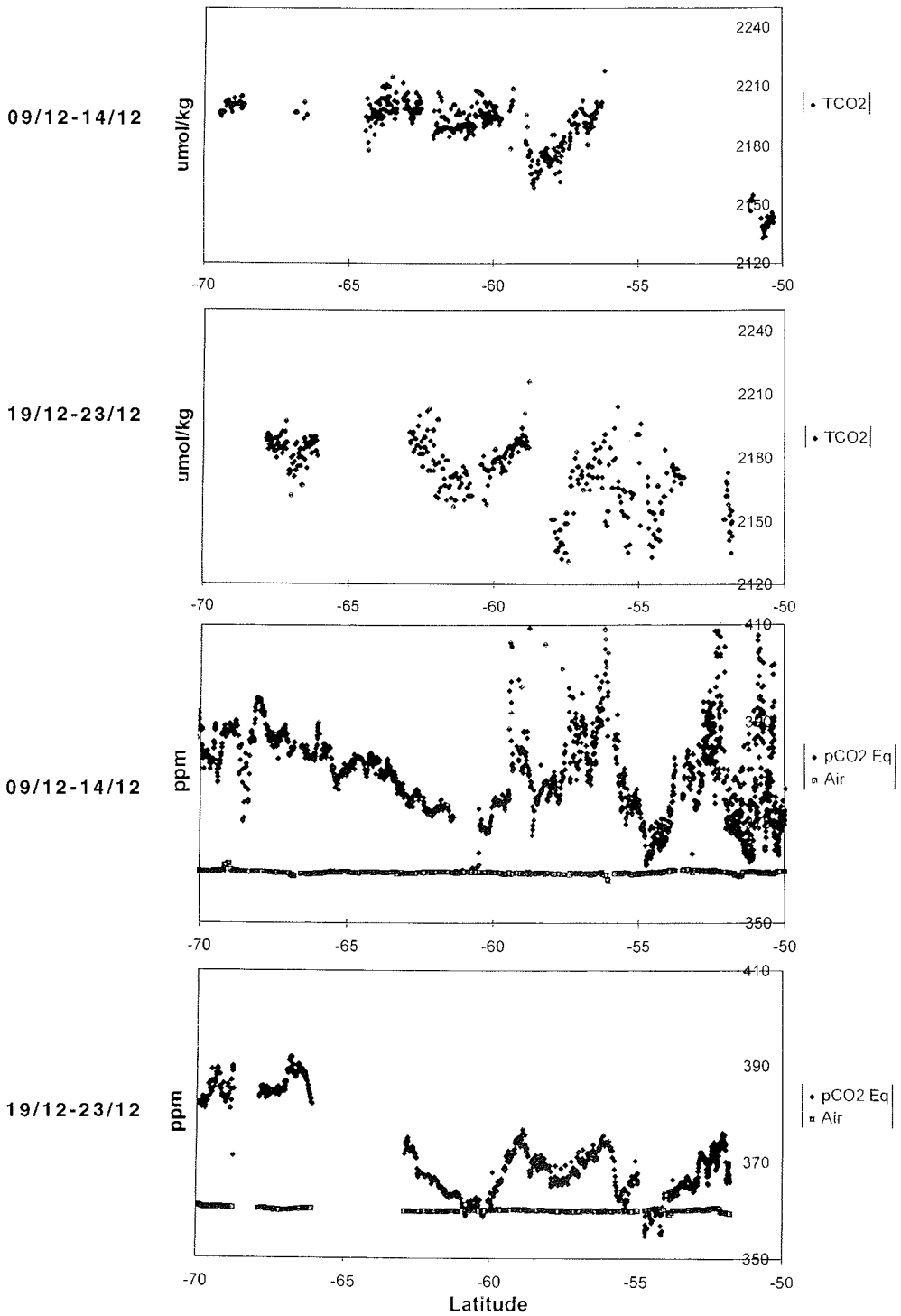

Figs. 11.1-11.4 TCO_2 (Fig. 11.1, 11.2) and pCO_2 (11.3, 11.4) from surface water registration of first two sections between 9 to 14 and 19 to 23 Dec. 95, respectively

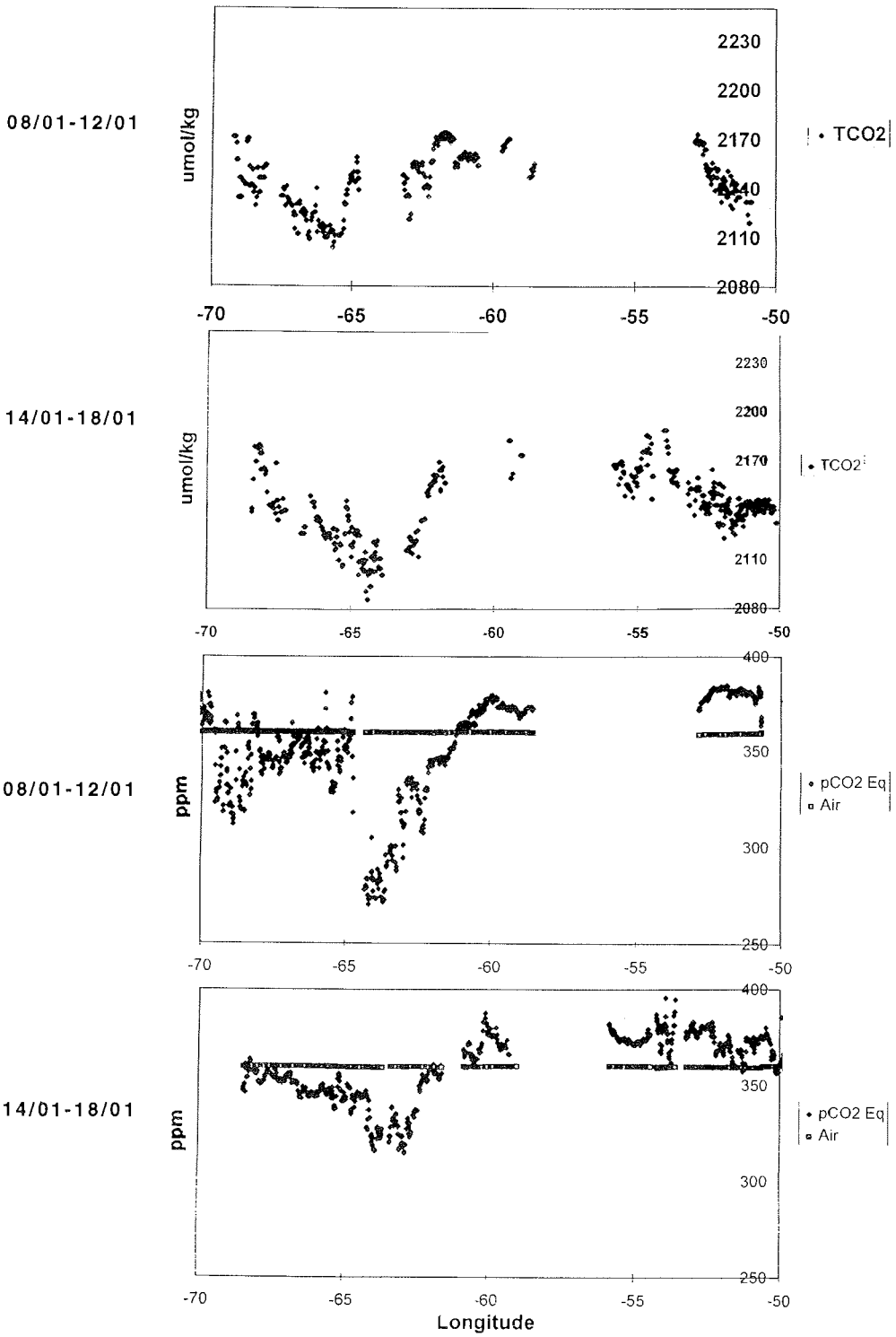

Figs. 11.5-11.8 TCO_2 (Fig. 11.5, 11.6) and pCO_2 (11.7, 11.8) from surface water registration of first two sections between 8 to 12 and 14 to 18 Jan. 96, respectively

TCO_2 was variable during both time periods but generally higher in the colder water regions south of 60°S. Aqueous pCO_2 was continuously oversaturated (relative to atmospheric values) with values as high as 400 µatm. Potential correlations with chlorophyll will be investigated later. On the return from Neumayer, less than two weeks later, pCO_2 in the region 55°S to 62°S was found to be about 10 ppm lower. Such observed changes could very well be mediated by local hydrographic structures.

The next pair of sections (08/01 to 12/01 and 14/01 to 18/01) were more eastwards but also extending from the CSS region to Neumayer and back (figures 11.3 & 11.4). Here, somewhat lower values for TCO_2 (about 20 to 25 µmol/kg lower) were recorded relative to the more westerly section.

The region south of 62°S was characterized by rather lower surface TCO_2 values in the range 2120 - 2140 µmol/kg. Though present, concentration changes with time were less pronounced than for the first section pair.
Surprisingly, pCO_2 values in the region south of 62°S were generally undersaturated while north of 62°S, values were oversaturated. However, close to the ice edge, values approached equilibrium. What clearly emerges is that nearly adjacent sections display considerable local variability mediated not only by local hydrography but also by local biological activity.

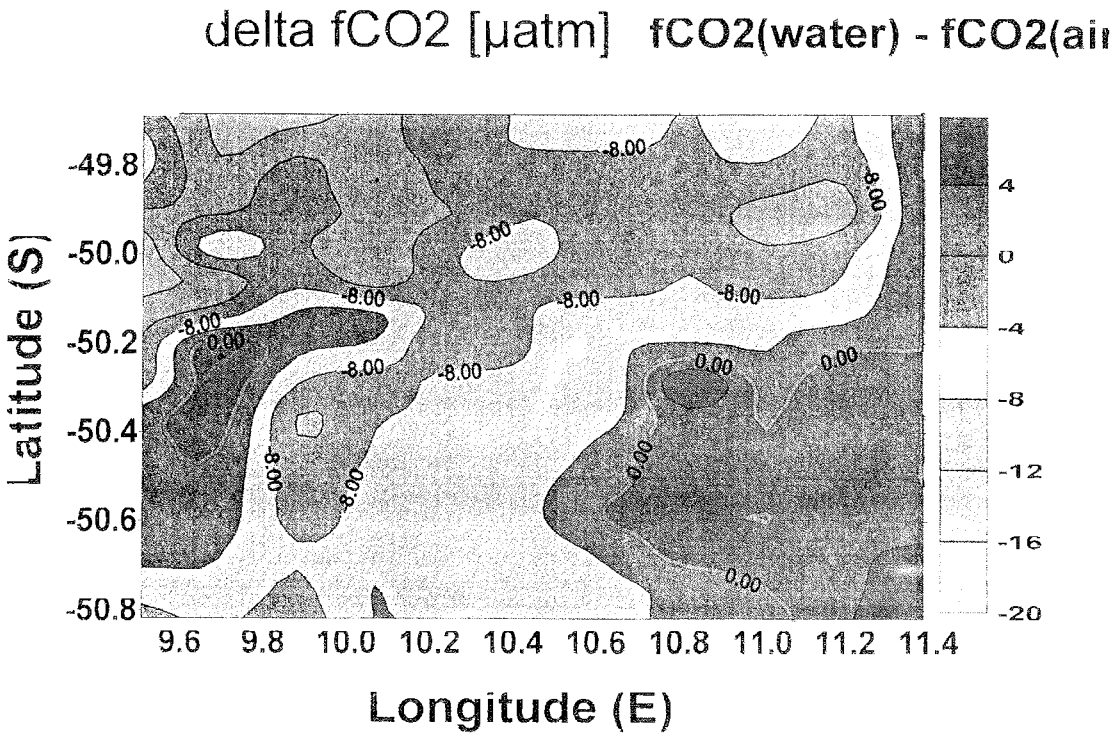

Fig. 11.9 Contouring of the pCO_2 distribution (Fig. 11.9) over the Fine Scale Survey (FSS) region showed a clear correlation with surface chlorophyll concentrations

12. PHYTOPLANKTON AND HETEROTROPHIC PROTIST COUNTS

C. Klaas, S. Kühn, S. Menden-Deuer, T. Reynarson, V. Smetacek

Introduction

The aim of this investigation was to determine the composition of the phytoplankton community (>20µm) and to estimate the relative abundance of dominant species with high spatial and temporal resolution. In this study, samples were assessed immediately after preservation. This unique approach counteracts the degeneration of preserved phytoplankton samples that occurs over time. As a result, chain lengths and condition of the cells could be assesed with fair certainty that the cells had not been affected by preservation. A further aim of this study is to link phytoplankton community structure and morphology with measurements of primary production and with SeaSoar derived data on the physical and biological environment.

Materials and methods

Sampling

This investigation was carried out during the SeaSoar deployment of coarse-grid transect 6 and fine-scale transect 8. Hourly surface water samples were taken with a stainless steel bucket lowered into the water from the aft deck of the ship. The bucket was judged to be the least destructive sampling method after examination of samples from the seawater pump on board revealed some damage to the cells. Three liters of the bucket sample were concentrated to 50ml by gently pouring the sample through a 20 µm mesh. This sample was then transferred to a settling chamber. To facilitate rapid settlement in the chamber, samples were preserved with Lugol's solution and optionally decoloured with sodiumthiosulfate. Additionally, a 200ml non-concentrated sample was preserved with 20% formalin (end concentration 3%) to be processed by Utermöhl-counting technique at the home laboratory in order to assess the <20µm component.

Analysis

Immediately after the sample was placed into a settling chamber, it was examined with a Zeiss inverted microscope at magnifications between 63x and 400x. To counteract the subjectivity of the assessment procedure, microscopists worked in overlapping shifts and their counts were cross-correlated.

The overall density of the sample was rated on a scale from 0 to 5 (highest), with 0.5 step intervals. The presence of frequently occurring plankton species was noted (see list below). The abundance of dominant species was rated as a percentage of total biomass for each sample. Independent of dominance, the relative abundance of following species was assessed whenever present: *Fragilariopsis kerguelensis*, *Chaetoceros atlanticum, Pseudonitzschia* cf. *lineola* and *Corethron criophilum*. The occurrence of *Phaeocystis* sp., *Acantharia* sp., thecate and athecate dinoflagellates, *Ceratium* sp., *Dinophysis* sp., foraminifera, copepods and nauplii was recorded.

The dominant chain-forming diatoms, *Fragilariopsis kerguelensis*, *Chaetoceros atlanticus* and *Pseudonitzschia* cf. *lineola* were examined with respect to the (i) chain-lengths, (ii) number of intact and empty cells per chain and (iii) number of dividing cells. Likewise, for *Corethron criophilum*, the number of intact, empty, dividing, auxospore and gametangial cells were determined.

Results

Phytoplankton blooms were either dominated (not homogeneously) by a group of *Chaetoceros atlanticus*. and *Chaetoceros bulbosum* (the latter species to be confirmed), *Pseudonitzschia* cf. *lineola* or *Thalassiotrix* spp. The south-east corner of the small scale grid was characterised by very low overall phytoplankton densities (Fig. 12.1). Similarly, there was a low density patch in the south

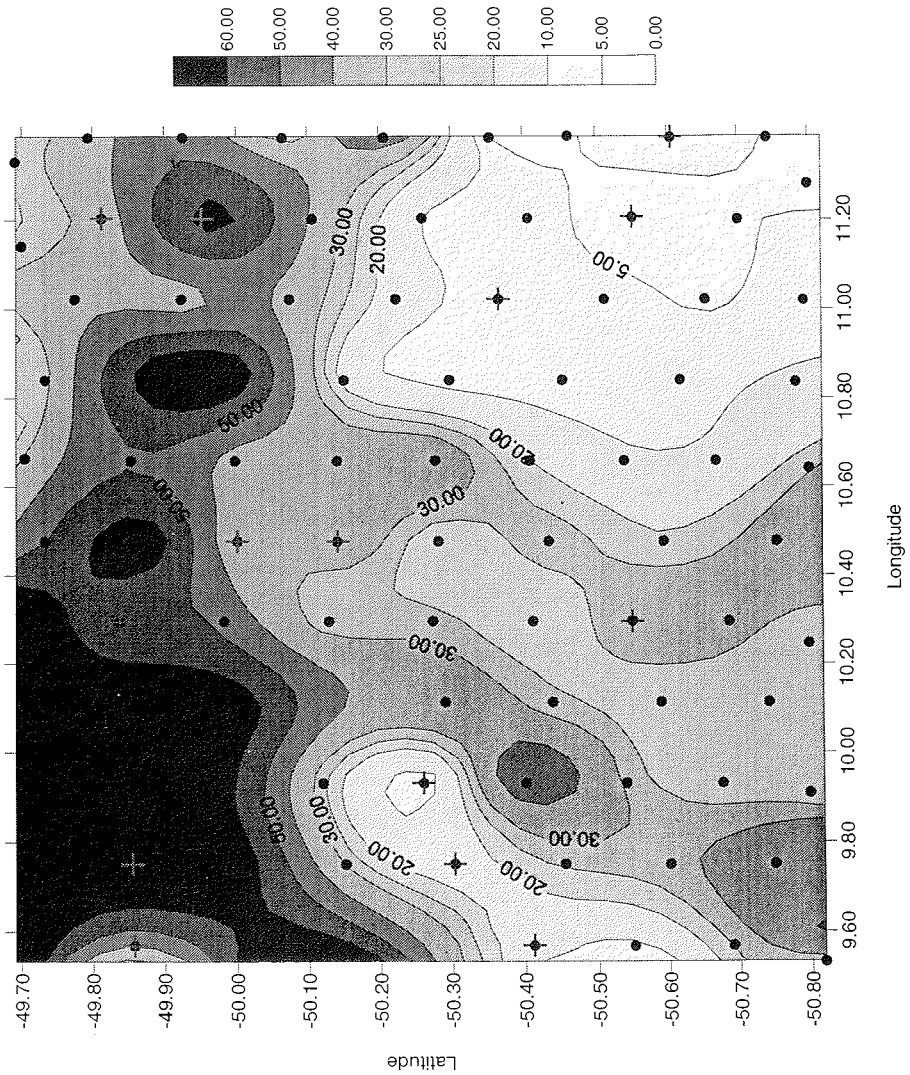

Fig. 12.1 Phytoplankton biomass of diatom species > 20µm (µgC/l) in the area of the small scale grid. Positions marked with a cross (⊕) refer to the calibration point where qualitative and quantitative microscopical analysis of the phytoplankton species was carried out. Dots (•) refer to positions where qualitative data were obtained.

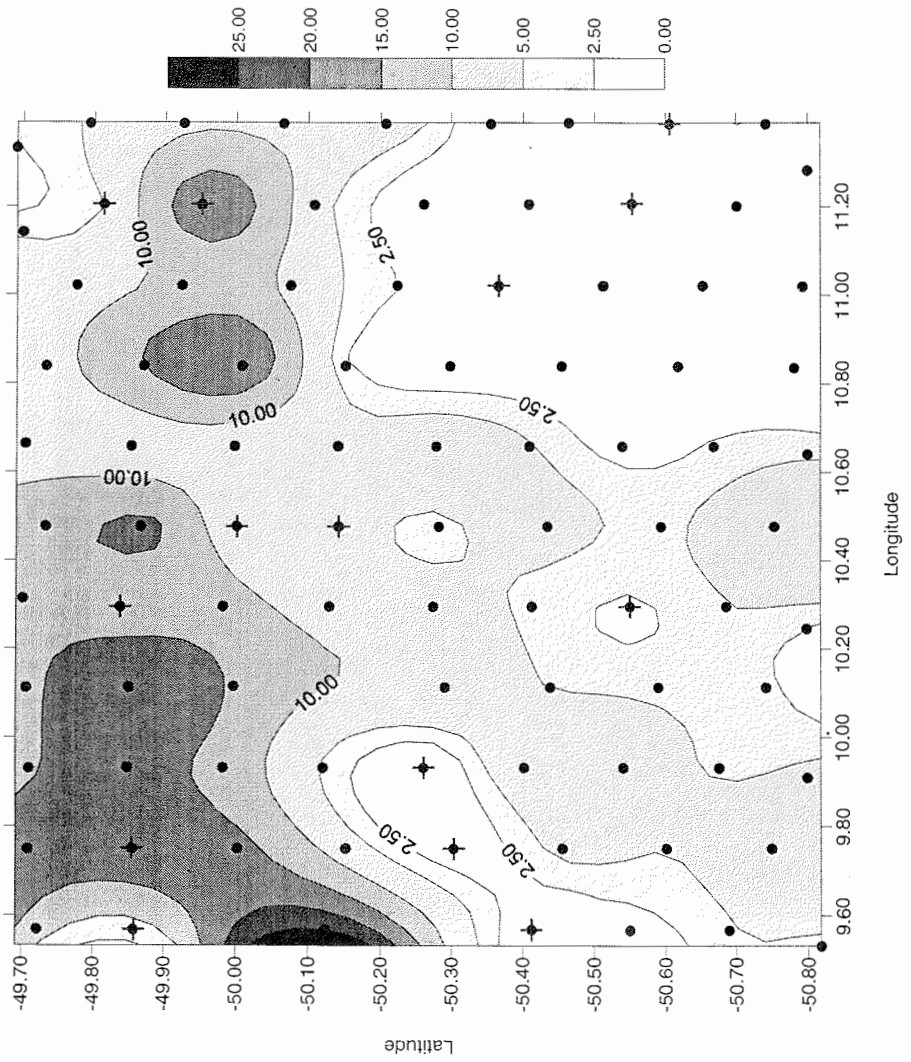

Fig. 12.2 *Chaetoceros atlanticus* and *Chaetoceros aequatorale* biomass (µgC/l) in Small Scale Grid survey area

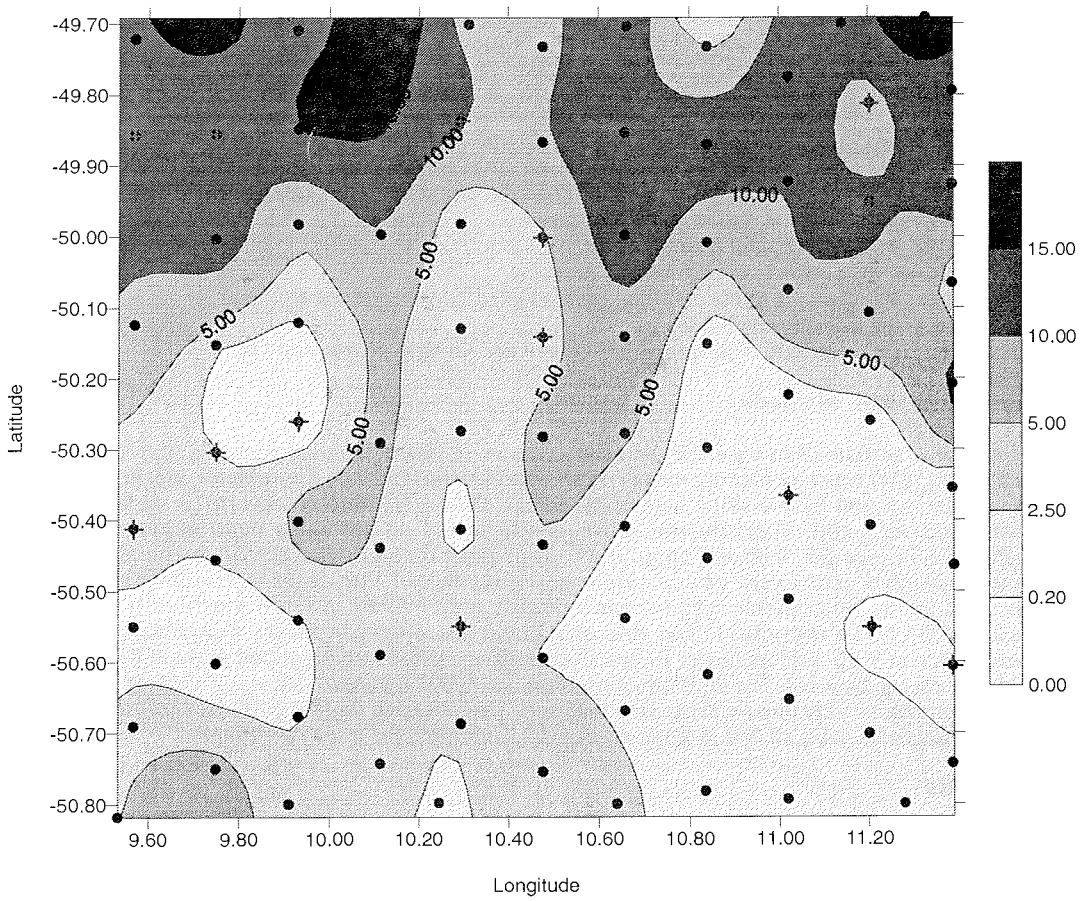

Fig. 12.3 Thalassiothrix spp. biomass (µgC/l) in Small Scale Grid survey area

western region of the grid. *Fragilariopsis kerguelensis* and *Corethron criophilum* dominate these low density patches but nonetheless these species occurred in low numbers almost homogeneously over the entire small scale grid, except for one low density tongue in the south west corner. Thus the apparent dominance of *Fragilariopsis kerguelensis* and *Corethron criophilum* is due rather to the absence of other species.
Comparison of the surface density and the distribution of *Chaetoceros atlanticus* (Fig. 12.2) and *Chaetoceros bulbosum* show great similarity which identifies this group as the overall dominating species. In contrast, *Thalassiothrix* spp. biomass show distinct maxima in the plankton rich northern part of the small scale grid (Fig. 12.3).
Rhizosolenia chunii and *R. cylindrus* contributed about 5% each to the diatom composition. *Dactylosolen antarctica* was identified in all samples but never contributed significantly to the biomass. The different species of the *Chaetoceros* spp. group were homogeneously present with little fluctuation in their composition and abundance but exhibiting low numbers: *(C. aequatoriale,, C. convolutus, C. criophilum, C. dichaeta, C. neglectum, C. socialis,)*. Other diatoms; *Corethron inerme, Eucampia* spp., *Membraneis* spp., *Pleurosigma* spp., *Pseudonitzschia heimii, Proboscia alata, Rhizosolenia antennata, Thalassiosira* spp. and *Thrichotoxon* spp. were noted but were relatively insignificant.

13. SURFACE PIGMENT CONCENTRATIONS

U. Bathmann, I. Hense, M. Nacken, T. Reynarson

Introduction

Surface chlorophyll concentrations may indicate the total amount and spatial extent of phytoplankton biomass in the sea. The phytoplankton pigment chlorophyll *a* is measured indirectly, *in situ* , by stimulating the phytoplankton with UV-light and record the fluorescence signal. At any time this signal is dependent on:
i) the amount of chlorophyll *a* (= biomass)
ii) species composition (e.g. chlorophyll per cell)
iii) physiological status of the cell (e.g. light adapted, growing phase etc.) and
iv) time of the day (photoinhibition).
Thus, the fluorescence to chlorophyll ratio may vary strongly in space and time.

Sampling and Methods

Underway surface (8 m water depths) fluorescence of phytoplankton pigments (expressed as chlorophyll *a*) was recorded by means of a Turner Design (TD 10) fluorometer attached to the sea water system by the ships membrane pump. Data were obtained every 10 seconds and averaged in 5 min. intervals and subsequently stored on the ships data logging system (POLDAT) together with the appropriate ships position and other physical, chemical and meteorological data. Every 3 hours, triplicates of normally 1 liter of sea water (drained from a bypass to the fluorometer system) were filtered onto Whatman GF/F glasfibre filters for calibration of the instrument. The chlorophyll and phaeopigment values were obtained after extraction in 90 % acetone/water as described after the procedure described in the JGOFS core measurement protocol. The determination limit was 0.001 µg chl*a*/l. Means of chlorophyll and phaeopigments were entered daily into data files (one for each day) in EXCEL 4.0 format. For the surface data base, all data were re-arranged according to the respective transect.

Results

Surface chlorophyll peaks along the transects to and from Neumayer (Figs. 13.1 and 13.2) indicate the surface biological expression of several fronts: the Subtropical Convergence (STC), the Subantarctic Front (SAF), the Antarctic Polar Front (APZ), the Antarctic Current - Weddell Front (AWF) and the Coastal Boundary Front (CBF).
In the south at the AWF and towards the CBF, sea-ice cover exceeded 50% (south of 65°30' S on transect 5, Fig. 13.1.; and south of 69°S on transect 11, Fig. 13.2) and caused the fluorescence signal to fluctuate wildly as sea-ice algae were sucked into the system when the ships bow crushed through the ice.
By comparing transects 5 and 10 the development of a phytoplankton bloom can be seen at about 63° to 65° south. Vertical profiles taken at St. 30 (63°S) indicated water column stabilisation at 18 m depth caused by a strong pyncnocline. The species composition of this bloom was dominated by *Phaeocystis* and several diatom species.
The surface distribution of chlorophyll *a* derived from fluorescence in the large scale grid and for the small scale grid is shown in Figs. 13.3 and 13.4. The pattern can be described as follows: In the north, the occurrence of a band of relatively high chlorophyll *a* values coincides with the position of the Polar Front (see Section 3). In the south-west and south-east corners of the grids, areas of relatively low chlorophyll concentrations were observed (see Section 12 for a detailed description of the differences in species composition in these two areas). The data for the composition of Figs. 13.3 and 13.4 are obtained along the cruise track with interpolation of the data between cruise lines. The interpolation results from the routine "Minimum Curvature" of the MS-DOS programme (SURFER). Tradeoffs of this routine are interpolation errors at the borders of the interpolation area. However, along the cruise tracks, the results of this interpolation are in good agreement with the observations.

Fig. 13.1 to 13.4 Surface sea water salinities and chlorophyll fluorescence along 4 transects between the main investigation area at the Polar Front and the Antarctic Continent at Neumayer Station

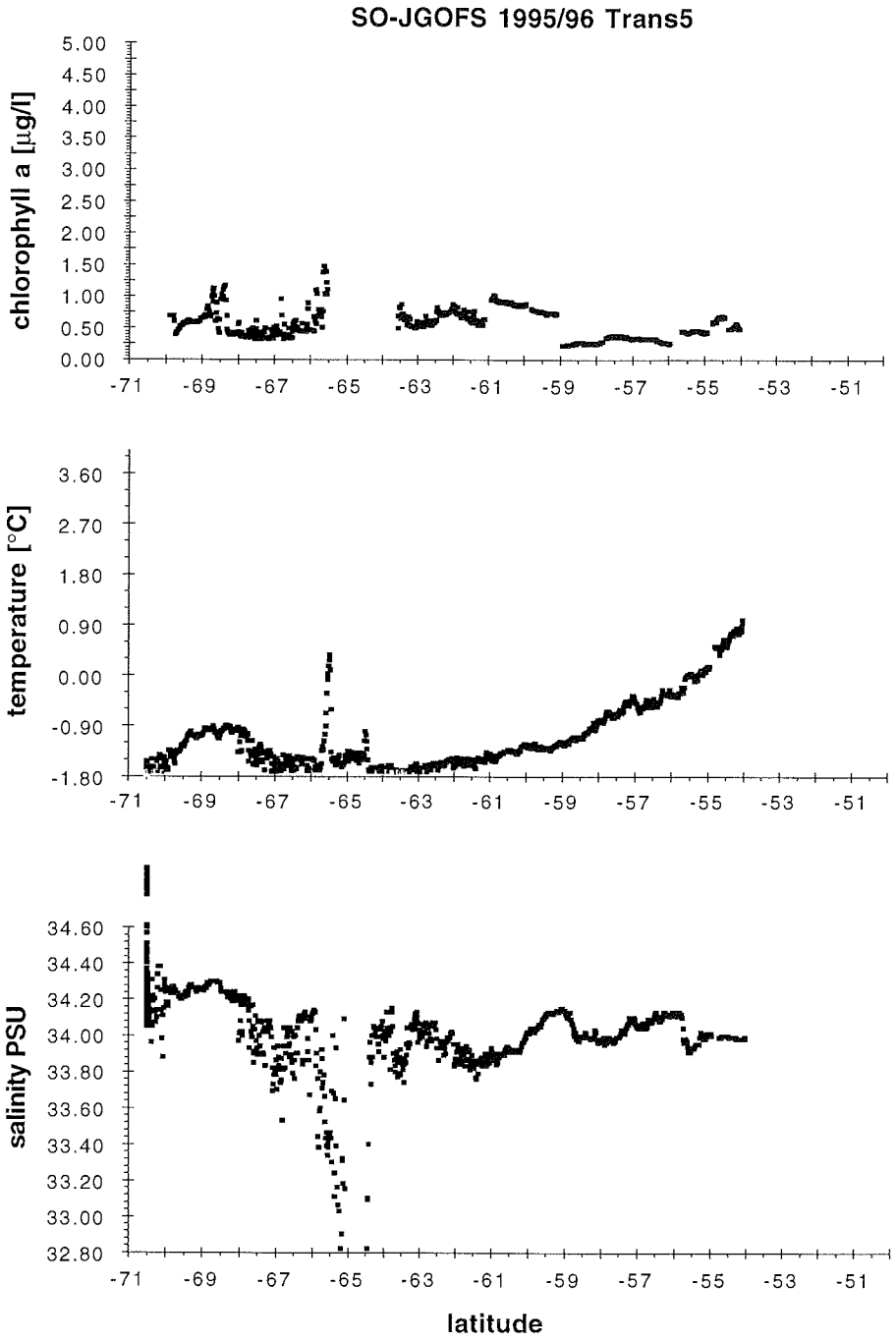

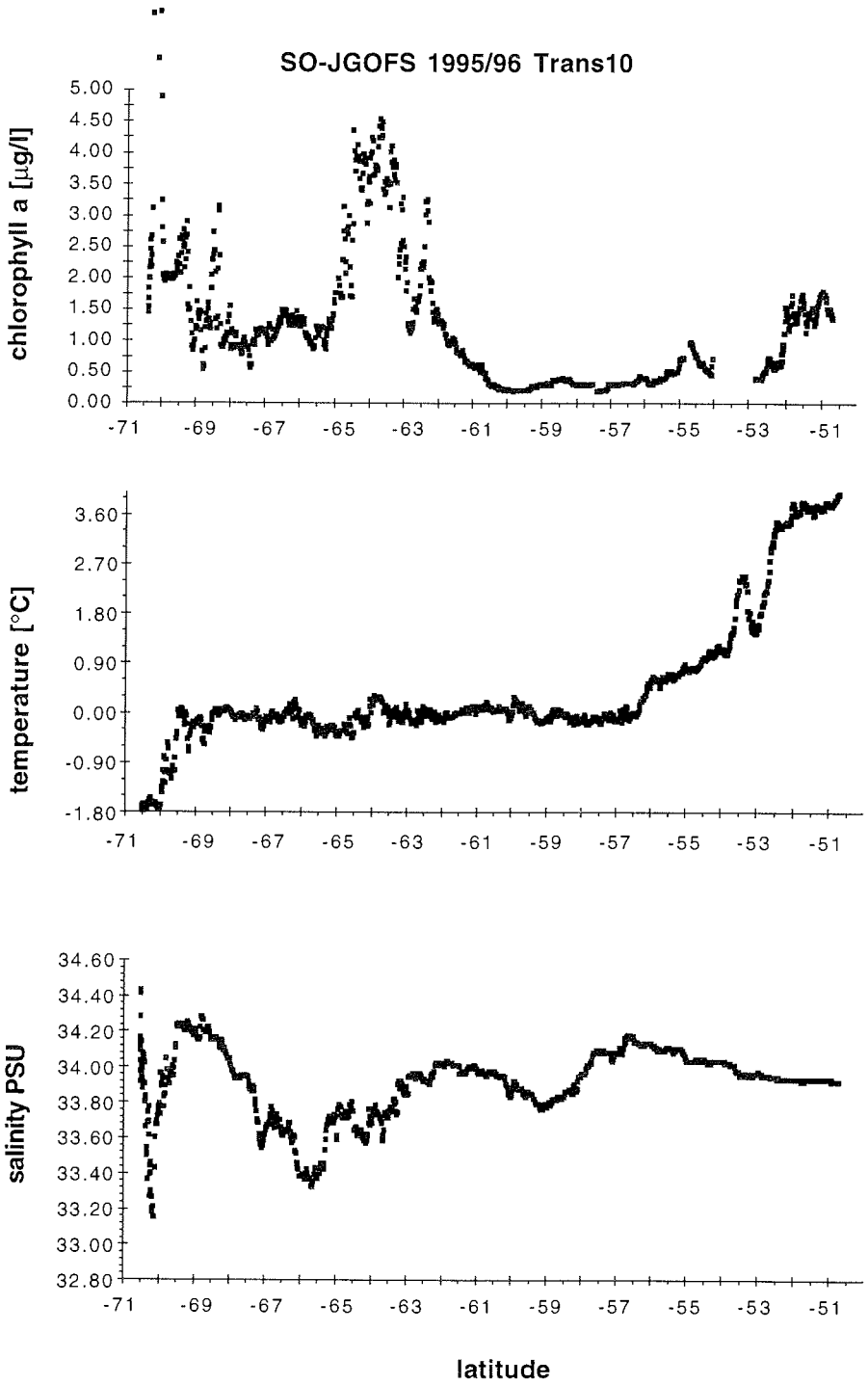
SO-JGOFS 1995/96 Trans10
chlorophyll a [µg/l]
5.00
4.50
4.00
3.50
3.00
2.50
2.00
1.50
1.00
0.50
0.00
-71 -69 -67 -65 -63 -61 -59 -57 -55 -53 -51
temperature [°C]
3.60
2.70
1.80
0.90
0.00
-0.90
-1.80
-71 -69 -67 -65 -63 -61 -59 -57 -55 -53 -51
salinity PSU
34.60
34.40
34.20
34.00
33.80
33.60
33.40
33.20
33.00
32.80
-71 -69 -67 -65 -63 -61 -59 -57 -55 -53 -51
latitude

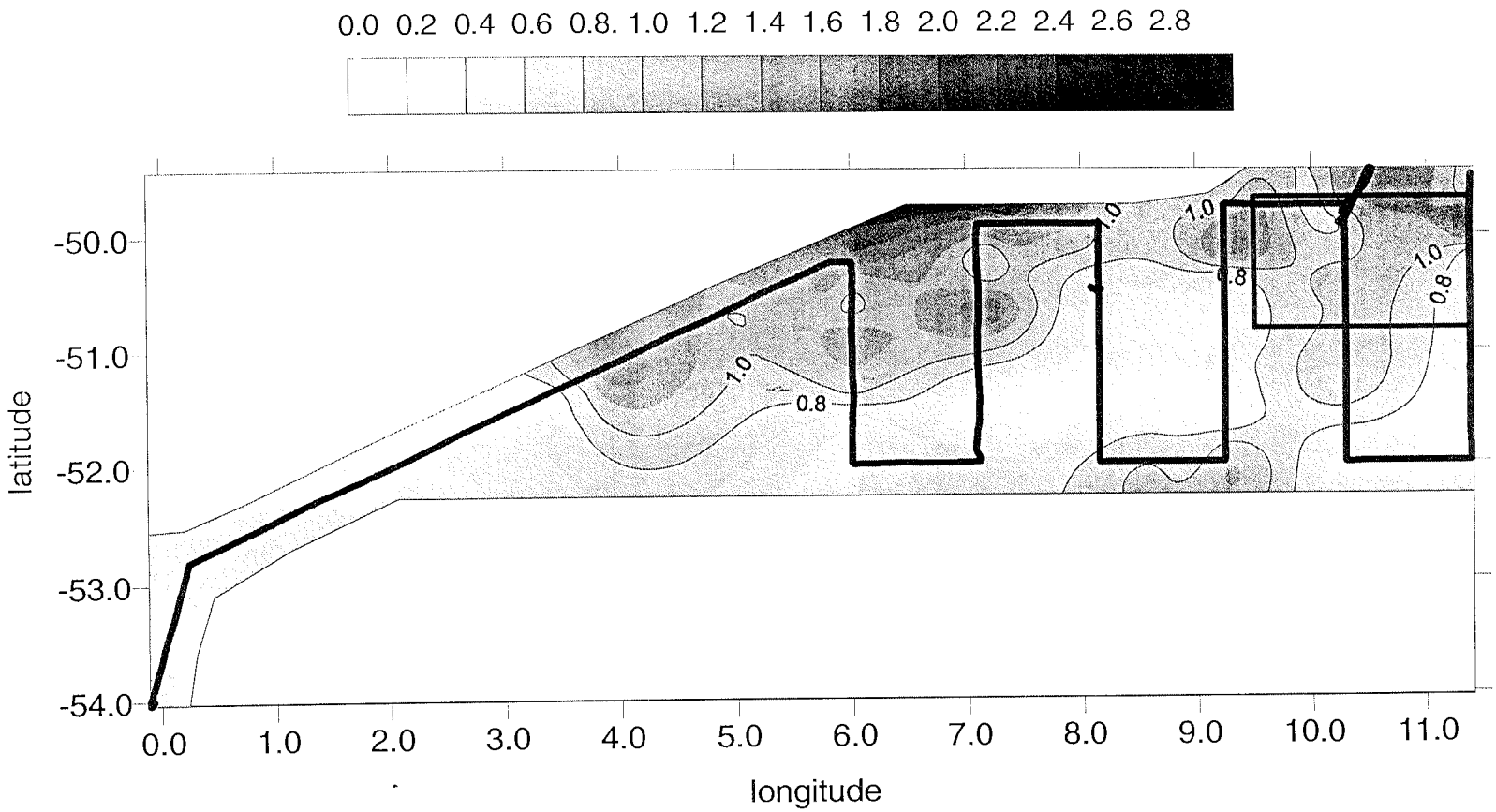
0.0 0.2 0.4 0.6 0.8 1.0 1.2 1.4 1.6 1.8 2.0 2.2 2.4 2.6 2.8
-50.0
-51.0
-52.0
-53.0
-54.0
latitude
0.0
1.0
2.0
3.0
4.0
5.0
6.0
7.0
8.0
9.0
10.0
11.0
longitude
1.0
0.8

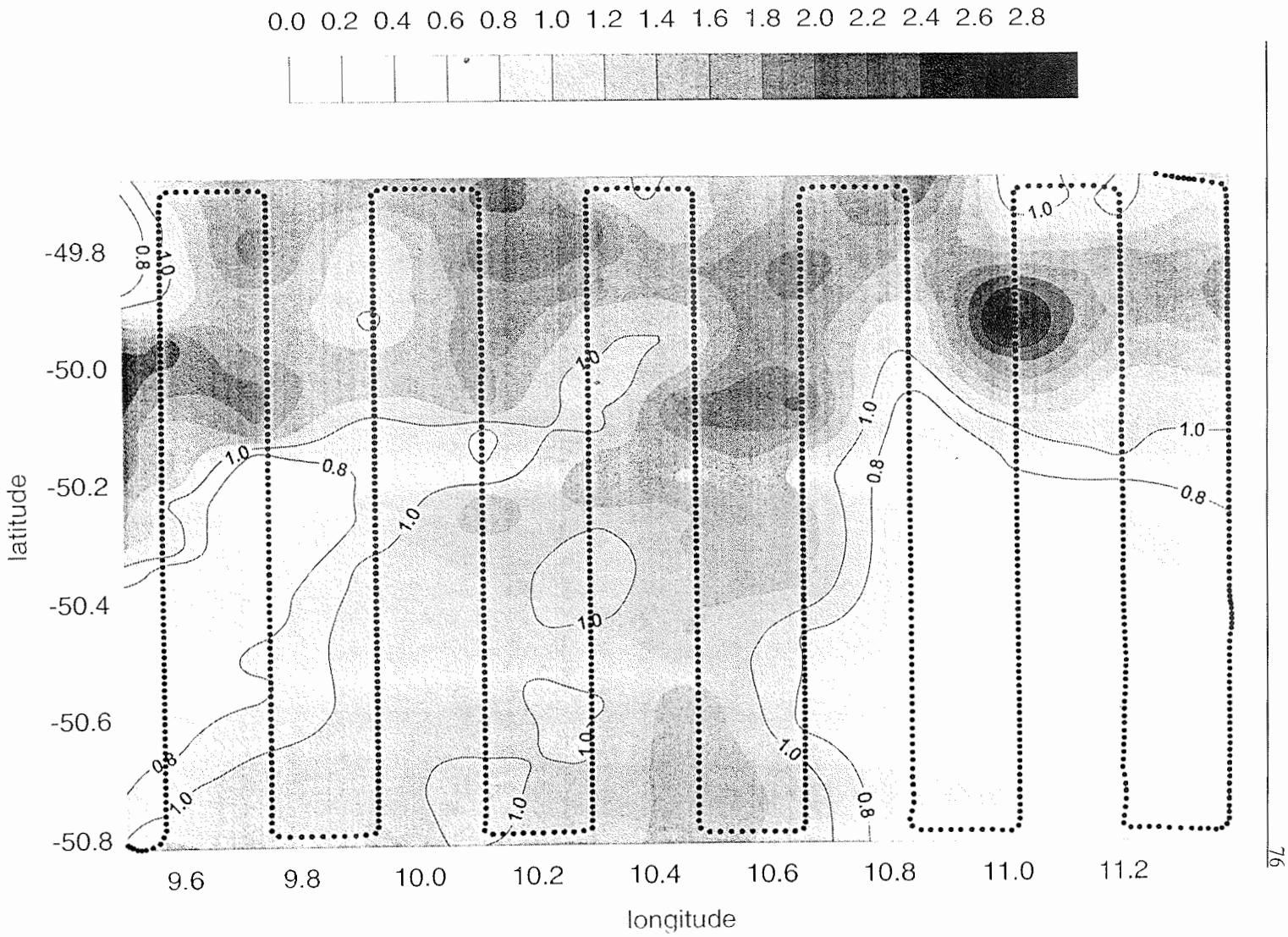
0.0 0.2 0.4 0.6 0.8 1.0 1.2 1.4 1.6 1.8 2.0 2.2 2.4 2.6 2.8
-49.8
-50.0
-50.2
-50.4
-50.6
-50.8
latitude
9.6
9.8
10.0
10.2
10.4
10.6
10.8
11.0
11.2
longitude
0.8
1.0

The surface distribution of chlorophyll *a* derived from fluorescence in both grids is shown in Figs. 13.5 and 13.6. In the north, a band of relatively high chlorophyll *a* values coincides with the position of the Polar Front. In the south-west and south-east corners of the grids, areas of relatively low chlorophyll concentrations were observed (see Section 12 for a detailed description of the differences in species composition in these two areas). The data for the composition of the two figures 13.5 and 13.6 are obtained along the cruise track with interpolation of the data between cruise lines, by applying a routine on the MS-DOS programme (SURFER). Such interpolations are suspicious at the edges of the figures. However, along the cruise tracks, the results of this interpolation are in good agreement with the observations.

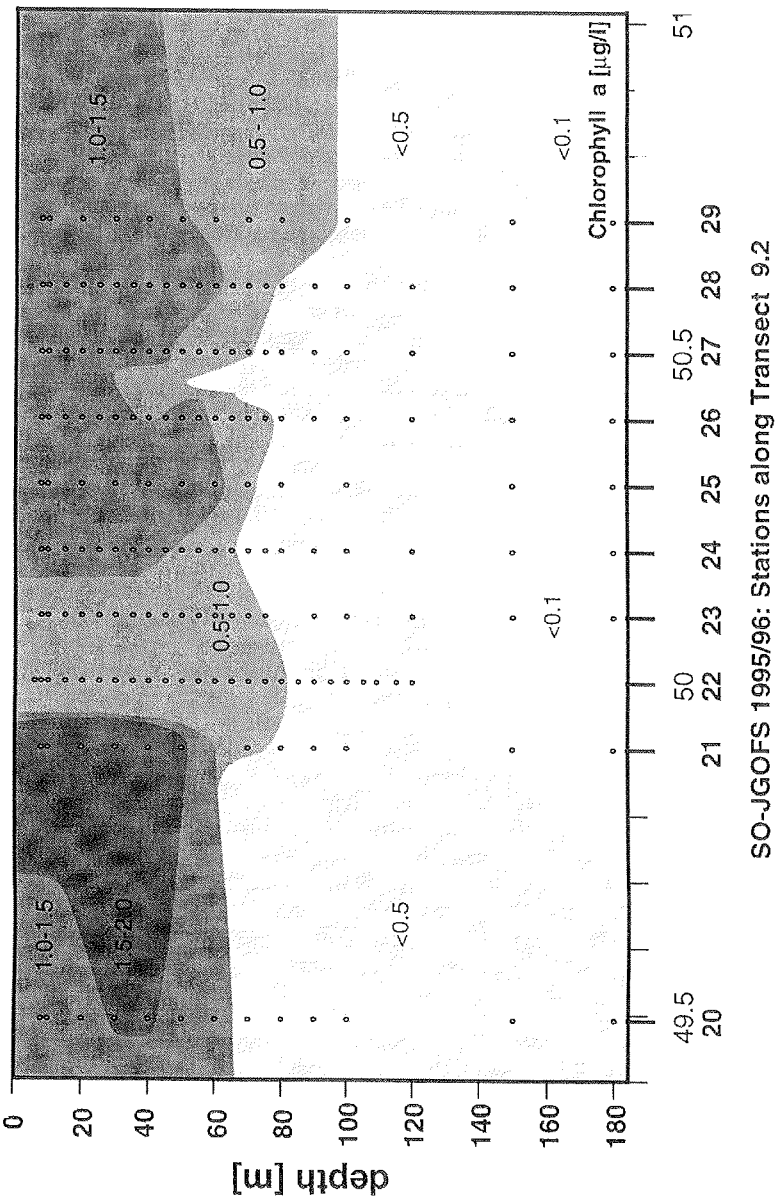

Fig. 13.5 Contour plot of chlorophyll *a* near sea surface (8 m) obtained along and interpolated between the cruise tracks (lines) during the large scale grid

14 PRIMARY PRODUCTION, NITROGEN CYCLING AND PHOTOSYNTHESIS-IRRADIANCE RELATIONSHIPS FOR PHYTOPLANKTON ASSOCIATED WITH THE ANTARCTIC POLAR FRONT IN SUMMER

M.I. Lucas, S.J. Bury, J-E Tremblay, A. Bracher, R. Lehmann, C. Bratrich, I. Ewen

Introduction

The International Joint Global Ocean Flux Study (JGOFS) initiated in 1989 concluded that the Southern Ocean may exert a significant impact on global climate change in terms of meridional heat flux and CO_2 exchange. Because of the extreme seasonality of the region, ocean-atmosphere fluxes of heat and CO_2 are likely to exhibit strong seasonal signals regulated both by physical and biological processes in the water column and by seasonal sea-ice cover. It is the exchange of CO_2 from surface waters into the deep ocean which is the critical rate-limiting step between atmospheric and oceanic carbon biogeochemical cycles.

In this respect phytoplankton biomass and photosynthesis provide the basis for transporting fixed carbon into the deep ocean by the processes of direct sedimentation of cells and through particle transformation into rapidly sinking faecal pellets as a result of krill and mesozooplankton grazing on larger (>20μm) net-phytoplankton cells. This is the "biological pump". The rate at which phytoplankton cells and other particles sink is to some extent size-dependent although physiological fitness considerably influences buoyancy and therefore sedimentation rates. Nevertheless, it is useful to consider phytoplankton biomass and production on a size basis;splitting them into net-plankton (>20μm), nano-plankton (2-20μm) and pico-plankton (<2μm). Small nano- and pico-plankton are not readily consumed by large zooplankton so they enter the micro-zooplankton food web characterised by little sedimentation but considerable regeneration of NH_4, urea and dissolved free amino acids, which are preferred and assimilated rapidly by phytoplankton.

A feature of the Southern Ocean generally is that primary production is lower than might be expected on the basis of available nutrients, particularly nitrogen. Explanations for this observation include light limitation, strong grazing pressure by microzooplankton, mesozooplankton and krill and the increasing probability that micro-nutrients, such as iron, limit algal growth.

Nitrate assimilation relative to total N assimilation by phytoplankton using ^{15}N tracers provides a useful index, the f-ratio, which indicates what proportion of phytoplankton growth is dependent upon NO_3 assimilation- i.e. "new" net production. Under long term equilibrium conditions, the f-ratio provides a measure of export production available to consumers or for sedimentation since NO_3 advection into surface waters must be related to N losses from surface waters. The f-ratio therefore provides a valuable tool for indirectly estimating vertical carbon flux. Furthermore, size-fractionated ^{15}N tracer studies can provide considerable insight into the structure and functioning of planktonic communities which has implications for planktonic trophodynamics and carbon flux.

SeaSoar has dramatically improved our resolution and understanding of both biological and physical mesoscale events. It's limitation is that it does not measure rate processes and nor does it perceive the intricacies of plankton community structure, form and function at the individual level. However, the strong group of microscopists on board can give us valuable insight into our somewhat "black-box approach." There is also a need to translate Sea-Soar data on the underwater light field and chlorophyll fluorescence into estimates of phytoplankton biomass and primary production. This can be done by careful calibration of deployed light meters (MER), by establishing chlorophyll to fluorescence ratios and by constructing photosynthesis-irradiance (PI) curves with respect to chlorophyll concentrations. Remotely sensed ocean colour

(SeaWiFS) will also depend on PI parameters for scaling-up while PI -derived rates of N and C assimilation provide important physiological indices of metabolic condition with respect to the nutrient and light fields; particularly with respect to spectral irradiance measurements. Together with the microscopists, this will allow us to more fully understand the interactions between light, nutrient availability and physiological processes that govern phytoplankton bloom development, and importantly, what may limit it's development.

From our cruise we have seen that diatom dominated blooms typify the Polar Frontal region of our study area. They form a remarkable assemblage of organisms ranging in size from 20µm to well over 500µm if their elongated and elaborate spines are taken into account. The question is: why do these blooms occur at the Polar Front and what is their role in the biogeochemical cycling of carbon, nitrogen and silica? Another is, what limits their growth and why do these blooms not achieve the same biomass that is frequently observed in the North Atlantic or coastal upwelling regions where nitrate, silica and other major nutrients often become limiting, especially nitrate? This is quite unlike these Polar Frontal waters where both nitrate and silicate are abundant. Could zooplankton grazing hold their biomass down? Data arising from the teams of microscopists, zooplanktologists and our measurements of primary production and nitrogen partitioning are trying to resolve these questions.

The Polar Front is marked by a steep gradient in silicate concentrations as it is crossed in a southerly direction while nitrate concentrations are abundant on both sides of the front. Careful analysis of the physical structure of the front shows that it is marked by a shallowing of the upper mixed layer, therefore providing phytoplankton cells with a more favourable light environment which stimulates their growth. This explains the presence of the bloom at the front but does not satisfactorily account for their limited growth in a high nutrient environment.

Broad Objectives

1. To measure size-fractionated water column primary production so that an estimate of photosynthetically fixed carbon potentially available for consumers or sedimentation is provided.

2. To measure size-fractionated ^{15}N-NO_3, Urea, NH_4 and DFAA uptake and $^{15}NH_4$ regeneration rates in the water column and in sea-ice communities with the aim of resolving nitrogen partitioning in the planktonic community and calculating the f-ratio to provide an estimate of export production.

3. To determine ^{14}C and ^{15}N photosynthesis-irradiance relationships for water-column and sea-ice phytoplankton communities. Associated with this, spectral measurements of the underwater light field were made while the response of chlorophyll to this field was also examined. Experiments to simulate the impact of UV irradiance on both ^{14}C and ^{15}N assimilation were also carried out.

Structure of Section

This section is divided into three main parts which reflect the three primary production groups involved-

(I) Lucas, Bury and Ewen: ..... ^{15}N production at standard light depths
(II) Tremblay: ..... ^{14}C at standard light depths and ^{15}N PI
(III) Bracher, Lehmann, Bratrich: ... ^{14}C PI and, UV & Bio-optical measurements

Methods

Study area and sample collection

The location of the production stations sampled along a series of SeaSoar transects across the Antarctic Polar Front, and between Neumayer and the main study area are given in Tab. 14.1 below. Station positions are shown graphically on the coarse scale SeaSoar survey grid which is overlaid on a contour map of surface chlorophyll concentrations (Fig. 14.1).

LONG	LAT	DATE/TIME	STN NAME
-03.19	-59.42	12-DEC 11:00	PS-08
-08.51	-70.46	15-DEC 15:00	ICE-1
-08.21	-70.27	19-DEC 13:00	ICE-2
-05.14	-66.92	20-DEC 05:00	UW-1
-02.67	-61.77	21-DEC 05:00	UW-2
-00.07	-54.00	22-DEC 17:40	PS-09
06.01	-50.71	24-DEC 07:00	UW-3
08.17	-50.48	25-DEC 21:45	PS-10
10.41	-49.63	27-DEC 19:00	UW-4
11.52	-49.89	29-DEC 14:00	PS-13
10.31	-51.10	30-DEC 18:00	PS-16
11.33	-49.69	01-JAN 09:00	UW-5
10.84	-50.79	02-JAN 11:00	UW-6
10.29	-49.84	03-JAN 13:00	UW-7
09.75	-50.30	04-JAN 17:00	UW-8
09.56	-50.70	05-JAN 08:00	PS-18
10.30	-49.90	06-JAN 15:30	PS-21
10.27	-50.69	07-JAN 23:00	PS29 --UW9
-07.94	-70.54	12-JAN 15:00	ICE-3
00.01	-63.67	16-JAN 10:00	PS-30
05.84	-57.33	17-JAN 16:30	PS-31
11.55	-49.90	20-JAN 06:00	PS-32

Tab. 14.1 Location of production stations during ANT XIII/2

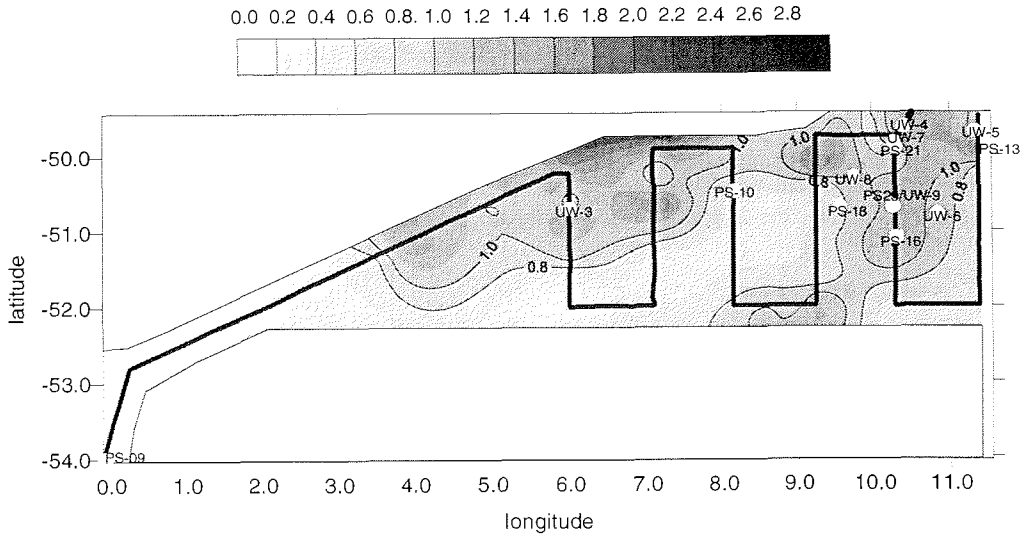

Fig. 14.1 Positions of the underway (UW) and profiled production stations overlaid on a contoured map of surface chlorophyll *a* from Bathmann et al., Para. 13

Water Samples

Water samples were obtained as follows:-

- Underway Stations and Surface Samples of CTD stations
Surface water was sampled by plastic bucket and poured carefully into a 60 l plastic container to pool the water. Water was then transferred into 2.4l polycarbonate incubation bottles which had previously been acid washed and rinsed twice with seawater. Samples which had been processed in this way were checked under the microscope for damage to the cells. Cells were found to be in excellent condition, even the long spines of *Chaetoceros criophilum* were completely intact.

- Water column Sampling - Production CTD's
Sampling of the euphotic zone at depths corresponding to 50%, 25%, 10%, 1% and 0.1% light depths was carried out using a 24 bottle (12L) General Oceanic CTD/Rosette array. Surface water was sampled as above. Sampling was carried out in conjunction with Jean-Eric Tremblay, Astrid Bracher and Meinhard Simon so that our results could be co-ordinated.

Ice Samples

For P.I., ^{15}N experiments and DIC measurements, two types of ice-sample were used. These were the ice-platelet layer beneath fast-ice adjacent to Neumayer, and brine derived from broken floes of slush ice. At each of the sampling stations the ice was melted into filtered seawater and the salinity, chlorophyll, DIC and nutrient concentrations were measured.

Ice Station: PS-ICE1, December 15th 1995, 15.00
Ice was sampled from the *Polarfuchs* by bucket and kept in a -4°C freezer for two days before thawing. Three blocks of 10 cm X10 cm and one of 5cm X 5 cm were melted into 10.5 L of filtered seawater.

	Salinity
FSW (3L)	34.2844
FSW + melted ice (32L)	30.5710

Ice Station: PS-ICE2, December 19th 1995, 13.00
Slush ice was sampled from the ship whilst we were steaming out from Neumayer through the pack ice. Ice and seawater were sampled (approx. 8 parts water, 2 parts slush ice) and the ice was melted in the -4°C freezer in the seawater from which it was sampled. No additional filtered seawater was added.

Ice Station: PS-ICE3, January 12th, 1996, 15.00
Three types of ice sample were taken from the fast ice adjacent to the Neumayer Ice Shelf. Seawater was sampled by bucket aft of the ship to make up filtered seawater in which to melt the ice. The filtered seawater plus melted ice samples were analysed for DIC, salinity, nutrients, and chlorophyll *a*.

Ice Sample 3A:
A large block of ice 30 x 40 cm with a layer of brown platelet algae (long chain diatoms) growing on the underside was sampled from the ice edge close to the ship. The block of ice was placed in a cool box without any seawater to cover the algae. The layer of algae was approximately 0.5-1 cm thick in places. A 1 cm layer was scraped off and placed in 4.5 x the ice volume of filtered seawater. This is the same ratio as the recommended JGOFS protocol (10 cm core length x 10 cm diameter of ice (785 cc) to 3500ml filtered seawater). The total volume of the ice plus algae was 990 cc and this was melted into 4414ml of filtered seawater.

Ice Sample 3B:
Similar smaller blocks of ice with long chain diatomaceous platelet algae were sampled as for sample A. These blocks were immediately placed in a cool box in seawater from the close

vicinity of the ice samples to prevent desiccation of the algae. The total volume of the ice was 505 cc which was melted into 2250ml of filtered seawater.

Ice Sample 3C:
Blocks of clear columnar ice were sampled by bucket from the aft of the ship. A volume of 8270 cc of ice was melted into 36.9 L of filtered seawater.

All three ice samples were incubated at 1% surface light intensity. Beneath 1.5 m of ice and 40 cm snow cover, light intensity was reported to be 1% of the surface irradiation for the same time of year in a previous cruise to the Weddell Sea (R. Gradinger and J. Weissenberger, 1992: Expedition Antarctis IX/1-4 *Polarstern* 1990/1, Cruise Report 100, Alfred Wegener Institute).

Standard Measurements

Size-Fractionated chlorophyll *a*

For each CTD production, underway and ice station, size-fractionated chlorophyll-*a* and phaeopigment samples were obtained by filtering 0.5 L of sea water onto Whatman 25 mm GF/F filters to yield total chlorophyll while a further 1.0 L was passed through a 20 mm mesh plankton screen and then filtered onto 25 mm GF/F filters as before to provide the <20µm fraction. A third 1.0 L sample was filtered through a 47 mm 2.0µm pore-size Nuclepore filter. The filtrate was retained for filtration through a 25 mm GF/F as before to yield the <2µm picoplankton fraction. Net plankton (>20µm) and nanoplankton, (<20, >2µm) are obtained by difference. It should be noted however that many of the small organisms <5 mm in diameter are sufficiently plastic to squeeze through the 2µm Nuclepore filters while the extreme morphological diversity of the spiny diatoms creates problems with size fraction classification.

Pigments retained on the GF/F filters were extracted in 9ml 90% Acetone after the sample had been macerated with glass beads. After 2-3 hours extraction in a dark freezer, the sample was centrifuged and the supernatant was transferred into quartz tubes and read on a Turner Designs scaling Fluorometer. Phaeopigments were measured following the addition of 2 drops of 5% 1N HCl. This was exactly the same protocol and instrumentation that other groups on the ship were using so that results should be directly comparable.

Nutrients

For each CTD production, underway and ice station, nitrate, nitrite, ammonium, silicate and phosphate concentrations were routinely measured by Dr. G. Kattner's group on a Technician TA II Auto analyser. Details of these methods are to be found in Section 8 of this report.

Ammonium and Urea
Manual analyses of ammonium and urea were determined on fresh samples corresponding with all ^{15}N incubation experiments using the methods of Grasshoff *et al.* (1983) scaled down to 5ml samples. Standards were prepared at the appropriate salinity of the sample. These manual analyses were not conducted routinely for any other samples. As both Autoanalyser and manual methods used the citrate, phenol and hypo chlorite method to form the indo-phenol blue complex which is read spectrophotometrically at 630 nm, we can inter-calibrate the two methods.

Underwater irradiance and PAR

Percent light depths for the production CTD's were calculated from both Secchi depth and MER deployments. Because of the heavy swell and poor visibility at times, we decided to adopt the top two light depths (50% & 25%) as given by the Secchi disc while adopting the bottom two depths (1% & 0.1%) from the MER. There was good agreement between both techniques at the 10% light depth, but the Secchi disc consistently underestimated the 0.1% depth by about 5-8m while surface MER values were erratic. Intercalibration of the SeaSoar light sensors and the MER sensors was conducted on board *Polarstern* and the final intercalibrated data set await confirmation.

14 I Dual-labelled measurements of phytoplankton production and nitrogen partitioning based on ^{13}C and ^{15}N isotopic tracer techniques

M. Lucas, S. Bury, T. Preston, I. Ewen

Methods

Nitrogen uptake measurements

For each of the production station light depths, 2.0 L incubation volumes, in polycarbonate bottles, were supplemented with 1.0 µmol/0.1ml $Na^{15}NO_3$ (98 atom%) to give a final concentration of 0.5 µmol l^{-1}; 0.05 µmol/0.1ml $CO(^{15}NH_2)_2$ (99.1 atom%) to give a final concentration of 0.025 µmol l^{-1}, and for NH_4-N uptake experiments, 2x2.0 L volumes were spiked with 0.1 µmol/0.1ml $^{15}NH_4Cl$ (98 atom%) to a final concentration of 0.05 µmol l^{-1}. One of these was incubated with the nitrate and urea incubations in the simulated *in situ* on deck incubator tubes covered with neutral density filter screen to give the appropriate shading. The bottles were cooled by surface seawater pumped through the tubes. The remaining 2.0 L bottle was immediately filtered onto a 47 mm GF/F filter which was retained and frozen for later particulate N analysis. The filtrate (900ml) was retained in a 1.0 L glass Schott bottle to which 1000ml NH_4Cl carrier was added before freezing the sample at -30°C for later isotopic dilution analysis at time zero (Ro). Uptake experiments were terminated after 24 hours by filtration on top re-ashed (450°C for 6 hours) Whatman 47 mm GF/F filters which were retained and frozen at -30°C for later analysis of PN and ^{15}N content on a Europa Scientific 20/20 mass spectrometer. At the end of the NH_4 uptake experiment, (Rt), 900ml filtrate and carrier was retained and frozen as before for isotopic dilution measurements of NH_4 regeneration.

Details of nitrate and urea uptake rates calculations can be found in Probyn & Painting (1985). Ammonium uptake rates were similarly calculated but corrected for isotopic dilution due to 14N excretion (Glibert et al. 1982). A relative preference index (RPI) was calculated for each nutrient assimilated (McCarthy et al. 1977).

Ammonium regeneration

Aqueous ammonium in the regeneration bottle samples (900ml frozen) is recovered by diffusion from the thawed samples back at our laboratory in Cape Town. Sufficient MgO is added to increase the pH to >9.0. A 25 mm GF/F filter moistened with 50 µl 6N H_2SO_4 is suspended above the sample and the bottle is re-capped. After standing for approximately 2 weeks at room temperature, >50% of the aqueous NH_4 is usually recovered on the filter as NH_4SO_4. The filters are then shaken in 5ml Milli-Q water and a sample is removed for colorimetric ammonium concentration determination. Ammonium regeneration rates are calculated from a modified form of the Blackburn (1979) and Caperon et al. (1979) models as described in Probyn (1987).

Size-fractionated uptake and NH_4 regeneration experiments were carried out on surface communities at each CTD production and for a number of underway stations. For each nutrient, 6.0 L of sample was inoculated with ^{15}N label at the same concentration as before. Two litres (NH_4 incubation) were also spiked for aqueous ammonium determinations and isotopic dilution measurements at time zero (Ro) as described earlier and immediately filtered onto a Whatman GF/F filter. At the end of the incubation period, the spiked samples for each nutrient (NO_3, NH_4, urea) were split into an intact community (2.0 L), a <20 µm fraction (2.0 L passed through a 20 µm mesh) and a <2 µm fraction (2.0 L passed through a 2.0 µm Nuclepore filter). Each separate fraction was then filtered onto 47mm GF/F filters and the particulate ^{15}N enrichment determined as previously. For the NH_4 incubation experiment, 900ml was collected from the filtrate for aqueous NH_4 measurements (Rt) as outlined before.

DFAA Experiments

For surface samples DFAA additions were made to 10% of the ambient concentrations. Samples were incubated on deck in 3 x 2L bottles in the flow through incubation system. DFAA samples were size-fractionated into total, <20µm and <2 µm at each depth. For the 0.1% light depth further size fractionations were carried out:- total, <20-0.7µm, <2-0.7µm, <2-0.3µm, <1-

0.3µm. In addition, t=0 and t=24 filtrate samples were taken from each depth from the nitrate, ammonium and DFAA incubation bottles to measure nitrification and regeneration rates.

^{13}C Uptake Measurements

To measure C:N uptake ratios and carbon fixation as a measure of primary production, ^{13}C was added to the nitrate bottle (to 5% of the ambient DIC concentration). A dark ^{13}C experiment was also carried out to correct for respiration. At the end of the experiments, the recovered ^{13}C-sodium bicarbonate filters were fumed for 2 minutes over concentrated HCl to remove inorganic carbon prior to drying of the filters. To estimate bacterial production, ^{13}C labelled leucine was added at a 10 nmolar concentration to the ammonium bottle. Filtrate samples (t=0 and t=24) were taken from the nitrate, ammonium and DFAA incubation bottles to measure nitrification and regeneration values. Samples were immediately frozen in -30°C degree freezer following filtration.

UVA and UVB Radiation Effects

The effect of UVA and UVB radiation on carbon, nitrate, ammonium, urea, DFAA and leucine uptake was investigated by carrying out incubations in teflon FEP bottles. Teflon FEP bottles (500ml) which are transparent to UVA and UVB light were used although these bottles cut out 50% of the visible radiation band. Incubations of surface water in 2.4 L polycarbonate bottles under 50% light were therefore carried out for comparison with the UVA and UVB clear bottles. The teflon bottles were incubated in an unscreened incubator.

Results and Discussion

For this report, only the "standard" and preliminary ^{15}N uptake measurements through the water column are presented together with very preliminary estimates of C:N uptake ratios. All of the other experiments await further analysis.

Water column profiles of chlorophyll, ^{15}N uptake rates & nutrients

Of the ten water column production stations (and nine surface underway stations), four representative water column stations are chosen here for presentation and discussion. They are production stations 21 and 31 which represent contrasting Polar Frontal (PF) and southern ACC waters respectively. Stations 13 and 32 are also illustrated since they accompanied the deployment and recovery of the mooring array at the eastern boundary of the fine scale grid survey.

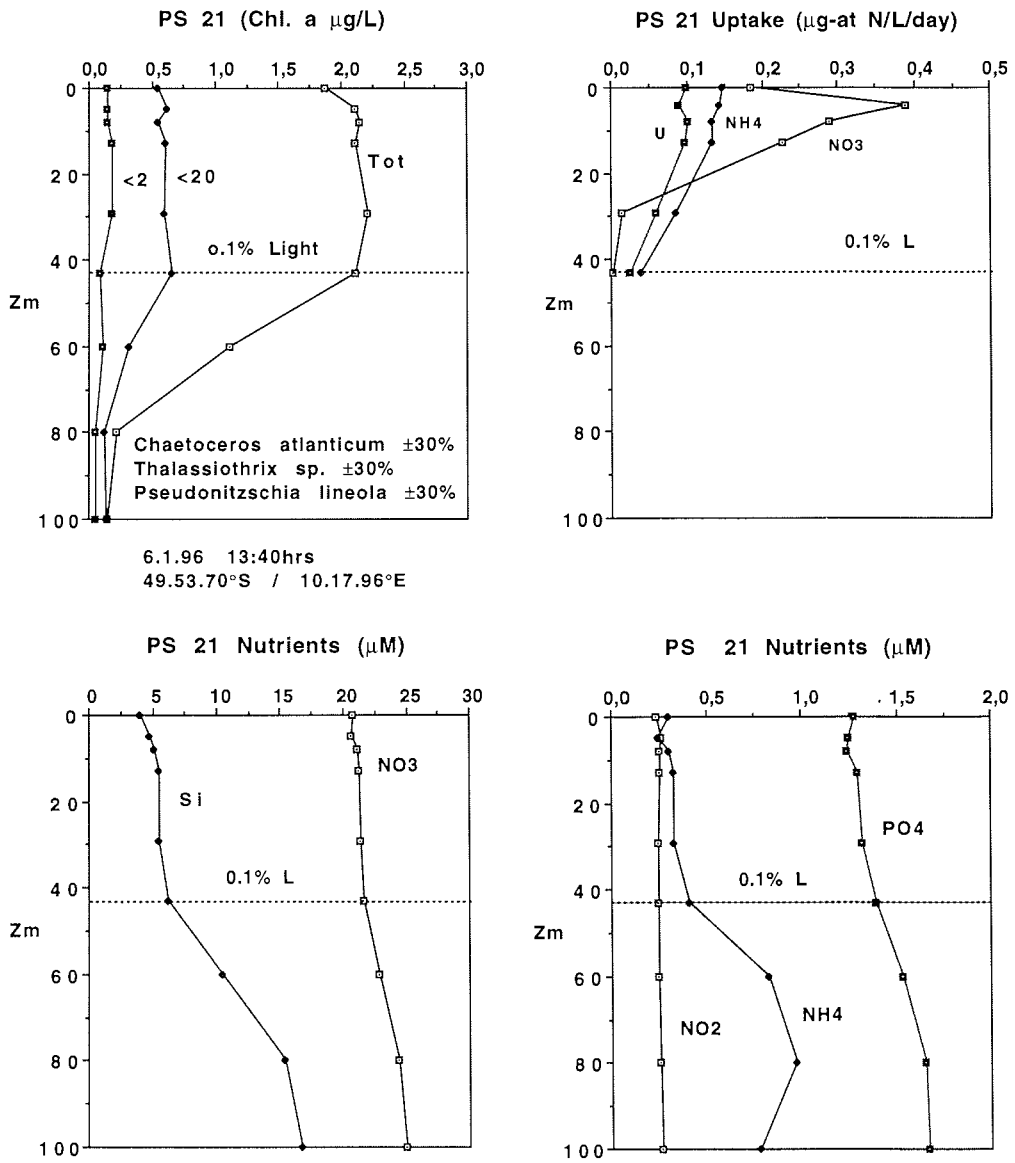

Figs. 14.2 a-d Profiles of chlorophyll *a*, nitrogen uptake and nutrient concentration for station 21. The nutrient data were kindly provided by Dr. G. Kattner's group.

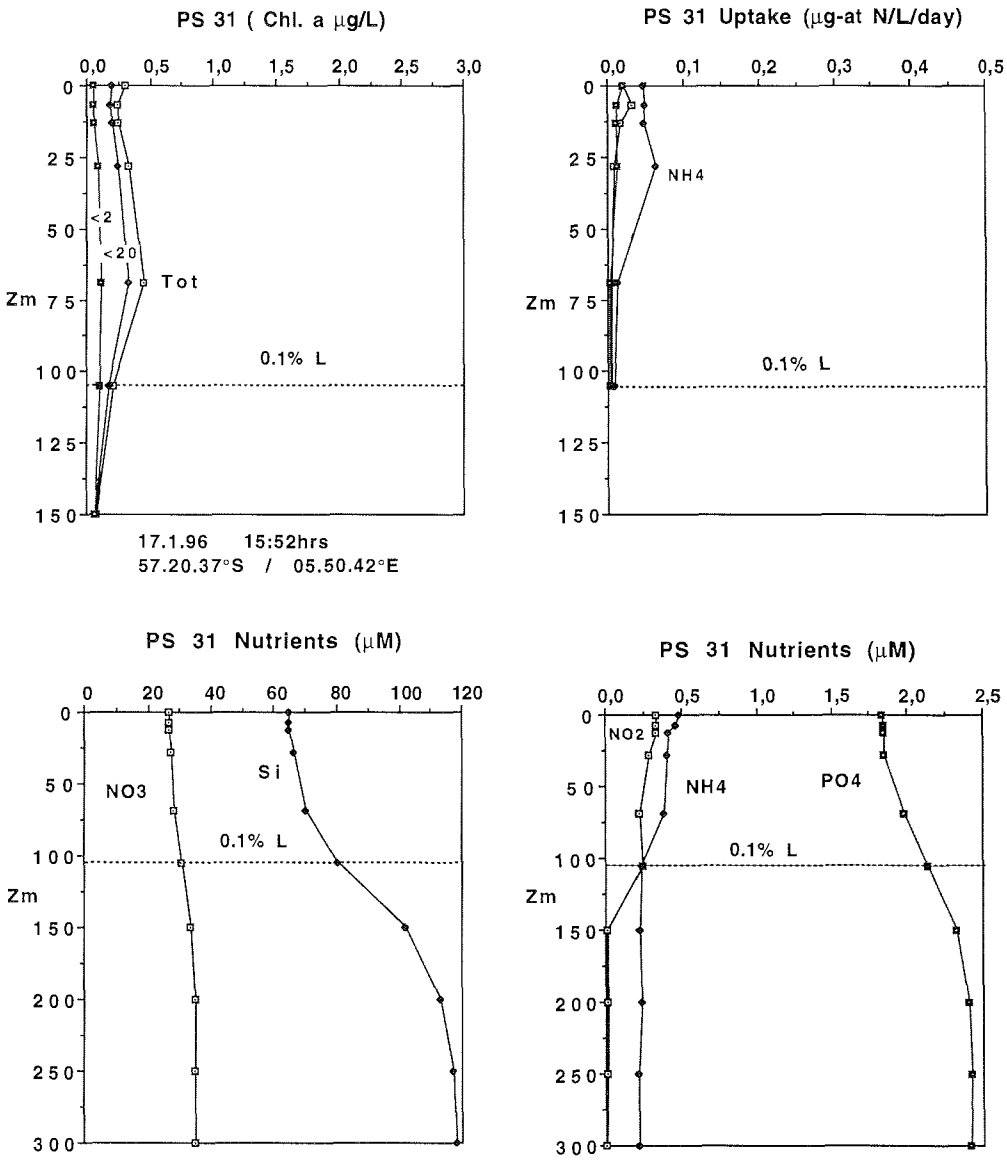

14.3 a-d Profiles of chlorophyll *a*, nitrogen uptake and nutrient concentration for station 31. The nutrient data were kindly provided by Dr. G. Kattner's group.

Figures 14.2 (a-d) and 14.3 (a-d) contrast water column profiles of chlorophyll *a*, nitrogen uptake rates and nutrient profiles for PF and ACC stations 21 and 31 respectively. As expected, the PF, characterised by a high chlorophyll biomass (±1.5 µg/L; PS 21) and dominated (67%) by netplankton, exhibited the highest uptake rates when nitrate uptake (pNO_3) typically exceeded that of either NH_4 uptake (pNH_4) or urea uptake (urea) in surface waters. The f-ratio, pNO_3 / (pNO_3 + pNH_4 + urea), had a maximum of 0.63 at the 50% light depth (4m) but decreased to <0.1 at the 1% (29m) and 0.1% light depths (43m). This is indicative of a "new" production based system in surface layers where diatom growth is optimal and relatively fast, leading to a requirement for NO_3 as well as preferred NH_4 and urea to satisfy nitrogen requirements. Deeper in the water column under less favourable light conditions, reduced

phytoplankton growth rates can be sustained by the supply of regenerated NH_4 and urea alone (f=<0.1) which is re-cycled by micro- and mesozooplankton grazers. The moderate (f >0.4) to high surface f-ratio values indicate the potential for limited export production. By contrast, low chlorophyll values and low regeneration based nitrogen uptake rates of the ACC waters (Stn. 31; Fig. 14.3 a-d) characterise nano-and picoplanktonic phytoplankton populations which are closely coupled to a microzooplankton grazer community where nitrogen is tightly re-cycled and most carbon is lost through respiration. Such communities are not associated with export production or significant CO_2 draw-down.

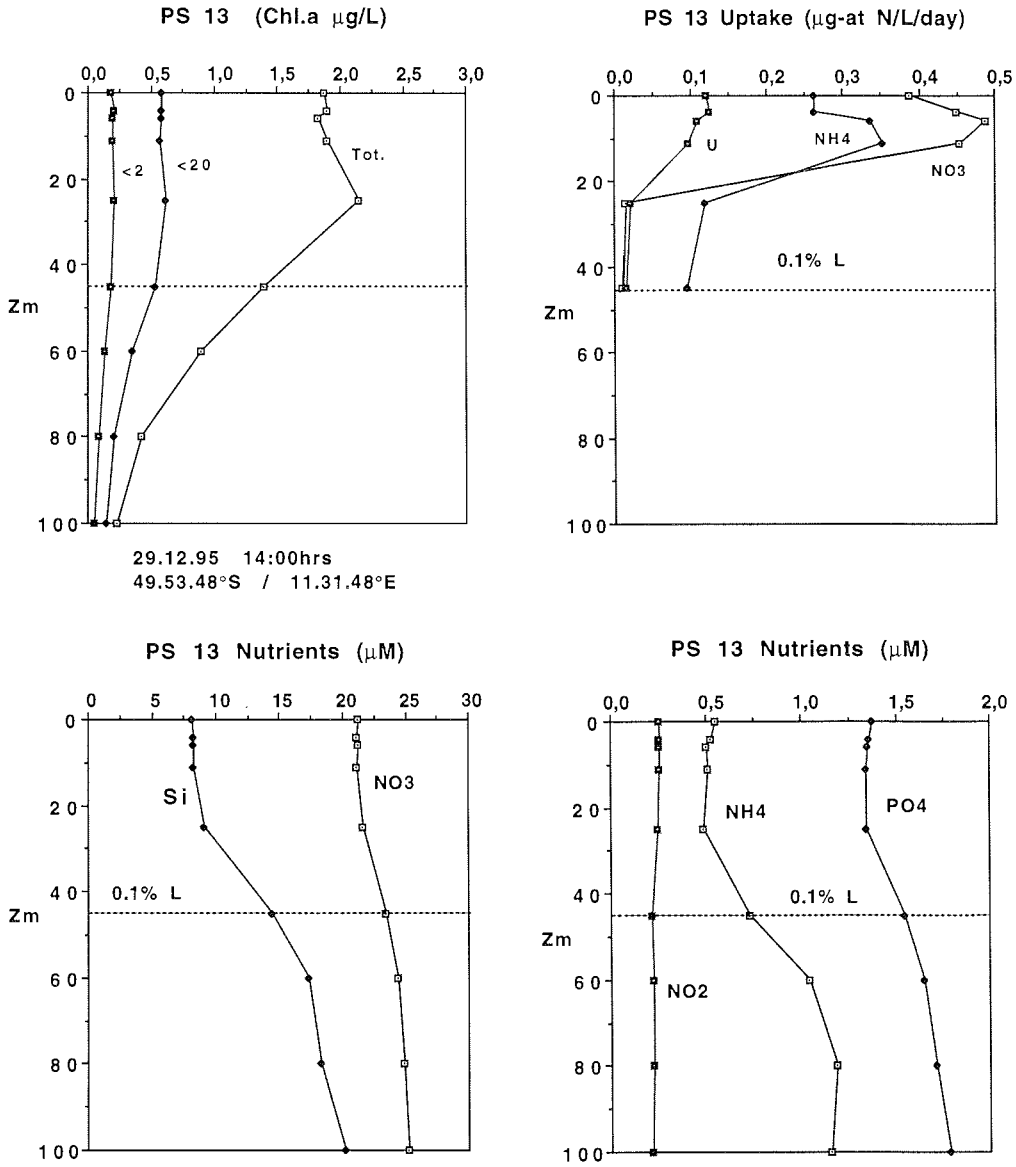

Figs. 14.4 a-d Profiles of chlorophyll *a*, nitrogen uptake and nutrient concentration for station 13. The nutrient data were kindly provided by Dr. Kattner's group.

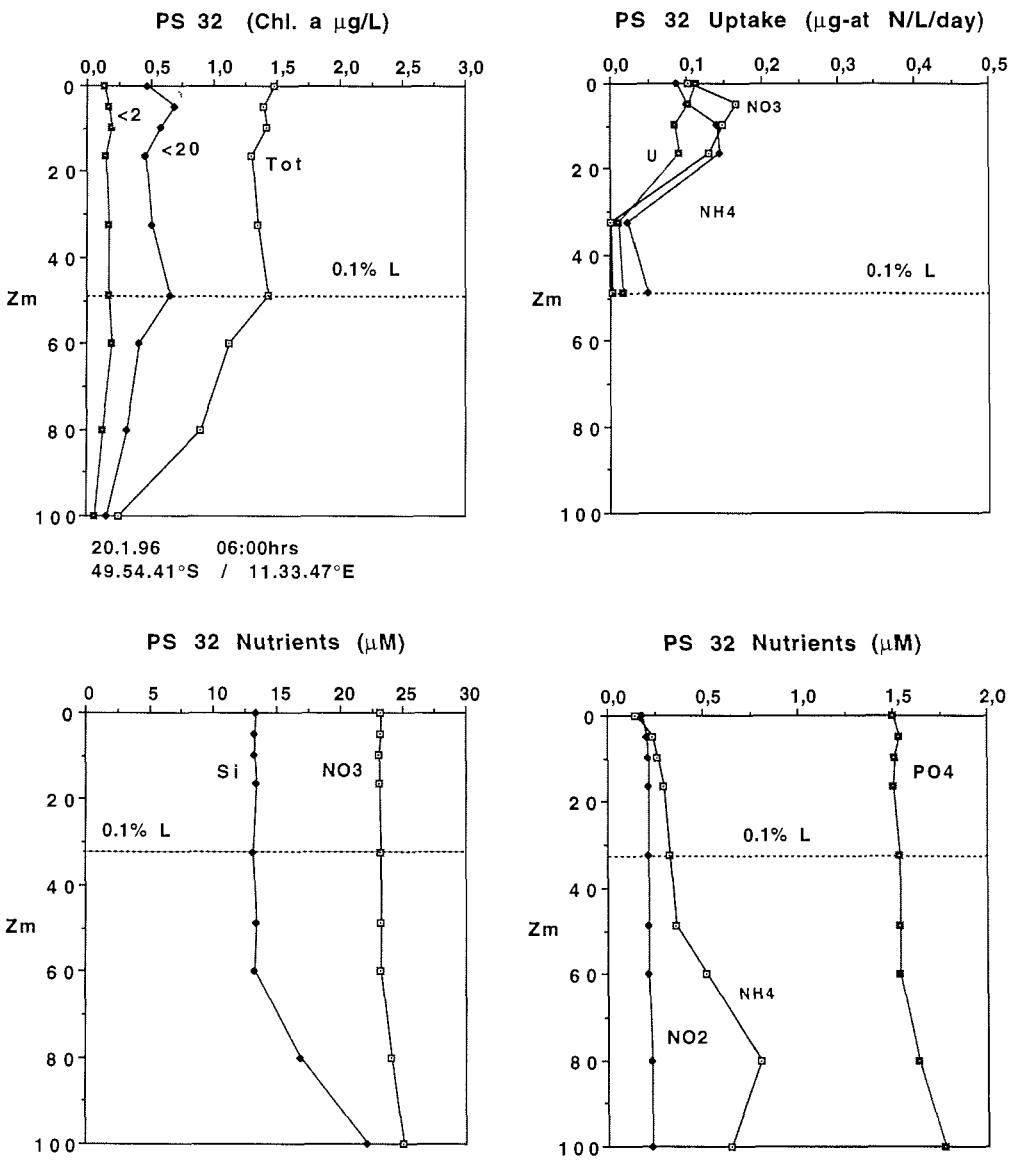

Figs. 14.5 a-d Profiles of chlorophyll *a*, nitrogen uptake and nutrient concentration for station 32. The nutrient data were kindly provided by Dr. G. Kattner's group.

The scenario at the mooring stations PS 13 & 32 (Figs. 14.4 a-d & 14.5 a-d) is very similar to that described for station 21. Of interest is the apparent reduction in chlorophyll concentrations and uptake rates in the three week period that separated sampling at this location. One might speculate that this represents losses due to grazing or export, this is not supported by the nutrient data which show that both nitrate and silicate concentrations have increased, indicating an influx of water from elsewhere, probably from the west or south west.

Everywhere, it is notable that maximum uptake rates are typically associated with the 50% light depth (normally < 10m depth) and maximal pNO_3. With increasing depth, there is a significant shift towards pNH_4 and urea, with pNO_3 becoming insignificant. Although "new" or export production is high at some stations, the overall trend is one of a largely regeneration based phytoplankton community with only moderate or little export production. This is summarised in Fig. 14.6; a plot of average f-ratios with depth for all water column productions stations.

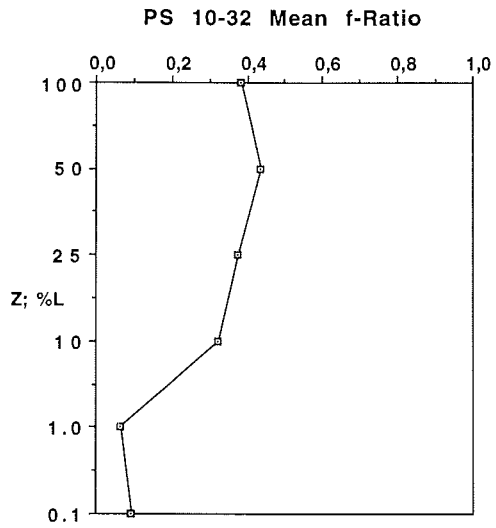

Fig 14.6 Average f-ratios with depth for stations PS 10,13,16,18,21,31& 32. Zero values were included in the calculation.

There are a number of explanations for the shift from NO_3 to NH_4 based nitrogen metabolism with depth. One is that with increasing depth and diminishing irradiance, nitrate uptake becomes light limited with respect to either pNH_4 or urea since pNO_3 is an energetically more expensive process. Linked to this is the observation that significant (upto approx. 40%) NH_4 uptake can occur in the dark (see Tremblay et al.; Part III). Whether this is autotrophic uptake or heterotrophic bacterial uptake remains to be seen and may be elucidated by both our measurements of heterotrophic Leucine uptake and Meinhard Simon's measurements of bacterial production in the water column (see section 16).

Nutrient profiles shown in Figs. 14.2-14.5 (c&d) offer a number of insights into the chemistry of Polar Frontal and ACC waters. In many of the profiles (e.g. PS 13, 21, and 31) an NH_4 maximum is evident beneath the euphotic zone between 60-80m. One explanation for this is that sedimenting PON is undergoing ammonification by heterotrophic bacteria. Another is that microzooplankton grazing at this depth results in NH_4 regeneration which accumulates in the absence of photo-assimilation. Within the euphotic zone, pNH_4 is significant and mostly exceeds or is balanced by regeneration processes; accounting for the typically low euphotic NH_4 concentrations. An exception is at station 31 in the central ACC where NH_4 regeneration in the euphotic zone must exceed uptake rates to account for the accumulation of NH_4 here (see Fig. 14.3d). However analyses of our NH_4 regeneration experiments (yet to be done) should remove some of this speculative discussion.

The silicate and nitrate profiles are themselves also informative. Firstly, it is quite clear that ambient concentrations for both nutrients typically far exceed demand. For example, at PS 31 in the ACC, the ambient surface concentration of NO_3 is nearly 30μM while that of Si is >65μM (see Fig. 14.3d). Nitrate uptake in surface waters at this station is about 0.025 μg-at / L / day which translates into 0.35 μg N / L / day. Assuming such growth rates were constant, it would take about 100 days for ambient NO_3 concentrations to become depleted. Clearly however, mixing events are likely to replenish ambient NO_3 concentrations within this period so that other limits to growth and biomass accumulation need to be advanced - such as water column instability, grazing pressure and/or iron limitation.

Nevertheless, within the Polar Frontal region there is some possibility that Si could become limiting at some stations depending on the NO_3 : Si uptake ratio adopted. For example, at station 21, pNO_3 rates would remove the approx. 5μM deficit between surface and aphotic NO_3 concentrations in approximately 10 days. The Si deficit here is about 10μM, implying that the NO_3:Si uptake ratio over the 10 day period is of the order 1:2. As ambient Si concentrations in surface waters here are about 5μM, the observed growth rates could be sustained for about a further 5 days only. Such back-of-the-envelope calculations imply that the entire euphotic zone nutrient load needs to be replenished every 10-15 days and that the diatom cells are accreting significant quantities of silicate.

Size-fractionated chlorophyll and nitrogen uptake rates

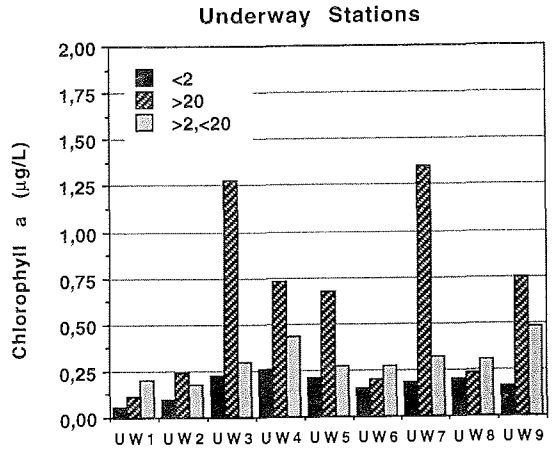

Fig 14.7 Size-fractionated surface chlorophyll concentrations for all underway production stations.

Size-fractionated chlorophyll profiles (Figs. 14.2a-14.5a & 14.7) indicate that regions of elevated chlorophyll are dominated (±70%) by the netplanktonic (>20μm) size-classes. Elsewhere in unproductive (often ACC) waters, the nano- and picoplanktonic fractions dominated with few phytoplankters exceeding 20μm. Picoplankton ubiquitously accounted for about 10% of the total chlorophyll biomass. It is worth noting here that the frequent practice of pre-screening the water sample to exclude mesozooplankton grazers would have been entirely inappropriate since many of the diatom spines exceeded 500μm or more in length.

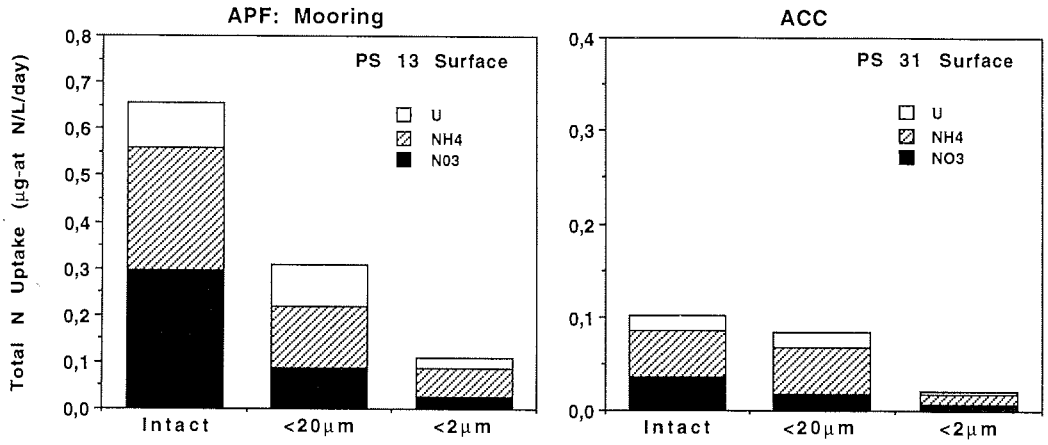

Fig 14.8 Examples of surface size-fractionated nitrogen uptake for stations 13 & 31.

Size-fractionated ^{15}N uptake rates (e.g. Fig. 14.8) mirrored the size-fractionated chlorophyll profiles. Where chlorophyll biomass was relatively high (e.g. > 1 µg /l), most of the ^{15}N uptake was recorded in the netplanktonic fraction and usually dominated by pNO_3. Conversely, where phytoplankton biomass was low, uptake rates were dominated by the smaller fractions where NH_4 and urea were the most important nutrient. As is now well known, the community structure elaborated in this way has wide implications for export production.

Integrated water column production

Summarised below are the integrated nitrogen and carbon uptake rates for both frontal and ACC regions. Data are integrated to the 0.1% light depth for the stations shown.

Stn.	0.1%Zm	pNO_3	pNH_4	urea	pTot.N	f-ratio
10	61	2.93	7.38	1.46	11.77	0.25
13	45	8.41	8.78	2.35	19.55	0.43
16	56	6.02	11.69	2.33	20.05	0.30
18	60	3.60	8.55	1.91	14.06	0.26
21	43	5.83	4.53	3.05	13.41	0.44
31	105	0.88	3.36	0.67	4.91	0.18
32	49	3.37	3.43	2.56	9.78	0.34

Stn.	0.1%Zm	pTot.C	PC	PN	POC/PON.	pC:N
10	61	33.4	14.8	03.30	4.45	2.84
13	45	59.8	16.10	3.20	5.06	3.06
16	56	57.6	15.80	2.80	5.61	2.87
18	60	50.2	17.00	1.70	10.27	3.57
21	43	48.3	11.20	2.60	4.26	3.85
31	105	14.9	9.81	2.30	4.25	3.03
32	49	41.7	10.20	2.60	3.93	4.26

Tab. 14.2 Integrated Nitrogen and Carbon Uptake Rates (mg-at / m^2 / day)

Note: A revision of the DIC data currently taking place will alter the pTot. C and pC:N values slightly.

Overall, the integrated pTot. C and pTot. N values (above) demonstrate that the entire region is characterised by low water column production rates, dependent primarily upon reduced nitrogen (mostly NH_4), as indicated by the low f-ratio values. The latter confirm that this system is not marked by significant export production at this time; somewhat contrary to other cruises to the region (e.g. ANT X/6, 1992 at 6°W). The low pC:N values are unexpected and require further consideration before comment can be made. We know however that both C:N uptake and sedimentation ratios can be de-coupled from Redfield ratio expectations which has wide ranging implications for carbon export production.

Acknowledgements

We would like to gratefully acknowledge the financial support to Drs. Lucas, Bury and Ms. Ewen provided from the South African Foundation for Research and Development (FRD; Division of International Liaison) and the University of Cape Town's Research Committee to participate on this German JGOFS cruise (ANT XIII/2). Further funding by FRD to pay for the analytical costs of ^{15}N mass spectrometry at Dr. Tom Preston's lab. within the Scottish Universities Research and Reactor Centre (SURRC) in East Kilbride is also greatly appreciated. Furthermore, I (MIL) want to express my gratitude to the AWI (Smetacek and Bathmann) for the generous funding I have received to spend several months at the AWI analysing the data from this cruise. Similarly, additional support provided to me from the Southampton Oceanographic Centre (SOC) through Dr. Raymond Pollard to continue with analyses of SeaSoar data at SOC is gratefully acknowledged also. The support and good humour of Victor Smetacek and Uli Bathmann throughout this period has been greatly appreciated by all of us; making ANT XIII/2 a memorable and successful cruise.

References

Dugdale and Goering (1967) Limnology & Oceanography 12: 196-206
Glibert et al (1982) Limnology & Oceanography 27: 639-650
Grasshof et al (1983) Methods of Seawater Analysis. Verlag Chemie, Germany
McCarthy et al (1977) Limnology & Oceanography 22: 996-1101
Probyn and Painting (1985) Limnology & Oceanography 30: 1327-1332
Probyn (1987) Marine Ecology Progress Series 37: 53-64

14 II Size-fractionated uptake of carbon and nitrogen in the Southern Ocean

J.-E. Tremblay

Introduction

To complement the standard water column measurements of nitrogen assimilation outlined in Part I, above, the physiological basis of carbon fixation and nitrogen assimilation with respect to light was investigated using on-deck and PI approaches. In particular, such PI approaches allow us to investigate the light requirements of NO_3, NH_4 and urea uptake to be investigated separately. This has implications for phytoplanktonic community development where, for example, diatom growth based on nitrate assimilation is regarded as having a high light dependency because of the energetic cost of transporting NO_3 across the cell membrane and reducing it to NH_4 prior to protein synthesis. Similarly, the proportion of dark NH_4 uptake relative to total NH_4 uptake can also be resolved through the PI approach.

Methods

Estimation of size-fractionated primary production

Subsamples from the surface (Underway stations) or from the six optical depths (CTD stations) were incubated (see part I for sampling procedures and incubator design) for 24 h in acid-washed 1.0 L culture flasks with 370 kBq $NaH^{15}NO_3$ (Amersham). Duplicate dark bottles were incubated with DCMU. Following incubations, size-fractions were obtained by parallel

filtration onto 20 µm Nylon mesh, 2 µm Nuclepore and GF/F glass fiber filters. After addition of 6N HCl to the filters in liquid scintillation vials and bubbling of carbonate for 1 h, 10ml QuickZint scintillation cocktail was added. The activity of samples and time-zero blanks, corrected for quenching, was determined with a scintillation counter, using the channel ratio method. Potential growth rates of netplankton were estimated using the exponential growth equation and assuming a chl *a* :carbon ratio of 30 (chl *a* data from Lucas et al., this report).

Simultaneous measurements of ^{13}C and ^{15}N uptake versus irradiance

Subsamples from the surface and the depth of 1% irradiance (CTD stations) or from the surface only (Underway stations) were incubated in the laboratory under controlled light conditions for 5 h. The incubation system, modified from Frenette et al. (in press), consists of six chambers placed radially around a 250-W arc lamp (OSRAM, HQI-T 250 W/D). In each chamber 12-600ml tissue-culture flasks are exposed to irradiances ranging from 12 to 1492 µmol m^{-2} s^{-1} (pre-determined by the attenuation of light along the chamber and use of neutral density filters between some of the flasks). Temperature was maintained by circulating seawater from 8 m depth. Incubations were started sequentially in order to ensure equal incubation time for all chambers. All samples were spiked with $NaH^{13}CO_3$ at ca. 10% of ambient dissolved inorganic carbon concentration and with ca. 10% of ambient nitrogen as follows:

Sample	Chamber	Nitrogen spike	
Surface	1	$K^{15}NO_3$	(nitrate)
Surface	2	$^{15}NH_4Cl$	(ammonium)
Surface	3	$CO(^{15}NH_2)_2$	(urea)
1%	4	$K^{15}NO_3$	
1%	5	$^{15}NH_4Cl$	
1%	6	$CO(^{15}NH_2)_2$	

At underway stations, enrichment experiments were conducted by adding saturating levels of ^{15}N-ammonium (chamber 4) and ^{15}N-urea (chamber 5) and the effect of ammonium on nitrate uptake was examined by simultaneous spiking with ^{15}N-nitrate and addition of ^{14}N-ammonium (chamber 6). At the end of the incubation, samples from each chamber were filtered (600ml) simultaneously onto pre-combusted 25 mm GF/F filters and stored frozen. Where chl *a* concentrations were sufficiently high (e.g. > 1.5 µg l^{-1}), size-fractions were obtained by filtering 300ml onto 20 µm Nylon screens or Nuclepore 2 µm filters, and collecting the filtrate onto GF/F filters. Another 300 ml was filtered directly onto GF/F filters. Filters were stored frozen for later analysis on a 20/20 Europa Scientific Mass Spectrometer (AWI).

Results and Discussions

Primary production

The high phytoplankton standing stock at the Polar Front contrasts sharply with background chlorophyll concentrations in nearby waters of the Antarctic Circumpolar Current (see Lucas et al., this report). However, higher standing stocks in the front do not necessarily correspond to higher rates of CO_2 fixation (a determinant variable for flux studies), so that estimates of photosynthesis are required for assessing the potential impact of the front on CO_2 drawdown by the Southern Ocean. Moreover, the partitioning of CO_2 between small and large phytoplankton is a key process, since large phytoplankton can be readily exported (i.e. direct sinking, grazing by large herbivores and advection of particulate and dissolved organic matter), whereas the small cells tend to be remineralized within the euphotic zone. Using preliminary results, we now report on estimates of daily size-fractionated (< 20 and > 20 µm) primary production.

Estimates of primary production were highly variable throughout the sampling area, ranging from 5 to 36 mg C m^{-3} d^{-1} at surface (Fig. 14.9a; Underway stations) and from 250 to 1968 mg C m^{-2} d^{-1} for depth-integrated samples (Fig. 14.9b; CTD stations). The highest values of primary production were in the Polar Front (e.g. stations UW3 and PS13), but there was

another peak at the southern edge of the sampling area (station PS30), where a bloom of *Phaeocystis* was

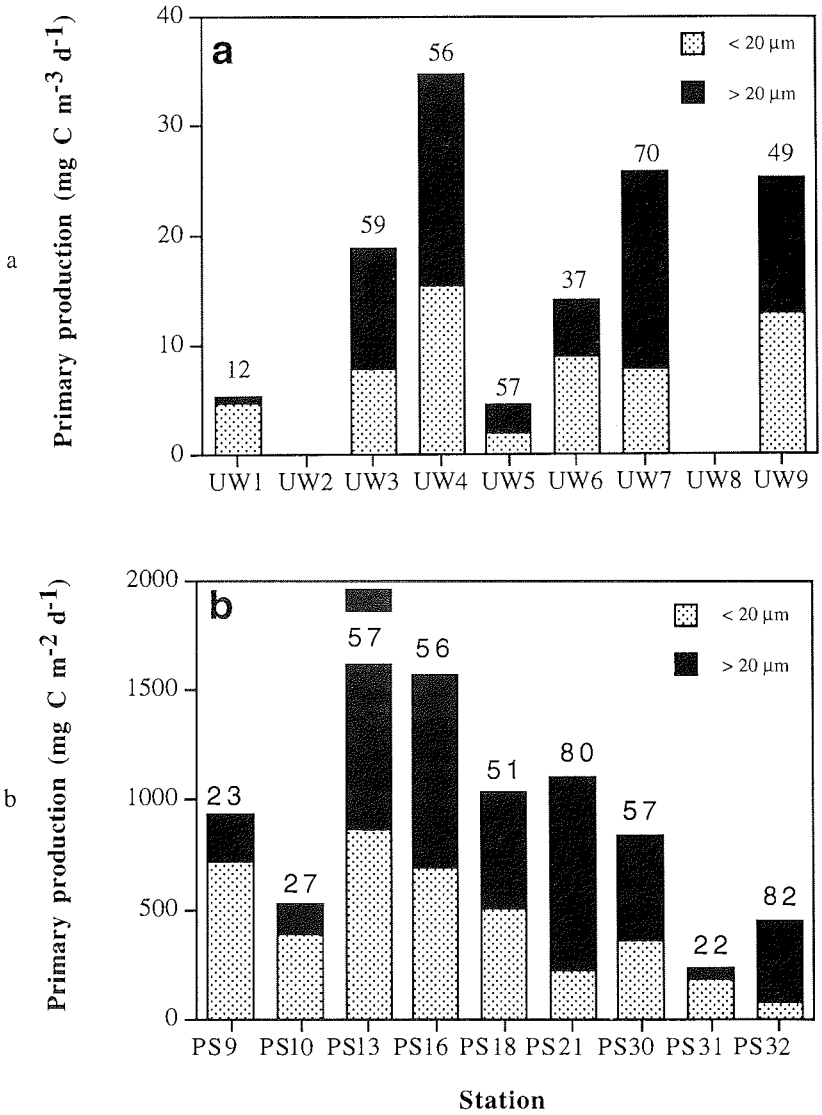

Fig. 14.9 a, b Primary production a) at surface for Underway stations and b) integrated over the euphotic zone for CTD stations. Station numbers correspond to those in the map (see Lucas et al., this report) and numbers above the bars indicate the percent contribution of netplankton (>20 µm) to total primary production

encountered. Netplankton (> 20 µm) dominated in the Polar Front, accounting for 51 to 80% of total primary production. The high rates of total carbon fixation in the front imply a relatively large drawdown of atmospheric CO_2 for the area and, since netplankton are dominant, a high potential for the downward export of this CO_2. It should be noted, however, that primary production in the Polar Front was relatively low compared to other systems of the World Ocean.

Physiological status and responses of phytoplankton size classes

Reasons for the occurrence of a bloom at the Polar Front are elusive since deep mixing should lead to light limitation of phytoplankton growth in both the front and surrounding waters. It is not known, however, whether the high chlorophyll signal in the front results from high growth rates *in situ* (because higher primary production does not imply higher growth rates) or

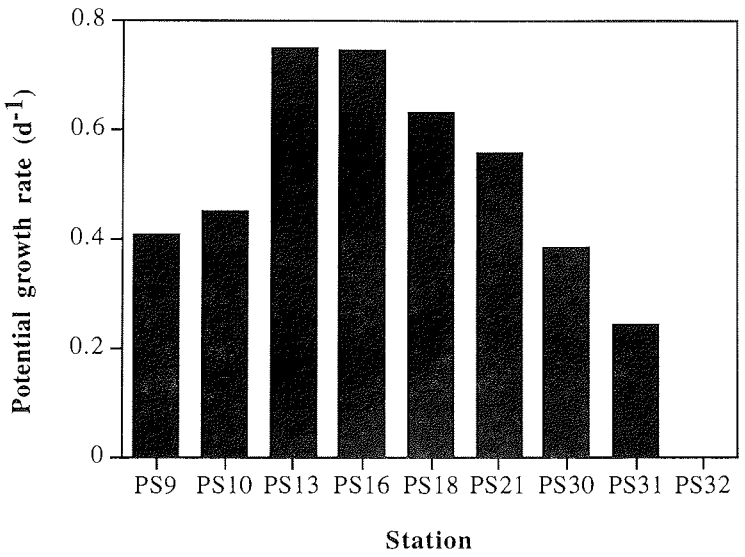

Fig. 14.10 Potential growth rates of netplankton (>20 μm) for CTD stations

physical accumulation. Assessing the physiological status and responses of phytoplankton size classes to physical forcing is a critical step toward understanding the ecological functioning of the front and modelling its impact on the CO_2 pump in the Southern Ocean. In general, netplankton showed higher potential growth rates in bloom areas of the Polar Front than in surrounding waters (Fig. 14.9b). This implies that the physiological condition of netplankton in the front was relatively good (note that high potential growth rates do not imply that the cells achieved higher realized growth rates, because the latter is dependent on loss processes). Results from irradiance vs. carbon (see Bracher et al., this report) and nitrogen uptake experiments will allow detailed conclusions on the physiological response of phytoplankton to physical forcing. This type of information will be useful for estimating large-scale primary production and *f*-ratios from remotely-sensed data.

14. III Responses in photosynthesis of Antarctic phytoplankton to light and UV-radiation

A. Bracher, C. Bratrich, R. Lehmann

Introduction

Modelling primary production in the Southern Ocean requires information on the optical properties of sea water, the absorption capabilities of suspended particles (especially phytoplankton), and the efficiency at which absorbed light energy is converted into particular matter. The goals of this study were to characterise the light environment within the ocean, and to define the responses of algal communities to their respective light regimes. The underwater light climate of the Southern Ocean is spatially and temporally very heterogeneous because of unstable hydrographical conditions. To a certain degree phytoplankton can adapt to the underwater light field by altering the photosynthetic pigment apparatus. These adaptive mechanisms can be seen as strategies to optimise the efficiency of light utilisation. In particular, our investigations focused upon the energetics of light utilisation, primary production and quantum yield of photosynthesis, in order to quantify the degree of photoadaptation of natural algae under different light conditions. The information obtained during this cruise will be used to test and refine existing bio-optical models of primary production, and to determine their applicability for the Polar Front region of the S. Atlantic sector of the Southern Ocean. In addition, effects of enhanced UV-radiation on phytoplankton photosynthesis due to ozone depletion were studied.

Materials and methods

Sampling at sea

We sampled 12 vertical stations (6 depths within the euphotic zone) and 5 surface-water-stations within the large transect at the polar front, and 5 vertical stations and 2 surface-water-stations on the way up and down to Neumayer Station. All stations were in the open ocean without any ice cover. *in situ* water samples were restricted to the upper 120m of the water column. Additionally we sampled 5 ice stations as described in Part I (Lucas *et al.*).

Radiation measurements

1. Underwater light spectra

Vertical profiles of the upwelling and downwelling spectral distribution of the underwater light field was measured using a MER-2040 underwater spectroradiometer equipped with a cosine receptor (Biospherical Instruments, San Diego, USA). Within the PAR (photosynthetically available radiation 400-700 nm) spectrum, spectral light intensities were measured at wavelengths of 412, 443, 465, 490, 510, 520, 550, 560, 615, 633, 665 and 683 nm (10 nm bandwidth). These included the wavelengths which will be measured by the SeaWiFS ocean colour satellite. In addition, two UV wavelengths (340 and 380 nm), scalar PAR and the solar-stimulated fluorescence of chlorophyll *a* were measured. During underwater cast, the on-deck spectroradiometer MER-2041 was measuring as reference the same PAR, UV parameters and solar-stimulated fluorescence of chlorophyll *a* as the underwater unit. The spectral distribution of underwater light was studied at all sampled CTD-stations (except for stations 9,10, 14 and 15) during daylight.

2. On-Deck- On-line- Measurements

In addition to the underwater measurements, photosynthetically available radiation (PAR, 400-700nm) and UV-B-(280-320nm) and UV-A-(320-400nm)-radiation at the sea surface was continuously measured throughout the cruise. PAR was measured with a Licor sensor (Li-193SA), UV-light with Dr. Groebel UV-A and UV-B cosinus sensors. These sensors were mounted on the forward superstructure of the ship where the sensor was not shaded from parts of the ship. Every 10 min PAR (in mol quanta / m^2*s) means were logged throughout the day to a Li Cor LI-1000 Data Logger.

Every 1 sec., UV-A- and UV-B-radiation means (in W/m^2) and every 1 hr, UV-A- and UV-B-radiation sums were logged throughout the day to a compaq 486 computer (procomm program). The ships global radiation measurements will also be compared to the on-line light measurements.

Water sample analysis and experiments

The following measurements were carried out using water sampled from a Bio-Rosette at CTD stations, ice stations and stations with only surface water samples taken with a bucket (see PART I). At CTD stations, the pigment composition, particulate light absorption and measurements of photosynthetic activity were determined at 6 depths in the euphotic zone (either at standard depths (0m, 20m, 40m, 60m, 80m, 100m) or 100%, 50%, 25%, 10%, 1% & 0.1% light depths). Photosynthesis/irradiance (PI) relationships and experiments studying UV- light effects were conducted with water samples from the surface and the 1% light depth only.

1. Photosynthesis-irradiance measurements

The functional relationship between algal photosynthesis and incident light intensity was experimentally examined at 17 open water stations and 5 ice stations. Samples were incubated at *in situ* temperatures in a small volume (20ml) "photosyntetron" (from S. Pilo, Israel). ^{14}C incorporation was used to provide measurements of dissolved and particulate carbon. A concentration between 0.763-0.953 µCi ^{14}C/ml (per vial between 15.26 to 19.66 µCi ^{14}C) was used for each 20ml sample. The concentration chosen related to the low chlorophyll of the samples (between 0.3-2.5 µg chl *a* /l). 18 samples per light depth were incubated under a 200W tungsten halogen lamp used as a light source. Photon flux (I) ranged from 1-1000 µmol q m^{-2} s^{-1} and irradiance levels in the photosyntetron were measured using a Biospherical Instrument probe (QSP200). Samples were filtered onto Sartorius cellulose nitrate filters (0.45 µm pore diameter) and then HCL-fumed in a desiccator for 15 min to release non-assimilated $^{14}CO_2$. Scintillation cocktail was added to the filters prior to counting in a Packard 1900CA Tri-Carb Liquid Scintillation Counter. The uptake of ^{14}C labelled bicarbonate into acid-stable organic material was converted to biomass-specific fixation rates using measured values of chlorophyll *a* and alkalinity.

2. Particulate light absorption

1-2 l of water samples taken from the same depths as the pigment composition samples were filtered onto GF/F filters (pre-soaked in filtered sea water) and particulate spectral absorption measured with a double beam spectrophotometer (Varian model cary 3).

3. Photosynthetic activity

A pulse amplitude modulation principle fluorometer (PAM-WALZ GmbH) was used for measurements of stimulated variable fluorescence yield of chlorophyll *a* (Fv/Fm) on dark adapted water samples. In order to detect a fluorescence signal, 1.0 L samples with a chl *a* content < 2.5 µg/l had to be concentrated to 100ml by pouring the sample gently through a 20 µm mesh. The information given by the Fv/Fm values will be used to asses the photosynthetic conversion efficiencies of phytoplankton.

4. Photosynthetic and UV-absorbing pigment composition

Pigment composition was determined by filtering 1.0 or 2.0 L samples through 25 mm Whatmann GF/F filters. The filters were placed in Eppendorf tubes and immediately deep frozen in liquid nitrogen before being stored at -70°C. Analyses of these samples by HPLC will be carried out at AWI, Bremerhaven.

5. Influence of enhanced UV-radiation on phytoplankton photosynthesis

Water samples from the surface and the 1% (only at CTD stations) light depths were chosen for these experiments. From each depth, three 50ml samples were spiked with 10 µCi ^{14}C. Another sample from each depth was concentrated from a 500ml sample to 50ml. Both ^{14}C and concentrated samples were incubated in the UV-incubator simulating ozone hole conditions (corresponding to a radiation field of 130 Dobson Units (DU)) over 4 hrs at *in situ* temperature. Approximately 1.0 L of the original sample obtained from the CTD was kept in the dark at *in situ* temperature. After the first incubation, this sample was prepared as the first, but incubated under radiation conditions outside the ozone hole (corresponding to a radiation field of 360 DU). After incubation, the ^{14}C spiked samples were treated identically to the samples originating from the PI and biomass-specific production rate experiments.

The concentrated sample was kept in the dark over 4 hr. Every hour, the quantum yield (Fv/Fm) of the sample was measured by using the PAM and compared to the quantum yield of the sample before the incubation.

Preliminary Results

Primary production as a function of light

The parameters of the PI relationships for stations within the Polar Front transects of both the FFS and CSS, showed Pmax values ranging from 0.68 to a 2.51 µg C/ µg chl *a* *hr, Ek values from 50 to 200 µE/ m^{-2}*s and alpha values between 0.00428 to 0.01507. In the south-eastern part of the survey area (stations 13,14,15,16,18 and 32), the 1% light depth phytoplankton samples (from 25 to 40m) exhibited higher Pmax values than those from the surface. Stations in the centre and north-western part of the region (stations 20, 21, 25 and 29) showed the reverse, where higher Pmax values for surface samples were found relative to the deeper samples. Both results indicate that at most stations, either the light history the phytoplankton community experiences changes with depth, or that the water column is separated into two distinct phytoplankton communities exhibiting differing PI characteristics. Differences might be related to stabilisation of the water column where communities have photoadapted to the particular light regime they experience. Further analyses of pigments and comparisons with the availability of macro- and micro-nutrient may provide further evidence to explain these observed differences. Examples of P-I-curves are shown in Fig. 14.11a-c.

a

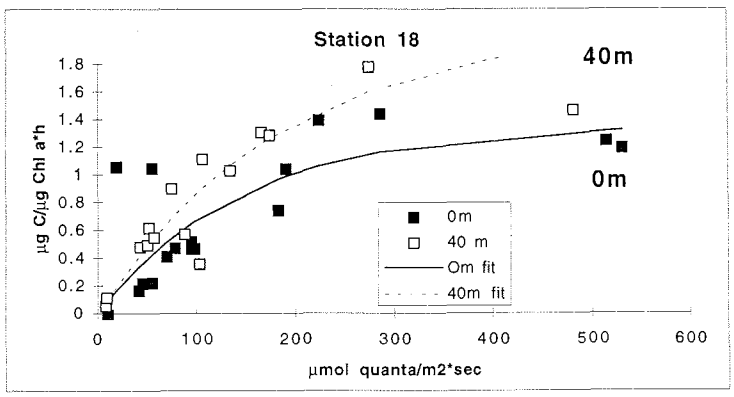

b

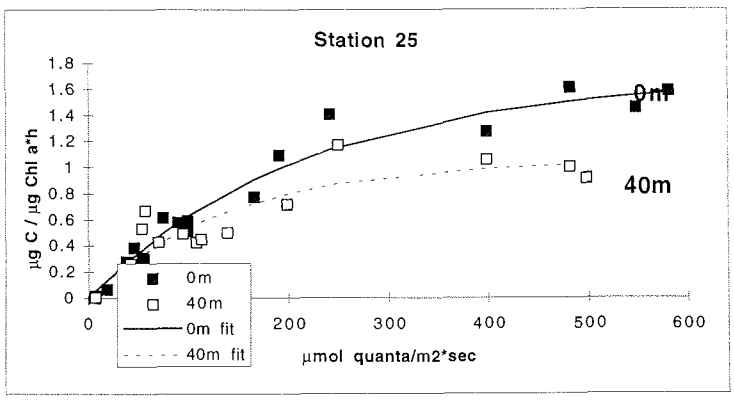

c

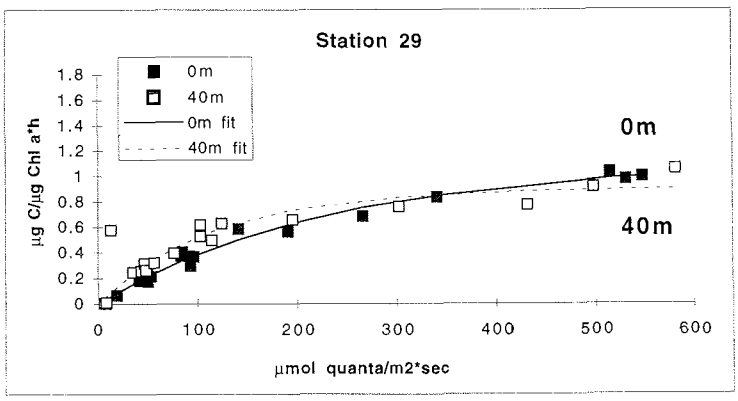

Fig. 14.11a-c Photosynthesis vs. irradiance (PI) relationships of samples taken within the Polar Front

Influence of enhanced UV- radiation due to stratospheric ozone depletion on phytoplankton photosynthesis:
Among samples taken from open water stations (total = 32), productivity was significantly depressed under simulated ozone hole conditions (spectra of 130 DU, high UV-B) for 15 of these samples (Fig.14.12a). However, 17 of the 32 samples, showed no significant difference relative to rates under normal UV conditions (360 DU). Photosynthetic activity (measured as the quantum yield = Fv/Fm) always showed a significant decrease after incubation under high UV compared to the control (measurements before the incubation) and to samples measured after incubation under low UV- light conditions (Fig.14.12b). Explanations for these different responses might be due to the physiological state of phytoplankton relative to their pigment content, including UV-absorbing compounds. Analyses of pigment samples should resolve such speculation.

a

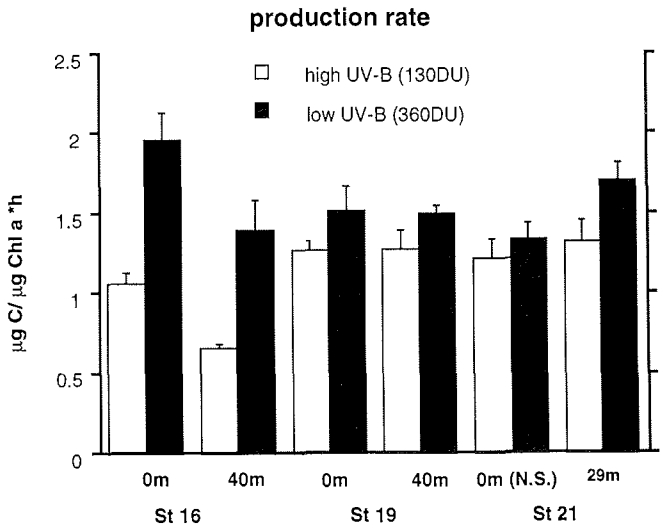

b

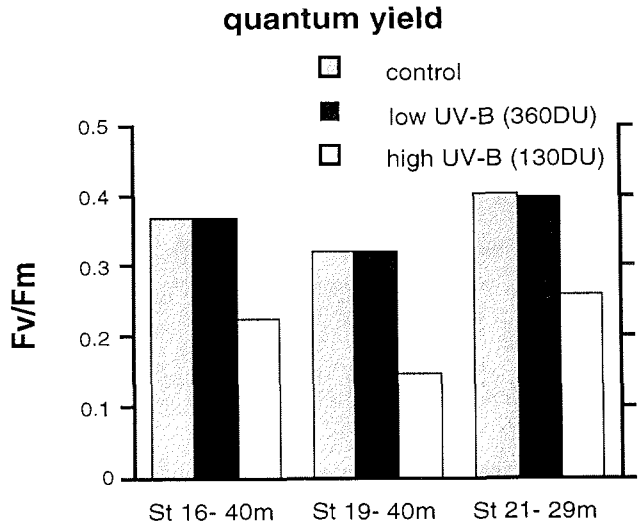

Fig. 14.12a, b Influence of enhanced UV- radiation due to stratospheric ozone depletion on phytoplankton photosynthesis

Experiments using ice- samples were designed to simulate a melting sea-ice situation where phytoplankton is released into the water column. On 3 out of 4 times, productivity was significantly lowered ($p < 0.05$) at ozone hole conditions relative to "normal " conditions. For sample 'ICE I' there was no significant difference ($p= 0.084$) (Fig.14.13a) despite a trend of lowered production under ozone hole conditions. Photosynthetic activity (Fv/Fm) showed a significant decrease after incubation under high UV compared to the controls (Fig.14.13b). Increasing UV light therefore seems to depress the primary production of ice algae.

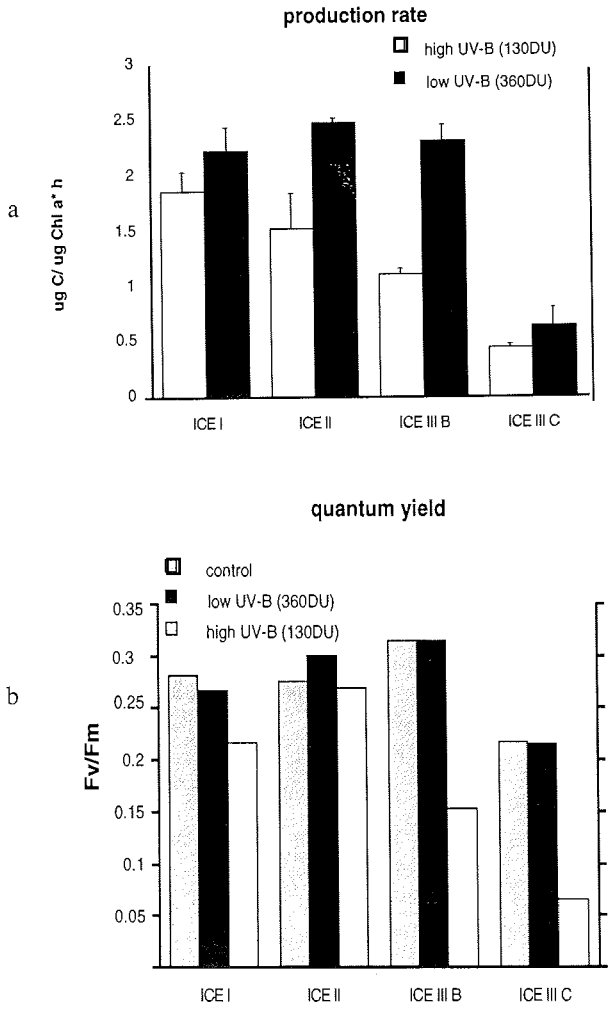

Fig. 14.13a, b Influence of enhanced UV- radiation due to stratospheric ozone depletion on phytoplankton photosynthesis at ice stations

15. ZOOPLANKTON DYNAMICS

C. Dubischar, U. Bathmann, S. Menden-Deuer, T. Rynearson

Introduction

Frontal systems in the oceans are often characterized by high concentrations of phyto- and zooplankton and enhanced biological activity. Underlying mechanisms controlling this phenomenon are varied depending on the physical characteristics of the front under consideration. One major aim of the *Polarstern*- cruise to the Antarctic Polar Front at about 10°E during austral summer 1995/6 was to investigate the hydrographic dynamics of the Polar Frontal Zone (PFZ) and its impact on zooplankton distribution and behaviour.
Zooplankton research activities during ANT XIII/2 concentrated on the determination of vertical and horizontal distributions of meso- and macrozooplankton in relation to water mass distribution in the Southern Ocean in spring. The main objective during this cruise was to gather information on biomass distribution, life cycle strategies, grazing and defecation rates of the dominant zooplankters and to assess the role of zooplankton in carbon cycling in the Southern Ocean as defined in the JGOFS implementation plan. Additionally, the impact of grazing on plankton species succession was studied.

Material and Methods

Zooplankton biomass and distribution

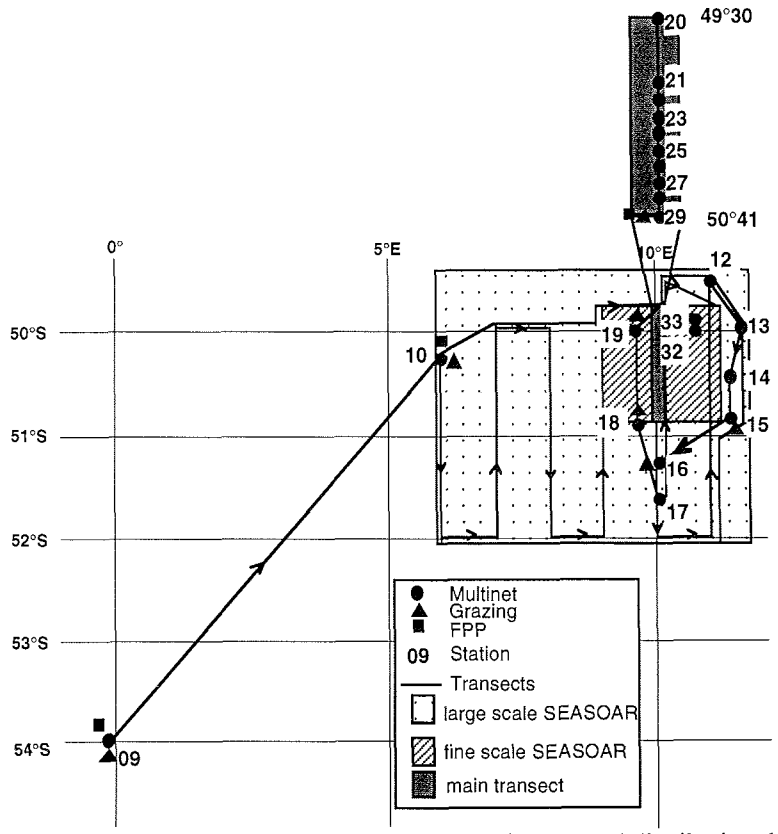

Fig. 15.1 Sampling stations to obtain zooplankton biomass and distribution during ANT XIII/2

Two methods were used during this study to determine zooplankton biomass and abundance:
1.) Net catches:
- Multinet (MN) -catches (100µm mesh-size) were carried out over 5 depth intervals (500-300 m, 300-100 m, 100-50 m, 50-25 m and 25-0 m) at stations indicated in Fig. 15.1.
- Rectangular Midwater Trawl (RMT)-catches (2000µm and 500µm mesh sizes) were carried out to a depth of 150 m at three positions in the Polar Frontal region.

2.) Optical Plankton Counter:
- Additional to net catches, the Optical Plankton Counter (OPC) was deployed to resolve the *in situ* small scale distribution of zooplankton with a high degree of resolution. Particle size is given as equivalent spherical diameter (ESD) of particles (= zooplankton) interfering with the passage of a red-light beam (640nm) to a photodiode (for details of the instrument, see Herman 1988, 1992). This instrument was used in two different ways: i) attached to the SeaSoar (see Pollard et al., Section 4 and Figs. 4.5, 4.7, 4.9) ii) deployed on station, where a second OPC was fixed on the Multinet to obtain vertical profiles of zooplankton distribution simultaneously with net catches. Because the OPC measures only the size and the number of particles in the water column, calibration of these data are very important requiring correlation of data from simultaneously obtained net catches and OPC-measurements.

The MN-samples were divided into subsamples with a Folsom plankton splitter; one half was stored in 4% seawater formalin solution (buffered with hexamethylenetetramine) for later analyses of species composition and abundance. Body volume determinations of the dominant species will be done by means of a video-image analyzer at the AWI. The other half of the sample was divided into different size fractions (100-200 µm, 200-500 µm, 500-1000 µm, 1000-2000 µm and >2000 µm) and each was filtered onto pre-weighed GF/C-filters (47 mm) for later analyses of AFDW (ash free dry weight). Other sub-samples were taken and deep-frozen for later POC-PON analyses with a Carlo Erba CHN 1500 analyzer at the AWI.

Zooplankton grazing and faecal pellet production

Grazing experiments and faecal pellet production experiments were carried out to assess the ecological role of zooplankton species on phytoplankton dynamics and to investigate the response of zooplankton species to changing physical and biological boundary conditions. These experiments were performed with dominant zooplankton species but mainly with *Rhincalanus gigas*, collected at different stations (Table 15.1, Fig. 15.1).

A Bongo-net (mesh-sizes 200 µm and 310 µm) with a sealed cod-end was used to catch undamaged animals for experiments. This net was lowered to a maximum depth of 200 m, depending on the physical structure of the water column. Grazing rates were determined by using two techniques: firstly, by following the JGOFS-protocol, gut fluorescence technique (Mackas and Bohrer 1976, JGOFS 1989) and secondly, by carrying out bottle-experiments and calculating the grazing rates (chlorophyll removal) using the formulae of Frost (1972). These measurements were accompanied by determining the faecal pellet production of *R. gigas* in order to estimate its impact on vertical flux. For bottle-experiments as well as for the faecal pellet production experiments, water samples were taken with a bucket at the different stations and passed through a 500 µm net to exclude larger zooplankton. Samples of the dominant species were taken for later analyses of the fatty acid composition.

Experiment	Date	Position
Faecal pellet production experiment No. I of *R. gigas.*,	22.12.95	Sta. 09
Faecal pellet production experiment No. II of *R. gigas.*	25.12.95	Sta. 10
Grazing Experiment (Bottle Experiment) No. I *R. gigas*	22.12.95	Sta. 09
Grazing Experiment (Bottle Experiment) No. II *R. gigas*	25.12.95	Sta. 10
Gut fluorescence experiment *R. gigas*	30.12.95	Sta. 15
Grazing Experiment (Bottle Experiment) No. III *R. gigas*	30.12.95	Sta. 16
Grazing Experiment (Bottle Experiment) No. **IV** *R. gigas*	02.01.96	Sta. 16,
Gut fluorescence experiment *Salpa thompsonii*	05.01.96	Sta. 18
Grazing Experiment (Bottle Experiment) No. **VI** *Salpa thompsonii* and *R. gigas*	05.01.96	Sta. 18
Grazing Experiment (Bottle Experiment) No. VII *R. gigas* and *Pleuromamma*	06.01.96	Sta. 19
Grazing Experiment (Bottle Experiment) No. VIII *R. giga s* and *Pleuromamma*	08.01.96	Sta. 29
Faecal pellet production experiment: *R. gigas* with and without additional cyclopoid copepods	08.01.96	Sta. 29

Tab. 15.1 List of the grazing and faecal pellet production experiments carried out on-board *Polarstern* during the cruise.

Preliminary results

Field observations

High resolution vertical profiles of particle concentration, for 4 stations out of a total of 30, are illustrated in Fig. 15.2.

On the left hand side, the total particle count of up to 15 000 particles per m^3 is plotted with depth. In adjacent columns, this total is broken down into the size categories indicated. Note the different scales for size classes 800-1000 µm and >1000 µm.

Stations 21, 23 and 27 are located on the north-south transect sampled in the Polar Frontal region (Fig. 15.1). Maximum particle abundance was generally found in the upper 70 m of the water column. In most cases, particles in the smallest size-class (250-350 µm) reached maximum concentrations at depths of about 100 m below the main pycnocline (ca. 70 m; Pollard et al. Section 4). The surface maximum was comprised of particles >500 µm ESD. Typically, <30 % of all particles recorded were >800 µm.

Station 30 was encountered at the ACC/Weddell Gyre boundary in the centre of an intensive phytoplankton bloom dominated by *Phaeocystis* sp. (see section Phytoplankton). The vertical profile and the size spectrum and abundance of particles recorded optically at this station differed significantly from all those at other stations. Maximum particle concentrations were recorded near the sea surface in the size category >1000 µm ESD. This signal at the sea surface was probably due to colonies of *Phaeocystis* .

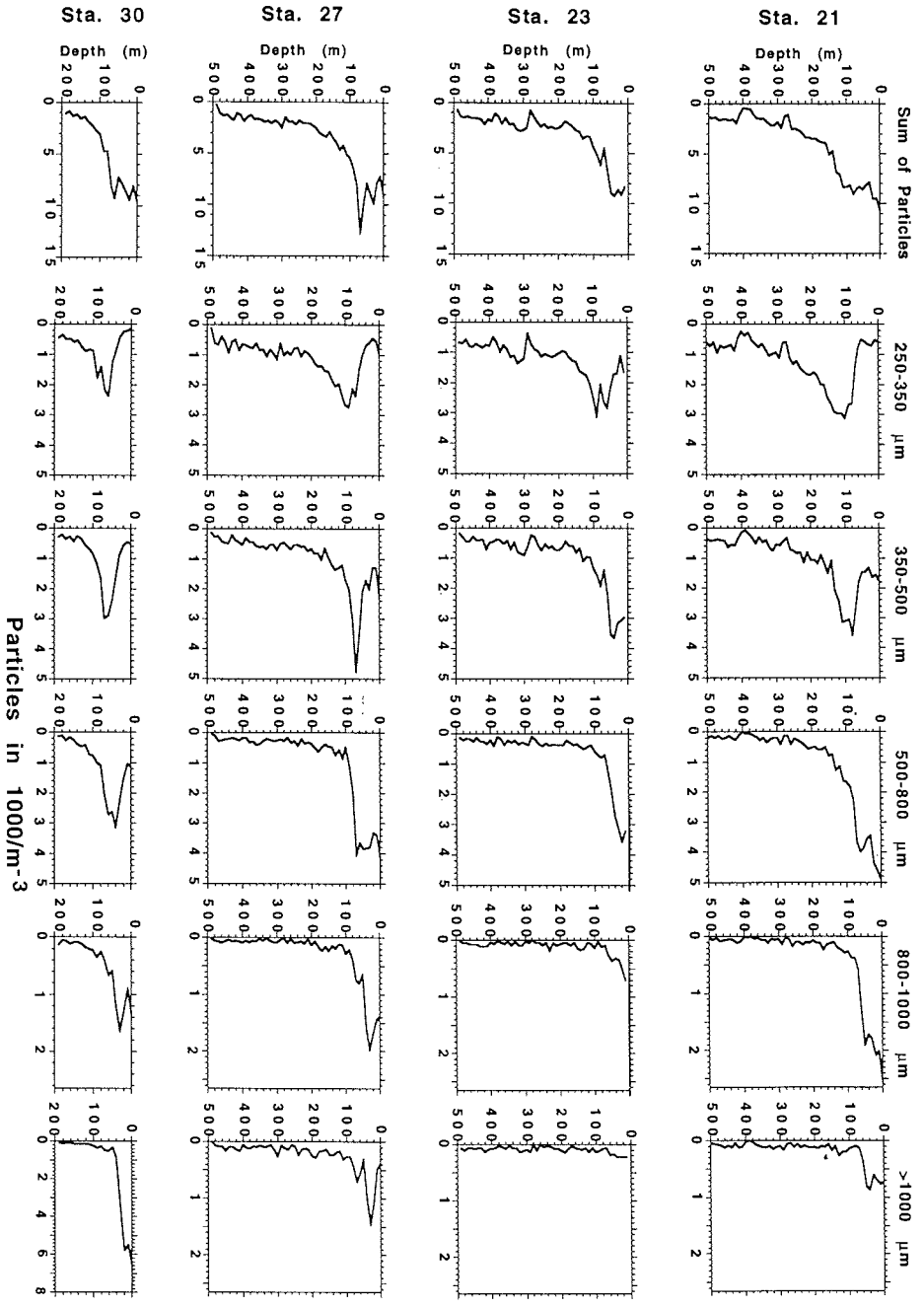

Fig. 15.2 Vertical profiles of particle concentrations obtained with the Optical Plankton Counter (OPC) mounted on the MN. Note the differences in scales between the sum of particles and the different size-classes, especially for the largest size-class at station 30

Feeding experiments

One example of the feeding experiments carried out with dominant zooplankton species (mainly *Rhincalanus gigas*) during the cruise (Table 15.1) is shown in Fig. 15.3 below. This shows chlorophyll *a* concentrations with time in controls and in experimental bottles containing *Pleuromamma* or *Rhincalanus gigas*. Chlorophyll *a* concentrations did not change significantly in controls or in bottles containing *Pleuromamma*, but decreased significantly in bottles containing *Rhincalanus gigas;* equivalent to a grazing rate of 50 - 140 ng Chl*a* ind^{-1} day^{-1} or 2.5 - 7.0 µg C ind^{-1} day^{-1} (phytoplankton carbon:Chl*a* = 50:1).

Grazing experiments to determine selectivity or avoidance of phytoplankton species await microscopical examination of the samples in the home laboratory before results from these experiments can be presented.

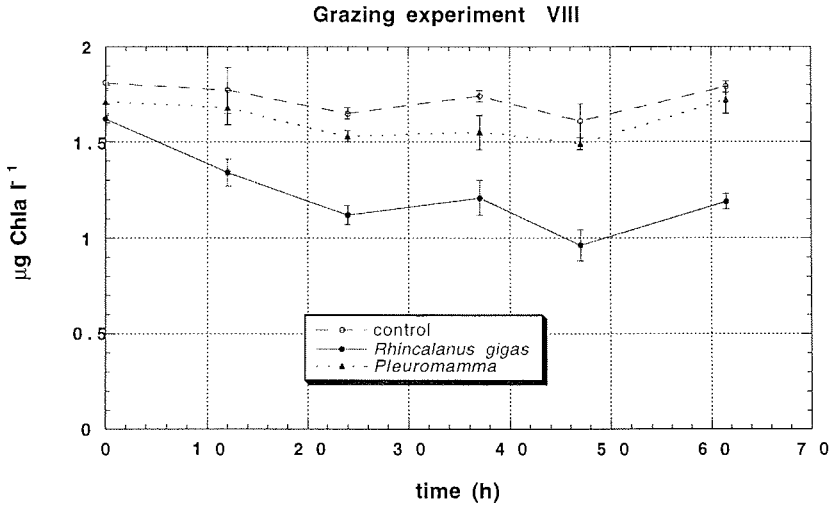

Fig. 15.3 Development of Chl*a* concentrations with time in experimental containers with and without grazers. Error-bars show standard deviations (n=3)

References

Frost B.W. (1972): Effects of size and concentration of food particles on the feeding behavior of the marine planktonic copepod *Calanus pacificus*. Limnol. Oceanogr. 17, 805-815

Herman A.W. (1988): Simoultaneous Measurement of Zooplankton and Light Attenuance with a New Optical Plankton Counter. Continental Shelf Research, 8, 205-221

Herman A.W. (1992): Design and calibration of a new optical plankton counter capable of sizing small small zooplankton. Deep Sea Research, 39, 395-415

JGOFS (1989): Core measurements protocols, reports of the core measurement working groups. In: Tidmarsh E. (Ed.): SCOR, JGOFS Report 6, 40 S.

Mackas D. und Bohrer R. (1976): Fluorescence analysis of zooplankton gut contents and an investigation of diel feeding patterns. J. exp. mar. Biol. Ecol. 25, 77-85

16. BACTERIA, VIRUSES AND MARINE SNOW

M. Simon, K. Hennes, B. Rosenstock

Introduction

Bacteria

Until recently, very limited information was available on the utilization of the major dissolved labile organic compounds by planktonic bacteria in the Southern Ocean. These compounds comprise dissolved free and combined amino acids (DFAA & DCAA), proteins and dissolved free mono- and polysaccharides (DMCHO & DPCHO). We therefore investigated the dynamics of these bacterial substrates in the Polar Front including measurements of *in situ* concentrations, the release of proteins, DFAA and DMCHO by phytoplankton and zooplankton grazing and their bacterial utilization in the context of bacterioplankton growth demands. In addition, we studied the adaptation of bacterioplankton growth to temperature in the Polar Front, at the northern and southern edge of the Antarctic Circumpolar Current (ACC) and in the pack ice zone near Neumayer Station.

Bacterioplankton abundance was enumerated by standard epifluorescence microscopy after DAPI staining. Bacterioplankton production was measured by the leucine (Leu) and thymidine (TdR) incorporation techniques using ^{14}C-leucine and ^{3}H-thymidine in a dual-label approach (Simon & Azam 1989, Fuhrman & Azam 1982). Added final concentrations of Leu and TdR were 10 nM each which ensured maximum uptake rates. For the preliminary evaluation of the data the following conversion factors were used: Leu: 3 kg C/mol; TdR: 1.1×10^{18} cells/mol (Björnsen & Kuparinen 1991). Three experiments for measuring intracellular isotope dilution of radiolabelled Leu to determine a precise conversion factor of Leu (Simon & Azam 1989) were carried out and will be evaluated in the home laboratory. Uptake of DFAA was determined by the turnover rate of a mixture of 10 ^{3}H-amino acids (0.1 nM, final concentration) and ambient concentrations of DFAA. Uptake of dissolved protein was measured by the incorporation of ^{14}C-protein (2 nM DFAA equivalents, final concentration) and the ambient concentration measured as 50% of Kt+Sn which was determined by concentration kinetics according to Wright & Hobbie (1965). Both rate measurements adopted a dual-label approach. Uptake of dissolved monosaccharides was measured via the turnover rates of ^{3}H-glucose and ^{3}H-galactose (0.2 nM, final total concentration) and the ambient concentration of DMCHO. Concentrations of DFAA, DCAA, DMCHO and DPCHO will be analysed in the home laboratory by high performance liquid chromatography (HPLC). Release of DFAA, dissolved proteins and DMCHO were measured by an isotope dilution approach and ambient concentrations and will be evaluated in the home laboratory.
To examine bacterioplankton temperature adaptation, we measured Leu and TdR incorporation at 0, 2, 5, 8, 12 and 18 or 20 °C.

Viruses

Bacteria-specific viruses (phages) have been shown to be important in controlling bacterioplankton growth in various marine environments. So far, however, true oceanic regions such as the Polar Front have not been included in these investigations. Therefore, we studied the distribution of free viruses and the fraction of infected bacteria in relation to bacterioplankton dynamics.

Free viruses were counted after staining with YOPRO by epifluorescence microscopy (Hennes & Suttle 1995). The fraction of phage-infected bacteria will be determined by transmission electron microscopy (TEM, Hennes & Simon 1995).

Phyto-aggregates (Marine Snow)

The aggregation of phytoplankton cells is known to often occur during late stages of blooms and is a major form in which senescent algae and particulate organic material sinks out of the mixed layer. The aim of this study was to examine the aggregation potential of phytoplankton at the Polar Front in relation to environmental parameters such as transparent exopolymer particles (TEP, Passow et al. 1994), phytoplankton species composition and the sinking flux.

Aggregation of bulk water samples of various depths was studied in rolling cylinders (1.1 and 2.8 liters) according to Shanks and Edmonson (1989) under simulated *in situ* conditions. For each experiment, 4 to 10 replicate cylinders were incubated. The cylinders were examined periodically to record the time until visible aggregates (2-3 mm diameter) occurred and then incubated further to examine the development of the aggregates, the ageing of algae and the colonization by bacteria. Periodically, aggregates were harvested and examined microscopically for phytoplankton species composition and, after staining with Alcian blue, for the occurrence of TEP. Subsamples for the analysis of the community structure of bacteria colonising the aggregates were deep frozen. Subsequent analyses by fluorescent rRNA-targeted oligonucleotide probes (Amann et al. 1995) will be done back at the home laboratory.

Results

Bacteria

Samples to determine bacterioplankton substrate dynamics were collected at the following stations: 5, 7, 9, 10, 11, 12, 13, 14, 15, 16, 17, 18, 19, 20, 22, 25, 29, 32, 33. Usually 7 depths between 20 m and 200 m were sampled. In addition, abundance and production of planktonic bacteria in the mesopelagic zone was measured in four samples between 300 m and 1000 m at stations 5, 7, 9, 13, 15, 18, 19, 25, 29, 32 and 33.

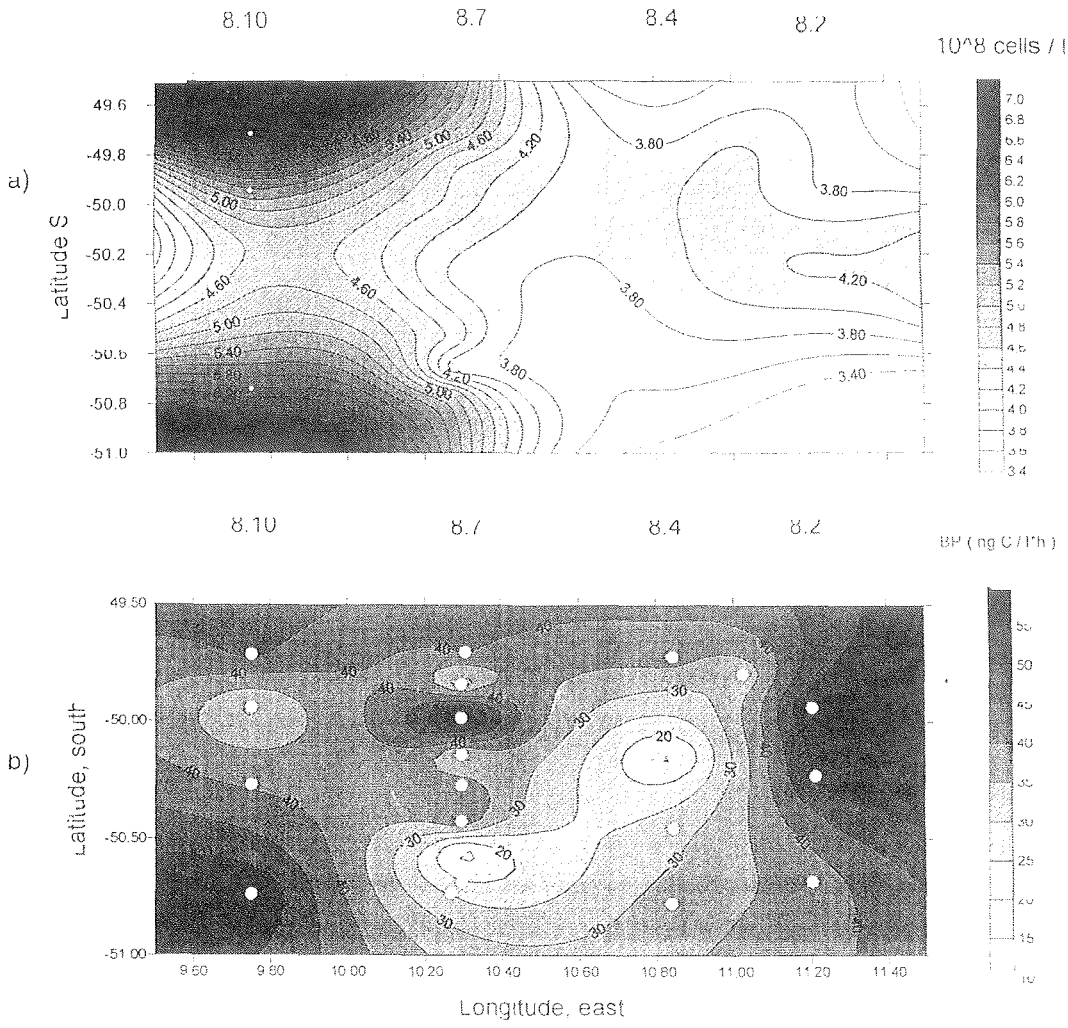

Fig. 16.1 Bacterial a) abundance and b) production rates within the small scale grid. (Transects 8.2, 8.4, 8.7 and 8.10.)

Bacterioplankton abundance ranged from $<4x10^8$ cells l^{-1} in the eastern area to $>6x10^8$ cells l^{-1} in the western part, indicating that the ACC water in the southeastern part contained fewer bacteria than the frontal water masses. This pattern was not reflected by that of bacterioplankton production. Maxima of >40 ng C l^{-1} h^{-1} occurred at the northeastern and southwestern edges of the area studied and close to the center of transect 8.7. Minima were recorded close to the center of this area. The turnover times of DFAA and dissolved proteins exhibited fairly similar patterns suggesting that they were important substrates for bacterioplankton production. Numbers of free viruses ranged between $0.7x10^{10}$ and $5.7x10^{10}$ viruses l^{-1}. Lowest numbers occurred in the southeastern area where low bacterial numbers were also found. Maxima occurred at stations with high bacterial production rates such as at the northern end of transect 8.2 and on transect 8.7. In general the patterns of bacterioplankton and virus dynamics reflected the horizontal distribution of phytoplankton and zooplankton abundances and indicated that the whole plankton community was fairly similarly affected by the physical pattern of the water masses at the Polar Front.

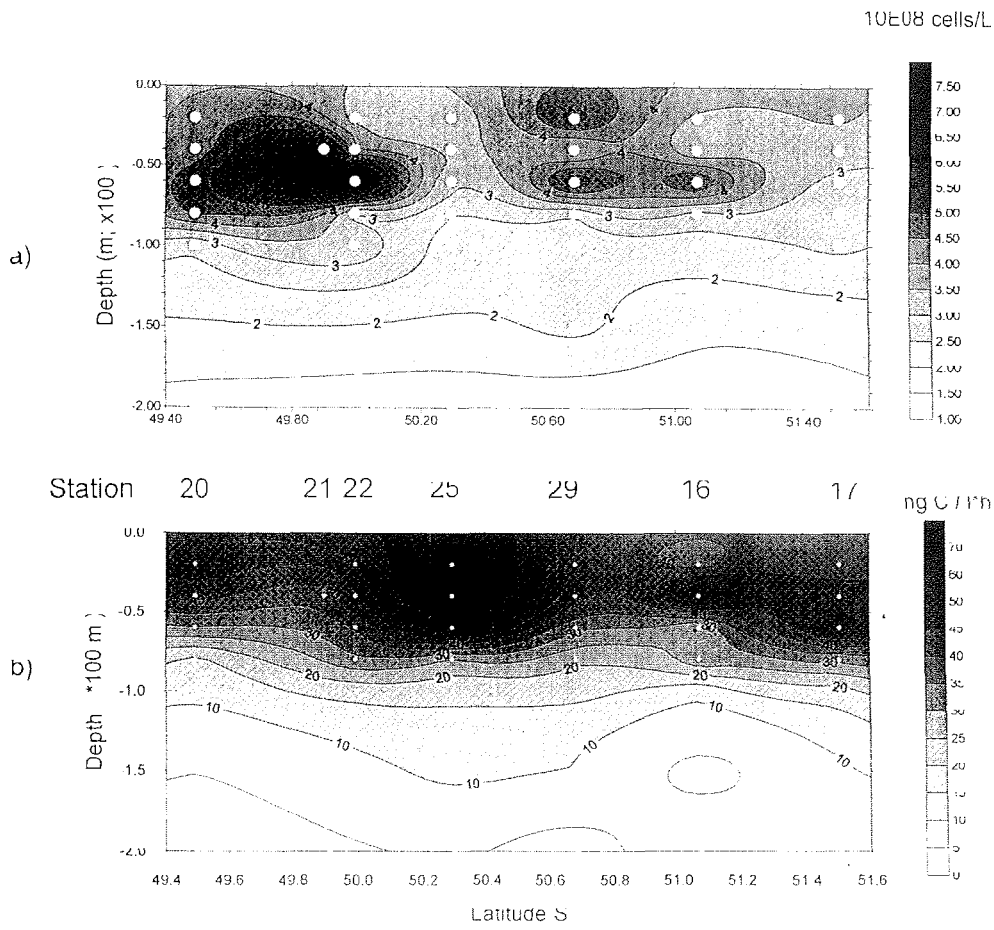

Fig. 16.2 Bacterioplankton a) abundance and b) production rates of the central transect (7.2 and 9.2, stations 20, 21, 22, 25, 29, 16, 17)

Highest cell numbers occurred at 60 m depth at stations 22, 29 and 16 at the bottom of the mixed layer. Highest rates of bacterial production, however, occurred at station 25 at 20 and 40 m, coinciding with the phytoplankton maximum, and at stations 16 and 17 where minima of turnover times of DFAA and dissolved proteins were found.

Bacterioplankton abundance in the upper 200 m ranged from 1 to $8x10^8$ cells l^{-1} and bacterial production rates in the same layer ranged from <5 to 75 ng C l^{-1} h^{-1}. Highest numbers and production rates occurred between 20 m and 60 m. Generation times, ranging between 2 and >20 d, covaried with production rates. Turnover times of DFAA exhibited great variations ranging from as short as <4 to >100 d. They were substantially shorter than those of DMCHO which ranged from 10 to >300 d. The spatial patterns of the turnover times of both substrates covaried only weakly. Whether the different turnover times were due to much higher concentrations of DMCHO and similar bacterial uptake rates of DFAA and DMCHO or to a much more rapid uptake of DFAA by bacteria relative to DMCHO can only be resolved when ambient concentrations have been analysed. Interestingly, the turnover of dissolved proteins was always faster than that of DFAA ranging between 1 and 10 d, and covaried with that of DFAA. The ambient concentration of dissolved proteins was between 40 and 140 nM (DFAA equivalents).

Temperature adaptation by bacteria

In all experiments we found elevated bacterial production with increasing temperature, indicating that bacteria were apparently not well adapted to the ambient temperature. The temperature optimum, however, differed in the various water masses. At the Polar Front, the optimum was not yet reached at 12 or 20°C. At the northern edge of the ACC it was at 12°C whereas it was at 8°C at the southern edge of the ACC. Bacterioplankton growth above these temperatures was reduced. In the pack ice, two levels were detected; one below 2°C and another distinct optimum at 12°C. Q_{10} values varied considerably. Usually, values for Leu were higher than for TdR (Tab. 16.1). Most values ranged between 1.7 and 3.1. Lower values occurred at the pack ice station below 2°C. Values considerably higher were found at the Polar Front, suggesting that bacterioplankton populations adapted differently to the varying temperature ranges tested.

Latitude		Temp (°C)		Q_{10}	
		in situ	range	Leu	TdR
49° 42' S	Polar Front	4.5	0 - 12	5.2	3.8
49° 45' S	Polar Front	4.5	0 - 12	3.1	2.3
49° 24' S	Polar Front	4.5	0 - 20	32.5	18.5
58° 56' S	northern ACC	0.12	0 -12	3.7	2.7
68° 50' S	southern ACC	0.11	0 - 8	1.7	1.9
70° 30' S	Pack ice	-1.67	-0.5 - 2	1.5	1.3
			4 - 11	2.6	1.8

Tab. 16.1 Bacterioplankton growth response to increasing temperature. Q_{10} values for Leu and TdR incorporation are given

Viruses

Abundances of free viruses in surface waters ranged from 0.7×10^{10} to 5.7×10^{10} viruses l^{-1}. In genera, higher numbers of viruses covaried with the abundance of bacterioplankton. An even closer covariation often occurred with bacterioplankton production rates. The ratio of virus/bacteria varied between 17 and 139. A detailed analysis of the data will be done later together with that of the fraction of virus-infected bacteria which will be determined on ultrathin sections of TEM-prepared specimens. This evaluation will yield production rates of viruses and bacterial mortality rates due to virus infection.

Phytoaggregates (Marine Snow)

Experiments were performed at 7 stations with samples from various depths (Tab. 16.2). In most experiments numerous aggregates (approx. 5-50 per cylinder) of 2-3 mm formed within 2 to 7 hours. At stations 5, 7 and 9 they further aggregated into larger, but fewer, aggregates with an equivalent spherical diameter of 8 to 20 mm after 7 to 20 hours. Later on, the size and shape remained fairly similar although they became more compact. In several cases aggregation was much slower (Sta 9, 100 m; Sta 11, 40 m), or no aggregates formed at all in several or all cylinders (Sta 7, 20 m; Sta 13, 15 m). At stations 11, 13 and 21 the initially very abundant (>50 per cylinder) small (2-3 mm) aggregates persisted for several days and did not further increase in size. In some cases when larger (8-15 mm) aggregates had been formed, they disintegrated again (Sta 11, 40 m; Sta 21, 25 m). The dominating algae in the bulk water and the aggregates were *Pseudonitzschia* spp, *Chaetoceros* spp, *Corethron* spp and *Thalassiothrix* spp. *Thalassiothrix* spp was abundant only at Sta 11, 13 and 21, suggesting that these extremely long (10-30 mm), needle-like cells or cell bundles hindered or even prevented aggregation. As shown by bright-field microscopy after staining with Alcian blue, algae were frequently (as

single cells or as aggregates) covered with acidic polysaccharides. However, distinct TEP particles were rarely found in aggregates or in bulk water. Quite a few algae exhibited only weak or no excretion of acidic polysaccharides, as indicated by only very dim or no blue coloration after Alcian blue staining. This was in particular true for samples where no aggregates formed, where the formation was delayed or when aggregates disintegrated again. As shown by epifluorescence microscopy after DAPI staining, bacterial colonization of aggregates was fairly slow. Within the first two days after aggregate formation, algal cells were either not colonized or colonized by only very few bacteria (<5 cells per algae). Aggregates became heavily colonized only after 7 to 9 days. At this stage many bacteria were found inside the algal cells and bacterial microcolonies were abundant in the aggregates.

These results suggest that the aggregation potential of ambient phytoplankton populations was weak and thus phytoplankton in form of phyto-detritus (marine snow) contributed only very little to the sinking flux which was apparently not very pronounced at the Polar Front during our survey.

Station	Position	Depth (m)	Time of Formation (h)
5	50° 11.57' S 05° 51.93' E	30	4
7	57° 19.60' S 01° 55.70' W	20 50 100	no aggregates 4 10
9	54° 00.00' S 00° 06.20' E	20 60 100	6.5 2.3 21.5
10	50° 28.70' S 08° 08.90' E	20 40	5 5
11	49° 51.08' S 10° 17.65' E	40	20.5 (aggs disintegrated after 40 h)
13	49° 51.92' S 11° 32.23' E	15	3.5
21	49° 54.30' S 10° 18.49' E	20 40	10 10

Table 16.2 Formation of aggregates in rolling tanks at the Polar Front.

References

Amann, RI, W Ludwig, KH Schleifer, 1995. Phylogenetic identification and *in situ* detection of individual microbial cells without cultivation. Microbiol Rev 59: 143-169.

Björnsen PK, J Kuparinen, 1991. Determination of bacterioplankton biomass, net production and growth efficiency in the Southern ocean. Mar Ecol Prog Ser 71: 185-194.

Fuhrman JA, F Azam, 1982. Thymidine incorporation as a measure of heterotrophic bacterioplankton production in marine surface waters. Evaluation and field results. Mar Biol 66: 109-120.

Hennes KP, M Simon, 1995. Significance of bacteriophages for controlling bacterioplankton growth in a mesotrophic lake. Appl Environ Microbiol 61: 333-340.

Hennes KP, CA Suttle, 1995. Direct counts of viruses in natural waters and laboratory cultures by epifluorescence microscopy. Limnol Oceanogr 40: 1050-1055.

Passow U, AL Alldredge, BE Logan, 1994. The role of particulate carbohydrate exudates in the flocculation of diatom blooms. Deep Sea Res 41: 335-357.

Shanks AL, EW Edmondson, 1989. Laboratory-made artificial marine snow: a biological model of the real thing. Mar Biol 101: 463-470.

Simon M, F Azam, 1989. Protein content and protein synthesis rates of planktonic marine bacteria. Mar Ecol Prog Ser. 51: 201-213.

Wright RT, JE Hobbie, 1965. The uptake of organic solutes in lake water. Limnol Oceanogr 10: 22-28.

17. EXPORT PRODUCTION MEASURED WITH THE NATURAL TRACER TH-234 AND SEDIMENT TRAPS

M.M. Rutgers van der Loeff, U.V. Bathmann, K.O. Buesseler

Introduction

During the SO JGOFS expedition ANT X/6 we used the natural radioisotope ^{234}Th as a tracer of export production and compared this to flux measurements obtained by sediment trap deployments. ^{234}Th is produced in seawater by decay of ^{238}U, an isotope which has such a long residence time in the ocean that its activity can be derived from salinity according to Chen et al. (1986). Deviations from secular equilibrium of ^{234}Th (24 days half-life) with its parent ^{238}U are caused by the particle reactive nature of Th. During ANT X/6, two steps in the development of the bloom in the Polar Front region could be distinguished: first, the progressive adsorption of Th onto particles as the suspended load and chlorophyll content increased; then the export of particles, which was evident from the development of ^{234}Th depletion in surface water of up to 37% relative to ^{238}U. From this depletion and the POC/^{234}Th ratio on suspended particles, carbon export of between 0.43 and 0.86 mol C m^{-2} was estimated for the 22-day period.

During the present expedition, it was our aim to use the same tracer not only to obtain an estimate of export production, but also to obtain information on the subtleties of upwelling, downwelling and the overlayering of water masses in the frontal region. Evidence for the latter is seen when chlorophyll maxima are sometimes observed at depths where light is insufficient for dense blooms to develop. In such situations, ^{234}Th might provide clues as to whether the particles have sunk (i.e. have been imported) to the respective depth, or whether the entire water mass has been overlain by clearer water.

Sampling strategy and methods

Horizontal particulate distribution

The horizontal distribution of particulate and dissolved ^{234}Th was obtained by frequent sampling from the ship's seawater supply; using the membrane pump seawater intake from the bow thruster tube (approx. 7m depth).

Two methods were used:

1) 32-liter samples were collected after passage through the in-line fluorimeter, in parallel with samples taken for chlorophyll calibration and POC measurements. Analysis began by pressure filtration of these samples through 1 µm Nuclepore filters, co-precipitation of dissolved Th onto a fresh MnO_2 precipitate which was collected on a similar filter, and direct beta counting of both filters (Rutgers van der Loeff in Kuhn, cruise report ANT XI/4, in press). This method was developed for measurements in the nepheloid layer. Application to surface waters requires two additional measurements which have to be made after the expedition. First, the contribution of beta emitters other than ^{234}Th has to be checked by following the decay of representative filters with time over several ^{234}Th half-lives. Similar checks made after ANT XI/4 showed that the effect of Ra-daughters must be small, but for greatest accuracy, it has to be evaluated here again, as the Ra concentration gradients in surface waters are appreciable. Second, some filters were so heavily loaded with particles, that self-adsorption has to be determined for each of these samples individually. These two checks imply that the results obtained on-board are still preliminary, but we estimate that the total correction will be below 10% of the total ^{234}Th activity measured in surface water.

2) In the main study area where the SeaSoar survey was conducted, greater resolution was obtained with the method of Hartman and Buesseler (1994). For this approach, 200-300L of seawater was passed at a flow rate of 4-8 L/min over a pre-combusted quartz filter and over two

MnO_2 absorbers. These samples will be analysed after the expedition for POC and dissolved and particulate ^{234}Th at Woods Hole Oceanographic Institute.

Vertical particulate distribution
The water from 2-4 Rosette bottles, closed at the same depth, was combined to give one 20-30 L sample for Th, as well as a 5-L sample for POC and biogenic Si analyses. The Th sample was filtered under pressure and analysed as described above under 1.

Sediment trap deployments
For a total of 14 days, we deployed two sediment traps in 500 and 1500 m water depth respectively on a mooring additionally equipped with mechanical and acoustic current meters and an up-ward looking ADCP at a geographical position at the north-eastern edge of the investigation area. Sampling cups were filled with a brine seawater solution (38 PSU) containing $HgCl_2$ as a preservative. Sampling interval was 48 hours. All sampling procedures were done according to JGOFS core parameter protocols (UNESCO 1994, JGOFS 1996). Data will be analyzed in home institutes.

Results

1. Horizontal distribution

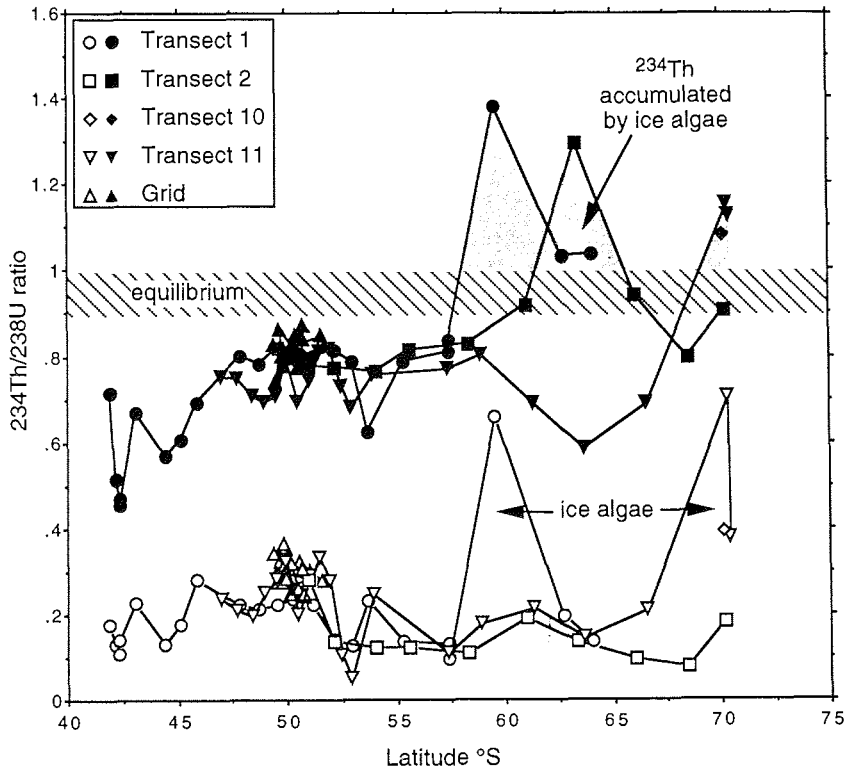

Fig. 17.1 Particulate (open symbols) and total (closed symbols) ^{234}Th in surface water, expressed as a ratio to ^{238}U, over the various N-S transects, showing the depletion of total ^{234}Th relative to ^{238}U near the subtropical front and at 54°S, and the excess activities in the south due to accumulation on ice algae. The hatched bar represents the uncertainty in the level of the $^{234}Th/^{238}U$ equilibrium

In a wide latitudinal band encompassing all transects made, there was only a very moderate, invariable depletion of ^{234}Th. All surface determinations made on-board in the survey area (and awaiting confirmation by the second method), fall within a narrow range. These results imply little or no export production. Alternatively, we missed the export event at the Polar Front similar to that observed three years before, or, we cannot exclude the possibility that significant export may have occurred over a wide area some 1-2 months earlier, followed by a partial return towards equilibrium associated with the development of a more re-cycling based plankton community. Nevertheless, the strongest depletion occurred at the Subtropical Front while another event was observed at 54°S. Here, SeaSoar identified a narrow band of deep chlorophyll-a penetration which persisted for at least 12 days when the location was again sampled (Sta. 9). Only much further south did dramatic changes occur in samples collected when the ship was breaking its way through melting ice, releasing a dense cloud of ice algae. The occasional large excess of ^{234}Th implies that ice and/or algae attached to the underside of the ice accumulate this isotope, to release it rapidly upon ice melt. As a similar process was postulated by Friedrich (1994) to explain the atypical vertical distribution of ^{210}Po in Antarctic Surface Water, samples were taken to analyse ^{210}Po and ^{210}Pb in these water masses after our return.

2. Vertical distribution

Remarkably similar profiles of dissolved and particulate ^{234}Th were obtained at 14 stations. Particulate ^{234}Th typically has the highest activity in the upper 60m, and gradually declines downward, simply reflecting the distribution of suspended particles. Total ^{234}Th, the sum of particulate and dissolved activities, is depleted relative to ^{238}U in the surface water by about 20%. This depletion disappears gradually towards 200m depth. Equilibrium with ^{238}U from 200m downwards was confirmed by some measurements in the clear water minimum at 2000-2500m depth.

Export production

In view of the expected corrections, we estimate that the actual depletion at all stations corresponds to at most 10% over a depth range of 100m. Applying the same assumptions and particulate $C_{org}/^{234}Th$ ratios as observed in 1992, this corresponds to an export production of at most 100 mg C m^{-2} d^{-1}. The remarkable similarity of all profiles implies that no major export event happened anywhere in the research area during the expedition. The only exception was at 54°S. (station 9), where the deep chlorophyll maximum, observed 12 days earlier, was gone. This station stands out with the highest ^{234}Th depletions at 60 and 100m, suggesting that an export event had occurred in the meantime.

The benthic nepheloid layer

At station 18, transmissiometer data showed that a nepheloid layer was well developed. One sample could be obtained at 4300m, at about 10m above the seafloor. Particulate ^{234}Th constituted 25% of total activity, but total ^{234}Th did not show depletion with respect to ^{238}U. This means that the particles had been in suspension during a period which is long in comparison with the 24 days halflife of ^{234}Th.

References

Chen, J. H., L. R. Edwards, and G. J. Wasserburg (1986) 238U, 234U and 232Th in seawater. *Earth Planet. Sci. Lett.,* 80, 241- 251.

Friedrich, J., and M. M. Rutgers van der Loeff (1994) Polonium-210 and lead-210 in surface waters of the Antarctic Circumpolar Current during development of plankton blooms. *EOS abstract,* 75, 219.

Hartman, M. C., and K. O. Buesseler (1994) Adsorbers for in-situ collection and at-sea gamma analysis of dissolved Thorium-234 in seawater, WHOI, Woods Hole,

JGOFS Report 19 (1996) Protocols for the Joint Global Ocean Flux Study (JGOFS) Core measurements. 170 pp.

Kuhn, G. (1995) Cruise Report ANT XI/4. *Reports on Polar Research,* in press.

UNESCO (1994) Protocols for the Joint Global Ocean Flux Study (JGOFS) Core measurements. *Manual and Guide* 29, 170 pp.

18. CENSUSES OF MARINE BIRDS AND MAMMALS

J. A. van Franeker, N. W. van den Brink

Introduction

The interdisciplinary approach of *Polarstern's* JGOFS studies offers an excellent framework for gaining knowledge of the pelagic ecology of marine top predators, as their numbers and distribution can be viewed in the light of environmental physico-chemical and biological conditions. The obtained information can assist in the compilation of population estimates for Antarctic species and in the identification of particular environments or geographical areas on which they depend (van Franeker 1996). Such information is needed in issues of management of the Antarctic environment, for example within the framework of the Convention for the Conservation of Antarctic Marine Living Resources (CCAMLR).

Although a previous study (van Franeker et al. in press) showed that Antarctic top predators play a minor role in terms of direct carbon consumption, they may be a forcing power in structuring the ecosystem. Moreover, their species composition, abundance and distributional patterns may assist in revealing trophic structure and abundance of lower ecosystem levels not easily studied directly. Top predators can therefore contribute to the JGOFS aim of understanding and quantifying carbon fluxes in marine systems.

Methods

Observations of seabirds, seals and whales were made from outdoor observation posts installed on top of the bridge of *Polarstern*. The unobstructed clear view to all sides is required for quantitative observations. Only from this position is it reasonably possible to identify which birds are associated with the ship and have to be omitted from quantitative density counts. Bird observations are based on the snapshot method (Tasker et al. 1984) which has an advantage over the BIOMASS (1984) method since it accounts for bias by bird movement. Quantitative differences between snapshot and BIOMASS methods have been evaluated in van Franeker (1994). Birds as well as seals are counted in a band transect in time blocks of ten minutes from the moving ship. Ship speed and transect width can be used to convert observed numbers of animals to densities per unit of surface area for each ten-minute period. The width of the transect band for seals and birds was usually 300m, taken as 150m on each side of the ship. Depending on viewing conditions such as sea-state, light and glare, the transect width was adapted to allow optimal quantitative observations. For seals and whales, line transect methods (Hiby and Hammond 1989) were tested simultaneously with the band transect methods. Although band-transect methods were the standard method for seal censuses (Laws 1980), the new Antarctic Pack Ice Seal Program (APIS) will probably switch to line-transect methods (SCAR Group of Specialists on Seals 1994; Anonymous 1995). Dedicated whale surveys use line-transect methods as a standard (Hiby and Hammond 1989), but these are not always possible in studies like this one due to the low number of animals observed. In this report 'effective transect widths' for different whale groups were estimated to make calculations. Preliminary results in this paper are thus all based on the band-transect system. Methods to convert top predator densities to their daily food or carbon requirements are based on published literature values of field metabolic rates described in detail in van Franeker (1992) and van Franeker et al (in press). Data for seals have yet to be adjusted for diurnal changes in haul-out behaviour of the Crabeater Seal (Erickson et al. 1989). In addition to the quantitative counts, qualitative information was collected on the occurrence of species outside transect bands or during oceanographic sampling stations.

Ten-minute records of ice conditions were made in association with the top predator study. These provide small-scale details that add to the ice observations according to the SO-JGOFS protocol (van den Brink & van Franeker, this volume). The 10-minute bird and ice observations will be included in the 'ANTXIII/2 surface-database' which combines all sorts of continuous measurements from the surface layer.

Results and Discussion

A total of 2305 quantitative ten-minute censuses was conducted during the cruise, representing a total surface band-transect of 2537 km^2. Additional 225 non-quantitative censuses were conducted at stations. The observations were fairly evenly spaced over a wide latitudinal range (37°S to 70°S) during the long transects to Neumayer (trans. 1-5 and 10-11). As far as permitted by weather and daylight, censuses were also conducted during the small scale grid in the Polar Front (trans. 6-9). All top predator data have been stored on an ORACLE-like database.

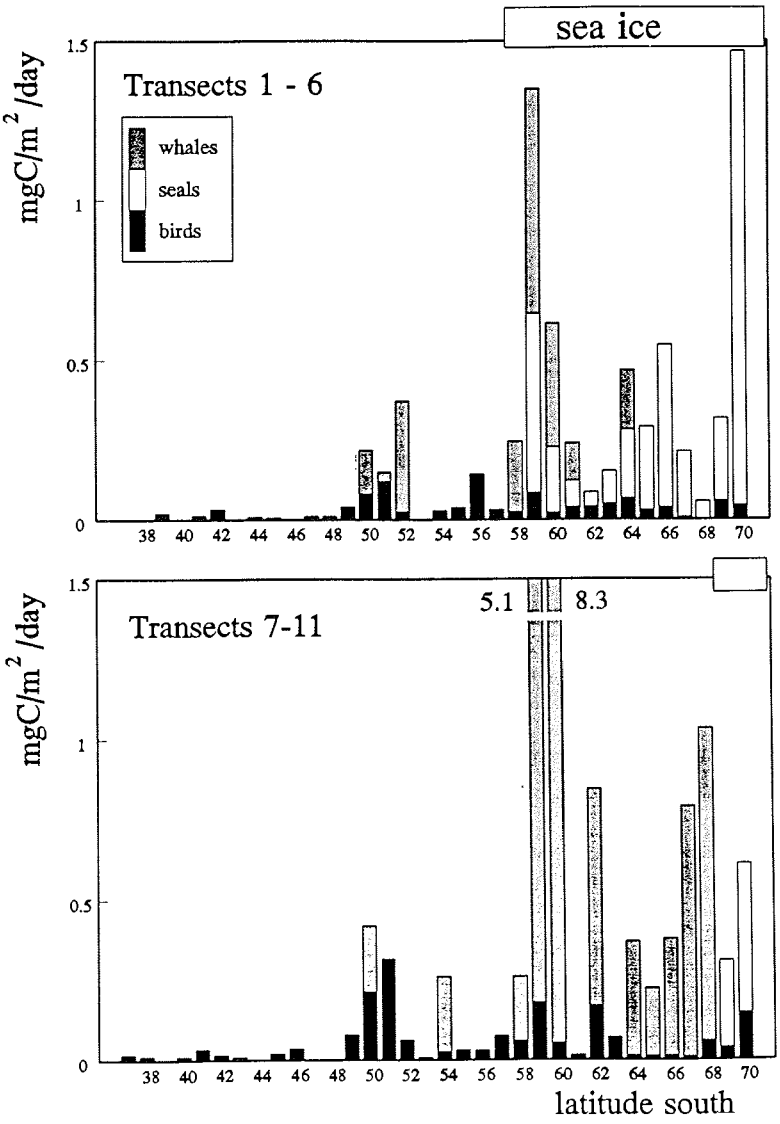

Fig. 18.1 Large scale patterns in carbon requirements of top predators (seabirds, seals and whales) during the long north-south voyages of ANT-XIII/2 (SO-JGOFS'95; n=2305 ten-minute counts)

Figure 18.1 shows a preliminary summary of the long north-south voyages, in which data have been pooled for trans. 1-6 (Cape Town - Neumayer - Polar Front; 5 - 29 Dec 1995) and trans. 7-11 (Polar Front - Neumayer - Cape Town; 29 Dec 1995 - 23 Jan 1996). Animal densities have been converted to their daily rate of carbon consumption ($mgC/m^2/day$), averaged per degree latitude. Data are based on observed animal numbers and have not yet been corrected for factors such as bird concentrations on icebergs outside the transect band or for day-time related variability in numbers of Crabeater Seals hauling out on ice. Final figures will somewhat increase as a consequence of adjustments. All marine bird and mammal species observed during the cruise have been listed in an appendix with some general indicators of abundance.

The two long transects show similar large scale patterns of animal distribution. Lowest bird numbers occurred north of the Polar Front. Bird numbers increased in the Polar Front, particularly those of the Antarctic Prion *Pachyptila vittata*. Mammals in this area were mainly represented by Hourglass Dolphins *Lagenorhynchus cruciger*, a few larger whales and a single Fur Seal *Arctocephalus sp.*. Further south the Antarctic Circumpolar Current was usually characterized by reduced animal numbers but these strongly increased in the area from 58°S to 60°S. This increase probably coincides with the northern rim of the Weddell Sea Gyre and occurred during both transects in spite of huge differences in ice conditions (related to time of season and a somewhat more eastern track of the second transect). During SO-JGOFS'92 (ANT-X/6) (van Franeker et al. in press) high top predator densities in this area were linked to ice edge phenomena, but present observations indicate the importance of the frontal system. Further analyses will focus on this aspect. Extreme top predator carbon consumption rates in this zone during the second long transect (transects 7-11) were related to considerable numbers of foraging Humpback Whales *Megaptera novaeangliae* and Killer Whales *Orcinus orca*, coinciding with high bird densities of, for example, Southern Fulmar *Fulmarus glacialoides* and Blue Petrel *Halobaena caerulea*. Chinstrap Penguins *Pygoscelis antarctica* were abundant in this area during the Oct/Nov'92 transects of ANTX/6, but only played a minor role during the current Dec'95/Jan'96 observations.

Throughout the extensive ice zone on the first long transect, Crabeater Seals *Lobodon carcinophagus* were the main consumers, with Minke Whales *Balaenoptera acutorostrata* being mainly restricted to the marginal ice areas. Relatively high carbon requirements persisted during the second long transect, when nearly this whole area was open water: small whales, among which Minke and the Southern Bottlenose Whale *Hyperoodon planifrons* determined this pattern.

The large scale patterns in Fig.18.1 are similar to those observed during the observations in spring 1992 (van Franeker et al. in press) but with evident seasonal changes such as an increasing number of whales later in the season. Carbon consumption rates by all top predators combined were similar for the various zones, and remained low relative to those observed in the western Weddell Sea (van Franeker 1992). Detailed small scale patterns were noted within various zones, such as a dense concentration of Blue Petrels within the Weddell Sea during the last northward transect. Analysis of various data-sets in the surface-database and SeaSoar data may reveal possible correlations with particular biotic or abiotic phenomena.

Extensive surveys were conducted during grid-transects 6 to 9 in the Polar Front. As indicated, high densities of Prions were observed in the area. Bird surveys revealed strong small scale gradients in densities. Fig. 18.2 shows the result of contour plotting of Prion densities in the small scale grid area (Transects 7-9). Although general patterns in this figure seem to correlate to contour plots of phytoplankton and zooplankton abundance in the area, there are differences that can only be interpreted after further analyses of all data available. It is evident however, that gradients as strong as in Fig. 182. have to reflect strong biotic and/or abiotic patterns in the underlying ocean.

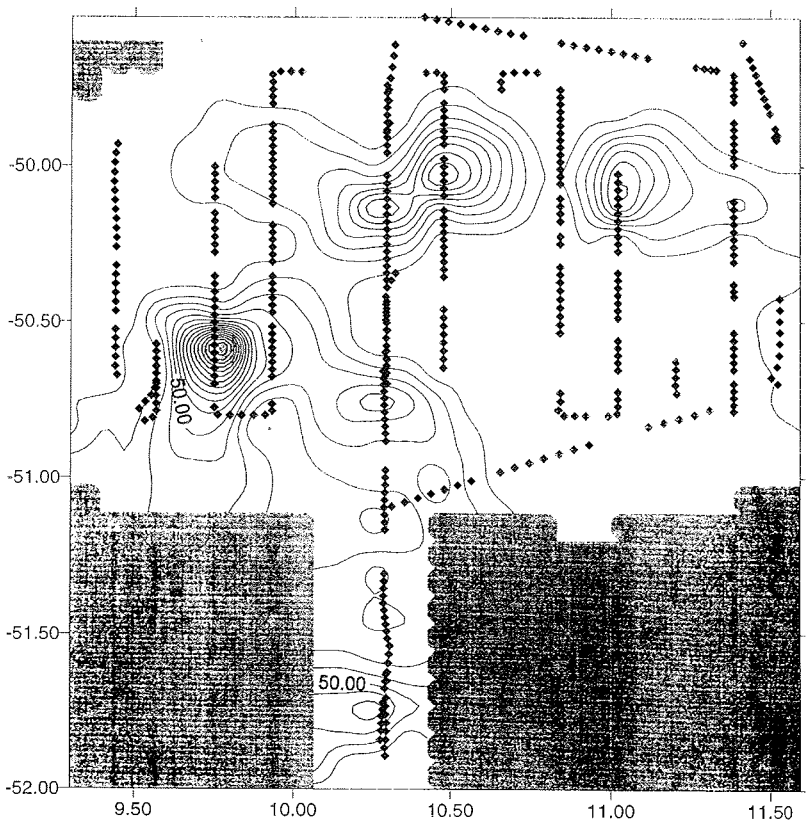

Fig 18.2 Contour plot of densities of Prions by geographical position (Latitude; Longitude) during the small scale grid (transects 7-9) in the Polar Front. Isolines for densities increment by steps of 10 birds/km^2 with increased shading for higher density areas.

References

Anonymous 1995. Report of the 1995 APIS Program planning meeting. APIS Report No.1. National Marine Mammal Laboratory, Seattle. 26pp.

BIOMASS Working Party on Bird Ecology. 1984. Recording observations of birds at sea (revised edition). BIOMASS Handb. 18: 1-20.

Erickson, A.W., Bledsoe L.J., & Hanson M.B. 1989. Bootstrap correction for diurnal activity cycle in census data for Antarctic seals. Mar. Mammal Sci. 5: 29-56.

Hiby A.R. & Hammond P.S. 1989. Survey techniques for estimating cetaceans. In: Donovan G.P.(ed). The comprehensive assessment of whale stocks: the early years. Rep. Int. Whal. Comm. (Special Issue II). Cambridge. pp 47-80.

Laws, R.M. (ed) 1980. Estimation of population sizes of seals. BIOMASS Handbook No. 2: 21 pp. SCAR, Cambridge.

SCAR Group of Specialists on Seals 1994. Antarctic Pack Ice Seals: indicators of environmental change and contributors to carbon flux. APIS Program, draft implementation plan, Aug. 1994. SCAR Group of Specialists on Seals, Seattle. 7 pp.

Tasker M.L., Hope Jones P, Dixon T, & Blake B.F. 1984. Counting seabirds at sea from ships: a review of methods employed and a suggestion for a standardized approach. Auk 101: 567-577.

van Franeker, J.A. 1992. Top predators as indicators for ecosystem events in the confluence zone and marginal ice zone of the Weddell and Scotia seas, Antarctica, November 1988 to January 1989 (EPOS Leg 2). Polar Biol. 12: 93-102.

van Franeker, J.A. 1994. A comparison of methods for counting seabirds at sea in the Southern Ocean. J. Field Ornithol. 65(1): 96-108
van Franeker, J.A.; Bathmann, U.V.; & Mathot, S. (*in press*). Carbon fluxes to Antarctic top predators. Deep Sea Research .
van Franeker, J.A. 1996. Pelagic distribution and numbers of the Antarctic Petrel *Thalassoica antarctica* in the Weddell Sea during spring. Polar Biology 14: in press.

Tab. 18.1 Marine birds and mammals observed during ANT-XIII/2, Dec'95-Jan'96 (south of 37°S; observations near South African coast omitted)

numb = total number of individuals recorded (2530 counts; in + out of transect band)
freq = number of quantitative counts during which species was recorded in transect
dens = average number of individuals per km² for all transects

name	numb	freq	dens	scientific name
PENGUINS				
Emperor Penguin	153	29	.015	Aptenodytes forsteri
Adelie Penguin	250	41	.050	Pygoscelis adeliae
Chinstrap Penguin	213	8	.022	Pygoscelis antarctica
Unid - Pygoscelis	20	5	.005	Pygoscelis sp.
Macaroni Penguin	1	0		Eudyptes chrysolophus
Unid - Eudyptes	4	3	.002	Eudyptes sp.
ALBATROSSES				
Wandering Alb.	261	9	.004	Diomedea exulans
Black-browed Alb.	98	7	.003	Diomedea melanophris
White-capped Alb.	4	0		Diomedea cauta
Yellow-nosed Alb.	24	2	.001	Diomedea chlororhynchos
Grey-headed Alb.	81	10	.004	Diomedea chrysostoma
Mollymauk sp.	3	1	.000	Diomedea 'mollymauk'
Sooty Albatross	7	2	.001	Phoebetria fusca
Light-m. Sooty Alb.	288	19	.014	Phoebetria palpebrata
PETRELS AND SHEARWATERS				
Southern Fulmar	1784	100	.185	Fulmarus glacialoides
Antarctic Petrel	2979	169	.099	Thalassoica antarctica
Cape Petrel	289	20	.017	Daption capense
Snow Petrel	612	124	.074	Pagodroma nivea
N. Giant Petrel	21	1	.000	Macronectes halli
S. Giant Petrel	31	8	.005	Macronectes giganteus
Giant Petrel sp.	77	11	.005	Macronectes sp.
Antarctic Prion	22134	545	2.934	Pachyptila vittata (des.)
Prion sp unid	133	18	.013	Pachyptila sp
Prion or Blue P.?	40	8	.006	Pachyptila/Halobaena sp.
Blue Petrel	5058	139	.678	Halobaena caerulea
Great-winged Petrel	47	11	.008	Pterodroma macroptera
White-headed Petrel	209	55	.027	Pterodroma lessonii
Kerguelen Petrel	450	133	.078	Pterodroma brevirostris
Soft-plumaged Petrel	2111	355	.212	Pterodroma mollis
Pterodroma sp.	3	1	.000	Pterodroma sp.
Grey Petrel	70	12	.006	Procellaria cinerea
White-chinned Petrel	302	26	.011	Procellaria aequinoctialis
Cory's Shearwater	15	0		Calonectris diomedea
Great Shearwater	469	85	.060	Puffinus gravis
Sooty Shearwater	42	9	.005	Puffinus griseus
Little Shearwater	78	12	.017	Puffinus assimilis

STORM-PETRELS & DIVING PETRELS				
Wilsons Storm-p.	28	4	.002	Oceanites oceanicus
Black-bellied St-p.	678	174	.103	Fregetta tropica
White-bellied St-p.	9	3	.002	Fregetta grallaria
Unid. Storm-petrel	2	0		Oceanitidae sp
Common Diving P.	1	1	.000	Pelecanoides urinatrix
Diving Petrel sp.	71	39	.021	Pelecanoides sp.
OTHER BIRDS				
South Polar Skua	4	0		Catharacta maccormicki
Antarctic Skua	11	2	.001	Catharacta (skua) lonnbergi
Large unid Skua	14	2	.001	Catharacta sp.
Pomarine Skua	1	1	.000	Stercorarius pomarinus
Arctic Skua	5	2	.001	Stercorarius parasiticus
Smaller unid Skua	5	3	.001	Stercorarius sp.
Sabine's Gull	1	1	.000	Larus sabini
Arctic Tern	532	14	.071	Sterna paradisaea
Small unid tern	2	1	.000	Sterna sp small
SEALS				
Crabeater Seal	228	72	.048	Lobodon carcinophagus
Leopard Seal	20	4	.002	Hydrurga leptonyx
Weddell Seal	6	0		Leptonychotes weddellii
Ross Seal	3	3	.001	Ommatophoca rossii
Seal (Phocid) sp	16	1	.000	Phocidae sp
Fur Seal	1	1	.000	Arctocephalus sp.
WHALES				
Minke Whale	15	11	.002	Balaenoptera acutorostrata
S. Bottlenose Whale	5	1	.000	Hyperoodon planifrons
Killer Whale	19	5	.002	Orcinus orca
Small whale sp.	22	13	.002	Cetacean small
Medium Whale sp.	3	2	.000	Cetacean medium
Humpback Whale	23	12	.002	Megaptera novaeangliae
Fin Whale	1	1	.000	Balaenoptera physalus
Hourglass Dolphin	42	5	.008	Lagenorhynchus cruciger
Dolphin sp.	1	1	.000	Dolphin sp.

19. SEA ICE REPORT

J. A. van Franeker, N. van den Brink

This table contains the sea-ice and iceberg observations according to SO-JGOFS Protocol (Ackley S.F., Eicken, H., van Franeker, J.A. & Wadhams, P. (1992) Protocol for ship and airborne observations on the structure, physical properties and coverage of sea ice in the framework of Southern Ocean (SO) JGOFS activities. AWI, Bremerhaven, 9pp). Observations in the JGOFS protocol integrate the conditions in a wider area (radius of several km's) around the point of observation.
Finer scale data are available from observations during 10 minute counts of birds/mammals: these data will be stored in the 'Surface database'.

Contrary to the general recommendation not to cite cruise reports we would like to ask you to cite the 'van den Brink & van Franeker' chapter on ice conditions in 'Berichte zur Polarforschung' if you use specific information from the cruise report, Surface-database, or this Ice-report. These ice data will not be published separately elsewhere.

INDEX OF COLUMNS USED IN THE ICE REPORT

TRNR	= ANT XIII/2 transect number
STATION	= ANT XIII/2 station number
DATUM	= date (day-mon-year) GMT
TIJD	= time (hh:mm:ss) GMT
LATD	= latitude decimal (from POLDAT at listed time)
LOND	= longitude decimal (from POLDAT at listed time)
T	= surface watertemperature (from POLDAT 10min avg before listed time/position)
SAL	= surface salinity o/oo (from POLDAT 10min avg before listed time/position)
WAT	= % of open water
TOT	= % of ice-covered water
NEW	= % of water covered by sludge,pancake,nilas and grey ice
FLOE	= % of water covered by first year or multi-year floes
MELT	= % of water covered by decaying ice remains (brash)
THICK	= estimated thickness of dominant type of floes (FLOE) in cm
SNOW	= estimated average thickness of snowlayer on floes in cm
FDIAM	= estimated average diameter of dominant type of floes in m
RIDGE	= % of total surface where ice is ridged
BROW	= % of ice coloured by algae etc
COLO	= 0=absent 1=light 2=light/medium 3=medium 4=medium/dark 5=dark
NBERG	= number of ice-bergs in 12 nm range (radar)

Original data partly contain more detail (e.g. percentages of more specific types of ice and size indications for icebergs: all these are listed in the lotus123 spreadsheet stat95.wk3. Please note that date/time-code in this spreadsheet refer to begin of 10 min time-blocks: to link data from this spreadsheet to POLDAT positions etc add 10 minutes.

no ice and no icebergs seen (visual or radar) before start of listing

TRNR	DATUM	TIJD	LATD	LOND	T	SAL	WAT	TOT	NEW	FLOE	MELT	THICK	SNOW	FDIAM	RIDG	BROW	COLO	NBERG	COMMENTS
3.00	11-Dec-95	20:20:00	-57.2235	-1.9890	-1.04	34.12	99.9	.1	.0	.0	.1	0	0	0	0	0	0	0	firstbergbits;nobergseen
4.00	12-Dec-95	03:40:00	-58.1198	-2.4591	-1.60	33.92	30.0	70.0	5.0	45.0	20.0	100	30	3	0	0	3	0	iceedge
4.00	12-Dec-95	05:10:00	-58.4051	-2.5683	-1.55	33.98	99.0	1.0	.0	.0	1.0	0	0	0	0	0	0	1	firstbergpassed(4.45h)
4.00	12-Dec-95	09:50:00	-59.2113	-3.0508	-1.68	34.16	40.0	60.0	1.0	44.0	15.0	80	20	10	5	100	4	5	
4.00	12-Dec-95	16:50:00	-59.4539	-3.1960	-1.62	34.13	30.0	70.0	1.0	54.0	15.0	50	20	8	5	100	4	0	
4.00	12-Dec-95	20:10:00	-60.0331	-3.3773	-1.72	34.08	50.0	50.0	5.0	35.0	10.0	75	25	8	5	100	2	0	
4.00	12-Dec-95	22:20:00	-60.4084	-3.4375	-1.71	34.06	35.0	65.0	.0	55.0	10.0	50	20	10	1	100	3	0	
4.00	13-Dec-95	03:10:00	-61.2458	-3.8789	-1.71	33.99	30.0	70.0	5.0	55.0	10.0	75	25	10	5	90	2	0	
4.00	13-Dec-95	06:50:00	-61.9025	-4.0976	-1.62	34.06	50.0	50.0	5.0	42.0	3.0	50	20	15	5	90	2		
4.00	13-Dec-95	09:10:00	-62.2968	-4.2947	-1.77	33.84	20.0	80.0	5.0	73.0	2.0	60	15	25	5	50	4	5	
4.00	13-Dec-95	11:30:00	-62.6211	-4.5144	-1.73	33.76	15.0	85.0	2.0	81.0	2.0	50	15	20	5	50	3	8	
4.00	13-Dec-95	14:00:00	-62.9979	-4.6789	-1.73	33.63	10.0	90.0	5.0	80.0	5.0	60	20	40	5	80	4	15	
4.00	13-Dec-95	16:20:00	-63.3840	-4.7429	-1.64	33.35	15.0	85.0	15.0	65.0	5.0	75	20	150	1	75	2	14	
4.00	13-Dec-95	19:00:00	-63.7779	-4.8421	-1.62	33.56	15.0	85.0	15.0	65.0	5.0	75	25	1000	1	100	2	6	
4.00	13-Dec-95	21:50:00	-64.1011	-4.9268	-1.70	34.03	10.0	90.0	.0	90.0	.0	100	20	1000	0	50	2	2	
4.00	14-Dec-95	02:40:00	-64.8935	-5.2705	-1.66	34.28	50.0	50.0	.0	50.0	.0	100	20	5000	5	50	2	11	
4.00	14-Dec-95	06:40:00	-65.5481	-5.5396	-1.71	33.75	20.0	80.0	15.0	65.0	.0	50	15	1000	5	100	4	4	
4.00	14-Dec-95	08:50:00	-65.9081	-6.0088	-1.59	34.17	50.0	50.0	18.0	30.0	2.0	50	10	500	5	100	2	12	
4.00	14-Dec-95	11:20:00	-66.3280	-6.2648	-1.56	34.13	50.0	50.0	15.0	30.0	5.0	50	20	500	5	50	3	2	
4.00	14-Dec-95	14:00:00	-66.7243	-6.2592	-1.42	34.16	50.0	50.0	10.0	35.0	5.0	50	10	3000	0	50	3	0	
4.00	14-Dec-95	16:20:00	-67.1417	-6.4431	-1.45	34.07	70.0	30.0	9.0	20.0	1.0	50	10	500	5	50	2	6	
4.00	14-Dec-95	18:50:00	-67.5677	-6.7549	-1.64	34.06	60.0	40.0	15.0	25.0	.0	80	20	150	50	100	4	20	
4.00	14-Dec-95	22:00:00	-68.1918	-7.1454	-1.03	34.3	95.0	5.0	.0	.0	5.0	0	0	0	0	0	0	2	
4.00	15-Dec-95	02:10:00	-69.0688	-7.7469	-1.15	34.28	99.9	.1	.0	.0	.1	0	0	0	0	0	0	0	
4.00	15-Dec-95	04:10:00	-69.4672	-8.0288	-1.56	34.08	70.0	30.0	3.0	25.0	2.0	50	15	2000	3	100	2	3	
4.00	15-Dec-95	08:50:00	-69.9431	-8.4761	-1.69	34.35	40.0	60.0	4.0	51.0	5.0	75	15	5000	10	100	4	21	
4.00	15-Dec-95	11:30:00	-70.2600	-8.5541	-1.69	34.29	15.0	85.0	10.0	55.0	20.0	75	40	2	50	80	5	5	
5.00	17-Dec-95	12:50:00	-70.5007	-8.1158	-1.76	34.22	1.0	99.0	.0	89.0	10.0	200	100	1000	50	50	4		
5.00	19-Dec-95	13:10:00	-70.2536	-8.2002	-1.74	34.13	.0	100.0	95.0	5.0	.0	50	15	1	0	0	0		
5.00	19-Dec-95	14:10:00	-70.0650	-7.9331	-1.67	33.93	35.0	65.0	5.0	50.0	10.0	50	20	10	1	50	1		
5.00	19-Dec-95	16:40:00	-69.5195	-7.3551	-1.27	34.21	90.0	10.0	.0	8.0	2.0	30	10	10	3	0	0	0	
5.00	19-Dec-95	19:30:00	-68.8572	-6.7264	-.98	34.27	100.0	.0	.0	.0	.0	0	0	0	0	0	0	1	
5.00	19-Dec-95	22:40:00	-68.1302	-6.2044	-.98	34.22	80.0	20.0	5.0	10.0	5.0	50	15	5	0	10	1	1	
5.00	20-Dec-95	02:10:00	-67.4985	-5.5506	-1.53	33.95	80.0	20.0	.0	15.0	5.0	40	10	20	3	90	2	11	
5.00	20-Dec-95	06:20:00	-66.6268	-4.9351	-1.54	33.97	75.0	25.0	5.0	15.0	5.0	40	10	20	3	30	1	1	
5.00	20-Dec-95	09:10:00	-66.0046	-4.4366	-1.50	34.09	75.0	25.0	.0	20.0	5.0	40	10	250	3	50	1	1	
5.00	20-Dec-95	11:40:00	-65.4868	-4.2257	.21	33.45	30.0	70.0	9.0	56.0	5.0	50	10	150	0	10	2	8	
5.00	20-Dec-95	14:10:00	-64.9825	-3.9606	-1.47	32.06	50.0	50.0	10.0	30.0	10.0	50	10	100	0	70	2	3	
5.00	20-Dec-95	16:10:00	-64.5905	-3.8320	-1.41	31.63	15.0	85.0	5.0	75.0	5.0	50	10	250	3	50	2	1	
5.00	20-Dec-95	19:20:00	-63.8715	-3.5857	-1.68	34.09	30.0	70.0	10.0	50.0	10.0	40	10	25	3	50	1	7	
5.00	20-Dec-95	21:50:00	-63.3036	-3.3813	-1.73	33.99	20.0	80.0	15.0	50.0	15.0	30	15	15	9	50	1	13	

TRNR	DATUM	TIJD	LATD	LOND	T	SAL	WAT	TOT	NEW	FLOE	MELT	THICK	SNOW	FDIAM	RIDG	BROW	COLO	NBERG	COMMENTS
5.00	21-Dec-95	02:20:00	-62.4156	-2.9448	-1.67	33.89	75.0	25.0	.0	15.0	10.0	40	10	5	10	25	2	9	
5.00	21-Dec-95	05:30:00	-61.7082	-2.6556	-1.55	33.88	85.0	15.0	.0	10.0	5.0	40	10	8	0	10	2	3	
5.00	21-Dec-95	08:00:00	-61.0999	-2.4411	-1.54	33.84	85.0	15.0	.0	10.0	5.0	50	10	8	10	100	2	4	
5.00	21-Dec-95	10:10:00	-60.5733	-2.2456	-1.38	33.92	98.0	2.0	.0	1.0	1.0	30	10	1	0	100	1	4	ice-edge diffuse
5.00	21-Dec-95	12:30:00	-60.0109	-2.0425	-1.24	34	99.0	1.0	.0	.0	1.0	0	0	0	0	0	0	4	
5.00	21-Dec-95	14:30:00	-59.5471	-1.8837	-1.30	34.09	99.0	1.0	.0	.0	1.0	0	0	0	0	0	0	4	
5.00	21-Dec-95	16:20:00	-59.1293	-1.7386	-1.26	34.13	100.0	.0	.0	.0	.0	0	0	0	0	0	0	3	
5.00	21-Dec-95	18:00:00	-58.7515	-1.6032	-1.16	34.08	100.0	.0	.0	.0	.0	0	0	0	0	0	0	3	
5.00	21-Dec-95	20:20:00	-58.2217	-1.4300	-.95	33.98	100.0	.0	.0	.0	.0	0	0	0	0	0	0	0	
5.00	22-Dec-95	03:00:00	-56.6825	-.9287	-.52	34.05	100.0	.0	.0	.0	.0	0	0	0	0	0	0	0	
5.00	22-Dec-95	05:40:00	-56.0750	-.7242	-.37	34.11	100.0	.0	.0	.0	.0	0	0	0	0	0	0	0	
5.00	22-Dec-95	09:30:00	-55.2022	-.4704	.02	34.01	100.0	.0	.0	.0	.0	0	0	0	0	0	0	0	
5.00	22-Dec-95	14:30:00	-54.0845	-.1251	.75	33.98	100.0	.0	.0	.0	.0	0	0	0	0	0	0	0	
6.01	22-Dec-95	15:10:00	-53.9989	-.1038	1.00	33.99	100.0	.0	.0	.0	.0	0	0	0	0	0	0	0	
6.01	22-Dec-95	20:00:00	-53.8097	-.0441	.90	33.99	100.0	.0	.0	.0	.0	0	0	0	0	0	0	0	
6.01	23-Dec-95	03:40:00	-52.6149	.6691	2.31	33.97	100.0	.0	.0	.0	.0	0	0	0	0	0	0	0	
6.01	23-Dec-95	06:10:00	-52.3508	1.2319	2.27	33.97	100.0	.0	.0	.0	.0	0	0	0	0	0	0	0	
6.01	23-Dec-95	08:00:00	-52.1757	1.6425	1.69	34	100.0	.0	.0	.0	.0	0	0	0	0	0	0	0	
6.01	23-Dec-95	10:20:00	-51.9315	2.1960	2.42	33.95	100.0	.0	.0	.0	.0	0	0	0	0	0	0	0	
6.01	23-Dec-95	15:10:00	-51.4304	3.2530	3.07	33.97	100.0	.0	.0	.0	.0	0	0	0	0	0	0	0	
6.01	23-Dec-95	17:40:00	-51.1850	3.7807	3.61	33.97	100.0	.0	.0	.0	.0	0	0	0	0	0	0	0	
6.01	24-Dec-95	04:00:00	-50.2376	5.9949	4.32	33.94	100.0	.0	.0	.0	.0	0	0	0	0	0	0	0	
6.02	24-Dec-95	06:20:00	-50.6001	6.0078	4.05	33.93	100.0	.0	.0	.0	.0	0	0	0	0	0	0	0	
6.02	24-Dec-95	08:10:00	-50.8804	6.0031	3.84	33.94	100.0	.0	.0	.0	.0	0	0	0	0	0	0	0	
6.02	24-Dec-95	13:20:00	-51.7194	6.0042	3.14	33.97	100.0	.0	.0	.0	.0	0	0	0	0	0	0	0	
6.02	24-Dec-95	16:30:00	-52.0025	6.3441	3.68	33.96	100.0	.0	.0	.0	.0	0	0	0	0	0	0	0	
6.03	25-Dec-95	04:30:00	-50.7361	7.1014	3.74	33.96	100.0	.0	.0	.0	.0	0	0	0	0	0	0	0	
6.03	25-Dec-95	10:50:00	-49.9106	7.2901	4.84	33.94	100.0	.0	.0	.0	.0	0	0	0	0	0	0	0	
6.04	25-Dec-95	14:20:00	-49.9250	8.1584	5.27	33.92	100.0	.0	.0	.0	.0	0	0	0	0	0	0	0	
6.04	25-Dec-95	19:30:00	-50.4778	8.1496	4.09	33.95	100.0	.0	.0	.0	.0	0	0	0	0	0	0	0	
6.04	26-Dec-95	04:00:00	-51.2408	8.1517	3.84	33.95	100.0	.0	.0	.0	.0	0	0	0	0	0	0	0	
6.04	26-Dec-95	08:00:00	-51.8594	8.1517	3.91	33.95	100.0	.0	.0	.0	.0	0	0	0	0	0	0	0	
6.05	26-Dec-95	13:10:00	-51.9742	9.2435	3.40	33.97	100.0	.0	.0	.0	.0	0	0	0	0	0	0	0	
6.05	26-Dec-95	15:40:00	-51.5964	9.2450	3.81	33.95	100.0	.0	.0	.0	.0	0	0	0	0	0	0	0	
6.05	26-Dec-95	19:30:00	-51.0018	9.2450	4.18	33.94	100.0	.0	.0	.0	.0	0	0	0	0	0	0	0	
6.06	27-Dec-95	09:30:00	-49.9144	10.2548	4.83	33.91	100.0	.0	.0	.0	.0	0	0	0	0	0	0	0	
6.06	27-Dec-95	14:00:00	-49.6592	10.4006	5.41	33.91	100.0	.0	.0	.0	.0	0	0	0	0	0	0	0	
6.06	28-Dec-95	04:00:00	-50.9495	10.2922	3.15	33.97	100.0	.0	.0	.0	.0	0	0	0	0	0	0	0	
6.06	28-Dec-95	08:10:00	-51.5555	10.2919	2.89	33.98	100.0	.0	.0	.0	.0	0	0	0	0	0	0	0	
6.06	28-Dec-95	11:40:00	-52.0021	10.4141	2.81	33.98	100.0	.0	.0	.0	.0	0	0	0	0	0	0	0	
6.07	28-Dec-95	15:40:00	-51.9728	11.3959	2.43	33.98	100.0	.0	.0	.0	.0	0	0	0	0	0	0	0	
6.07	28-Dec-95	20:00:00	-51.3534	11.3885	2.96	33.98	100.0	.0	.0	.0	.0	0	0	0	0	0	0	0	

TRNR	DATUM	TIJD	LATD	LOND	T	SAL	WAT	TOT	NEW	FLOE	MELT	THICK	SNOW	FDIAM	RIDG	BROW	COLO	NBERG	COMMENTS
6.07	29-Dec-95	04:00:00	-50.1438	11.3850	3.43	33.96	100.0	.0	.0	.0	.0	0	0	0	0	0	0	0	
7.01	29-Dec-95	08:40:00	-49.4682	11.4032	5.42	33.91	100.0	.0	.0	.0	.0	0	0	0	0	0	0	0	
7.01	29-Dec-95	14:20:00	-49.8931	11.5343	4.34	33.96	100.0	.0	.0	.0	.0	0	0	0	0	0	0	0	
7.01	30-Dec-95	04:00:00	-50.3065	11.5367	3.51	33.95	100.0	.0	.0	.0	.0	0	0	0	0	0	0	0	
7.01	30-Dec-95	06:10:00	-50.6984	11.5221	3.55	33.96	100.0	.0	.0	.0	.0	0	0	0	0	0	0	0	
7.01	30-Dec-95	15:20:00	-51.1007	10.2902	3.56	33.94	100.0	.0	.0	.0	.0	0	0	0	0	0	0	0	
7.02	31-Dec-95	04:10:00	-51.5145	10.2947	3.10	33.96	100.0	.0	.0	.0	.0	0	0	0	0	0	0	0	
7.03	31-Dec-95	14:00:00	-51.2840	10.2909	3.04	33.97	100.0	.0	.0	.0	.0	0	0	0	0	0	0	0	
7.03	31-Dec-95	18:50:00	-50.6170	10.2853	3.22	33.96	100.0	.0	.0	.0	.0	0	0	0	0	0	0	0	
7.03	01-Jan-96	04:10:00	-49.5277	10.2911	5.15	33.91	100.0	.0	.0	.0	.0	0	0	0	0	0	0	0	
7.03	01-Jan-96	08:10:00	-49.6671	11.1896	5.05	33.9	100.0	.0	.0	.0	.0	0	0	0	0	0	0	0	
8.01	01-Jan-96	14:10:00	-50.3793	11.3850	3.42	33.96	100.0	.0	.0	.0	.0	0	0	0	0	0	0	0	
8.01	01-Jan-96	17:40:00	-50.8031	11.3481	3.40	33.97	100.0	.0	.0	.0	.0	0	0	0	0	0	0	0	
8.02	01-Jan-96	19:50:00	-50.5770	11.2053	3.36	33.97	100.0	.0	.0	.0	.0	0	0	0	0	0	0	0	
8.03	02-Jan-96	04:00:00	-49.9239	11.0217	4.08	33.93	100.0	.0	.0	.0	.0	0	0	0	0	0	0	0	
8.03	02-Jan-96	08:10:00	-50.5364	11.0217	3.46	33.97	100.0	.0	.0	.0	.0	0	0	0	0	0	0	0	
8.04	02-Jan-96	15:00:00	-50.1514	10.8400	3.35	33.97	100.0	.0	.0	.0	.0	0	0	0	0	0	0	0	
8.04	02-Jan-96	18:00:00	-49.7328	10.8400	4.69	33.91	100.0	.0	.0	.0	.0	0	0	0	0	0	0	0	
8.06	03-Jan-96	03:50:00	-50.7809	10.4760	3.34	33.96	100.0	.0	.0	.0	.0	0	0	0	0	0	0	0	
8.06	03-Jan-96	08:10:00	-50.1186	10.4767	4.07	33.95	100.0	.0	.0	.0	.0	0	0	0	0	0	0	0	
8.07	03-Jan-96	14:20:00	-50.0312	10.2950	4.20	33.92	100.0	.0	.0	.0	.0	0	0	0	0	0	0	0	
8.07	03-Jan-96	18:10:00	-50.5723	10.2950	3.57	33.95	100.0	.0	.0	.0	.0	0	0	0	0	0	0	0	
8.08	04-Jan-96	03:40:00	-49.7534	10.1133	4.48	33.9	100.0	.0	.0	.0	.0	0	0	0	0	0	0	0	
8.09	04-Jan-96	08:10:00	-50.1438	9.9316	4.12	33.93	100.0	.0	.0	.0	.0	0	0	0	0	0	0	0	
8.10	04-Jan-96	14:20:00	-50.7003	9.7502	4.06	33.95	100.0	.0	.0	.0	.0	0	0	0	0	0	0	0	
8.10	04-Jan-96	18:10:00	-50.1271	9.7500	4.30	33.93	100.0	.0	.0	.0	.0	0	0	0	0	0	0	0	
8.11	05-Jan-96	03:50:00	-50.5275	9.5684	4.24	33.92	100.0	.0	.0	.0	.0	0	0	0	0	0	0	0	
9.01	05-Jan-96	07:30:00	-50.6986	9.5675	4.30	33.94	100.0	.0	.0	.0	.0	0	0	0	0	0	0	0	
9.01	05-Jan-96	14:40:00	-50.4973	9.4398	4.42	33.93	100.0	.0	.0	.0	.0	0	0	0	0	0	0	0	
9.01	05-Jan-96	18:40:00	-49.8991	9.5614	5.64	33.89	100.0	.0	.0	.0	.0	0	0	0	0	0	0	0	
9.02	06-Jan-96	09:30:00	-49.6118	10.3205	5.09	33.89	100.0	.0	.0	.0	.0	0	0	0	0	0	0	0	
9.02	06-Jan-96	13:00:00	-49.8988	10.2943	4.51	33.9	100.0	.0	.0	.0	.0	0	0	0	0	0	0	0	
9.02	07-Jan-96	08:30:00	-50.2853	10.3311	3.74	33.94	100.0	.0	.0	.0	.0	0	0	0	0	0	0	0	
9.02	07-Jan-96	10:10:00	-50.4035	10.2936	3.81	33.94	100.0	.0	.0	.0	.0	0	0	0	0	0	0	0	
9.02	07-Jan-96	16:40:00	-50.7007	10.2895	4.12	33.93	100.0	.0	.0	.0	.0	0	0	0	0	0	0	0	
10.00	08-Jan-96	05:20:00	-51.9727	9.3830	3.71	33.93	100.0	.0	.0	.0	.0	0	0	0	0	0	0	0	
10.00	08-Jan-96	08:00:00	-52.5529	8.9698	3.03	33.94	100.0	.0	.0	.0	.0	0	0	0	0	0	0	0	
10.00	08-Jan-96	11:30:00	-53.3441	8.3818	2.44	33.95	100.0	.0	.0	.0	.0	0	0	0	0	0	0	0	
10.00	08-Jan-96	15:00:00	-54.1166	7.8152	1.15	34.03	100.0	.0	.0	.0	.0	0	0	0	0	0	0	0	
10.00	08-Jan-96	19:30:00	-55.0942	7.0528	.72	34.09	100.0	.0	.0	.0	.0	0	0	0	0	0	0	0	
10.00	09-Jan-96	00:40:00	-56.2191	6.2019	.26	34.12	100.0	.0	.0	.0	.0	0	0	0	0	0	0	0	
10.00	09-Jan-96	03:20:00	-56.8050	5.7337	-.03	34.08	100.0	.0	.0	.0	.0	0	0	0	0	0	0	0	First ice berg, 15nm on Radar

TRNR	DATUM	TIJD	LATD	LOND	T	SAL	WAT	TOT	NEW	FLOE	MELT	THICK	SNOW	FDIAM	RIDG	BROW	COLO	NBERG	COMMENTS
10.00	09-Jan-96	06:10:00	-57.4331	5.2156	-.14	34.08	100.0	.0	.0	.0	.0	0	0	0	0	0	0	1	
10.00	09-Jan-96	08:00:00	-57.8491	4.8967	-.20	34	100.0	.0	.0	.0	.0	0	0	0	0	0	0	1	
10.00	09-Jan-96	11:30:00	-58.6321	4.2318	.00	33.83	100.0	.0	.0	.0	.0	0	0	0	0	0	0	3	
10.00	09-Jan-96	14:20:00	-59.2600	3.6984	-.16	33.79	100.0	.0	.0	.0	.0	0	0	0	0	0	0	5	
10.00	09-Jan-96	16:20:00	-59.7084	3.3105	.14	33.88	100.0	.0	.0	.0	.0	0	0	0	0	0	0	7	
10.00	09-Jan-96	18:00:00	-60.0805	2.9884	-.09	33.86	100.0	.0	.0	.0	.0	0	0	0	0	0	0	4	
10.00	09-Jan-96	20:00:00	-60.5305	2.5798	.03	33.96	100.0	.0	.0	.0	.0	0	0	0	0	0	0	14	
10.00	09-Jan-96	22:00:00	-60.9864	2.1862	.05	33.99	100.0	.0	.0	.0	.0	0	0	0	0	0	0	20	
10.00	10-Jan-96	03:10:00	-62.1622	1.0936	-.15	34.01	100.0	.0	.0	.0	.0	0	0	0	0	0	0	8	
10.00	10-Jan-96	05:10:00	-62.6147	.6668	-.16	33.96	100.0	.0	.0	.0	.0	0	0	0	0	0	0	9	
10.00	10-Jan-96	07:10:00	-63.0676	.2172	-.02	33.86	100.0	.0	.0	.0	.0	0	0	0	0	0	0	9	
10.00	10-Jan-96	08:00:00	-63.2585	.0301	-.03	33.73	100.0	.0	.0	.0	.0	0	0	0	0	0	0	6	
10.00	10-Jan-96	11:30:00	-64.0603	-.7592	.17	33.72	100.0	.0	.0	.0	.0	0	0	0	0	0	0	6	
10.00	10-Jan-96	14:00:00	-64.6384	-1.3356	-.16	33.73	100.0	.0	.0	.0	.0	0	0	0	0	0	0	16	
10.00	10-Jan-96	16:00:00	-65.0998	-1.8119	-.28	33.71	100.0	.0	.0	.0	.0	0	0	0	0	0	0	16	
10.00	10-Jan-96	18:00:00	-65.5562	-2.2779	-.39	33.4	100.0	.0	.0	.0	.0	0	0	0	0	0	0	17	
10.00	10-Jan-96	22:10:00	-66.5019	-3.3239	-.08	33.61	100.0	.0	.0	.0	.0	0	0	0	0	0	0	3	
10.00	11-Jan-96	02:40:00	-67.5121	-4.4498	-.10	33.94	100.0	.0	.0	.0	.0	0	0	0	0	0	0	9	
10.00	11-Jan-96	04:30:00	-67.9296	-4.9243	-.08	33.97	95.0	5.0	.0	5.0	.0	30	10	1	0	0	0	7	First ice fields, on Radar
10.00	11-Jan-96	06:30:00	-68.3779	-5.4632	-.03	34.15	99.0	1.0	.0	.0	1.0	0	0	0	0	0	0	19	
10.00	11-Jan-96	08:00:00	-68.7178	-5.8715	-.28	34.19	100.0	.0	.0	.0	.0	0	0	0	0	0	0	10	
10.00	11-Jan-96	11:30:00	-69.4657	-7.0495	.01	34.23	100.0	.0	.0	.0	.0	0	0	0	0	0	0	8	
10.00	11-Jan-96	14:00:00	-70.0107	-7.7831	-1.71	33.78	5.0	95.0	.0	65.0	30.0	50	10	10	5	80	3	24	sharp ice-edge
10.00	11-Jan-96	15:40:00	-70.2563	-7.9602	-1.68	33.34	1.0	99.0	.0	90.0	9.0	100	25	100	20	100	4		
10.00	11-Jan-96	18:10:00	-70.5226	-7.9430	-1.71	34.06	1.0	99.0	.0	95.0	4.0	120	75	100	75	100	4	20	
11.01	14-Jan-96	22:50:00	-70.4904	-8.2424	-1.76	34.13	.0	100.0	1.0	80.0	19.0	90	40	100	80	100	3	5	
11.02	15-Jan-96	02:10:00	-70.2306	-7.9575	-1.60	33.76	11.0	89.0	4.0	60.0	25.0	90	20	20	0	95	3	8	
11.02	15-Jan-96	04:20:00	-69.9073	-7.5196	-1.70	33.35	5.0	95.0	10.0	80.0	5.0	75	20	25	10	95	3	5	
11.02	15-Jan-96	06:30:00	-69.5553	-6.8432	-.52	32.37	20.0	80.0	.0	70.0	10.0	60	15	25	10	95	3	20	
11.02	15-Jan-96	07:00:00	-69.4539	-6.7227	-1.22	33.42	1.0	99.0	.0	39.0	60.0	60	15	5	0	100	3	20	sharpice-edge
11.02	15-Jan-96	08:00:00	-69.2314	-6.4469	-.90	34.19	100.0	.0	.0	.0	.0	0	0	0	0	0	0	3	
11.02	15-Jan-96	11:30:00	-68.4557	-5.4654	.44	34.14	100.0	.0	.0	.0	.0	0	0	0	0	0	0	13	
11.02	15-Jan-96	14:00:00	-67.8952	-4.7748	.46	33.98	100.0	.0	.0	.0	.0	0	0	0	0	0	0	6	
11.02	15-Jan-96	16:20:00	-67.3741	-4.1465	.64	33.91	100.0	.0	.0	.0	.0	0	0	0	0	0	0	6	
11.02	15-Jan-96	18:00:00	-67.0047	-3.7156	.60	33.89	100.0	.0	.0	.0	.0	0	0	0	0	0	0	3	
11.02	15-Jan-96	21:20:00	-66.2520	-2.8909	.31	33.7	100.0	.0	.0	.0	.0	0	0	0	0	0	0	7	
11.02	15-Jan-96	22:30:00	-65.9908	-2.5911	.43	33.65	100.0	.0	.0	.0	.0	0	0	0	0	0	0	17	
11.02	16-Jan-96	02:40:00	-65.0804	-1.4896	-.03	33.75	100.0	.0	.0	.0	.0	0	0	0	0	0	0	13	
11.02	16-Jan-96	04:20:00	-64.7155	-1.1071	.38	33.61	100.0	.0	.0	.0	.0	0	0	0	0	0	0	7	
11.02	16-Jan-96	08:10:00	-63.8713	-.1933	.76	33.71	100.0	.0	.0	.0	.0	0	0	0	0	0	0	6	
11.03	16-Jan-96	10:10:00	-63.6679	.0082	.60	33.72	100.0	.0	.0	.0	.0	0	0	0	0	0	0	10	
11.03	16-Jan-96	13:00:00	-63.3272	.3390	.65	33.76	100.0	.0	.0	.0	.0	0	0	0	0	0	0	4	

TRNR	DATUM	TIJD	LATD	LOND	T	SAL	WAT	TOT	NEW	FLOE	MELT	THICK	SNOW	FDIAM	RIDG	BROW	COLO	NBERG	COMMENTS
11.03	16-Jan-96	15:00:00	-62.8827	.7927	1.00	33.94	100.0	.0	.0	.0	.0	0	0	0	0	0	0	8	
11.03	16-Jan-96	19:40:00	-61.8513	1.8052	.62	33.99	100.0	.0	.0	.0	.0	0	0	0	0	0	0	3	
11.03	16-Jan-96	22:00:00	-61.3333	2.2909	.58	33.92	100.0	.0	.0	.0	.0	0	0	0	0	0	0	3	
11.03	17-Jan-96	02:50:00	-60.2525	3.2931	.59	33.96	100.0	.0	.0	.0	.0	0	0	0	0	0	0	8	
11.03	17-Jan-96	05:20:00	-59.6837	3.8109	.71	33.94	100.0	.0	.0	.0	.0	0	0	0	0	0	0	7	
11.03	17-Jan-96	07:00:00	-59.3064	4.1477	.62	33.84	100.0	.0	.0	.0	.0	0	0	0	0	0	0	7	
11.03	17-Jan-96	10:30:00	-58.5133	4.8236	.44	33.83	100.0	.0	.0	.0	.0	0	0	0	0	0	0	0	
11.03	17-Jan-96	13:00:00	-57.9609	5.3066	.58	33.92	100.0	.0	.0	.0	.0	0	0	0	0	0	0	1	
11.03	17-Jan-96	14:50:00	-57.5509	5.6602	.51	34	100.0	.0	.0	.0	.0	0	0	0	0	0	0	0	
11.03	17-Jan-96	16:10:00	-57.3344	5.8370	.65	34.03	100.0	.0	.0	.0	.0	0	0	0	0	0	0	1	
11.04	17-Jan-96	20:00:00	-56.7429	6.3358	.41	34.03	100.0	.0	.0	.0	.0	0	0	0	0	0	0	0	
11.04	18-Jan-96	02:40:00	-55.2653	7.5292	.91	34.1	100.0	.0	.0	.0	.0	0	0	0	0	0	0	0	
11.04	18-Jan-96	06:00:00	-54.5605	8.1317	.95	34.1	100.0	.0	.0	.0	.0	0	0	0	0	0	0	0	
11.04	18-Jan-96	09:40:00	-53.8377	8.8883	1.39	34.01	100.0	.0	.0	.0	.0	0	0	0	0	0	0	0	
11.04	18-Jan-96	11:50:00	-53.4204	9.2970	2.03	33.95	100.0	.0	.0	.0	.0	0	0	0	0	0	0	0	
11.04	18-Jan-96	18:20:00	-52.2082	10.2577	3.37	33.92	100.0	.0	.0	.0	.0	0	0	0	0	0	0	0	
11.04	19-Jan-96	04:00:00	-50.5066	11.5267	3.89	33.93	100.0	.0	.0	.0	.0	0	0	0	0	0	0	0	
11.05	19-Jan-96	10:50:00	-49.6854	11.3166	3.88	33.91	100.0	.0	.0	.0	.0	0	0	0	0	0	0	0	
11.06	20-Jan-96	04:10:00	-49.8967	11.5525	3.60	33.91	100.0	.0	.0	.0	.0	0	0	0	0	0	0	0	
11.07	21-Jan-96	04:20:00	-47.8715	12.3987	5.52	33.88	100.0	.0	.0	.0	.0	0	0	0	0	0	0	0	
11.07	21-Jan-96	11:50:00	-46.5137	13.0116	7.55	34.01	100.0	.0	.0	.0	.0	0	0	0	0	0	0	0	

FILE C:\DATA\123DATA\SEA\JGOFS95\STAT95.WK3					========	<===	JGOFS PROTOCOL OBSERVATIONS							=====	=====	=====	=====	=====	=====	=====	=====	=======	=====	=====	=====	===>	<= bergs in 12nm =>				=+=+=+=+=+=+=+=+=+=+=+=+=
Iceconditions and iceberg counts at stations and other positions						V.	WA	SLU	PAN	DNI	LNI		WHI	SEC	MUL	MELT	TOT	ICE	THI		F					N	L	M	S	
					STATION	range	TER	DGE	CAKE	LAS	LAS	GREY	TE	YEAR	YEAR	ICE	ICE	WAT	CK	SNOW	DIAM	RAFT	RIDG	BROW	COLO	BERG	BERG	BERG	BERG	COMMENTS
					========	<===	=====	=====	=====	=====	=====	=====	=====	=====	=====	=====	=====	=====	=====	=====	======	=====	=====	=====	===>	<===	=====	=====	===>	=+=+=+=+=+=+=+=+=+=+=+=+=
TRNF	Date	hh:mm	LATD	LOND	nr	km	%	%	%	%	%	%	%	%	%	%	%	%	%	cm	cm	m	%	%	%	code	n	n	n	n	text
4	12-Dez-95	03:40	-58.1198	-2.4591		0.5	30	0	5	0	0	0	40	5	0	20	70	100	100	30	3	0	0	0	3	0				ice edge
						5	99	0	0	0	0	0	0	0	0	1	1	100	0	0	0	0	0	0	0	1				first berg passed (4.45h)
4	12-Dez-95	09:50	-59.2113	-3.0508		0.5	40	0	1	0	0	0	40	4	0	15	60	100	80	20	10	1	5	100	4	5				
4	12-Dez-95	16:50	-59.4539	-3.196		10	30	0	1	0	0	0	50	4	0	15	70	100	50	20	8	1	5	100	4	0				
4	12-Dez-95	20:10	-60.0331	-3.3773		10	50	0	5	0	0	0	30	5	0	10	50	100	75	25	8	1	5	100	2	0				
4	12-Dez-95	22:20	-60.4084	-3.4375		10	35	0	0	0	0	0	50	5	0	10	65	100	50	20	10	1	1	100	3	0				
4	13-Dez-95	03:10	-61.2458	-3.8789		10	30	3	2	0	0	0	50	5	0	10	70	100	75	25	10	5	5	90	2	0				
4	13-Dez-95	06:50	-61.9025	-4.0976		10	50	3	2	0	0	0	40	2	0	3	50	100	50	20	15	5	5	90	2					
4	13-Dez-95	09:10	-62.2968	-4.2947		10	20	1	1	1	1	1	70	3	0	2	80	100	60	15	25	5	5	50	4	5				
4	13-Dez-95	11:30	-62.6211	-4.5144		10	15	0.5	0.5	0.3	0.2	0.5	80	1	0	2	85	100	50	15	20	5	5	50	3	8				
4	13-Dez-95	14:00	-62.9979	-4.6789		10	10	1	1	1	1	1	80	0	0	5	90	100	60	20	40	5	5	80	4	15				
4	13-Dez-95	16:20	-63.384	-4.7429		10	15	1.5	1.5	1	1	10	60	5	0	5	85	100	75	20	150	0	1	75	2	14				
4	13-Dez-95	19:00	-63.7779	-4.8421		10	15	1.5	1.5	1	1	10	60	5	0	5	85	100	75	25	1000	1	1	100	2	6				
4	13-Dez-95	21:50	-64.1011	-4.9268		10	10	0	0	0	0	0	90	0	0	0	90	100	100	20	1000	0	0	50	2	2				
4	14-Dez-95	02:40	-64.8935	-5.2705		10	50	0	0	0	0	0	50	0	0	0	50	100	100	20	5000	0	5	50	2	11				
4	14-Dez-95	06:40	-65.5481	-5.5396		10	20	0	0	3	2	10	65	0	0	0	80	100	50	15	1000	0	5	100	4	4				
4	14-Dez-95	08:50	-65.9081	-6.0088		10	50	1.5	1.5	0	0	15	30	0	0	2	50	100	50	10	500	0	5	100	2	12				
4	14-Dez-95	11:20	-66.328	-6.2648		10	50	2.5	2.5	0	0	10	30	0	0	5	50	100	50	20	500	5	5	50	3	2				
4	14-Dez-95	14:00	-66.7243	-6.2592		10	50	2.5	2.5	0	0	5	35	0	0	5	50	100	50	10	3000	0	0	50	3	0				
4	14-Dez-95	16:20	-67.1417	-6.4431		10	70	0	2	1	1	5	20	0	0	1	30	100	50	10	500	0	5	50	2	6				
4	14-Dez-95	18:50	-67.5677	-6.7549		10	60	0	0	0	5	10	25	0	0	0	40	100	80	20	150	0	50	100	4	20				
4	14-Dez-95	22:00	-68.1918	-7.1454		10	95	0	0	0	0	0	0	0	0	5	5	100	0	0	0	0	0	0	0	2				
4	15-Dez-95	02:10	-69.0688	-7.7469		10	99.9	0	0	0	0	0	0	0	0	0.1	0.1	100	0	0	0	0	0	0	0	0				
4	15-Dez-95	04:10	-69.4672	-8.0288		5	70	0	0	1	1	1	25	0	0	2	30	100	50	15	2000	0	3	100	2	3				
4	15-Dez-95	08:50	-69.9431	-8.4761		10	40	0	0	0	0	4	50	1	0	5	60	100	75	15	5000	0	10	100	4	21				
4	15-Dez-95	11:30	-70.26	-8.5541		10	15	0	0	0	5	5	45	10	0	20	85	100	75	40	2	0	50	80	5	5				
5	17-Dez-95	12:50	-70.5007	-8.1158		5	1	0	0	0	0	0	89	0	0	10	99	100	200	100	1000	0	50	50	4					
5	19-Dez-95	13:10	-70.2536	-8.2002		10	0	0	0	95	0	0	5	0	0	0	100	100	50	15	1	0	0	0	0					
5	19-Dez-95	14:10	-70.065	-7.9331		10	35	1	1	1	2	0	50	0	0	10	65	100	50	20	10	5	1	50	1					
5	19-Dez-95	16:40	-69.5195	-7.3551		15	90	0	0	0	0	0	7	1	0	2	10	100	30	10	10	0	3	0	0	0				
5	19-Dez-95	19:30	-68.8572	-6.7264		20	100	0	0	0	0	0	0	0	0	0	0	100	0	0	0	0	0	0	0	1				
5	19-Dez-95	22:40	-68.1302	-6.2044		10	80	1	1	1	1	1	10	0	0	5	20	100	50	15	5	0	0	10	1	1				
5	20-Dez-95	02:10	-67.4985	-5.5506		10	80	0	0	0	0	0	15	0	0	5	20	100	40	10	20	0	3	90	2	11				
5	20-Dez-95	06:20	-66.6268	-4.9351		10	75	0	0	0	0	5	15	0	0	5	25	100	40	10	20	0	3	30	1	1				
5	20-Dez-95	09:10	-66.0046	-4.4366		10	75	0	0	0	0	0	20	0	0	5	25	100	40	10	250	0	3	50	1	1				
5	20-Dez-95	11:40	-65.4868	-4.2257		10	30	1	1	2	0	5	55	1	0	5	70	100	50	10	150	5	0	10	2	8				
5	20-Dez-95	14:10	-64.9825	-3.9606		10	50	1	1	1	2	5	30	0	0	10	50	100	50	10	100	1	0	70	2	3				
5	20-Dez-95	16:10	-64.5905	-3.832		15	15	0	0	0	0	5	75	0	0	5	85	100	50	10	250	0	3	50	2	1				
5	20-Dez-95	19:20	-63.8715	-3.5857		15	30	0	0	0	5	5	50	0	0	10	70	100	40	10	25	0	3	50	1	7				
5	20-Dez-95	21:50	-63.3036	-3.3813		10	20	10	0	0	0	5	50	0	0	15	80	100	30	15	15	1	9	50	1	13				
5	21-Dez-95	02:20	-62.4156	-2.9448		5	75	0	0	0	0	0	15	0	0	10	25	100	40	10	5	0	10	25	2	9				
5	21-Dez-95	05:30	-61.7082	-2.6556		15	85	0	0	0	0	0	10	0	0	5	15	100	40	10	8	0	0	10	2	3				
5	21-Dez-95	08:00	-61.0999	-2.4411		15	85	0	0	0	0	0	10	0	0	5	15	100	50	10	8	0	10	100	2	4				
5	21-Dez-95	10:10	-60.5733	-2.2456		10	98	0	0	0	0	0	1	0	0	1	2	100	30	10	1	0	0	100	1	4				ice-edge diffuse
5	21-Dez-95	12:30	-60.0109	-2.0425		10	99	0	0	0	0	0	0	0	0	1	1	100	0	0	0	0	0	0	0	4				
5	21-Dez-95	14:30	-59.5471	-1.8837		10	99	0	0	0	0	0	0	0	0	1	1	100	0	0	0	0	0	0	0	4				
5	21-Dez-95	16:20	-59.1293	-1.7386		10	100	0	0	0	0	0	0	0	0	0	0	100	0	0	0	0	0	0	0	3				
5	21-Dez-95	18:00	-58.7515	-1.6032		10	100	0	0	0	0	0	0	0	0	0	0	100	0	0	0	0	0	0	0	3				
5	21-Dez-95	20:20	-58.2217	-1.43		10	100	0	0	0	0	0	0	0	0	0	0	100	0	0	0	0	0	0	0	0				
5	22-Dez-95	03:00	-56.6825	-0.9287		10	100	0	0	0	0	0	0	0	0	0	0	100	0	0	0	0	0	0	0	0				
5	22-Dez-95	05:40	-56.075	-0.7242		10	100	0	0	0	0	0	0	0	0	0	0	100	0	0	0	0	0	0	0	0				
5	22-Dez-95	09:30	-55.2022	-0.4704		10	100	0	0	0	0	0	0	0	0	0	0	100	0	0	0	0	0	0	0	0				
5	22-Dez-95	14:30	-54.0845	-0.1251		10	100	0	0	0	0	0	0	0	0	0	0	100	0	0	0	0	0	0	0	0				
6.1	22-Dez-95	15:10	-53.9989	-0.1038	38.009a	10	100	0	0	0	0	0	0	0	0	0	0	100	0	0	0	0	0	0	0	0				
6.1	22-Dez-95	20:00	-53.8097	-0.0441		10	100	0	0	0	0	0	0	0	0	0	0	100	0	0	0	0	0	0	0	0				
6.1	23-Dez-95	03:40	-52.6149	0.6691		10	100	0	0	0	0	0	0	0	0	0	0	100	0	0	0	0	0	0	0	0				
6.1	23-Dez-95	06:10	-52.3508	1.2319		10	100	0	0	0	0	0	0	0	0	0	0	100	0	0	0	0	0	0	0	0				
6.1	23-Dez-95	08:00	-52.1757	1.6425		10	100	0	0	0	0	0	0	0	0	0	0	100	0	0	0	0	0	0	0	0				
6.1	23-Dez-95	10:20	-51.9315	2.196		10	100	0	0	0	0	0	0	0	0	0	0	100	0	0	0	0	0	0	0	0				
6.1	23-Dez-95	15:10	-51.4304	3.253		10	100	0	0	0	0	0	0	0	0	0	0	100	0	0	0	0	0	0	0	0				
6.1	23-Dez-95	17:40	-51.185	3.7807		10	100	0	0	0	0	0	0	0	0	0	0	100	0	0	0	0	0	0	0	0				
6.1	24-Dez-95	04:00	-50.2376	5.9949		10	100	0	0	0	0	0	0	0	0	0	0	100	0	0	0	0	0	0	0	0				
6.2	24-Dez-95	06:20	-50.6001	6.0078		10	100	0	0	0	0	0	0	0	0	0	0	100	0	0	0	0	0	0	0	0				

FILE C:\DATA\123DATA\SEA\JGOFS95\STAT95.WK3 ======== <=== JGOFS PROTOCOL OBSERVATIONS ===== ===== ===== ===== ===== ===== ===== ===== ====== ===== ===== ===== ===> <= bergs in 12nm => =+=+=+=+=+=+=+=+=+=+=+=+=+

Iceconditions and iceberg counts at stations and other positions

						V.	WA	SLU	PAN	DNI	LNI		WHI	SEC	MUL	MELT	TOT	ICE	THI			F				N	L	M	S	
					STATION	range	TER	DGE	CAKE	LAS	LAS	GREY	TE	YEAR	YEAR	ICE	ICE	WAT	CK	SNOW	DIAM	RAFT	RIDG	BROW	COLO	BERG	BERG	BERG	BERG	COMMENTS
					========	<===	=====	=====	=====	=====	=====	=====	=====	=====	=====	=====	=====	=====	=====	=====	======	=====	=====	=====	===>	<===	=====	=====	===>	=+=+=+=+=+=+=+=+=+=+=+=+=+
TRNR	Date	hh:mm	LATD	LOND	nr	km	%	%	%	%	%	%	%	%	%	%	%	%	%	cm	cm	m	%	%	%	code	n	n	n	n	text
6.2	24-Dez-95	08:10	-50.8804	6.0031		10	100	0	0	0	0	0	0	0	0	0	0	100	0	0	0	0	0	0	0	0					
6.2	24-Dez-95	13:20	-51.7194	6.0042		10	100	0	0	0	0	0	0	0	0	0	0	100	0	0	0	0	0	0	0	0					
6.2	24-Dez-95	16:30	-52.0025	6.3441		10	100	0	0	0	0	0	0	0	0	0	0	100	0	0	0	0	0	0	0	0					
6.3	25-Dez-95	04:30	-50.7361	7.1014		10	100	0	0	0	0	0	0	0	0	0	0	100	0	0	0	0	0	0	0	0					
6.3	25-Dez-95	10:50	-49.9106	7.2901		10	100	0	0	0	0	0	0	0	0	0	0	100	0	0	0	0	0	0	0	0					
6.4	25-Dez-95	14:20	-49.925	8.1584		10	100	0	0	0	0	0	0	0	0	0	0	100	0	0	0	0	0	0	0	0					
6.4	25-Dez-95	19:30	-50.4778	8.1496	38.010	10	100	0	0	0	0	0	0	0	0	0	0	100	0	0	0	0	0	0	0	0					
6.4	26-Dez-95	04:00	-51.2408	8.1517		10	100	0	0	0	0	0	0	0	0	0	0	100	0	0	0	0	0	0	0	0					
6.4	26-Dez-95	08:00	-51.8594	8.1517		10	100	0	0	0	0	0	0	0	0	0	0	100	0	0	0	0	0	0	0	0					
6.5	26-Dez-95	13:10	-51.9742	9.2435		10	100	0	0	0	0	0	0	0	0	0	0	100	0	0	0	0	0	0	0	0					
6.5	26-Dez-95	15:40	-51.5964	9.245		10	100	0	0	0	0	0	0	0	0	0	0	100	0	0	0	0	0	0	0	0					
6.5	26-Dez-95	19:30	-51.0018	9.245		10	100	0	0	0	0	0	0	0	0	0	0	100	0	0	0	0	0	0	0	0					
6.6	27-Dez-95	09:30	-49.9144	10.2548	38.011	10	100	0	0	0	0	0	0	0	0	0	0	100	0	0	0	0	0	0	0	0					
6.6	27-Dez-95	14:00	-49.6592	10.4006		10	100	0	0	0	0	0	0	0	0	0	0	100	0	0	0	0	0	0	0	0					
6.6	28-Dez-95	04:00	-50.9495	10.2922		10	100	0	0	0	0	0	0	0	0	0	0	100	0	0	0	0	0	0	0	0					
6.6	28-Dez-95	08:10	-51.5555	10.2919		10	100	0	0	0	0	0	0	0	0	0	0	100	0	0	0	0	0	0	0	0					
6.6	28-Dez-95	11:40	-52.0021	10.4141		10	100	0	0	0	0	0	0	0	0	0	0	100	0	0	0	0	0	0	0	0					
6.7	28-Dez-95	15:40	-51.9728	11.3959		10	100	0	0	0	0	0	0	0	0	0	0	100	0	0	0	0	0	0	0	0					
6.7	28-Dez-95	20:00	-51.3534	11.3885		10	100	0	0	0	0	0	0	0	0	0	0	100	0	0	0	0	0	0	0	0					
6.7	29-Dez-95	04:00	-50.1438	11.385		10	100	0	0	0	0	0	0	0	0	0	0	100	0	0	0	0	0	0	0	0					
7.1	29-Dez-95	08:40	-49.4682	11.4032	38.012	10	100	0	0	0	0	0	0	0	0	0	0	100	0	0	0	0	0	0	0	0					
7.1	29-Dez-95	14:20	-49.8931	11.5343	38.013	10	100	0	0	0	0	0	0	0	0	0	0	100	0	0	0	0	0	0	0	0					
7.1	30-Dez-95	04:00	-50.3065	11.5367	38.014	10	100	0	0	0	0	0	0	0	0	0	0	100	0	0	0	0	0	0	0	0					
7.1	30-Dez-95	06:10	-50.6984	11.5221	38.015	10	100	0	0	0	0	0	0	0	0	0	0	100	0	0	0	0	0	0	0	0					
7.1	30-Dez-95	15:20	-51.1007	10.2902	38.016	10	100	0	0	0	0	0	0	0	0	0	0	100	0	0	0	0	0	0	0	0					
7.2	31-Dez-95	04:10	-51.5145	10.2947	38.017	10	100	0	0	0	0	0	0	0	0	0	0	100	0	0	0	0	0	0	0	0					
7.3	31-Dez-95	14:00	-51.284	10.2909		10	100	0	0	0	0	0	0	0	0	0	0	100	0	0	0	0	0	0	0	0					
7.3	31-Dez-95	18:50	-50.617	10.2853		10	100	0	0	0	0	0	0	0	0	0	0	100	0	0	0	0	0	0	0	0					
7.3	01-Jan-96	04:10	-49.5277	10.2911		10	100	0	0	0	0	0	0	0	0	0	0	100	0	0	0	0	0	0	0	0					
7.3	01-Jan-96	08:10	-49.6671	11.1896		10	100	0	0	0	0	0	0	0	0	0	0	100	0	0	0	0	0	0	0	0					
8	01-Jan-96	14:10	-50.3793	11.385		10	100	0	0	0	0	0	0	0	0	0	0	100	0	0	0	0	0	0	0	0					
8	01-Jan-96	17:40	-50.8031	11.3481		10	100	0	0	0	0	0	0	0	0	0	0	100	0	0	0	0	0	0	0	0					
8	01-Jan-96	19:50	-50.577	11.2053		10	100	0	0	0	0	0	0	0	0	0	0	100	0	0	0	0	0	0	0	0					
8	02-Jan-96	04:00	-49.9239	11.0217		10	100	0	0	0	0	0	0	0	0	0	0	100	0	0	0	0	0	0	0	0					
8	02-Jan-96	08:10	-50.5364	11.0217		10	100	0	0	0	0	0	0	0	0	0	0	100	0	0	0	0	0	0	0	0					
8	02-Jan-96	15:00	-50.1514	10.84		10	100	0	0	0	0	0	0	0	0	0	0	100	0	0	0	0	0	0	0	0					
8	02-Jan-96	18:00	-49.7328	10.84		10	100	0	0	0	0	0	0	0	0	0	0	100	0	0	0	0	0	0	0	0					
8.1	03-Jan-96	03:50	-50.7809	10.476		10	100	0	0	0	0	0	0	0	0	0	0	100	0	0	0	0	0	0	0	0					
8.1	03-Jan-96	08:10	-50.1186	10.4767		10	100	0	0	0	0	0	0	0	0	0	0	100	0	0	0	0	0	0	0	0					
8.1	03-Jan-96	14:20	-50.0312	10.295		10	100	0	0	0	0	0	0	0	0	0	0	100	0	0	0	0	0	0	0	0					
8.1	03-Jan-96	18:10	-50.5723	10.295		10	100	0	0	0	0	0	0	0	0	0	0	100	0	0	0	0	0	0	0	0					
8.1	04-Jan-96	03:40	-49.7534	10.1133		10	100	0	0	0	0	0	0	0	0	0	0	100	0	0	0	0	0	0	0	0					
8.1	04-Jan-96	08:10	-50.1438	9.9316		10	100	0	0	0	0	0	0	0	0	0	0	100	0	0	0	0	0	0	0	0					
8.10	04-Jan-96	14:20	-50.7003	9.7502		10	100	0	0	0	0	0	0	0	0	0	0	100	0	0	0	0	0	0	0	0					
8.10	04-Jan-96	18:10	-50.1271	9.75		10	100	0	0	0	0	0	0	0	0	0	0	100	0	0	0	0	0	0	0	0					
8.1	05-Jan-96	03:50	-50.5275	9.5684		10	100	0	0	0	0	0	0	0	0	0	0	100	0	0	0	0	0	0	0	0					
9.1	05-Jan-96	07:30	-50.6986	9.5675	38.018	10	100	0	0	0	0	0	0	0	0	0	0	100	0	0	0	0	0	0	0	0					
9.1	05-Jan-96	14:40	-50.4973	9.4398		10	100	0	0	0	0	0	0	0	0	0	0	100	0	0	0	0	0	0	0	0					
9.1	05-Jan-96	18:40	-49.8991	9.5614	38.019	10	100	0	0	0	0	0	0	0	0	0	0	100	0	0	0	0	0	0	0	0					
9.2	06-Jan-96	09:30	-49.6118	10.3205		10	100	0	0	0	0	0	0	0	0	0	0	100	0	0	0	0	0	0	0	0					
9.2	06-Jan-96	13:00	-49.8988	10.2943	38.021	10	100	0	0	0	0	0	0	0	0	0	0	100	0	0	0	0	0	0	0	0					
9.2	07-Jan-96	08:30	-50.2853	10.3311	38.025	10	100	0	0	0	0	0	0	0	0	0	0	100	0	0	0	0	0	0	0	0					
9.2	07-Jan-96	10:10	-50.4035	10.2936	38.026	10	100	0	0	0	0	0	0	0	0	0	0	100	0	0	0	0	0	0	0	0					
9.2	07-Jan-96	16:40	-50.7007	10.2895	38.029	10	100	0	0	0	0	0	0	0	0	0	0	100	0	0	0	0	0	0	0	0					
10	08-Jan-96	05:20	-51.9727	9.383		10	100	0	0	0	0	0	0	0	0	0	0	100	0	0	0	0	0	0	0	0					
10	08-Jan-96	08:00	-52.5529	8.9698		10	100	0	0	0	0	0	0	0	0	0	0	100	0	0	0	0	0	0	0	0					
10	08-Jan-96	11:30	-53.3441	8.3818		10	100	0	0	0	0	0	0	0	0	0	0	100	0	0	0	0	0	0	0	0					
10	08-Jan-96	15:00	-54.1166	7.8152		10	100	0	0	0	0	0	0	0	0	0	0	100	0	0	0	0	0	0	0	0					
10	08-Jan-96	19:30	-55.0942	7.0528		10	100	0	0	0	0	0	0	0	0	0	0	100	0	0	0	0	0	0	0	0					
10	09-Jan-96	00:40	-56.2191	6.2019		10	100	0	0	0	0	0	0	0	0	0	0	100	0	0	0	0	0	0	0	0					
10	09-Jan-96	03:20	-56.805	5.7337		10	100	0	0	0	0	0	0	0	0	0	0	100	0	0	0	0	0	0	0	0					First iceberg, 15nm on radar
10	09-Jan-96	06:10	-57.4331	5.2156		10	100	0	0	0	0	0	0	0	0	0	0	100	0	0	0	0	0	0	0	1	0	1	0	
10	09-Jan-96	08:00	-57.8491	4.8967		10	100	0	0	0	0	0	0	0	0	0	0	100	0	0	0	0	0	0	0	1	0	1	0	

FILE C:\DATA\123DATA\SEA\JGOFS95\STAT95.WK3

Iceconditions and iceberg counts at stations and other positions

					========	<===	JGOFS PROTOCOL OBSERVATIONS						=====	=====	=====	=====	=====	=====	=====	=====	=====	======	=====	=====	=====	===>	<= bergs in 12nm =>				=+=+=+=+=+=+=+=+=+=+=+
					STATION	V_ range	WA TER	SLU DGE	PAN CAKE	DNI LAS	LNI LAS	GREY	WHI TE	SEC YEAR	MUL YEAR	MELT ICE	TOT ICE	ICE WAT	THI CK	SNOW	F DIAM	RAFT	RIDG	BROW	COLO	N BERG	L BERG	M BERG	S BERG	COMMENTS
					========	<===	=====	=====	=====	=====	=====	=====	=====	=====	=====	=====	=====	=====	=====	=====	======	=====	=====	=====	===>	<===	=====	=====	===>	=+=+=+=+=+=+=+=+=+=+=+
TRNF	Date	hh:mm	LATD	LOND	nr	km	%	%	%	%	%	%	%	%	%	%	%	%	cm	cm	m	%	%	%	code	n	n	n	n	text
10	09-Jan-96	11:30	-58.6321	4.2318		10	100	0	0	0	0	0	0	0	0	0	0	100	0	0	0	0	0	0	0	3	0	0	3	
10	09-Jan-96	14:20	-59.26	3.6984		10	100	0	0	0	0	0	0	0	0	0	0	100	0	0	0	0	0	0	0	5	0	5	0	
10	09-Jan-96	16:20	-59.7084	3.3105		10	100	0	0	0	0	0	0	0	0	0	0	100	0	0	0	0	0	0	0	7	1	6	0	
10	09-Jan-96	18:00	-60.0805	2.9884		10	100	0	0	0	0	0	0	0	0	0	0	100	0	0	0	0	0	0	0	4	0	2	2	
10	09-Jan-96	20:00	-60.5305	2.5798		10	100	0	0	0	0	0	0	0	0	0	0	100	0	0	0	0	0	0	0	14	0	11	3	
10	09-Jan-96	22:00	-60.9864	2.1862		10	100	0	0	0	0	0	0	0	0	0	0	100	0	0	0	0	0	0	0	20	0	8	12	
10	10-Jan-96	03:10	-62.1622	1.0936		10	100	0	0	0	0	0	0	0	0	0	0	100	0	0	0	0	0	0	0	8	0	6	2	
10	10-Jan-96	05:10	-62.6147	0.6668		10	100	0	0	0	0	0	0	0	0	0	0	100	0	0	0	0	0	0	0	9	0	4	5	
10	10-Jan-96	07:10	-63.0676	0.2172		10	100	0	0	0	0	0	0	0	0	0	0	100	0	0	0	0	0	0	0	9	0	3	6	
10	10-Jan-96	08:00	-63.2585	0.0301		10	100	0	0	0	0	0	0	0	0	0	0	100	0	0	0	0	0	0	0	6	0	2	4	
10	10-Jan-96	11:30	-64.0603	-0.7592		10	100	0	0	0	0	0	0	0	0	0	0	100	0	0	0	0	0	0	0	6	0	3	3	
10	10-Jan-96	14:00	-64.6384	-1.3356		10	100	0	0	0	0	0	0	0	0	0	0	100	0	0	0	0	0	0	0	16	0	5	11	
10	10-Jan-96	16:00	-65.0998	-1.8119		10	100	0	0	0	0	0	0	0	0	0	0	100	0	0	0	0	0	0	0	16	0	10	6	
10	10-Jan-96	18:00	-65.5562	-2.2779		10	100	0	0	0	0	0	0	0	0	0	0	100	0	0	0	0	0	0	0	17	0	10	7	
10	10-Jan-96	22:10	-66.5019	-3.3239		10	100	0	0	0	0	0	0	0	0	0	0	100	0	0	0	0	0	0	0	3	0	0	3	
10	11-Jan-96	02:40	-67.5121	-4.4498		10	100	0	0	0	0	0	0	0	0	0	0	100	0	0	0	0	0	0	0	9	0	6	3	
10	11-Jan-96	04:30	-67.9296	-4.9243		10	95	0	0	0	0	0	5	0	0	0	5	100	30	10	1	0	0	0	0	7	0	0	7	First icefields, on radar
10	11-Jan-96	06:30	-68.3779	-5.4632		0.5	99	0	0	0	0	0	0	0	0	1	1	100	0	0	0	0	0	0	0	19	1	10	8	
10	11-Jan-96	08:00	-68.7178	-5.8715		10	100	0	0	0	0	0	0	0	0	0	0	100	0	0	0	0	0	0	0	10	0	6	4	
10	11-Jan-96	11:30	-69.4657	-7.0495		10	100	0	0	0	0	0	0	0	0	0	0	100	0	0	0	0	0	0	0	8	1	4	3	
10	11-Jan-96	14:00	-70.0107	-7.7831		1	5	0	0	0	0	0	65	0	0	30	95	100	50	10	10	5	5	80	3	24	2	7	15	sharp ice-edge
10	11-Jan-96	15:40	-70.2563	-7.9602		10	1	0	0	0	0	0	90	0	0	9	99	100	100	25	100	0	20	100	4					
10	11-Jan-96	18:10	-70.5226	-7.943		1	1	0	0	0	0	0	95	0	0	4	99	100	120	75	100	1	75	100	4	20	1	11	8	
						1	0	0	0	0	0	1	80	0	0	19	100	100	90	40	100	0	80	100	3	5	1	4	0	
						10	11	0	0	1	2	1	60	0	0	25	89	100	90	20	20	0	0	95	3	8	1	3	4	
						10	5	0	0	2	3	5	80	0	0	5	95	100	75	20	25	0	10	95	3	5	0	0	5	
						10	20	0	0	0	0	0	70	0	0	10	80	100	60	15	25	0	10	95	3	20	0	7	13	
						0.5	1	0	0	0	0	0	39	0	0	60	99	100	60	15	5	0	0	100	3	20	0	7	13	sharp ice-edge
						10	100	0	0	0	0	0	0	0	0	0	0	100	0	0	0	0	0	0	0	3	0	0	3	
						10	100	0	0	0	0	0	0	0	0	0	0	100	0	0	0	0	0	0	0	13	1	4	8	
						10	100	0	0	0	0	0	0	0	0	0	0	100	0	0	0	0	0	0	0	6	0	6	0	
						10	100	0	0	0	0	0	0	0	0	0	0	100	0	0	0	0	0	0	0	6	0	6	0	
						10	100	0	0	0	0	0	0	0	0	0	0	100	0	0	0	0	0	0	0	3	0	3	0	
						10	100	0	0	0	0	0	0	0	0	0	0	100	0	0	0	0	0	0	0	7	0	4	3	
						10	100	0	0	0	0	0	0	0	0	0	0	100	0	0	0	0	0	0	0	17	0	12	5	
						10	100	0	0	0	0	0	0	0	0	0	0	100	0	0	0	0	0	0	0	13	0	8	5	
						10	100	0	0	0	0	0	0	0	0	0	0	100	0	0	0	0	0	0	0	7	0	4	3	
						10	100	0	0	0	0	0	0	0	0	0	0	100	0	0	0	0	0	0	0	6	0	6	0	
						10	100	0	0	0	0	0	0	0	0	0	0	100	0	0	0	0	0	0	0	10	0	7	3	
						10	100	0	0	0	0	0	0	0	0	0	0	100	0	0	0	0	0	0	0	4	0	2	2	
						10	100	0	0	0	0	0	0	0	0	0	0	100	0	0	0	0	0	0	0	8	0	5	3	
						10	100	0	0	0	0	0	0	0	0	0	0	100	0	0	0	0	0	0	0	3	0	3	0	
						10	100	0	0	0	0	0	0	0	0	0	0	100	0	0	0	0	0	0	0	3	0	3	0	
						10	100	0	0	0	0	0	0	0	0	0	0	100	0	0	0	0	0	0	0	8	0	5	3	
						10	100	0	0	0	0	0	0	0	0	0	0	100	0	0	0	0	0	0	0	7	0	4	3	
						10	100	0	0	0	0	0	0	0	0	0	0	100	0	0	0	0	0	0	0	7	0	7	0	
						10	100	0	0	0	0	0	0	0	0	0	0	100	0	0	0	0	0	0	0	0	0	0	0	
						10	100	0	0	0	0	0	0	0	0	0	0	100	0	0	0	0	0	0	0	1	0	1	0	
						10	100	0	0	0	0	0	0	0	0	0	0	100	0	0	0	0	0	0	0	0	0	0	0	
					38.031	10	100	0	0	0	0	0	0	0	0	0	0	100	0	0	0	0	0	0	0	1	0	1	0	
						10	100	0	0	0	0	0	0	0	0	0	0	100	0	0	0	0	0	0	0	0	0	0	0	
						10	100	0	0	0	0	0	0	0	0	0	0	100	0	0	0	0	0	0	0	0	0	0	0	
						10	100	0	0	0	0	0	0	0	0	0	0	100	0	0	0	0	0	0	0	0	0	0	0	
						10	100	0	0	0	0	0	0	0	0	0	0	100	0	0	0	0	0	0	0	0	0	0	0	
						10	100	0	0	0	0	0	0	0	0	0	0	100	0	0	0	0	0	0	0	0	0	0	0	
						10	100	0	0	0	0	0	0	0	0	0	0	100	0	0	0	0	0	0	0	0	0	0	0	
						10	100	0	0	0	0	0	0	0	0	0	0	100	0	0	0	0	0	0	0	0	0	0	0	
						10	100	0	0	0	0	0	0	0	0	0	0	100	0	0	0	0	0	0	0	0	0	0	0	
					38.032	10	100	0	0	0	0	0	0	0	0	0	0	100	0	0	0	0	0	0	0	0	0	0	0	
						10	100	0	0	0	0	0	0	0	0	0	0	100	0	0	0	0	0	0	0	0	0	0	0	
						10	100	0	0	0	0	0	0	0	0	0	0	100	0	0	0	0	0	0	0	0	0	0	0	

20. STATIONS-LIST ANT XIII/2

Stat.38/	Date	Time	Latitude	Longitude	Depth	Operation
003	05.12.95	13:22	39° 04,7'S	14° 44,0'E	4725	SeaSoar-D
003a		18:21	39° 37,5'S	14° 16,4'E	4745	SeaSoar-R
004	06.12.95	08:08	41° 48,9'S	12° 43,0'E	4873	CTD, MN, SeaSoar-D
004a	09.12.95	03:03	50° 13,5'S	05° 45,7'E	3838	SeaSoar-R
005		04:00	50° 11,1'S	05° 30,8'E	3853	CTD, MN, KV, CTD, Hy, R- PF-8 negative
006		12:32	50° 21,7'S	05° 30,7'E	3542	CTD, MN, MER, Bucket, SeaSoar-D
007	11.12.95	21:00	57° 19,0'S	02° 05,3'E	3928	SeaSoar-R, CTD, MN, BO
008	12.12.95	11:20	59° 25,8'S	03° 12,5'E	5253	MER, MN, CTD, MN, KV, Hy, R-AWI-227 neg.
009	22.12.95	15:05	53° 59,9'S	00° 06,2'E	2752	CTD, SD, KV, MN, BO, CTD, SeaSoar-D, D-FeP
010	25.12.95	17:59	50° 28,8'S	08° 09,1'E	4456	R-FeP, SeaSoar-R, CTD, SD, KV, MN, BO CTD, SeaSoar-D
011	27.12.95	09:00	49° 54,8'S	10° 17,6'E	4082	SeaSoar-R, CTD, SeaSoar-D,
	28.12.95	11:08	52° 00,0'S	10° 17,5'E	3764	D-FeP,
	29.12.95	08:10	49° 30,1'S	11° 23,4'E	4228	R-FeP, SeaSoar-R
012	29.12.95	09:07	49° 29,3'S	11° 23,3'E	4205	CTD, MN
013		13:35	49° 54,0'S	11° 31,6'E	4174	MER, SD, CTD, D-AWI-235, ADCP, CTD, KV MN, CTD
014	30.12.95	00:19	50° 18,1'S	11° 31,6'E	2902	CTD, MN, Bucket, CTD
015		06:05	50° 41,8'S	11° 31,0'E	3966	CTD, KV, MN, APSN, BO,
016		15:20	51° 06,1'S	10° 17,4'E	3993	CTD, SD, MER, KV, CTD, APSN, BO, CTD MN, CTD
017	31.12.95	02:05	51° 30,1'S	10° 17,5'E	3785	CTD, APSN, MN, CTD, CTD,
	01.01.96	08:57	49° 41,4'S	11° 19,6'E	3807	SeaSoar-D,
	02.01.96	01:41	49° 42,7'S	11° 12,2'E	3835	D-FeP,
	05.01.96	05:50	50° 48,0'S	09° 34,1'E	4286	SeaSoar-R
018		07:25	50° 42,0'S	09° 34,1E	4284	MER, CTD, KV, CTD, MN, BO, CTD, APSN
019		18:27	49° 54,0'S	09° 34,1'E	4023	MER, CTD, KV, MN, BO, CTD,
	06.01.96	00:12	49° 53,2'S	09° 34,1'E	3996	RMT
Stat.38/	Date	Time	Latitude	Longitude	Depth	Operation
020		03:40	49° 30,0'S	10° 17,8'E	3537	CTD, KV, CTD, APSN, MN, CTD, MER
021		11:00	49° 54,1'S	10° 17,9'E	4066	CTD, MN, CTD, MER, Bucket, CTD, CTD, KV CTD, CTD, APSN
022		19:52	49° 59,5'S	10° 17,3'E	4105	MN, CTD
023		21:54	50° 05,9'S	10° 17,6'E	4105	CTD, MN
024	07.01.96	00:20	50° 11,9'S	10° 17,5'E	3967	CTD, MN, RMT,
025		02:57	50° 18,0'S	10° 17,5'E	4246	CTD, KV, CTD, APSN, MN, CTD, BO, MER
026		09:58	50° 24,0'S	10° 17,6'E	4435	CTD, MN
027		12:06	50° 30,0'S	10° 17,8'E	3544	CTD, APSN, MN,
028		14:15	50° 36,0'S	10° 17,6'E	4007	CTD, MN,
029		16:30	50° 42,0'S	10° 17,5'E	4041	CTD, MER, SD, CTD, KV, CTD, MN, CTD BO
	15.01.96	14:15	67° 50,1'S	04° 42,1'E	4591	D-FeP
030	16.01.96	09:10	63° 40,0'S	00° 00,4'E	5237	R-FeP, MN, MER, CTD, KV, D-FeP, R-FeP
031	17.01.96	17:01	57° 20,0'S	05° 50,0'E	4733	MER, SD, APSN, CTD, MN,
032	20.01.96	04:02	49° 53,8'S	11° 33,1'E	4176	SD, CTD, Hy, R-AWI-235, MER, CTD, MN Bucket, CTD, KV, RMT,
033		15:57	49° 42,2'S	11° 31,5'E	4042	CTD, MN, APSN

Operation/Gear used:

ADCP = Acoustic Doppler Current Profiler	APSN = Apstein Net	BO = Bongo Net
Bucket = Stainless Steelbucket for Surface Samples	CTD = Conductivity, Temperature, Pressure Probe	D- = Deployment of Instruments
FeP = Fe-Probe, for Underway Iron Samples	Hy = Hydrophone	KV = Kevlar, Winch for Iron Samples
MER = Under Water Spectral Radiometer	MN = Multinet	R- = Recovering of Instruments
RMT = Rectangular Midwater Trawl	SD = Secchi Disk	SeaSoar-D = Deployment
SeaSoar-R = Recovery		

21. PARTICIPANTS / FAHRTTEILNEHMER

ANT XIII/1

Name	Institution	Nation
Brockhoff, Jörg	GECON	D
Dugge, Peter	STN	D
El Naggar, Saad El Dine	AWI	D
England, Joachim	DWD	D
Gerchow, Peter	AWI	D
Großklaus, Martin	IFMK	D
Grumme, Ingo	GEO	D
Johannsen, Hergen	IFMK	D
Kall, Edelgard	AWI	D
Köhler, Herbert	DWD	D
Körtzinger, Arne	IFMK	D
Schweinsberg, SusanneI	FMK	D
Segl, Monika	UNIB	D

ANT XIII/2

Name	Institution	Nation
Allen, John T.	JRC	UK
Bathmann, Ulrich	AWI	D
Bracher, Astrid	AWI	D
Bratrich, Christine M.	Ulm	D
Brink, N. W. van den	IBN-DLO	NL
Bury, Sarah	SURRC	UK
de Jong, Edwin	NIOZ	NL
de Jong, Jeroen	NIOZ	NL
den Das, Johan	NIOZ	NL
Dubischar, Corinna	AWI	D
England, Joachim	DWD	D
Ewen, Ingeborg	UCT	SA
Fischer, Haika	AWI	D
Franeker, Jan A. van	IBN-DLO	NL
Griffiths, Mike J.	JRC	UK
Hartmann, Carmen	AWI	D
Hollmann, Beate	AWI	D
Hennes, Kilian	LIUK	D
Hense, Inga	AWI	D
Hofmann, Matthias	AWI	D
Kattner, Gerd	AWI	D
Klaas, Christine	AWI	SUI
Kühn, Stefanie	AWI	D
Lehmann, Renate	AWI	D
Lucas, Mike	UCT	SA
Menden-Deuer, Susanne	AWI	D
Nacken, Maret	AWI	D
Naveira Garabato, Alberto C.	UL	UK / ESP
Pollard, Raymond	JRC	UK
Read, Jane F.	JRC	UK
Richter, Kai-Uwe	AWI	D
Rosenstock, Bernd	LIUK	D
Rutgers v.d. Loeff, M.	AWI	NL
Rynearson, Tatiana	AWI	USA
Schledlbauer, Oliver	IACUR	D

Simon, Meinhard	LIUK	D
Smetacek; Victor	AWI	IND
Strass, Volker	AWI	D
Terbrüggen, Anja	AWI	D
Timmermann, Ralph	AWI	D
Tremblay, Jean-Eric	ULQ, AWI	CAN
Wischmeyer, Andre	AWI	D
Zondervan, Ingrid	NIOZ	NL
Köhler, Herbert	DWD	D
Hillebrandt, Marc-Oli	Wasserthal	D

to Neumayer

Arck, Martin	AWI	D
Besuden, Eicke R.	Radio Bremen	D
Bimberg, Karin	AWI	D
Brüninghaus, Mathias	Radio Bremen	D
Gaw, Viola	AWI	D
Jockwer, Gustav	AWI	D
Johannes, Walter	Radio Bremen	D
Leitzke, Rüdiger	AWI	D
Nitsch, Olaf	AWI	D
Plato von, Christian	Radio Bremen	D
Schmidt, Anke	AWI	D
Schmidt, Dr. Thomas	AWI	D
Schubert, Helga	AWI	D

Summer Camp

Gödecke, Lothar	AWI	D
Gwilliam, Patrick, T.	AWI	UK
Heidland, Dr. Klemens	AWI	D
Meyer, Uwe F.	AWI	D
Miller, Johann G.	Kässborer	D
Minikin, Andreas	AWI	Ire
Nolting, Michael	AWI	D
Schmidt, Eike	AWI	D
Trefzer, Ulrich O.	AWI	D
Weynand, Markus	AWI	D
Wohltmann, Holger	AWI	D

22. PARTICIPANTING INSTITUTES / BETEILIGTE INSTITUTE

ANT XIII/1

A W I	Alfred-Wegener-Institut für Polar- und Meeresforschung Columbusstrasse 27515 Bremerhaven GERMANY
DWD	Deutscher Wetterdienst, Seewetteramt Bernhard-Nocht-Str. 76 20359 Hamburg GERMANY
GECON	Systemtechnik GmbH Wildrosenweg 3 24119 Kronshagen GERMANY
STN	STN Atlas Elektronik, Abt. MME4 Sebaldsbrücker Heerstr. 235 28305 Bremen GERMANY
IFM	Institut für Meereskunde, Uni Kiel Abt. Meereschemie Düsternbrooker Weg 20 24105 Kiel GERMANY
GEO	Fa. Geo++ GmbH Osteriede 8-10 30827 Garbsen GERMANY
UNIB	Universität Bremen Geowissenschaften, FB 5 Postfach 33 04 40 28334 Bremen GERMANY

ANT XIII/2

A W I	Alfred-Wegener-Institut für Polar- und Meeresforschung Columbusstrasse 27515 Bremerhaven GERMANY
DWD	Deutscher Wetterdienst, Seewetteramt Bernhard-Nocht-Str. 76 20359 Hamburg GERMANY
IACUR	Univ. Regensburg Institut für Anorganische Chemie Universitätsstr. 31 93040 Regensburg GERMANY

IBN-DLO	Institute for Forestry & Nature Research Postbox 167 NL-1790 AB Den Burg (Texel) THE NETHERLANDS
JRC	James Rennell Centre for Ocean Circulation Division of the Southampton Oceanography Centre Empress Dock Southampton, SO14 3ZH ENGLAND
KB	Georg Miller Kässbohrer Geländefahrzeug GmbH Rittinghaus-Str. 2 89250 Senden GERMANY
LIUK	Limnologisches Institut Universität Konstanz Postfach 55 60 78434 Konstanz GERMANY
NIOZ	Nederlands Instituut voor Onderzoek der Zee Postbox 59 NL-1790 AB Den Burg/Texel THE NETHERLANDS
RB	Radio Bremen Hans-Bredow-Str. 10 28353 Bremen GERMANY
SURRC	Scottish Universities Research and Reactor Centre (SURRC) Isotope Biochem. Lab. East Kilbride, Glasgow, G75 0QU ENGLAND
UCT	Southern Ocean Group Zoology Department University of Cape Town Rondebosch 7700 SOUTH AFRICA
UL	Dept. of Earth Sciences The University Liverpool, L69 3BX ENGLAND
ULQ	GIROQ Pavillon Vachon, Univ. Laval Quebec, P.Q. G1K 7P4 CANADA

23. SCHIFFSBESATZUNG/SHIPS CREW

ANT XIII/1 und ANT XIII/2

Dienstgrad	Name
Kapitän	H.G.W. Jonas
1. Offizier	I. Varding
Naut. Offizier	U. Pahl
Naut. Offizier	S. Schwarze
zusl.Offizier	M. Block
Arzt	F.M. Paulus
Funkoffizier	W. Thonhauser
Funkoffizier	J. Butz
Ltd. Ingenieur	V. Schulz
1. Ingenieur	W. Delff
2. Ingenieur	W. Simon
2. Ingenieur	H. Folta
Elektriker	G. Schuster
Elektroniker	U. Lembke
Elektroniker	H.E. Pabst
Elektroniker	M. Fröb
Elektroniker	A. Piskorzynski
Koch	H-J. Schäfer
Kochsmaat	M. Yavuz
Kochsmaat	H. Hüneke
Stewardess	A. Hopp
Stewardess/Nurse	C. Lehmbecker
Stewardess	R. Klemet
2. Steward	B. Amran
2. Steward	J-M. Tu
2. Steward	E. Golose
2. Steward	K.F. Mui
Wäscher	K-Y. Yu
Bootsmann	R.R. Loidl
Zimmermann	P. Kassubeck
Matrose	S. Moser
Matrose	H. Voges
Matrose	B. Clasen
Matrose	W.W. Neisner
Matrose	B.B. Iglesias
Matrose	J. Novo Loveira
Matrose	A. Suarez Paisal
Matrose	E. Dominguez-Quintas
Lagerhalter	B. Barth
Masch-Wart	A.H.F. Schade
Masch-Wart	H. Bloedorn
Masch-Wart	E. Heurich
Masch-Wart	G. Fritz
Matrose	E. Arias Iglesias

Folgende Hefte der Reihe „Berichte zur Polarforschung" sind bisher erschienen:

* **Sonderheft Nr. 1/1981** – „Die Antarktis und ihr Lebensraum"
Eine Einführung für Besucher – Herausgegeben im Auftrag von SCAR

Heft Nr. 1/1982 – „Die Filchner-Schelfeis-Expedition 1980/81"
zusammengestellt von Heinz Kohnen

* **Heft-Nr. 2/1982** – „Deutsche Antarktis-Expedition1980/81 mit FS ‚Meteor'"
First International BIOMASS Experiment (FIBEX) – Liste der Zooplankton- und Mikronektonnetzfänge
zusammengestellt von Norbert Klages.

Heft Nr. 3/1982 – „Digitale und analoge Krill-Echolot-Rohdatenerfassung an Bord des Forschungsschiffes ‚Meteor'" (im Rahmen von FIBEX 1980/81, Fahrtabschnitt ANT III), von Bodo Morgenstern

Heft Nr. 4/1982 – „Filchner-Schelfeis-Expedition 1980/81"
Liste der Planktonfänge und Lichtstärkemessungen
zusammengestellt von Gerd Hubold und H. Eberhard Drescher

* **Heft Nr. 5/1982** – "Joint Biological Expedition on RRS 'John Biscoe', February 1982"
by G. Hempel and R. B. Heywood

* **Heft Nr. 6/1982** – „Antarktis-Expedition 1981/82 (Unternehmen ‚Eiswarte')"
zusammengestellt von Gode Gravenhorst

Heft Nr. 7/1982 – „Marin-Biologisches Begleitprogramm zur Standorterkundung 1979/80 mit MS ‚Polarsirkel' (Pre-Site Survey)" – Stationslisten der Mikronekton- und Zooplanktonfänge sowie der Bodenfischerei
zusammengestellt von R. Schneppenheim

Heft Nr. 8/1983 – "The Post-Fibex Data Interpretation Workshop"
by D. L. Cram and J.-C. Freytag with the collaboration of J. W. Schmidt, M. Mall, R. Kresse, T. Schwinghammer

* **Heft Nr. 9/1983** – "Distribution of some groups of zooplankton in the inner Weddell Sea in summer 1979/80"
by I. Hempel, G. Hubold, B. Kaczmaruk, R. Keller, R. Weigmann-Haass

Heft Nr. 10/1983 – „Fluor im antarktischen Ökosystem" – DFG-Symposium November 1982
zusammengestellt von Dieter Adelung

Heft Nr. 11/1983 – "Joint Biological Expedition on RRS 'John Biscoe', February 1982 (II)"
Data of micronecton and zooplankton hauls, by Uwe Piatkowski

Heft Nr. 12/1983 – „Das biologische Programm der ANTARKTIS-I-Expedition 1983 mit FS ‚Polarstern'"
Stationslisten der Plankton-, Benthos- und Grundschleppnetzfänge und Liste der Probennahme an Robben und Vögeln, von H. E. Drescher, G. Hubold, U. Piatkowski, J. Plötz und J. Voß

* **Heft Nr. 13/1983** – „Die Antarktis-Expedition von MS ‚Polarbjörn' 1982/83" (Sommerkampagne zur Atka-Bucht und zu den Kraul-Bergen), zusammengestellt von Heinz Kohnen

* **Sonderheft Nr. 2/1983** – „Die erste Antarktis-Expedition von FS ‚Polarstern' (Kapstadt, 20. Januar 1983 – Rio de Janeiro, 25. März 1983)", Bericht des Fahrtleiters Prof. Dr. Gotthilf Hempel

Sonderheft Nr. 3/1983 – „Sicherheit und Überleben bei Polarexpeditionen"
zusammengestellt von Heinz Kohnen

* **Heft Nr. 14/1983** – „Die erste Antarktis-Expedition (ANTARKTIS I) von FS ‚Polarstern' 1982/83"
herausgegeben von Gotthilf Hempel

Sonderheft Nr. 4/1983 – "On the Biology of Krill *Euphausia superba*" – Proceedings of the Seminar and Report of the Krill Ecology Group, Bremerhaven 12.–16. May 1983, edited by S. B. Schnack

Heft Nr. 15/1983 – "German Antarctic Expedition 1980/81 with FRV 'Walther Herwig' and RV 'Meteor'" – First International BIOMASS Experiment (FIBEX) – Data of micronekton and zooplankton hauls
by Uwe Piatkowski and Norbert Klages

Sonderheft Nr. 5/1984 – "The observatories of the Georg von Neumayer Station", by Ernst Augstein

Heft Nr. 16/1984 – "FIBEX cruise zooplankton data"
by U. Piatkowski, I. Hempel and S. Rakusa-Suszczewski

Heft Nr. 17/1984 – „Fahrtbericht (cruise report) der ‚Polarstern'-Reise ARKTIS I, 1983"
von E. Augstein, G. Hempel und J. Thiede

Heft Nr. 18/1984 – „Die Expedition ANTARKTIS II mit FS ‚Polarstern' 1983/84",
Bericht von den Fahrtabschnitten 1, 2 und 3, herausgegeben von D. Fütterer

Heft Nr. 19/1984 – „Die Expedition ANTARKTIS II mit FS ‚Polarstern' 1983/84",
Bericht vom Fahrtabschnitt 4, Punta Arenas–Kapstadt (Ant-II/4), herausgegeben von H. Kohnen

Heft Nr. 20/1984 – „Die Expedition ARKTIS II des FS ‚Polarstern' 1984, mit Beiträgen des FS ‚Valdivia' und des Forschungsflugzeuges ‚Falcon 20' zum Marginal Ice Zone Experiment 1984 (MIZEX)"
von E. Augstein, G. Hempel, J. Schwarz, J. Thiede und W. Weigel

Heft Nr. 21/1985 – "Euphausiid larvae in plankton samples from the vicinity of the Antarctic Peninsula, February 1982" by Sigrid Marschall and Elke Mizdalski

Heft Nr. 22/1985 – "Maps of the geographical distribution of macrozooplankton in the Atlantic sector of the Southern Ocean" by Uwe Piatkowski

Heft Nr. 23/1985 – „Untersuchungen zur Funktionsmorphologie und Nahrungsaufnahme der Larven des Antarktischen Krills *Euphausia superba* Dana" von Hans-Peter Marschall

Heft Nr. 24/1985 – „Untersuchungen zum Periglazial auf der König-Georg-Insel Südshetlandinseln/ Antarktika. Deutsche physiogeographische Forschungen in der Antarktis. – Bericht über die Kampagne 1983/84" von Dietrich Barsch, Wolf-Dieter Blümel, Wolfgang Flügel, Roland Mäusbacher, Gerhard Stablein, Wolfgang Zick

* **Heft-Nr. 25/1985** – „Die Expedition ANTARKTIS III mit FS ‚Polarstern' 1984/1985" herausgegeben von Gotthilf Hempel.

***Heft-Nr. 26/1985** – "The Southern Ocean"; A survey of oceanographic and marine meteorological research work by Hellmer et al.

Heft Nr. 27/1986 – „Spatpleistozäne Sedimentationsprozesse am antarktischen Kontinentalhang vor Kapp Norvegia, östliche Weddell-See" von Hannes Grobe

Heft Nr. 28/1986 – „Die Expedition ARKTIS III mit ‚Polarstern' 1985" mit Beiträgen der Fahrtteilnehmer, herausgegeben von Rainer Gersonde

* **Heft Nr. 29/1986** – „5 Jahre Schwerpunktprogramm ‚Antarktisforschung' der Deutschen Forschungsgemeinschaft." Rückblick und Ausblick. Zusammengestellt von Gotthilf Hempel, Sprecher des Schwerpunktprogramms

Heft Nr. 30/1986 – "The Meteorological Data of the Georg-von-Neumayer-Station for 1981 and 1982" by Marianne Gube and Friedrich Obleitner

Heft Nr. 31/1986 – „Zur Biologie der Jugendstadien der Notothenioidei (Pisces) an der Antarktischen Halbinsel" von A. Kellermann

Heft Nr. 32/1986 – „Die Expedition ANTARKTIS IV mit FS ‚Polarstern' 1985/86" mit Beiträgen der Fahrtteilnehmer, herausgegeben von Dieter Fütterer

Heft Nr. 33/1987 – „Die Expedition ANTARKTIS-IV mit FS ‚Polarstern' 1985/86 – Bericht zu den Fahrtabschnitten ANT-IV/3–4" von Dieter Karl Fütterer

Heft Nr. 34/1987 – „Zoogeographische Untersuchungen und Gemeinschaftsanalysen an antarktischem Makroplankton" von U. Piatkowski

Heft Nr. 35/1987 – „Zur Verbreitung des Meso- und Makrozooplanktons in Oberflächenwasser der Weddell See (Antarktis)" von E. Boysen-Ennen

Heft Nr. 36/1987 – „Zur Nahrungs- und Bewegungsphysiologie von *Salpa thompsoni* und *Salpa fusiformis*" von M. Reinke

Heft Nr. 37/1987 – "The Eastern Weddell Sea Drifting Buoy Data Set of the Winter Weddell Sea Project (WWSP)" 1986 by Heinrich Hoeber und Marianne Gube-Lehnhardt

Heft Nr. 38/1987 – "The Meteorological Data of the Georg von Neumayer Station for 1983 and 1984" by M. Gube-Lenhardt

Heft Nr. 39/1987 – „Die Winter-Expedition mit FS ‚Polarstern' in die Antarktis (ANT V/1–3)" herausgegeben von Sigrid Schnack-Schiel

Heft Nr. 40/1987 – "Weather and Synoptic Situation during Winter Weddell Sea Project 1986 (ANT V/2) July 16–September 10, 1986" by Werner Rabe

Heft Nr. 41/1988 – „Zur Verbreitung und Ökologie der Seegurken im Weddellmeer (Antarktis)" von Julian Gutt

Heft Nr. 42/1988 – "The zooplankton community in the deep bathyal and abyssal zones of the eastern North Atlantic" by Werner Beckmann

Heft Nr. 43/1988 – "Scientific cruise report of Arctic Expedition ARK IV/3" Wissenschaftlicher Fahrtbericht der Arktis-Expedition ARK IV/3, compiled by Jörn Thiede

Heft Nr. 44/1988 – "Data Report for FV 'Polarstern' Cruise ARK IV/1, 1987 to the Arctic and Polar Fronts" by Hans-Jürgen Hirche

Heft Nr. 45/1988 – „Zoogeographie und Gemeinschaftsanalyse des Makrozoobenthos des Weddellmeeres (Antarktis)" von Joachim Voß

Heft Nr. 46/1988 – "Meteorological and Oceanographic Data of the Winter-Weddell-Sea Project 1986 (ANT V/3)" by Eberhard Fahrbach

Heft Nr. 47/1988 – „Verteilung und Herkunft glazial-mariner Gerölle am Antarktischen Kontinentalrand des östlichen Weddellmeeres" von Wolfgang Oskierski

Heft Nr. 48/1988 – „Variationen des Erdmagnetfeldes an der GvN-Station" von Arnold Brodscholl

* **Heft Nr. 49/1988** – „Zur Bedeutung der Lipide im antarktischen Zooplankton" von Wilhelm Hagen

Heft Nr. 50/1988 – „Die gezeitenbedingte Dynamik des Ekström-Schelfeises, Antarktis" von Wolfgang Kobarg

Heft Nr. 51/1988 – „Ökomorphologie notothenioider Fische aus dem Weddellmeer, Antarktis" von Werner Ekau

Heft Nr. 52/1988 – „Zusammensetzung der Bodenfauna in der westlichen Fram-Straße" von Dieter Piepenburg

* **Heft Nr. 53/1988** – „Untersuchungen zur Ökologie des Phytoplanktons im südöstlichen Weddellmeer (Antarktis) im Jan./Febr. 1985" von Eva-Maria Nöthig

Heft Nr. 54/1988 – „Die Fischfauna des östlichen und südlichen Weddellmeeres: geographische Verbreitung, Nahrung und trophische Stellung der Fischarten" von Wiebke Schwarzbach

Heft Nr. 55/1988 – "Weight and length data of zooplankton in the Weddell Sea in austral spring 1986 (Ant V/3)" by Elke Mizdalski

Heft Nr. 56/1989 – "Scientific cruise report of Arctic expeditions ARK IV/1, 2 & 3" by G. Krause, J. Meincke und J. Thiede

Heft Nr. 57/1989 – „Die Expedition ANTARKTIS V mit FS ‚Polarstern' 1986/87" Bericht von den Fahrtabschnitten ANT V/4–5 von H. Miller und H. Oerter

* **Heft Nr. 58/1989** – „Die Expedition ANTARKTIS VI mit FS ‚Polarstern' 1987/88" von D. K. Fütterer

Heft Nr. 59/1989 – „Die Expedition ARKTIS V/1a, 1b und 2 mit FS ‚Polarstern' 1988" von M. Spindler

Heft Nr. 60/1989 – „Ein zweidimensionales Modell zur thermohalinen Zirkulation unter dem Schelfeis" von H. H. Hellmer

Heft Nr. 61/1989 – „Die Vulkanite im westlichen und mittleren Neuschwabenland, Vestfjella und Ahlmannryggen, Antarktika" von M. Peters

* **Heft-Nr. 62/1989** – "The Expedition ANTARKTIS VII/1 and 2 (EPOS I) of RV 'Polarstern' in 1988/89", by I. Hempel

Heft Nr. 63/1989 – „Die Eisalgenflora des Weddellmeeres (Antarktis): Artenzusammensetzung und Biomasse sowie Ökophysiologie ausgewählter Arten" von Annette Bartsch

Heft Nr. 64/1989 – "Meteorological Data of the G.-v.-Neumayer-Station (Antarctica)" by L. Helmes

Heft Nr. 65/1989 – „Expedition Antarktis VII/3 in 1988/89" by I. Hempel, P. H. Schalk, V. Smetacek

Heft Nr. 66/1989 – „Geomorphologisch-glaziologische Detailkartierung des arid-hochpolaren Borgmassivet, Neuschwabenland, Antarktika" von Karsten Brunk

Heft-Nr. 67/1990 – „Identification key and catalogue of larval Antarctic fishes", edited by Adolf Kellermann

Heft-Nr. 68/1990 – „The Expediton Antarktis VII/4 (Epos leg 3) and VII/5 of RV 'Polarstern' in 1989", edited by W. Arntz, W. Ernst, I. Hempel

Heft-Nr. 69/1990 – „Abhängigkeiten elastischer und rheologischer Eigenschaften des Meereises vom Eisgefüge", von Harald Hellmann

Heft-Nr. 70/1990 – „Die beschalten benthischen Mollusken (Gastropoda und Bivalvia) des Weddellmeeres, Antarktis", von Stefan Hain

Heft-Nr. 71/1990 – „Sedimentologie und Paläomagnetik an Sedimenten der Maudkuppe (Nordöstliches Weddellmeer)", von Dieter Cordes.

Heft-Nr. 72/1990 – „Distribution and abundance of planktonic copepods (Crustacea) in the Weddell Sea in summer 1980/81", by F. Kurbjeweit and S. Ali-Khan

Heft-Nr. 73/1990 – „Zur Frühdiagenese von organischem Kohlenstoff und Opal in Sedimenten des südlichen und östlichen Weddellmeeres", von M. Schlüter

Heft-Nr. 74/1990 – „Expeditionen ANTARKTIS-VIII/3 und VIII/4 mit FS ‚Polarstern' 1989" von Rainer Gersonde und Gotthilf Hempel

Heft-Nr. 75/1991 – „Quartäre Sedimentationsprozesse am Kontinentalhang des Süd-Orkey-Plateaus im nordwestlichen Weddellmeer (Antarktis)", von Sigrun Grünig

Heft-Nr. 76/1990 – „Ergebnisse der faunistischen Arbeiten im Benthal von King George Island (Südshetlandinseln, Antarktis)", von Martin Rauschert

Heft-Nr. 77/1990 – „Verteilung von Mikroplankton-Organismen nordwestlich der Antarktischen Halbinsel unter dem Einfluß sich ändernder Umweltbedingungen im Herbst", von Heinz Klöser

Heft-Nr. 78/1991 – „Hochauflösende Magnetostratigraphie spätquartärer Sedimente arktischer Meeresgebiete", von Norbert R. Nowaczyk

Heft-Nr. 79/1991 – „Ökophysiologische Untersuchungen zur Salinitäts- und Temperaturtoleranz antarktischer Grünalgen unter besonderer Berücksichtigung des ß-Dimethylsulfoniumpropionat (DMSP) - Stoffwechsels", von Ulf Karsten

Heft-Nr. 80/1991 – „Die Expedition ARKTIS VII/1 mit FS ‚Polarstern' 1990", herausgegeben von Jörn Thiede und Gotthilf Hempel

Heft-Nr. 81/1991 – „Paläoglaziologie und Paläozeanographie im Spätquartär am Kontinentalrand des südlichen Weddellmeeres, Antarktis", von Martin Melles

Heft-Nr. 82/1991 – „Quantifizierung von Meereseigenschaften: Automatische Bildanalyse von Dünnschnitten und Parametrisierung von Chlorophyll- und Salzgehaltsverteilungen", von Hajo Eicken

Heft-Nr. 83/1991 – „Das Fließen von Schelfeisen - numerische Simulationen mit der Methode der finiten Differenzen", von Jürgen Determann

Heft-Nr. 84/1991 – „Die Expedition ANTARKTIS-VIII/1-2, 1989 mit der Winter Weddell Gyre Study der Forschungsschiffe „Polarstern" und „Akademik Fedorov", von Ernst Augstein, Nikolai Bagriantsev und Hans Werner Schenke

Heft-Nr. 85/1991 – „Zur Entstehung von Unterwassereis und das Wachstum und die Energiebilanz des Meereises in der Atka Bucht, Antarktis", von Josef Kipfstuhl

Heft-Nr. 86/1991 – „Die Expedition ANTARKTIS-VIII mit „FS Polarstern" 1989/90. Bericht vom Fahrtabschnitt ANT-VIII / 5", von Heinz Miller und Hans Oerter

Heft-Nr. 87/1991 –"Scientific cruise reports of Arctic expeditions ARK VI / 1-4 of RV "Polarstern" in 1989", edited by G. Krause, J. Meincke & H. J. Schwarz

Heft-Nr. 88/1991 – „Zur Lebensgeschichte dominanter Copepodenarten (*Calanus finmarchicus, C. glacialis, C. hyperboreus, Metridia longa)* in der Framstraße", von Sabine Diel

Heft-Nr. 89/1991 – „Detaillierte seismische Untersuchungen am östlichen Kontinentalrand des Weddell-Meeres vor Kapp Norvegia, Antarktis", von Norbert E. Kaul

Heft-Nr. 90/1991 – „Die Expedition ANTARKTIS-VIII mit FS „Polarstern" 1989/90. Bericht von den Fahrtabschnitten ANT-VIII/6-7", herausgegeben von Dieter Karl Fütterer und Otto Schrems

Heft-Nr. 91/1991 – "Blood physiology and ecological consequences in Weddell Sea fishes (Antarctica)", by Andreas Kunzmann

Heft-Nr. 92/1991 – „Zur sommerlichen Verteilung des Mesozooplanktons im Nansen-Becken, Nordpolarmeer", von Nicolai Mumm

Heft-Nr. 93/1991 – „Die Expedition ARKTIS VII mit FS „Polarstern", 1990. Bericht vom Fahrtabschnitt ARK VII/2", herausgegeben von Gunther Krause

Heft-Nr. 94/1991 – „Die Entwicklung des Phytoplanktons im östlichen Weddellmeer (Antarktis) beim Übergang vom Spätwinter zum Frühjahr", von Renate Scharek

Heft-Nr. 95/1991 – „Radioisotopenstratigraphie, Sedimentologie und Geochemie jungquartärer Sedimente des östlichen Arktischen Ozeans", von Horst Bohrmann

Heft-Nr. 96/1991 – „Holozäne Sedimentationsentwicklung im Scoresby Sund, Ost-Grönland", von Peter Marienfeld

Heft-Nr. 97/1991 – „Strukturelle Entwicklung und Abkühlungsgeschichte der Heimefrontfjella (Westliches Dronning Maud Land/Antarktika)", von Joachim Jacobs

Heft-Nr. 98/1991 – „Zur Besiedlungsgeschichte des antarktischen Schelfes am Beispiel der Isopoda (Crustacea, Malacostraca)", von Angelika Brandt

Heft-Nr. 99/1992 – "The Antarctic ice sheet and environmental change: a three-dimensional modelling study", by Philippe Huybrechts

* **Heft-Nr. 100/1992** – „Die Expeditionen ANTARKTIS IX/1-4 des Forschungsschiffes „Polarstern" 1990/91", herausgegeben von Ulrich Bathmann, Meinhard Schulz-Baldes, Eberhard Fahrbach, Victor Smetacek und Hans-Wolfgang Hubberten

Heft-Nr. 101/1992 – „Wechselbeziehungen zwischen Schwermetallkonzentrationen (Cd, Cu, Pb, Zn) im Meewasser und in Zooplanktonorganismen (Copepoda) der Arktis und des Atlantiks", von Christa Pohl

Heft-Nr. 102/1992 – „Physiologie und Ultrastruktur der antarktischen Grünalge *Prasiola crispa* ssp. *antarctica* unter osmotischem Streß und Austrocknung", von Andreas Jacob

Heft-Nr. 103/1992 – „Zur Ökologie der Fische im Weddelmeer", von Gerd Hubold

Heft-Nr. 104/1992 – „Mehrkanalige adaptive Filter für die Unterdrückung von multiplen Reflexionen in Verbindung mit der freien Oberfläche in marinen Seismogrammen", von Andreas Rosenberger

Heft-Nr. 105/1992 – „Radiation and Eddy Flux Experiment 1991 *(REFLEX I)*", von Jörg Hartmann, Christoph Kottmeier und Christian Wamser

Heft-Nr. 106/1992 – „Ostracoden im Epipelagial vor der Antarktischen Halbinsel - ein Beitrag zur Systematik sowie zur Verbreitung und Populationsstruktur unter Berücksichtigung der Saisonalität", von Rüdiger Kock

Heft-Nr. 107/1992 – „ARCTIC '91: Die Expedition ARK-VIII/3 mit FS „Polarstern" 1991", von Dieter K. Fütterer

Heft-Nr. 108/1992 – „Dehnungsbeben an einer Störungszone im Ekström-Schelfeis nördlich der Georg-von-Neumayer Station, Antarktis. – Eine Untersuchung mit seismologischen und geodätischen Methoden", von Uwe Nixdorf.

Heft-Nr. 109/1992 – „Spätquartäre Sedimentation am Kontinentalrand des südöstlichen Weddellmeeres, Antarktis", von Michael Weber.

Heft-Nr. 110/1992 – „Sedimentfazies und Bodenwasserstrom am Kontinentalhang des nordwestlichen Weddellmeeres", von Isa Brehme.

Heft-Nr. 111/1992 – „Die Lebensbedingungen in den Solekanälchen des antarktischen Meereises", von Jürgen Weissenberger.

Heft-Nr. 112/1992 – „Zur Taxonomie von rezenten benthischen Foraminiferen aus dem Nansen Becken, Arktischer Ozean", von Jutta Wollenburg.

Heft-Nr. 113/1992 – „Die Expedition ARKTIS VIII/1 mit FS "Polarstern" 1991", herausgegeben von Gerhard Kattner.

* **Heft-Nr. 114/1992** – „Die Gründungsphase deutscher Polarforschung, 1865-1875", von Reinhard A. Krause.

Heft-Nr. 115/1992 – „Scientific Cruise Report of the 1991 Arctic Expedition ARK VIII/2 of RV "Polarstern" (EPOS II)", by Eike Rachor.

Heft-Nr. 116/1992 – „The Meteorological Data of the Georg-von-Neumayer-Station (Antarctica) for 1988, 1989, 1990 and 1991", by Gert König-Langlo.

Heft-Nr. 117/1992 – „Petrogenese des metamorphen Grundgebirges der zentralen Heimefrontfjella (westliches Dronning Maud Land / Antarktis)", von Peter Schulze.

Heft-Nr. 118/1993 – „Die mafischen Gänge der Shackleton Range / Antarktika: Petrographie, Geochemie, Isotopengeochemie und Paläomagnetik", von Rüdiger Hotten.

* **Heft-Nr. 119/1993** – „Gefrierschutz bei Fischen der Polarmeere", von Andreas P.A. Wöhrmann.

* **Heft-Nr. 120/1993** – „East Siberian Arctic Region Expedition '92: The Laptev Sea - its Significance for Arctic Sea-Ice Formation and Transpolar Sediment Flux", by D. Dethleff, D. Nürnberg, E. Reimnitz, M. Saarso and Y. P. Sacchenko. – „Expedition to Novaja Zemlja and Franz Josef Land with RV.'Dalnie Zelentsy'", by D. Nürnberg and E. Groth.

* **Heft-Nr. 121/1993** – „Die Expedition ANTARKTIS X/3 mit FS 'Polarstern' 1992", herausgegeben von Michael Spindler, Gerhard Dieckmann und David Thomas.

Heft-Nr. 122/1993 – „Die Beschreibung der Korngestalt mit Hilfe der Fourier-Analyse: Parametrisierung der morphologischen Eigenschaften von Sedimentpartikeln", von Michael Diepenbroek.

* **Heft-Nr. 123/1993** – „Zerstörungsfreie hochauflösende Dichteuntersuchungen mariner Sedimente", von Sebastian Gerland.

Heft-Nr. 124/1993 – „Umsatz und Verteilung von Lipiden in arktischen marinen Organismen unter besonderer Berücksichtigung unterer trophischer Stufen", von Martin Graeve.

Heft-Nr. 125/1993 – „Ökologie und Respiration ausgewählter arktischer Bodenfischarten", von Christian F. von Dorrien.

Heft-Nr. 126/1993 – „Quantitative Bestimmung von Paläoumweltparametern des Antarktischen Oberflächenwassers im Spätquartär anhand von Transferfunktionen mit Diatomeen", von Ulrich Zielinski

Heft-Nr. 127/1993 – „Sedimenttransport durch das arktische Meereis: Die rezente lithogene und biogene Materialfracht", von Ingo Wollenburg.

Heft-Nr. 128/1993 – „Cruise ANTARKTIS X/3 of RV 'Polarstern': CTD-Report", von Marek Zwierz.

Heft-Nr. 129/1993 – „Reproduktion und Lebenszyklen dominanter Copepodenarten aus dem Weddellmeer, Antarktis", von Frank Kurbjeweit

Heft-Nr. 130/1993 – „Untersuchungen zu Temperaturregime und Massenhaushalt des Filchner-Ronne-Schelfeises, Antarktis, unter besonderer Berücksichtigung von Anfrier- und Abschmelzprozessen", von Klaus Grosfeld

Heft-Nr. 131/1993 – „Die Expedition ANTARKTIS X/5 mit FS 'Polarstern' 1992", herausgegeben von Rainer Gersonde

Heft-Nr. 132/1993 – „Bildung und Abgabe kurzkettiger halogenierter Kohlenwasserstoffe durch Makroalgen der Polarregionen", von Frank Laturnus

Heft-Nr. 133/1994 – "Radiation and Eddy Flux Experiment 1993 *(REFLEX II)*", by Christoph Kottmeier, Jörg Hartmann, Christian Wamser, Axel Bochert, Christof Lüpkes, Dietmar Freese and Wolfgang Cohrs

* **Heft-Nr. 134/1994** – "The Expedition ARKTIS-IX/1", edited by Hajo Eicken and Jens Meincke

Heft-Nr. 135/1994 – „Die Expeditionen ANTARKTIS X/6-8", herausgegeben von Ulrich Bathmann, Victor Smetacek, Hein de Baar, Eberhard Fahrbach und Gunter Krause

Heft-Nr. 136/1994 – „Untersuchungen zur Ernährungsökologie von Kaiserpinguinen *(Aptenodytes forsteri)* und Königspinguinen *(Aptenodytes patagonicus)*", von Klemens Pütz

* **Heft-Nr. 137/1994** – „Die känozoische Vereisungsgeschichte der Antarktis", von Werner U. Ehrmann

Heft-Nr. 138/1994 – „Untersuchungen stratosphärischer Aerosole vulkanischen Ursprungs und polarer stratosphärischer Wolken mit einem Mehrwellenlängen-Lidar auf Spitzbergen *(79° N, 12° E)*", von Georg Beyerle

Heft-Nr. 139/1994 – „Charakterisierung der Isopodenfauna (Crustacea, Malacostraca) des Scotia-Bogens aus biogeographischer Sicht: Ein multivariater Ansatz", von Holger Winkler.

Heft-Nr. 140/1994 – „Die Expedition ANTARKTIS X/4 mit FS 'Polarstern' 1992", herausgegeben von Peter Lemke

Heft-Nr. 141/1994 – „Satellitenaltimetrie über Eis – Anwendung des GEOSAT-Altimeters über dem Ekströmisen, Antarktis", von Clemens Heidland

Heft-Nr. 142/1994 – "The 1993 Northeast Water Expedition. Scientific cruise report of RV'Polarstern' Arctic cruises ARK IX/2 and 3, USCG 'Polar Bear' cruise NEWP and the NEWLand expedition", edited by Hans-Jürgen Hirche and Gerhard Kattner

Heft-Nr. 143/1994 – „Detaillierte refraktionsseismische Untersuchungen im inneren Scoresby Sund Ost-Grönland", von Notker Fechner

Heft-Nr. 144/1994 – „Russian-German Cooperation in the Siberian Shelf Seas: Geo-System Laptev Sea", edited by Heidemarie Kassens, Hans-Wolfgang Hubberten, Sergey M. Pryamikov und Rüdiger Stein

* **Heft-Nr. 145/1994** – „The 1993 Northeast Water Expedition. Data Report of RV 'Polarstern' Arctic Cruises IX/2 and 3", edited by Gerhard Kattner and Hans-Jürgen Hirche.

Heft-Nr. 146/1994 – "Radiation Measurements at the German Antarctic Station Neumayer 1982-1992", by Torsten Schmidt and Gert König-Langlo.

Heft-Nr. 147/1994 – „Krustenstrukturen und Verlauf des Kontinentalrandes im Weddell Meer / Antarktis", von Christian Hübscher.

Heft-Nr. 148/1994 – "The expeditions NORILSK/TAYMYR 1993 and BUNGER OASIS 1993/94 of the AWI Research Unit Potsdam", edited by Martin Melles.

** **Heft-Nr. 149/1994** – "Die Expedition ARCTIC' 93. Der Fahrtabschnitt ARK-IX/4 mit FS 'Polarstern' 1993", herausgegeben von Dieter K. Fütterer.

Heft-Nr. 150/1994 – "Der Energiebedarf der Pygoscelis-Pinguine: eine Synopse", von Boris M. Culik.

Heft-Nr. 151/1994 – „Russian-German Cooperation: The Transdrift I Expedition to the Laptev Sea", edited by Heidemarie Kassens and Valeriy Y. Karpiy.

Heft-Nr. 152/1994 – „Die Expedition ANTARKTIS-X mit FS 'Polarstern' 1992. Bericht von den Fahrtabschnitten / ANT-X / 1a und 2", herausgegeben von Heinz Miller.

Heft-Nr. 153/1994 – "Aminosäuren und Huminstoffe im Stickstoffkreislauf polarer Meere", von Ulrike Hubberten.

Heft-Nr. 154/1994 – "Regional und seasonal variability in the vertical distribution of mesozooplankton in the Greenland Sea", by Claudio Richter.

Heft-Nr. 155/1995 – "Benthos in polaren Gewässern", herausgegeben von Christian Wiencke und Wolf Arntz.

Heft-Nr. 156/1995 – "An adjoint model for the determination of the mean oceanic circulation, air-sea fluxes und mixing coefficients", by Reiner Schlitzer.

Heft-Nr. 157/1995 – "Biochemische Untersuchungen zum Lipidstoffwechsel antarktischer Copepoden", von Kirsten Fahl.

** **Heft-Nr. 158/1995** – "Die Deutsche Polarforschung seit der Jahrhundertwende und der Einfluß Erich von Drygalskis", von Cornelia Lüdecke.

Heft-Nr. 159/1995 – The distribution of $\partial^{18}O$ in the Arctic Ocean: Implications for the freshwater balance of the haocline and the sources of deep and bottom waters", by Dorothea Bauch.

* **Heft-Nr. 160/1995** – "Rekonstruktion der spätquartären Tiefenwasserzirkulation und Produktivität im östlichen Südatlantik anhand von benthischen Foraminiferenvergesellschaftungen", von Gerhard Schmiedl.

Heft-Nr. 161/1995 – "Der Einfluß von Salinität und Lichtintensität auf die Osmolytkonzentrationen, die Zellvolumina und die Wachstumsraten der antarktischen Eisdiatomeen *Chaetoceros* sp. und *Navicula* sp. unter besonderer Berücksichtigung der Aminosäure Prolin", von Jürgen Nothnagel.

Heft-Nr. 162/1995 – "Meereistransportiertes lithogenes Feinmaterial in spätquartären Tiefseesedimenten des zentralen östlichen Arktischen Ozeans und der Framstraße", von Thomas Letzig.

Heft-Nr. 163/1995 – "Die Expedition ANTARKTIS-XI/2 mit FS "Polarstern" 1993/94", herausgegeben von Rainer Gersonde.

Heft-Nr. 164/1995 – "Regionale und altersabhängige Variation gesteinsmagnetischer Parameter in marinen Sedimenten der Arktis", von Thomas Frederichs.

Heft-Nr. 165/1995 – "Vorkommen, Verteilung und Umsatz biogener organischer Spurenstoffe: Sterole in antarktischen Gewässern", von Georg Hanke.

Heft-Nr. 166/1995 – "Vergleichende Untersuchungen eines optimierten dynamisch-thermodynamischen Meereismodel mit Beobachtungen im Weddellmeer", von Holger Fischer.

Heft-Nr. 167/1995 – "Rekonstruktionen von Paläo-Umweltparametern anhand von stabilen Isotopen und Faunen-Vergesellschaftungen planktischer Foraminiferen im Südatlantik", von Hans-Stefan Niebler

Heft-Nr. 168/1995 – "Die Expedition ANTARKTIS XII mit FS 'Polarstern' 1993/94. Bericht von den Fahrtabschnitten ANT XII/1 und 2", herausgegeben von Gerhard Kattner und Dieter Karl Fütterer.

Heft-Nr. 169/1995 – "Medizinische Untersuchung zur Circadianrhythmik und zum Verhalten bei Überwinterern auf eine antarktischen Forschungsstation", von Hans Wortmann.

Heft-Nr. 170/1995 – DFG-Kolloquium: Terrestrische Geowissenschaften - Geologie und Geophysik der Antarktis.

Heft-Nr. 171/1995 – "Strukturentwicklung und Petrogenese des metamorphen Grundgebirges der nördlichen Heimefrontfjella (westliches Dronning Maud Land/Antarktika)", von Wilfried Bauer.

Heft-Nr. 172/1995 – "Die Struktur der Erdkruste im Bereich des Scoresby Sund, Ostgrönland: Ergebnisse refraktionsseismischer und gravimetrischer Untersuchungen", von Holger Mandler.

Heft-Nr. 173/1995 – "Paläozoische Akkretion am paläopazifischen Kontinentalrand der Antarktis in Nordvictorialand – P-T-D-Geschichte und Deformationsmechanismen im Bowers Terrane", von Stefan Matzer.

Heft-Nr. 174/1995 – "The Expedition ARKTIS-X/2 of RV 'Polarstern' in 1994", edited by Hans-W. Hubberten.

Heft-Nr. 175/1995 – "Russian-German Cooperation: The Expedition TAYMYR 1994", edited by Christine Siegert and Dmitry Bolshiyanov.

Heft-Nr. 176/1995 – "Russian-German Cooperation: Laptev Sea System", edited by Heidemarie Kassens, Dieter Piepenburg, Jörn Thiede, Leonid Timokhov, Hans-Wolfgang Hubberten and Sergey M. Priamikov.

Heft-Nr. 177/1995 – "Organischer Kohlenstoff in spätquartären Sedimenten des Arktischen Ozeans: Terrigener Eintrag und marine Produktivität", von Carsten J. Schubert.

Heft-Nr. 178/1995 – "Cruise ANTARKTIS XII/4 of RV 'Polarstern' in 1995: CTD-Report", by Jüri Sildam.

Heft-Nr. 179/1995 – "Benthische Foraminiferenfaunen als Wassermassen-, Produktions- und Eisdriftanzeiger im Arktischen Ozean", von Jutta Wollenburg.

Heft-Nr. 180/1995 – "Biogenopal und biogenes Barium als Indikatoren für spätquartäre Produktivitätsänderungen am antarktischen Kontinentalhang, atlantischer Sektor", von Wolfgang J. Bonn.

Heft-Nr. 181/1995 – "Die Expedition ARKTIS X/1 des Forschungsschiffes ‚Polarstern' 1994", herausgegeben von Eberhard Fahrbach.

Heft-Nr. 182/1995 – "Laptev Sea System: Expeditions in 1994", edited by Heidemarie Kassens.

Heft-Nr. 183/1996 – "Interpretation digitaler Parasound Echolotaufzeichnungen im östlichen Arktischen Ozean auf der Grundlage physikalischer Sedimenteigenschaften", von Uwe Bergmann.

Heft-Nr. 184/1996 – "Distribution and dynamics of inorganic nitrogen compounds in the troposphere of continental, coastal, marine and Arctic areas", by María Dolores Andrés Hernández.

Heft-Nr. 185/1996 – "Verbreitung und Lebensweise der Aphroditiden und Polynoiden (Polychaeta) im östlichen Weddellmeer und im Lazarevmeer (Antarktis)", von Michael Stiller.

Heft-Nr. 186/1996 – "Reconstruction of Late Quaternary environmental conditions applying the natural radionuclides ^{230}Th, ^{10}Be, ^{231}Pa and ^{238}U: A study of deep-sea sediments from the eastern sector of the Antrctic Circumpolar Current System", by Martin Frank.

Heft-Nr. 187/1996 – "The Meteorological Data of the Neumayer Station (Antarctica) for 1992, 1993 and 1994", by Gert König-Langlo and Andreas Herber.

Heft-Nr. 188/1996 – "Die Expedition ANTARKTIS-XI/3 mit FS 'Polarstern' 1994", herausgegeben von Heinz Miller und Hannes Grobe.

Heft-Nr. 189/1996 – "Die Expedition ARKTIS-VII/3 mit FS 'Polarstern' 1990", herausgegeben von Heinz Miller und Hannes Grobe.

Heft-Nr. 190/1996 – "Cruise report of the Joint Chilean-German-Italian Magellan 'Victor Hensen' Campaign in 1994", edited by Wolf Arntz and Matthias Gorny.

Heft-Nr. 191/1996 – "Leitfähigkeits- und Dichtemessung an Eisbohrkernen", von Frank Wilhelms.

Heft-Nr. 192/1996 – "Photosynthese-Charakteristika und Lebensstrategie antarktischer Makroalgen", von Gabriele Weykam.

Heft-Nr. 193/1996 – "Heterogene Raktionen von N_2O_5 und HBr und ihr Einfluß auf den Ozonabbau in der polaren Stratosphäre", von Sabine Seisel.

Heft-Nr. 194/1996 – "Ökologie und Populationsdynamik antarktischer Ophiuroiden (Echinodermata)", von Corinna Dahm.

Heft-Nr. 195/1996 – "Die planktische Foraminifere *Neogloboquadrina pachyderma* (Ehrenberg) im Weddellmeer, Antarktis", von Doris Berberich.

Heft-Nr. 196/1996 – "Untersuchungen zum Beitrag chemischer und dynamischer Prozesse zur Variabilität des stratosphärischen Ozons über der Arktis", von Birgit Heese.

Heft-Nr. 197/1996 – "The Expedition ARKTIS-XI/2 of 'Polarstern' in 1995", edited by Gunther Krause.

Heft-Nr. 198/1996 – "Geodynamik des Westantarktischen Riftsystems basierend auf Apatit-Spaltspuranalysen", von Frank Lisker.

Heft-Nr. 199/1996 – "The 1993 Northeast Water Expedition. Data Report on CTD Measurements of RV 'Polarstern' Cruises ARKTIS IX/2 and 3", by Gereon Budéus and Wolfgang Schneider.

Heft-Nr. 200/1996 – "Stability of the Thermohaline Circulation in analytical and numerical models", by Gerrit Lohmann.

Heft-Nr. 201/1996 – "Trophische Beziehungen zwischen Makroalgen und Herbivoren in der Potter Cove (King George-Insel, Antarktis)", von Katrin Iken.

Heft-Nr. 202/1996 – "Zur Verbreitung und Respiration ökologisch wichtiger Bodentiere in den Gewässern um Svalbard (Arktis)", von Michael K. Schmid.

Heft-Nr. 203/1996 – "Dynamik, Rauhigkeit und Alter des Meereises in der Arktis - Numerische Untersuchungen mit einem großskaligen Modell", von Markus Harder.

Heft-Nr. 204/1996 – "Zur Parametrisierung der stabilen atmosphärischen Grenzschicht über einem antarktischen Schelfeis", von Dörthe Handorf.

Heft-Nr. 205/1996 – "Textures and fabrics in the GRIP ice core, in relation to climate history and ice deformation", by Thorsteinn Thorsteinsson.

Heft-Nr. 206/1996 – "Der Ozean als Teil des gekoppelten Klimasystems: Versuch der Rekonstruktion der glazialen Zirkulation mit verschieden komplexen Atmosphärenkomponenten", von Kerstin Fieg.

Heft-Nr. 207/1996 – "Lebensstrategien dominanter antarktischer Oithonidae (Cyclopoida, Copepoda) und Oncaeidae (Poecilostomatoida, Copepoda) im Bellingshausenmeer", von Cornelia Metz.

Heft-Nr. 208/1996 – "Atmosphäreneinfluß bei der Fernerkundung von Meereis mit passiven Mikrowellenradiometern", von Christoph Oelke.

Heft-Nr. 209/1996 – "Klassifikation von Radarsatellitendaten zur Meereiserkennung mit Hilfe von Line-Scanner-Messungen", von Axel Bochert.

Heft-Nr. 210/1996 – "Die mit ausgewählten Schwämmen (Hexactinellida und Demospongiae) aus dem Weddellmeer, Antarktis, vergesellschaftete Fauna", von Kathrin Kunzmann.

* vergriffen/out of print.

** nur noch beim Autor/only from the author.

Heft-Nr. 211/1996 – "Russian-German Cooperation: The Expediton TAYMYR 1995 and the Expedition KOLYMA 1995", by Dima Yu. Bolshiyanov and Hans-W. Hubberten.

Heft-Nr. 212/1996 – "Surface-sediment composition and sedimentary processes in the central Arctic Ocean and along the Eurasian Continental Margin", by Ruediger Stein, Gennadij I. Ivanov, Michael A. Levitan, and Kirsten Fahl.

Heft-Nr. 213/1996 – "Gonadenentwicklung und Eiproduktion dreier Calanus-Arten (Copepoda): Freilandbeobachtungen, Histologie und Experimente", von Barbara Niehoff.

Heft-Nr. 214/1996 – "Numerische Modellierung der Übergangszone zwischen Eisschild und Eisschelf", von Christoph Mayer.

Heft-Nr. 215/1996 – "Arbeiten der AWI-Forschungsstelle Potsdam in Antarktika, 1994/95", herausgegeben von Ulrich Wand.

Heft-Nr. 216/1996 – "Rekonstruktion quartärer Klimaänderungen im atlantischen Sektor des Südpolarmeeres anhand von Radiolarien", von Uta Brathauer.

Heft-Nr. 217/1996 – "Adaptive Semi-Lagrange-Finite-Elemente-Methode zur Lösung der Flachwassergleichungen: Implementierung und Parallelisierung", von Jörn Behrens.

Heft-Nr. 218/1997 – "Radiation and Eddy Flux Experiment 1995 (REFLEX III)", by Jörg Hartmann, Axel Bochert, Dietmar Freese, Christoph Kottmeier, Dagmar Nagel and Andreas Reuter.

Heft-Nr. 219/1997 – "Die Expedition ANTARKTIS-XII mit FS 'Polarstern' 1995. Bericht vom Fahrtabschnitt ANT-XII/3", herausgegeben von Wilfried Jokat und Hans Oerter.

Heft-Nr. 220/1997 – "Ein Beitrag zum Schwerefeld im Bereich des Weddellmeeres, Antarktis. Nutzung von Altimetermessungen des GEOSAT und ERS-1", von Tilo Schöne.

Heft-Nr. 221/1997 – "Die Expeditionen ANTARKTIS-XIII/1-2 des Forschungsschiffes 'Polarstern' 1995/96", herausgegeben von Ulrich Bathmann, Mike Lucas und Victor Smetacek.

* vergriffen/out of print.

** nur noch beim Autor/only from the author.